Distribution Agreement

In presenting this thesis or dissertation as a partial fulfillment of the requirements for an advanced degree from Emory University, I hereby grant to Emory University and its agents the non-exclusive license to archive, make accessible, and display my thesis or dissertation in whole or in part in all forms of media, now or hereafter known, including display on the world wide web. I understand that I may select some access restrictions as part of the online submission of this thesis or dissertation. I retain all ownership rights to the copyright of the thesis or dissertation. I also retain the right to use in future works (such as articles or books) all or part of this thesis or dissertation.

Signature:

_____ _____

Filomene Grace Morrison Date

Mechanisms of Olfactory Fear Learning and Memory in Adult Mice
By

Filomene Grace Morrison

Doctor of Philosophy

Graduate Division of Biological and Biomedical Science
Neuroscience

_____
Kerry J. Ressler, M.D., Ph.D.
Advisor

_____
Shannon Gourley, Ph.D.
Committee Member

_____
Tanja Jovanovic, Ph.D.
Committee Member

_____
John Scott, Ph.D.
Committee Member

_____
James Zheng, Ph.D
Committee Member

Accepted:

_____
Lisa A. Tedesco, Ph.D.
Dean of the James T. Laney School of Graduate Studies

_____

Date

Mechanisms of Olfactory Fear Learning and Memory in Adult Mice

By

Filomene Grace Morrison
B.A., University of California, Berkeley, 2011

Advisor: Kerry J. Ressler, M.D., Ph.D.

An abstract of a dissertation submitted to the Faculty of the James T. Laney School of Graduate Studies of Emory University in partial fulfillment of the requirements for the degree of Doctor of Philosophy in Graduate Division of Biological and Biomedical Science, Neuroscience
2017

Abstract

Mechanisms of Olfactory Fear Learning and Memory in Adult Mice

By Filomene Grace Morrison

A significant amount is known regarding the molecular mechanisms underlying the processing of emotional stimuli in the central nervous system; however, fewer studies have investigated the mechanisms accompanying emotional learning at the level of specific sensory modalities. This dissertation utilizes the olfactory system, whose primary sensory receptive field maps are exquisitely organized, respond dynamically to cues in the environment, and remain plastic from development through adulthood, to understand the mechanisms underlying fear learning and memory at the primary sensory system level. Using a transgenic mouse in which olfactory sensory neurons (OSNs) expressing the M71 odorant receptor (OR) may be visualized by LacZ histochemistry (M71-LacZ mouse line), we have previously demonstrated that olfactory fear conditioning leads to increased odorant-specific receptor representation in the main olfactory epithelium (MOE) and in glomeruli within the olfactory bulb (OB). This dissertation reports on the effects of cue-specific extinction, as well as on the mechanisms underlying the behavioral and structural plasticity of the olfactory system in mice following the acquisition of cued olfactory fear. We first demonstrate that olfactory extinction training specific to the conditioned odor stimulus reverses the conditioning-associated freezing behavior and odor learning-induced structural changes in the olfactory epithelium and olfactory bulb in an odorant ligand-specific manner. These data suggest that learning-induced freezing behavior, structural alterations, enhanced neural sensory representation, and histone modifications at the M71 locus can be reversed in adult mice following extinction training. Second, we used 5-Ethynyl-2'-deoxyuridine (EdU) labeling of MOE OSNs to understand the dynamics of OSN cell turnover as a function of fear learning. Finally, using intranasal or intraperitoneal (I.P.) administration of Tropomysin receptor kinase B (TrkB) agonists and antagonists prior to olfactory fear conditioning, we demonstrate a role for brain-derived neurotrophic factor (BDNF) signaling through its receptor, TrkB in mediating the structural plasticity accompanying olfactory fear learning. The studies contained in this dissertation provide novel evidence of the mechanisms underlying the behavioral and structural plasticity of the olfactory system in mice following the acquisition and extinction of cued olfactory fear, and contribute to a growing body of literature suggesting a critical role for primary sensory systems, particularly the olfactory system, in emotional learning and memory.

Mechanisms of Olfactory Fear Learning and Memory in Adult Mice

By

Filomene Grace Morrison
B.A., University of California, Berkeley, 2011

Advisor: Kerry J. Ressler, M.D., Ph.D.

A dissertation submitted to the Faculty of the James T. Laney School of Graduate Studies of Emory University in partial fulfillment of the requirements for the degree of Doctor of Philosophy in Graduate Division of Biological and Biomedical Science, Neuroscience
2017

Acknowledgements

I would like to first thank my infinitely loving parents, Susan and Frank, for always supporting me and continually inspiring me with your hard work, curiosity and wisdom. To Huntly, I feel so fortunate to have such a compassionate, talented, hilarious and wise younger brother. Thank you to my Grandma Sixta, whose joyful outlook on the world is a constant inspiration. Thank you to the Vinluan, Hill, and Doria families, and my friends in Atlanta and elsewhere, I am so lucky to have your love and support. To Melly, Kev Kev, and Huxley, I can't even begin to imagine the last six years without you. And finally, thank you to Kennedy (and Ellie) for being the best lab, adventure, and travel partner and friend I could have hoped for.

In my academic life, I must thank Dr. Malu Tansey, Dr. Victor Faundez, Dr. Gary Bassell, Dr. Yoland Smith, Dr. Shawn Hochman, Dr. Ron Calabrese, Gary Longstreet, as the past and present leadership of the Emory Neuroscience program, as well as the Emory Neuroscience students. Thank you to my friends and lab mates in the Ressler lab, Yerkes fifth floor, and McLean Hospital; it's been such a pleasure to work with a group of not only incredibly talented and smart people, but also the nicest and most fun people around.

Thank you to my incredible dissertation committee members for their guidance, time and support throughout the development of my dissertation, Dr. Shannon Gourley, Dr. Tanja Jovanovic, Dr. John Scott and Dr. James Zheng. Lastly, thank you to my advisor, Dr. Kerry Ressler for his mentorship these past six years. Kerry has been unspeakably supportive and has truly pushed me to think critically and really develop as a scientist, and I will always be grateful to have worked with him.

Table of Contents

List of Figures

CHAPTER 1: INTRODUCTION

Preamble

This dissertation aims to advance and refine our understanding of the mechanisms underlying olfactory learning and memory processes. This introductory chapter will discuss the broad impact of Posttraumatic Stress Disorder (PTSD), the circuitry underlying dysregulated fear responses in PTSD, and the role of the olfactory system within this context. In the following chapters, I will examine the behavioral, structural and molecular processes underlying the acquisition and extinction of a learned olfactory association. Finally, in the concluding chapter, I will summarize the findings of this dissertation and place them into a broader context and framework of learning and memory processes from rodent models to translational clinical models, aiming to further our understanding of human fear and anxiety related disorders.

Context, Author's Contribution, and Acknowledgement of Reproduction

The following chapter reviews the fear circuitry that likely underlies anxiety and fear-related disorders such as specific and social phobia, panic disorder, and posttraumatic stress disorder (PTSD). Additionally, this chapter reviews the modeling of fear learning and memory using classical Pavlovian fear conditioning. Finally, this chapter will review principles of olfactory system neuroanatomy and processing, as well as prior research on associative plasticity in the olfactory system. The work presented here was conceptualized, organized, researched, and written by the dissertation author under the guidance of Dr. Ressler. The chapter is reproduced from sections with minor edits from Morrison, F.G. and Ressler, K.J. (2013) "From the Neurobiology of Extinction

to Improved Clinical Treatments." *Depression and Anxiety*.

Introduction

The neural circuitry underlying the fear response is extremely well conserved across mammalian species, which has allowed for the rapid translation of research findings in rodent models of fear to therapeutic interventions in human populations. Many aspects of exposure-based psychotherapy treatments in humans, which are widely used in the treatment of PTSD, Panic Disorder, Phobias, and other anxiety disorders, are closely paralleled by extinction training in rodent fear conditioning models. This introductory chapter will first discuss how the neural circuitry of fear learning and extinction in rodent animal models may be used to understand the underlying neural circuitry of fear related disorders such as PTSD in humans. We examine the factors that contribute to the pathology and development of PTSD. Next, we will review how fear is measured in animal models using classical Pavlovian fear conditioning paradigms, as well as brain regions such as the amygdala, which are involved in the fear response across species. Within this context, we will also discuss the primary olfactory system and its role in fear learning and memory across species.

Olfactory cues serve as potent and long lasting triggers of emotional memories. When a particular odorant is paired with a traumatic event, the subsequent exposure to that odor (or even the olfactory hallucination of it) may act as a strong and immediate trigger for PTSD symptoms. The mechanisms by which the brain encodes the representation of environmentally relevant odors, both at the level of its primary sensory system (first order neurons in the nose and their projections to the olfactory bulb) and also within the central nervous system (regions of olfactory cortex and areas such as the

hippocampus and amygdala), remain to be determined. Convergent findings from human studies and rodent models point toward the importance of the primary olfactory system in the processes underlying emotional memory formation and storage in adult, developmental and transgenerational contexts. Additionally, recent evidence indicates that primary sensory systems, such as the olfactory sensory system, could provide a tractable and plastic target that may be manipulated in the treatment of anxiety like disorders such as PTSD. Within this introductory chapter, we will 1) provide an overview of the recent and growing body of literature on rodent models of the structural plasticity of the olfactory system in emotional learning and memory, and 2) highlight the strength of the olfactory system as a model to investigate the mechanisms of threat-induced alterations in behavior, plasticity and neural representation. The vast clinical potential and opportunities for taking advantage of the plasticity of the primary olfactory sensory system in the treatment of psychiatric disorders such as PTSD will be explored in greater detail in Chapter 5.

PTSD as a disorder of fear dysregulation

Fear learning is an adaptive and evolutionarily advantageous response to traumatic events and experiences; however, dysregulated processes of fear regulation, such as sensitization and over-generalization, can be harmful to the individual. Normal fear responses involve both the consolidation and manifestation of fear memories in fearful situations and also the suppression and extinction of fear behaviors in safe contexts. The extinction of fear memories involves the gradual decline in fear responses upon repeated presentations of the fearful cue in non-threatening situations. The over-generalization of fear and the inability to extinguish fear memories comprise two of the

key symptoms of fear related disorders such as phobias and posttraumatic stress disorder (PTSD) (Myers and Davis, 2007). This section will focus specifically on PTSD, a debilitating fear related disorder in which fear memories of a traumatic incident become over-generalized and are difficult to extinguish. Estimates indicate that PTSD occurs in 5-10% of the general population (Kessler et al., 2005) and populations that are exposed to chronic physical and emotional trauma experience even higher lifetime rates of PTSD of up to 20-30% (Breslau, 2001).

In the Psychiatric Diagnostic Manual, DSM-V, there are three main clusters of PTSD symptoms: re-experiencing, avoidance and hyperarousal. Re-experiencing symptoms are provoked by reminders of the trauma and include intrusive and distressing thoughts of the traumatic incident, recurring nightmares, or experiences of intense emotional upset or physiological reactivity following exposure to reminders of the trauma. Re-experiencing symptoms can be thought of in terms of classical Pavlovian fear conditioning, in that a cue associated with the trauma will trigger an often painful emotional and/or physiological response, in addition to concomitant nightmares and flashbacks. The avoidance symptom cluster may be thought of as a type of operant conditioning, in which the avoidance of reminders of the trauma in and of itself becomes a reinforcing process. Finally hyperarousal symptoms include central and autonomic nervous system processes that lead to behaviors such as being easily startled or having trouble sleeping. Hyperarousal symptoms are the cluster most commonly targeted with currently available medications; however, these medications treat only the biological processes of hyperarousal, failing to address the specific trauma memory underlying the fear disorder (Cain et al., 2012; Steckler and Risbrough, 2012).

Underlying the three main clusters present in PTSD is a dysregulated fear response, which characterizes most anxiety disorders including phobias and PTSD. A number of factors make it feasible to translate research on PTSD and other fear related disorders conducted at the laboratory bench to clinical settings. First, the neural circuitry and phenotypic outputs of the fear response are well understood and have been studied since the time of Ivan Pavlov (in addition to appetitive conditioning, Pavlov had also studied aversive fear conditioning) (Davis, 1992). Second, the fear processing and behaviors following trauma exposure are highly evolutionarily conserved across mammalian species, thus allowing for translational research in rodent models towards the treatment of human fear disorders (Belzung and Philippot, 2007; Lang et al., 2000). And finally, PTSD is the only psychiatric disorder in which the instigating event – the trauma, is known, and in many instances the traumatic incident leading to PTSD development may be recalled and is readily identifiable, leading to more efficacious and tailored prevention and intervention approaches.

This section will discuss the neurobiology of fear learning and extinction. One of the primary goals of modern psychiatry related to fear disorders has been to identify therapies/drugs that modulate signaling pathways involved in synaptic plasticity of fear learning in associated brain regions such as the amygdala in order to enhance the neurocircuitry of extinction. The genetic, molecular and behavioral literature on extinction processes is vast and complex and interested readers are directed to additional reviews for further and more comprehensive reading (Myers and Davis, 2007; Parsons and Ressler, 2013).

Factors and stages underlying the development of PTSD

Although estimates suggest that 90% of individuals will be exposed to a significant traumatic event in their lifetime (Kessler et al., 2005), the rates of PTSD are relatively low at 5-20% (Breslau, 2001), depending on the cohort and trauma exposure levels. Thus a critical question in the study of PTSD is why some trauma victims go on to develop PTSD, while others experiencing the same event do not; and they appear instead to be resilient to the effects of the trauma. A number of factors contribute to the variability in an individual's risk of developing PTSD (Yehuda and LeDoux, 2007) (Figure 1.1). Pre-existing genetic sensitivities or early life experiences such as child abuse represent factors that contribute to risk for PTSD following exposure to trauma in adulthood. Twin studies indicate that risk for PTSD following trauma is in part genetically mediated (Milad et al., 2008). Additionally, many studies have now demonstrated a strong interaction between genetics and early life environment in predicting adult PTSD (Mehta and Binder, 2012). Certain gene pathways (such as FKBP5) interact with early life trauma (but not adult trauma) to predict adult PTSD (Binder, 2009; Binder et al., 2008; Klengel et al., 2012). For example, FKBP5 regulates key aspects of the HPA axis and may play a role in stress and glucocorticoid-dependent critical periods of amygdala and hippocampal development (Binder et al., 2008; Moriceau et al., 2006). Specifically, certain gene variants of FKBP5 when combined with exposure to early life stress may result in amygdala sensitization, thus affecting adult responses to trauma (Binder et al., 2004, 2008; Klengel et al., 2012; Mehta and Binder, 2012). How genetic background and early environmental factors such as childhood

trauma interact and impact adult vulnerability and resilience following trauma exposure is a critical area of ongoing research (Banerjee, Morrison, and Ressler, 2016).

The subjective severity of a traumatic experience can also contribute significantly to learning the fear memory. For example, a physical attack could be extremely traumatic for one individual and less so for another. In addition, the minutes, hours, and days directly following the traumatic event define the consolidation period of the trauma memory, representing the time frame in which the memory transitions from a labile state to a chronic stable state. Much current translational research is focused on therapeutic interventions that may be administered during the consolidation window to decrease the emotional memory that leads in the long term to the development of PTSD. Reconsolidation is also being increasingly explored as a process in which a fear memory may be reactivated and made to re-enter a labile state for therapeutic interventions (Agren et al., 2012; Alberini et al., 2006) (however, the extent to which reconsolidation occurs in humans remains somewhat unclear).

Following the formation of the fear memory, individuals may retrieve and express their fear through intrusive memories, nightmares, flashbacks and startle responses. In addition to individual variations in genetic makeup and consolidation effects, the ability of an individual to recover from the trauma is important. Individuals who go on to develop PTSD may generalize and sensitize these fears, whereas those who are able to recover will learn to discriminate and will extinguish the fear memory over time (Figure 1.1). Generalization occurs when the fear responses occur to a broader range of cues that become stimulated in parallel with the initial trauma cue, leading to a more general fear-response (symptom triggering) pattern across cues and contexts. Sensitization occurs

when fear symptoms in response to the trauma cue become worse over time. On the other hand, discrimination refers to the ability to differentiate between trauma cues and non-trauma cues, and extinction refers to the diminished fear response to cues over time or with repeated presentations of the trauma cue.

An understanding of the factors that account for resilience in certain individuals would contribute significantly to the development of targeted treatments as well as the prevention of PTSD in individuals with a predisposition to developing PTSD. In addition, the identification of vulnerable individuals could lead to specialized interventions that would prevent the development of disorders such as PTSD by enhancing resiliency. Furthermore, an understanding of the time course of the pathogenesis of PTSD may allow for therapeutic interventions at multiple time points across the progression and development of the fear disorder. As mentioned above, both pharmacological and behavioral interventions during consolidation are currently being explored. For example, recent studies have investigated the effects of exposure-based psychotherapy given in the hours directly following a trauma exposure and have found protective effects of treatment when PTSD symptoms were assessed 4 and 12 weeks following the intervention (Rothbaum et al., 2012). Unfortunately, therapeutic interventions may not always be possible during the consolidation window in the hours directly following the traumatic incident. Thus, recent efforts in the field have focused on therapies that may enhance the extinction of the fear memory. Additionally, PTSD is characterized by a hypersensitivity to environmental cues, which may be the result of enhanced primary sensory system representation of the trauma cue; this integration and reconceptualization of PTSD to

include primary sensory system regulation will be explored throughout the present dissertation (Figure 1.1).

How we model fear responses in animals: classical Pavlovian fear conditioning

Classic Pavlovian fear conditioning paradigms have been used to dissect the neural mechanisms involved in the acquisition and extinction of learned fear responses. In this paradigm (Figure 1.2), a conditioned stimulus (CS; for example, a light, tone, or odor that is initially inoffensive) is paired with an aversive unconditioned stimulus (US; such as a mild foot shock), such that after several CS-US pairings the subject exhibits a conditioned fear response (CR) to presentations of the conditioned stimulus (CS; odor, tone, light, etc.).

Within Pavlovian fear conditioning paradigms, "fear" is defined operationally as freezing (the complete lack of all bodily movements except those involved in respiration), fear potentiated startle responses (increases in acoustically elicited startle responses), increases in blood pressure, changes in respiration in the presence of the conditioned stimulus (CS; odor, tone, light, etc.) or avoidance of the fear conditioning context. Rodent model systems commonly measure fear responses with freezing behavior and potentiated startle, which are easily quantified objectively and in an automated fashion by computer programs. The fear potentiated startle assesses the increase (potentiation) in the acoustic startle reflex when the organism is presented with the conditioned stimulus (CS; odor, tone, light, etc.) that was previously paired with an aversive unconditioned stimulus (US; shock). The acoustic startle reflex is a three-synapse circuit between the ear and spinal cord that activates a reflexive skeletal musculature contraction response and is directly modulated by the amygdala (McDonald and Jackson, 1987; LeDoux et al., 1990; Turner

and Kerkenham, 1991; Yasui et al., 1991; Mascagni et al., 1993; Romanski and LeDoux, 1993; Shi and Cassell, 1997). In humans, acoustic startle response and skin conductance responses are physiological responses that are commonly used as behavioral measures of fear (Fani et al., 2014; Jovanovic et al., 2005; Myers and Davis, 2004).

To study extinction of the learned fear, the previously fear conditioned organism is exposed to the conditioned stimulus (CS; tone, light, odor, etc.) in the absence of the aversive unconditioned stimulus (US; shock). Repeated or prolonged exposures to the fear-eliciting CS results in a gradual decline in the conditioned fear response (CR); this procedure is referred to as fear extinction (Myers and Davis, 2007). Notably, the diminished conditioned fear responses (CRs) following extinction training are often not permanent and are subject to reinstatement, renewal and spontaneous recovery. Renewal consists of the re-emergence of the extinguished conditioned fear response when animals are exposed to the CS in a novel context (separate from the one in which extinction training occurred). Spontaneous recovery refers to the reappearance of the extinguished CRs after enough time has passed following extinction training. Reinstatement occurs when the extinguished fear response is triggered and reappears upon exposure to the unconditioned stimulus (US) (after the organism has undergone extinction training).

Extinction learning leading to active inhibition of the fear response forms the basis of most exposure based psychotherapies in the treatment of human fear disorders. Extinction training in rodent fear conditioning paradigms parallels many aspects of exposure-based psychotherapy treatments used in human subjects and thus has high face validity. These parallels have fueled translational research, allowing therapeutic interventions for fear related disorders to progress very rapidly from the research lab to

the clinic. The effects of cue specific olfactory extinction will be investigated in greater detail in chapter 2.

The fear response is a hardwired process involving the amygdala

There are several brain regions involved in fear processing and fear related disorders. The key brain regions belong to the limbic system (which regulates emotional processing across species) and include the hippocampus, amygdala and prefrontal cortex (other regions such as the parahippocampal gyrus, orbitofrontal cortex, sensorimotor cortex, the thalamus and the anterior cingulate cortex are also involved) (Mahan and Ressler, 2012; Myers and Davis, 2007). Amygdala activation is a hallmark of all fear related disorders (Figure 1.3) (Davis, 1992). Functional brain imaging studies demonstrate increased amygdala activation during the presentation of fearful faces, fearful cues, as well as during fear acquisition and expression (Etkin and Wager, 2012). Individuals diagnosed with PTSD or other fear related disorders exhibit hyperactive amygdala activity compared to normal subjects. The amygdala is composed of many subnuclei including the basolateral complex (BLA; lateral, basal and accessory basal nuclei) and the central (CeA) nuclei. The BLA is critical in the acquisition, expression and extinction of fear (Fanselow and Ledoux, 1999). In the context of rodent classical fear conditioning, multimodal sensory information from thalamic and sensory cortical areas (auditory, visual, somatosensory cortex, etc.), specific to the conditioned stimulus (CS) project to the lateral nucleus of the amygdala (LA) (Campeau and Davis, 1995; Ledoux et al., 1990). In parallel, information specific to the unconditioned stimulus (US) is relayed to the LA from somatosensory thalamic and cortical areas and the periaqueductal gray (Lanuza et al., 2004; Shi and Davis, 1999). The LA is thus thought of

as a site critical for synaptic plasticity and Hebbian learning that occurs during paired presentations of the CS and US during fear learning (Blair et al., 2001; Maren, 2005; McKernan and Shinnick-Gallagher, 1997; Pape and Pare, 2010; Sah et al., 2008; Sigurdsson et al., 2007; Tsvetkov et al., 2002). Broadly, the amygdala receives sensory input from the environment and serves as a "hub" to sample motifs of traumatic experiences. The integration of olfactory sensory inputs will be discussed in greater detail below.

The CeA has primarily been regarded as the fear output structure that sends projections to brain regions, which activate a host of downstream behavioral fear responses/symptoms (Ciocchi et al., 2010; Haubensak et al., 2010; LeDoux et al., 1988; Wilensky et al., 2006). For example, the CeA projects to: the lateral hypothalamus (initiates increase heart rate and blood pressure), the dorsal vagal nucleus (bradycardia and ulcers), the parabrachial nucleus (panting and respiratory distress), the basal forebrain (arousal, vigilance, attention), the reticular pontis caudalis (increased startle response), the central gray area (freezing and social interactions) and the paraventricular nucleus (corticosteroid release) (Davis, 1992). It is important to note that the amygdala is equally involved in appetitive learning processes that are not discussed in this review. Long-term potentiation (LTP) and synaptic plasticity at any point along this circuit contributes to alterations in pathways that underlie the fear response (Blair et al., 2001; Maren, 2005; McKernan and Shinnick-Gallagher, 1997; Pape and Pare, 2010; Sah et al., 2008; Sigurdsson et al., 2007; Tsvetkov et al., 2002). From a translational perspective, the hardwired fear reflex outputs following amygdala activation provide a specific set of neural circuits to understand the mechanisms underlying fear related disorders.

The amygdala is in turn modulated by several brain regions including the prefrontal cortex (PFC) and the hippocampus. In the context of classical fear conditioning models, the PFC has primarily been thought to provide inhibitory modulation to the amygdala. However, the complexity of the PFC is only recently starting to be understood (Blair et al., 2001; Maren, 2005; McKernan and Shinnick-Gallagher, 1997; Sah et al., 2008; Sigurdsson et al., 2007; Tsvetkov et al., 2002). Inactivation of the infralimbic cortex (IL) using small doses of the GABAa agonist muscimol, had no effect on fear expression, but impaired the within-session acquisition of extinction as well as extinction expression (Sierra-Mercado et al., 2011). In contract, inactivation of the prelimbic cortex (PL) using muscimol, impaired fear expression, but did not effect extinction acquisition or memory (Sierra-Mercado et al., 2011). Thus, the IL (ventromedial prefrontal cortex in humans) is required for fear extinction but not fear acquisition, while the PL (thought to be similar to the dorsal anterior cingulate cortex in humans) is required for fear acquisition but not extinction (Sierra-Mercado et al., 2011). In healthy human subjects, the acquisition and retrieval of extinction has been associated with increased activity in the ventromedial prefrontal cortex (vmPFC; homologous to rodent IL) and the hippocampus (Milad et al., 2007; Phelps et al., 2004). In contrast, individuals with PTSD show deactivation in the vmPFC and hippocampus, coupled with hyperactivation of the dorsal anterior cingulate (dACC; homologous to the rodent PL) (Milad et al., 2007). Furthermore, prior work has shown increased BOLD activity in the vmPFC and amygdala during extinction training in health human subjects, compared with depressed BOLD activity in these regions in subjects with PTSD (Milad et al., 2007) (Milad et al., 2009; Bremner et al., 2005).

Our understanding of the role of the hippocampus in spatial regulation and declarative learning and memory is vast. In the context of fear learning and memory, the hippocampus is crucial for the regulation and discrimination of contextual fear learning and extinction, and like the PFC, it also heavily modulates amygdala activity (Heldt et al., 2007; Knight et al., 2004). The current knowledge of the neural circuitry underlying the fear response is growing rapidly and its breadth lies beyond the scope of this review (Orsini and Maren, 2012). For the remainder of this review we will specifically discuss the role of the olfactory system as an important mediator of emotional learning and memory.

Odors can be potent and long lasting emotional and trauma memory cues

The olfactory system, remarkably well conserved across species from rodents to humans, is exquisitely tuned to detect and process olfactory sensory information in an organisms surrounding environment. Often dismissed within the hierarchy of sensory systems importance for humans, the olfactory system is nevertheless incredibly sensitive to salient olfactory cues, which often serve as potent and long lasting triggers of emotional memories. For example, when a particular odorant is paired with a traumatic event, the subsequent exposure to that odor may act as a strong and immediate trigger for PTSD symptoms. On the flip side, odorants paired with pleasant events and experiences can, upon subsequent presentation, elicit feelings of nostalgia, happiness, or fondness for old times. Olfactory memories across most individuals are likely not scant, and anecdotal evidence of such olfactory triggering of emotional memories is likely widespread. An excellent question is how these memories are processed, formed, and re-experienced within the brain and peripheral olfactory regions.

While the immediate processing and sensory transduction of olfactory stimuli has been well studied, with the organizational layout of the olfactory system becoming very well understood over the last tens of years, the plasticity occurring within the olfactory system in response to behavioral experiences and learning remains less well understood. A recent surge of work has begun to investigate the mechanisms by which the brain encodes the representation of environmentally relevant odors, both at the level of its primary sensory system (e.g. the first order neurons in the nose and their projections to the olfactory bulb) and also within the central nervous system (e.g. regions of the olfactory cortex and areas such as the amygdala). Furthermore, convergent findings from humans and rodent models point toward the importance of the primary olfactory system in the processes underlying emotional memory formation and storage in adult, developmental, and transgenerational contexts.

We will now highlight some of the increasing number of recent publications addressing learning and experience induced plasticity in the rodent primary olfactory system, and we will also discuss the growing body of research on the processing of olfactory cues in humans. Recent evidence supports the idea that primary sensory systems, such as the olfactory sensory system, could provide a powerfully tractable and plastic target that may be manipulated in the treatment of anxiety like disorders such as PTSD. This exciting potential to manipulate the olfactory system in the treatment of such disorders is novel within the field of psychiatric treatment research, yet may provide a powerful avenue for treatment. Psychiatric disorders such as PTSD are often characterized by hypersensitivity to environmental cues, as has also been shown across animal models of PTSD. Work in mouse models has recently highlighted the plasticity of

the main olfactory epithelium (MOE) and olfactory bulb (OB) circuitry in response to learned cues and experiences in the environment from developmental critical periods through adulthood. Additionally, plasticity at the level of the primary olfactory system has been shown to occur in an *in utero* and also in a transgenerational context (Todrank et al., 2011; Dias and Ressler, 2014). Observations of plasticity within the human olfactory system (Parma et al., 2015; Li, 2014; Li et al., 2008; Krusemark et al., 2013) additionally highlight the translational relevance of investigations of the early stages of olfactory processing.

The value of the olfactory system as a model to study learning and plasticity

A number of factors make the olfactory system an excellent model to study the underpinnings of learning and memory. Among these factors are 1) the specificity of the olfactory system stimuli and pathway, 2) available molecular biological tools, 3) constant turnover in olfactory cell populations, 4) the ability to perform physiology early in the processing system, and 5) the accessibility of bottom-up and top-down convergence points.

The visual and auditory systems are commonly used for studying the plasticity of sensory cortical regions in response to environmental stimuli and learning. Both the visual and auditory systems possess complex layered processing for the identification of the qualities of sensory stimuli; for example, the visual system possesses the dorsal and ventral streams of visual information processing. In contrast, the olfactory system consists of a pathway of only a few synapses from primary sensory neurons to important processing regions such as the BLA. The olfactory pathway provides a specific and direct connection from the neurons that sense signals in the environment, projecting directly to

higher brain regions for further processing, including direct projections to emotion and memory hubs. Although there are inputs from the primary olfactory system to the medialdorsal thalamus, there are direct projections to nuclei of the amygdala that do not require a thalamic relay. The presence of such direct pathways yield a simple pathway for tracing studies (Luskin and Price, 1983).

In addition to such direct projections to higher processing regions, many of the cell populations within the olfactory system, including the granule cells, juxtaglomerular cells, and OSNs, undergo adult neurogenesis (Corotto et al., 1994; Rochefort et al., 2002) (Mackay-Sim and Kittel, 1991). Such constant cell turnover makes the olfactory system uniquely plastic throughout adult life, and also provides an excellent system to monitor effects of environmental learning on primary sensory system plasticity, which will be discussed in further detail below and in chapter 3.

The olfactory system also provides a number of tractable advantages related to the diversity of olfactory stimuli. Odorants provide a huge number of discrete cues that are sensed by a family of approximately one thousand different receptors in rats and mice (Buck and Axel, 1991; Ressler et al., 1993), as described in greater detail below; such a system is in contrast to other sensory systems in which only a few types of receptors detect signals along a continuous range. With a few exceptions, each OSN expresses only one type of odorant receptor (Goldman et al., 2005; Li et al., 2004; Mombaerts, 2004; Shykind et al., 2004). The specificity of odorant receptor expression and the molecular specificity of the olfactory pathway allows for the anatomical study of individual odor cues by labeling molecularly unique receptors; such labeling may be accomplished with transgenic mouse models, or *in situ* labeling (Bozza et al., 2002; Vassalli et al., 2002a).

Another advantage of the olfactory system is at the levels of behavioral studies; rodents have the ability to learn olfactory tasks quickly, sometimes in as little as one trial (Lovelace and Slotnick, 1995; Paschall and Davis, 2002a, 2002b). Rodents also possess the ability to discriminate between different odorants (Jones et al., 2005), thus allowing the experimenter the ability to present a variety of odor stimuli within the same behavioral protocol (Dudchenko et al., 2000).

Anatomy and circuitry of the olfactory system

Olfactory signal transduction and upstream stages of olfactory processing: From the main olfactory epithelium to the olfactory bulb

The perception of a particular odor (composed of a multitude of distinct odorant molecules) begins in the main olfactory epithelium (MOE) of the nasal cavity, with the activation of olfactory receptors (ORs) expressed by olfactory sensory neurons (OSNs) (Figure 1.4). ORs are expressed on the olfactory cilia of OSN dendrites extending out of the surface of the epithelium, and are the first stage in the triggering of olfactory transduction. ORs are transmembrane G-protein coupled receptors and activation of an OR by its cognate odor ligand triggers coupling through G alpha olf (a G alpha s isoform enriched specifically in OSNs), followed by cAMP/PKA signaling, which subsequently leads to OSN depolarization and other intracellular events such as the transcription of cAMP-regulated genes. Odor induced depolarization of OSNs within the epithelium trigger action potentials that are propagated down the OSN axon to the olfactory bulb. OSN axons projecting to the OB synapse onto the projection neurons of the OB, the mitral and tufted cells, within discrete structures called glomeruli (Figure 1.4).

The exquisite specificity of odorant detection is achieved through a distinct neuroanatomical organization of the olfactory system. First, each OSN expresses only one allele of the large family of odorant receptors, of which there are approximately 1,200 in the mouse and 700 in humans. This singularity of OR expression is referred to as the 'one receptor, one neuron' rule and is achieved by a complex mechanism that involves an activation process wherein a single OR allele is stochastically chosen, followed by a maintenance phase in which the activation of additional OR alleles is prevented (Magklara and Lomvardas, 2013; Monahan and Lomvardas, 2015), all of which relies on complex epigenetic mechanisms that will be described in greater detail below. Although a specific odorant may have a high affinity for a specific OR subtype, and likewise, a particular OR subtype may have a high affinity for a specific odorant, this system is in fact more promiscuous with a single odorant being able to bind multiple ORs, and one OR being capable of activation via multiple odorants.

The second principle guiding the distinct neuroanatomical organization of the primary olfactory system is that axons of OSNs that express the same odorant receptor converge into the same glomerulus in the olfactory bulb (Mombaerts et al., 1996; Potter et al., 2001) (Figure 1.4). OSNs expressing the same OR are distributed broadly and in specific zones along the dorsal-ventral axis of the olfactory epithelium, however, the glomeruli in the OB onto which their axons converge are in a spatially invariant manner, and in a corresponding dorsal-ventral zone pattern (Mombaerts et al., 1996; Ressler et al., 1994a, 1994b; Vassar et al., 1994). This incredible consistency in projection patterns is achieved through a number of guidance molecules and mechanisms that will not be reviewed in the present manuscript, however, the authors direct the reader to an excellent

review (Mombaerts, 2006). Overall, the two organizing principles described above lend the primary olfactory system its specific organization, represent the first step in its ability to identify which of the ~1,200 ORs (in mouse) has been activated, and provide the basic principles of the olfactory sensory map.

Downstream olfactory processing: From the olfactory bulb to higher brain regions

In the next step of the olfactory pathway, OSN axons projecting to OB glomeruli synapse with the dendrites of mitral and tufted cells, the primary projection neurons of the OB (Figure 1.4). The targeting of OSN axons to specific OB glomeruli is dependent upon a number of factors including cAMP signaling, as well as axon guidance molecules (for an excellent review the authors direct the reader to Mori and Sakano, 2011). The axons of mitral and tufted cells project along the lateral olfactory tract (LOT) to several regions such as the anterior olfactory nucleus, olfactory tubercle, piriform cortex, amygdala and rostral entorhinal cortex; together, these regions are referred to as the primary olfactory cortex (Figure 1.5). Regions of the primary olfactory cortex send projections to regions including the orbitofrontal cortex (OFC), agranular insula, hypothalamus, lateral and basolateral amygdala, perirhinal cortex, hippocampus, and striatum (Brain et al., 1998; Gottfried et al., 2010). The olfactory system pathway is one of only a few synapses from primary sensory neurons to regions critical for emotional processing, learning, and memory (among many other roles that will be discussed in further detail below). Thus, compared to auditory or visual systems in which auditory and visual sensory information may reach the BLA through direct thalamic-amygdala pathway and/or indirect thalami-cortico-amygdala pathways, the olfactory system has a subset of pathways that are able to bypass the thalamus.

Adult neurogenesis in the olfactory system

Another distinct feature of the olfactory system is that several populations of neurons within the olfactory system, such as the granule, juxtaglomerular, and olfactory sensory neuron cells, undergo adult neurogenesis, thus lending the system a high level of plasticity in structure through the constant turnover of cells throughout life. New neurons produced throughout the lifespan must be added to the existing circuitries outlined above, and their production and integration into such circuitries may be influenced by environmental factors such as learning. Astrocytes in the subventricular zone (SVZ) are thought to act as a neurogenic niche, providing a pool of neural stem cells capable of producing neuroblasts that migrate to the olfactory bulb along the rostral migratory stream (RMS), and thus providing the inhibitory interneurons of the olfactory bulb - the granule and periglomerular cells.

Within the olfactory epithelium, new olfactory sensory neurons are renewed from a source of basal cells in the epithelium, which give rise to new neurons with a half-life ranging from 30-120 days (Caggiano et al., 1994; Graziadei, 1973; Graziadei and Graziadei, 1979; Kitte, 1990; Mackay-Sim and Kittel, 1991; Graziadei and Graziadei, 1989). Based on environmental influence, the continuously produced population of OB adult neurons and their continuously integrated synaptic connections, and newly born MOE OSNs, could potentially provide the organism with an efficient means to adapt to new and changing olfactory environments (Lledo et al., 2006); further evidence to suggest such an influence will be discussed throughout the present review as well as in Chapter 3.

Associative plasticity in the rodent olfactory system

Olfactory plasticity across development

Recent work has investigated the effect of early developmental postnatal odorant stimulation on behavior as well as OSN wiring and glomerular refinement (Kerr and Belluscio, 2006). Work from Kerr and Belluscio used a conditioned odorant aversion protocol through the daily application of octanal (a component of citrus oil, thought to produce an aversive response) to the nipples of a lactating mother. Pups in the octanal conditioned group spent significantly less time in an octanal scented zone compared to controls on a preference task, indicating aversion learning behavior. Accompanying the observed behavioral aversion, by P13, octanal conditioned pups showed accelerated glomerular maturation resulting in the early elimination of supernumerary glomeruli, which are slowly eliminated across early development. The accelerated glomerular refinement was not the result of either changes in the number of OSNs, nor rates of OSN turnover, suggesting that the enhanced glomerular refinement may be regulated within the OB rather than through the proliferation or elimination of MOE OSNs.

Such work closely parallels findings showing that naris occlusion in early development prevents the elimination of ectopic axonal projection sites in the OB, which gradually disappear during postnatal development, further suggesting that odorant stimulation and experience is involved in glomerular refinement and development (Nakatani et al., 2003). Furthermore, glomerular maturation appears to proceed along different time courses depending on the given OR population, and also requires sensory input during distinct sensitive periods.

Further work has investigated the neural circuitries underlying attachment learning in rodent pups. During early development, sensory stimuli play a crucial role in driving attachment to the mother. Rodent pups are born deaf and blind, and thus rely heavily on the olfactory system for the detection and learning of the maternal odor, which promotes approach behaviors to the mother, physical contact, and nipple attachment, all of which are essential to survival (Moriceau et al., 2009; Pedersen and Blass, 1982; Rudy and Cheatle, 1977; Sullivan et al., 1986; Teicher and Blass, 1977). Maternal odor learning is supported by a unique neural circuit that promotes attachment learning; within this circuit, large amounts of norepinephrine (NE) are released from the locus coeruleus (LC) onto the olfactory bulb and induce physiological and neuroanatomical changes and neural plasticity in order to promote maternal odor learning. During early periods of development, rodent pups are so strongly primed for attachment learning that the pairing of an odor and pain (such as a mild foot shock or tail pinch) results in learned approach behaviors to the aversively conditioned odor (Camp and Rudy, 1988; Raineki et al., 2012; Wilson et al., 2004). Such paradoxical odor preference learning promotes attachment to the mother in early life, despite her level of care, and later in development, after the emergence of functional amygdala-dependent fear learning, maternal presence may still act to socially buffer the pup by suppressing shock induced CORT release. Indeed in transitional sensitive periods, studies demonstrate that manipulation of pup CORT levels can act as a switch to drive amygdala plasticity and fear learning behavior (Moriceau and Sullivan, 2006; Moriceau et al., 2006; Raineki et al., 2010, 2012). Further discussion of the above work can be referenced in a number of excellent reviews (Callaghan et al., 2014; Landers and Sullivan, 2012; Sullivan and Wilson, 2003).

Olfactory plasticity in adulthood

Research from our laboratory has demonstrated dynamic structural plasticity in the primary olfactory system following olfactory learning and memory events (Jones et al., 2008a). Using the M71-LacZ transgenic mouse line, in which OSNs expressing the M71 odorant receptor could be visualized by LacZ immunohistochemistry (Vassali et al., 2002), the authors performed cue specific olfactory fear conditioning with acetophenone, an odorant shown to specifically activate the M71 OR (Bozza et al., 2002). Cue-specific fear conditioning to acetophenone resulted in an increased number of M71-expressing OSNs in the olfactory epithelium; this increase was also directly correlated with an increase in the M71 glomerular cross-sectional area and volume within the olfactory bulbs. Notably, when mice received the same odor-shock pairings to another odorant that did not activate the M71 OR, there were no detectable changes in the M71 neuron population or glomeruli. At a functional level, the authors found that mice exhibited enhanced freezing and fear potentiated startle to the conditioned odor stimulus following the conditioning session. The authors also observed a similar increase in the number of M71 OSNs and glomerulus area when mice underwent cocaine odor place preference with acetophenone, thus demonstrating enhanced structural plasticity in the primary olfactory system in response to both aversive and appetitive conditioning.

Chapter 2 of the present dissertation consists of follow-up work to the above Jones et al., 2008 study, replicating the enhancement in M71 representation with fear conditioning to acetophenone, and also demonstrating that extinction training specific to the conditioned odorant cue is able to reverse the conditioning-associated increases in freezing behavior and M71-specific OSN number and glomerular area (Chapter 2;

Morrison et al., 2015). In Chapter 2, we demonstrate that behavioral and structural enhancements are long lasting with effects persisting at least 6 weeks following acquisition of fear conditioning, and at least 3 weeks after extinction.

The above behavioral and structural work has been complemented at the neurophysiological level in work demonstrating changes in the synaptic output of OSNs in mice following associative odor conditioning (Kass et al., 2013). Kass et al. use a transgenic mouse line in which the fluorescent exocytosis indicator synapto-pHluorin (a pH sensitive green fluorescent protein variant) is expressed under the olfactory marker protein (OMP) promoter (which is expressed by all mature OSNs). By combining this transgenic mouse line with *in vivo* fluorescent imaging (Bozza et al., 2004), the authors found that discriminative olfactory fear conditioning resulted in an increase in the magnitude of spH responses in response to the conditioned odorant stimulus, while no increases were observed in response to a control odorant. spH is a fluorescent exocytosis indicator, and thus spH responses indicated neurotransmitter release from OSN presynaptic terminals in the OB glomeruli. Although the authors did not observe any structural increase in the number of CS responsive neurons at a short, 3-day time point following conditioning, presumably the observed physiological changes underlie the early phases following a learning event and likely operate in parallel to more long-term structural changes such as OSN number and glomerular size as seen in Jones, et al., 2008.

Glucocorticoid signaling and the HPA axis have been shown to play a critical role in regulating rates of adult neurogenesis, with high levels of stress and glucocorticoid signaling leading to decreased rates of both olfactory bulb and hippocampal neurogenesis. In a rodent model of anxiety/depression-like states in which mice receive

chronic corticosterone (CORT) administration, Siopi et al., 2016 recently found that chronic CORT administration leads to significant deficits in olfactory acuity, fine discrimination of odorants, and olfactory memory (Siopi et al., 2016). In addition to these observed deficits, mice exhibited significant decreases in rates of adult neurogenesis in the DG of the hippocampus and the OB, while observing no effect of chronic CORT on rates of cell proliferation in the MOE. Furthermore, treatment with the antidepressant fluoxetine in animals receiving chronic CORT reversed deficits in adult neurogenesis, behavior as well as olfactory memory (but not olfactory acuity or discrimination). Fluoxetine treatment alone did not increase adult neurogenesis in the dentate gyrus or OB compared to vehicle treated mice; Fluoxetine treatment only restored levels of neurogenesis in animals that had received chronic CORT treatment. The deficit and subsequent increase in OB neurogenesis with fluoxetine treatment could potentially explain the CORT-affected olfactory deficits and improvements, as OB interneurons play a critical role in odorant detection, discrimination, and olfactory learning and memory (Alonso et al., 2012; Belnoue et al., 2011; Breton-Provencher et al., 2009; Lazarini and Lledo, 2011; Moreno et al., 2009; Mouret et al., 2009; Sakamoto et al., 2014). This work highlights the important role of the HPA axis on both olfactory and hippocampal neurogenesis as well as olfactory behavior. Additionally, these data may explain the prevalence of olfactory impairments in patients suffering from major depressive disorders, of which hypercortisolemia is often a cardinal symptom.

There are several lines of research to support an environmentally sensitive and adaptive view of OB neurogenesis. Rates of new neuron production within the SVZ have been shown to be influenced by environmental factors and unique demands such as

pheromone exposure (Mak et al., 2007) and pregnancy. Furthermore, 2 to 3 weeks following neuronal cell birth, adult born neurons undergo high rates of cell death that are negatively correlated with olfactory activity (Petreanu and Alvarez-Buylla, 2002; Rochefort et al., 2002; Saghatelyan et al., 2005; Yamaguchi and Mori, 2005). Such a model may also extend to olfactory sensory neurons in the MOE. Recently, the histone variant H2be has been identified in playing a significant role in a "use it or lose it" model of olfactory neuronal survival wherein H2be expression in OSNs is negatively regulated by neuron activity, and the level of H2be expression regulated the lifespan of the neuron with H2be gene knockout greatly extending neuronal average lifespan, and overexpression significantly shortening it (Santoro and Dulac, 2012). This significant study has many implications for our understanding of how neuron population representation in the olfactory epithelium may be shaped by environmental influences such as exposure to odorants with learning as in the above-described studies (Jones et al., 2008a). Adult born neurons within the olfactory bulb and MOE are also sensitive to afferent activity from higher brain regions (Lledo et al., 2006)(Mouret et al., 2008), which may further reflect mechanisms by which specific neurons are selected to survive, based not only on environmental factors and odorant experience, but also on experiences such as learning. Ablation of SVZ neurogenesis leads to behavioral disruptions in olfactory-cued fear conditioning along with reductions in the size of the granule cell layer (GCL) (Valley et al., 2009).

Transgenerational and *in utero* olfactory plasticity

Enhancements in primary olfactory sensory representation for a learned odorant have also been recently shown to persist in both an *in utero* context, and also

transgenerationally. Todrank et al., 2011 investigated the effect on pups exposed *in utero* to an experimental odorant by scenting the maternal diet both during gestation as well as postnatally throughout nursing (Todrank et al., 2011). Pups that were exposed to the experimental odorant in the maternal diet had significantly larger glomeruli comprising OSNs responsive to the experimental odor. These pups also showed enhanced preference for the experimental maternal diet odor. The neuroanatomical developments at the level of the primary olfactory system likely result from the environmental diet of the mother, and thus reflect the environmental milieu being inhabited by the mother. As such, the observed plasticity in the neural circuitry of the primary olfactory system may likely result in adaptive behaviors by indicating the availability of foods in the environment, as well as the safety of available foods. Such results were also observed in a similar study in rabbits that tied postnatal preferences for the odor of juniper berries with physiological responses in the MOE upon juniper berry presentation, after *in utero* exposure via a maternal diet scented with juniper berry (Semke et al., 1995). Such alterations may represent one strategy by which organisms share environmental information and cues with their offspring to aid in their future survival.

At the level of aversive learning, Dias and Ressler (2014) recently discovered that the offspring (both F1 and F2) of a parental generation (F0) fear conditioned to acetophenone also exhibited increased numbers of M71 OR expressing OSNs, M71 glomerulus area, as well as enhanced behavioral sensitivity to the M71 activating odorant (Dias and Ressler, 2013). While the mechanism underlying the observed heritability remains to be determined, the authors did observe a hypomethylation at the M71 gene locus in the sperm of F0 fear conditioned mice compared to controls, thus pointing to a

potential epigenetic mechanism of heritability. Further work is required to determine if the reversal in behavior and structural responses seen in Chapter 2 (Morrison et al., 2015) may also be transmitted to subsequent generations, as was observed following fear conditioning alone in the parental generation.

Overview of Dissertation Goals:

The perception of an odorant in the environment and the subsequent triggering of an emotional memory is a common experience. Olfactory cues may also be paired with traumatic experiences in humans (for example, the smell of a physical abuser), and following such traumatic experiences, exposure to the environmental odor cue may serve as a reminder of the traumatic event and may trigger anxiety, phobia, and PTSD symptoms. As was discussed above, estimates from epidemiological studies indicate that PTSD occurs in up to 10% of the general population (Kessler et al., 2005) and populations that are exposed to chronic physical and emotional trauma experience even higher lifetime rates of PTSD of up to 20-30% (Breslau, 2001; Breslau et al., 1990). Underlying the main symptom clusters present in PTSD is a dysregulated fear response. While fear learning is an adaptive and evolutionarily advantageous response to traumatic events, dysregulated processes of fear regulation, such as the sensitization and over-generalization to sensory stimuli associated with a traumatic experience, can be extremely harmful to the individual.

Although the central nervous system is known to regulate the core components of the dysregulated fear responses underlying PTSD, an understanding of how peripheral sensory systems process environmental stimuli associated with the trauma event would also contribute to the development of therapeutic treatments. Furthermore, understanding the mechanisms by which sensory stimuli become associated with a traumatic experience requires understanding how the primary sensory epithelia perceive the sensory stimulus and, in turn, transmit such perception to the brain. A significant amount is known regarding the molecular mechanisms underlying the processing of emotional stimuli in

the central nervous system; however, very few studies have investigated the mechanisms accompanying emotional learning at the level of specific sensory modalities. The olfactory system provides a molecularly tractable system to understand the structural mechanisms underlying fear-dependent neural processes at the level of a sensory system.

The significance of the present dissertation is its goal to understand how environmental stimuli, which mediate emotional learning, recruit specific cellular and molecular signaling cascades in the individual primary sensory neurons that detect these environmental stimuli. Experiments contained within this dissertation work towards the following goals:

- Chapter 2: Identifies the effects of cue-specific olfactory fear extinction in adult mice at the level of behavior, neuroanatomy and the epigenome.
- Chapter 3: Explores the role of cell turnover and survival in the structural plasticity accompanying olfactory fear conditioning.
- Chapter 4: Investigates the activity-dependent signaling of BDNF at its receptor Tropomysin receptor kinase B (TrkB) and its role in olfactory fear learning regulation.
- Chapter 5: Collates experimental evidence in chapters 2 through 4 into an expanded model of odor fear learning and identifies translational implications of the present body of work.

Table 1: Other systems regulating consolidation and extinction of fear learning that are not discussed in this review.

System	Function	Summary of supporting evidence	Ref.
GABA	Consolidation	Auditory fear learning enhanced with genetic deletion of alpha-1 subunit of GABA-A receptor	(Wiltgen et al., 2009)
		Deficits in conditioned fear with GABAergic inactivation of amygdala, hippocampus, PFC or striatum	(Sierra-Mercado et al., 2011; Raybuck et al., 2011; Corbit and Janak, 2010)
	Extinction	Impaired by inverse agonist of GABA-A receptor (FG-7142)	(Delamater et al., 2009)
		Impaired by GABAergic inactivation of infralimbic cortex, BLA or ventral hippocampus	(Sierra-Mercado et al., 2011; Raybuck et al., 2011; Corbit and Janak, 2010)
		Enhanced by systemic administration of GABA antagonist picrotoxin	(McGaugh et al, 1990)
		Enhanced extinction of contextual freezing by intra-BLA infusion of GABA receptor antagonist bicuculline	(Berlau and McGaugh, 2006)
Dopamine (DA)	Consolidation	Enhanced by dopamine D2 receptor agonists in the VTA	(Borowski and Kokkinidis, 1996)
		Disrupted by dopamine receptor antagonists or lesions of midbrain dopamine systems	(Greba et al., 2001; Guarraci et al., 1999; Greba and Kokkinidis, 2000)
		FPS impaired by D2 receptor antagonists in the BLA	(de Oliveira et al., 2011)
	Extinction	Impaired by loss of D1 receptor (genetic KO or siRNA in hippocampus)	(Ortiz et al., 2010)
		Impaired with systemic or intra-IL PFC infusion of D2 antagonist	(Mueller et al., 2010)
		Impaired with systemic D2 receptor agonist quinpirole	(Nader and LeDoux, 1999)
		Facilitated with systemic administration of D2 receptor antagonist	(Ponnusamy et al., 2005)
Endocannabinoid	Consolidation	Enhanced with administration of CB1 inverse agonist in the CEA or BLA	(Lisboa et al., 2010)
		Impaired by CB1 receptor agonist or anandamide transport inhibition in vmPFC	(Lisboa et al., 2010)
	Extinction	Disrupted by genetic deletion or blockade of CB1 receptors	(Chhatwal et al., 2009)
Acetylcholine (Ach)	Consolidation	Impaired by alpha-7 nAch receptor antagonists	(Chess et al., 2009)

		Enhanced with nicotinic Ach agonists in the hippocampus	(Andre et al., 2011; Kenney et al., 2010; Davis and Gould, 2007)
	Extinction	Impaired by systemic administration of scopolamine, muscarinic acetylcholine receptor antagonist	(Prado-Alcalá et al., 1994)
Norepinephrine (NE)	Consolidation	Enhanced with alpha-1 adrenergic receptor blockade/antagonists (LA)	(Lazzaro et al., 2010)
		Impaired by siRNA for beta-1 adrenergic receptors (BLA)	(Fu et al., 2007)
	Extinction	Enhanced by systemic administration of yohimbine, alpha-2 autoreceptor antagonist	(Cain et al., 2004)
		Within session extinction facilitated by administration of propranolol (beta-adrenoreceptor antagonist)	(Brelau and McGaugh, 2006)
Opioids	Consolidation	Facilitated acquisition of conditioned fear with administration of opiate antagonists (e.g. naloxone)	(Fanselow, 1984; Fanselow and Bolles, 1979)
		Immediate morphine treatment following trauma may prevent PTSD development	(Holbrook et al., 2010; Saxe et al., 2001; Good and Westbrook, 1995)
		Impaired fear learning with administration of k-opioid antagonists	(Van't Veer et al., 2012)
		The NOP-R agonist SR-8993 impairs cued-fear memory consolidation in mice	(Andero et al., 2013)
	Extinction	Impaired by systemic administration of naloxone, opiate antagonist (before extinction training)	(McNally and Westbrook, 2003)
		Impaired by infusion of naloxone into the ventrolateral PAG	(McNally et al., 2004)
		Enhanced by u-opioid pathway activation	(McNally and Westbrook, 2003)

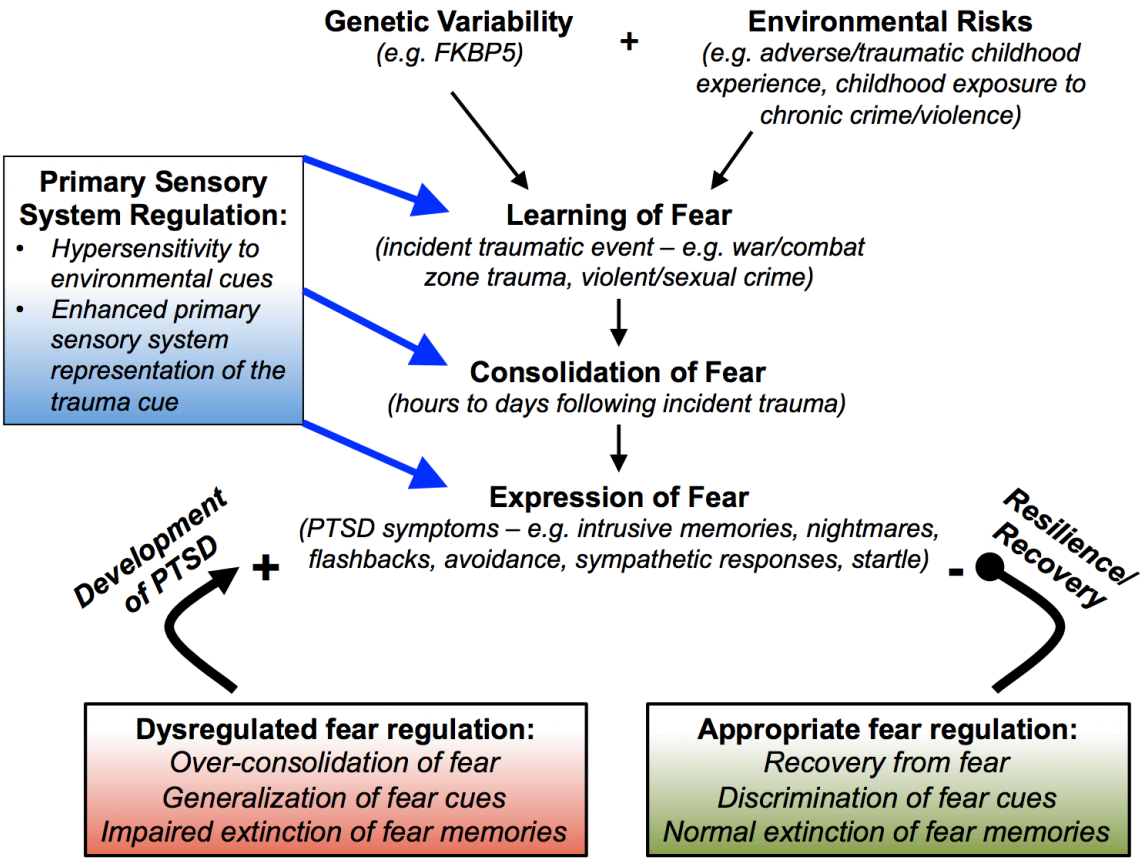

Figure 1.1: Factors contributing to the development and pathology of posttraumatic stress disorder. Variability in individual risk of developing PTSD may be attributed to a number of factors. Pre-existing sensitivities such as genetic variability may interact with early life trauma to predict adult PTSD. Upon experience of the incident trauma in adulthood, the individual will undergo consolidation of the fear memory, which occurs in the minutes, hours and days following the traumatic event. After the formation of the fear memory, individuals will express their fear in the form of PTSD symptoms that can include intrusive thoughts or memories related to the trauma, nightmares, flashbacks, avoidance of trauma cues that might trigger memories of the trauma event, or sympathetic responses. Individuals that go on to develop PTSD exhibit dysregulated fear regulation in the form of over-consolidation of fear, generalization of fear cues and impaired extinction of fear memories. On the other hand, resilient individuals who recover from the trauma will display appropriate fear regulation consisting of recovery from the fear, discrimination of fear cues and normal extinction of fear memories. Current therapeutic research approaches for PTSD seek to enhance the extinction learning that forms of the basis of common cognitive behavioral therapies such as exposure therapy, thus enhancing the resilience and recovery of individuals susceptible to PTSD. Overall, we propose a re-conceptualization of PTSD to include a greater consideration of primary sensory system effects and regulation.

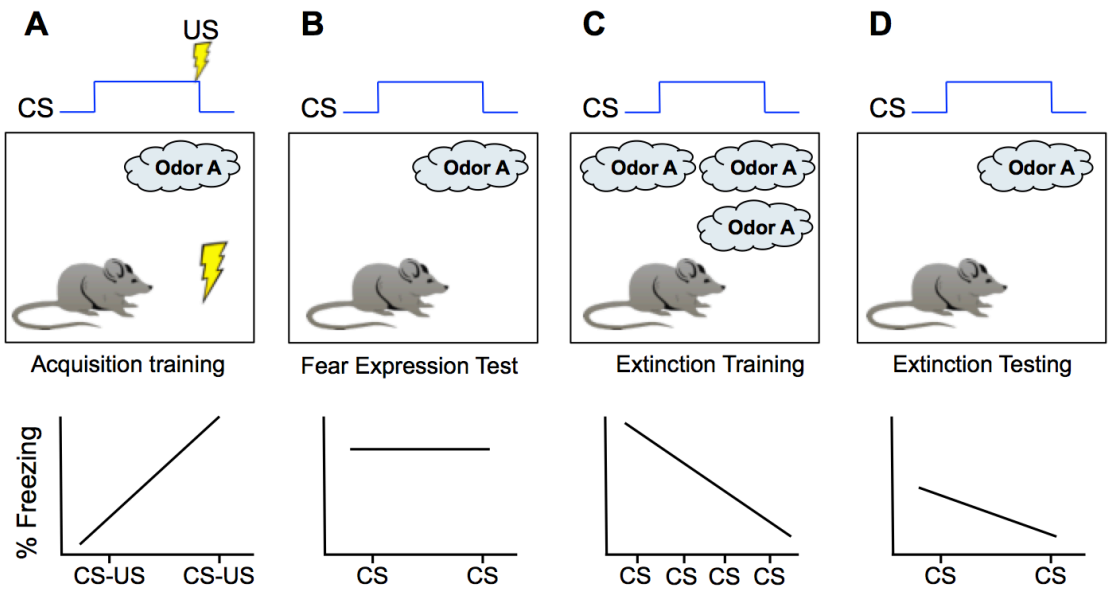

Figure 1.2: Basic procedure for fear conditioning in rodent models. Classic Pavlovian fear conditioning is used to study the acquisition and extinction of learned fear responses in rodent animal models. A) During acquisition training the conditioned stimulus (CS; tone) is paired with an aversive unconditioned stimulus (US; mild foot shock). After several CS-US pairings the organism will learn the CS-US association and will exhibit a conditioned fear response (CR) to the CS (tone), as evidenced by increased levels of freezing over the course of several CS-US pairings as well as B) after training during the presentation of the CS alone. C) During extinction training the previously fear conditioned organism is exposed the CS (tone) in the absence of the aversive US (shock). The repeated or prolonged exposure to the CS (tone) will result in a gradual decline in the conditioned fear response (CR) as evidenced by decreasing levels of freezing both during extinction training as well as D) after extinction training upon presentation of the CS

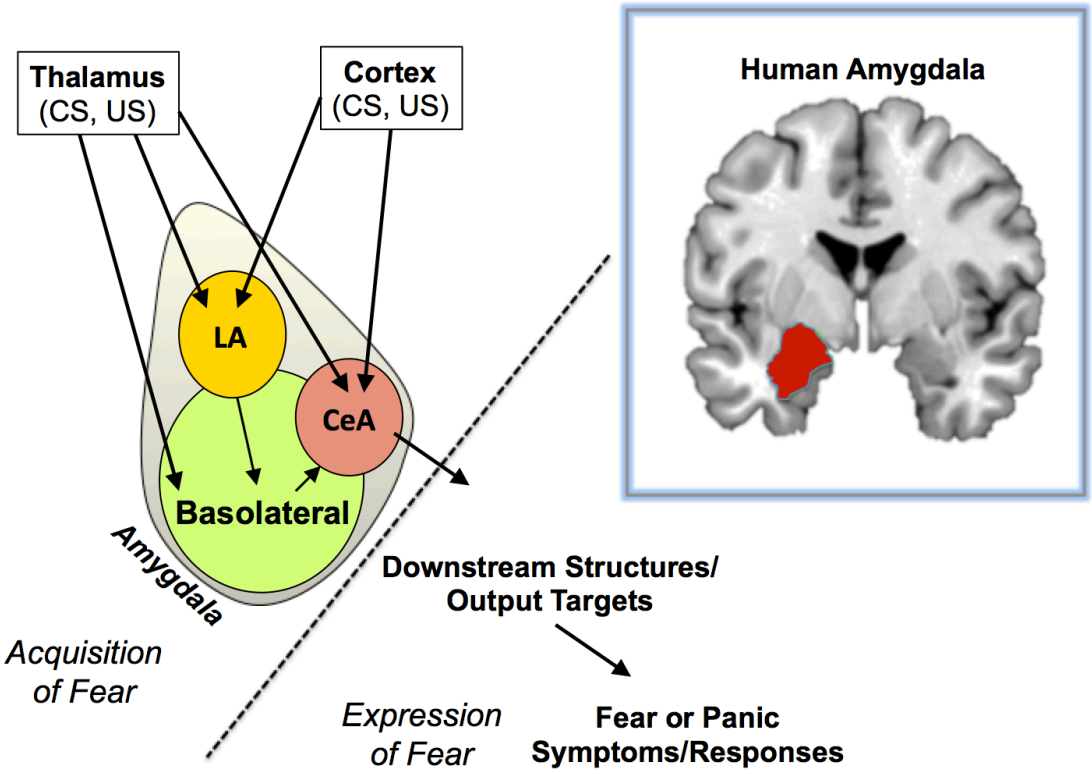

Figure 1.3: Simplified diagram of amygdala nuclei and circuits underlying the acquisition and expression of fear. The amygdala is a key region involved in fear learning. The human amygdala is shown in the upper right box. Multimodal sensory information is first processed in thalamic and sensory cortical areas before converging on the amygdala. The lateral amygdala is critical for synaptic plasticity involved in fear acquisition. The central nucleus (CeA) has traditionally been viewed as the "fear output structure" that sends projections to brain regions which activate downstream behavioral fear responses. Recent data supports a role for the lateral division of the central amygdala (CEl) in the acquisition of fear; we direct the reader to a number of excellent reviews on the detailed microcircuitry underlying amygdala-dependent learning.

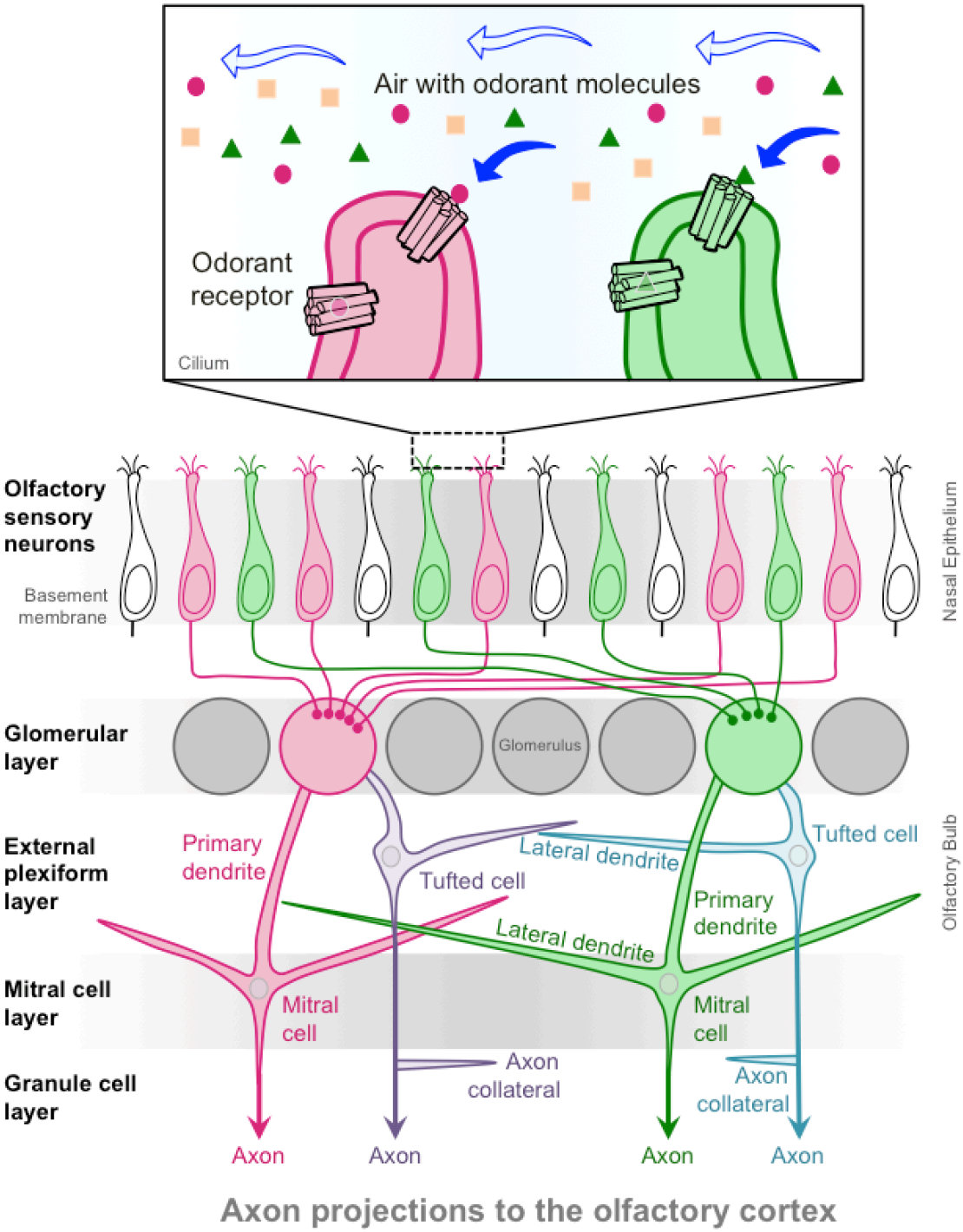

Figure 1.4: Neuroanatomy of odor processing in main olfactory epithelium and olfactory bulb. Odorants in the air make contact with olfactory receptors on the cilia of olfactory sensory neurons in the nasal epithelium. OSNs that express the same OR converge into the same glomerulus in the olfactory bulb. OSNs synapse with second-order neurons known as mitral and tufted cells, which are the two types of projection neurons from the OB to olfactory cortical regions (figure modified from Mori and Sakano, 2011).

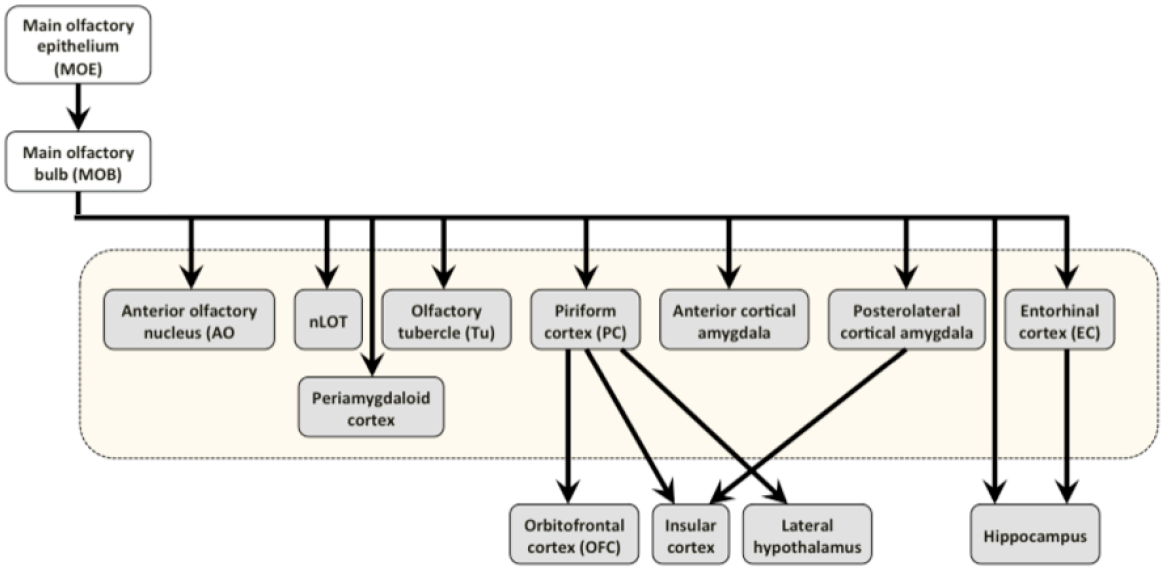

Figure 1.5: Anatomy and projection patters of the rodent and human olfactory system. (Top) Schematic diagrams showing a ventral view of axon projections of mitral and tufted cells to regions of the olfactory cortex in the mouse brain (left). (Bottom) Regions of olfactory cortex are also shown on the human brain (right) (Figure modified from Mori and Sakano, 2011).

CHAPTER 2: EXTINCTION REVERSES OLFACTORY FEAR CONDITIONED INCREASES IN NEURON NUMBER AND GLOMERULAR SIZE

Context, Author's Contribution, and Acknowledgement of Reproduction

The following chapter presents evidence of behavioral, neuroanatomical and epigenetic effects of cue-specific olfactory fear extinction. The context of the study was an effort to better understand the effects of extinction on conditioning associated plasticity at the level of the primary olfactory system. The dissertation author contributed to the paper by designing and running experiments, analyzing the data, and was a main contributor to the writing of the paper. The chapter is reproduced with minor edits from Morrison, F.G., Dias, B.G., and Ressler K.J. Learning-dependent functional and structural responses to a conditioned odor stimulus are reversed with olfactory extinction training. *Proceedings of the National Academy of Sciences* (2015)

Abstract

While much work has investigated the contribution of brain regions such as the amygdala, hippocampus and prefrontal cortex to the processing of fear learning and memory, fewer studies have examined the role of sensory systems, in particular the olfactory system, in the detection and perception of cues involved in learning and memory. The primary sensory receptive field maps of the olfactory system are exquisitely organized and respond dynamically to cues in the environment, remaining plastic from development through adulthood. We have previously demonstrated that olfactory fear conditioning leads to increased odorant-specific receptor representation in the main olfactory epithelium and in glomeruli within the olfactory bulb. We now demonstrate that olfactory extinction training specific to the conditioned odor stimulus reverses the conditioning-associated freezing behavior and odor learning-induced

structural changes in the olfactory epithelium and olfactory bulb in an odorant ligand-specific manner. These data suggest that learning-induced freezing behavior, structural alterations, and enhanced neural sensory representation can be reversed in adult mice following extinction training.

Significance Statement

Olfactory cues may be paired with traumatic experiences in humans (e.g., the smell of a physical abuser), and subsequent exposure to the environmental odor cue may serve as a reminder of the traumatic event and trigger PTSD symptoms. Very few studies have investigated the mechanisms accompanying the processing of emotional learning at the level of specific sensory modalities. The present study demonstrates that extinction specific to the conditioned odor acetophenone (which activates the M71 receptor) reverses conditioning-associated increases in freezing behavior and M71-specific OSN number and glomerular area in adult mice These data highlight the potential to exploit sensory system plasticity as a means of ameliorating negative emotional memories that may be tied to peripheral sensory systems.

Introduction

Increasing evidence suggests that the cellular, neuroanatomical and receptive field organizations of vertebrate sensory systems are continually reshaped throughout adulthood by cues from the external environment. Activity-dependent changes are known to occur both during critical periods of development and also in the adult brain, allowing the animal to optimally perform behaviors based on the demands of the surrounding environment. Post-mitotic organizational changes, along with activity-dependent plasticity, have been largely implicated in shaping sensory circuits from development

through adulthood (King et al., 2013; Lodovichi and Belluscio, 2012; Rincón-Cortés and Sullivan, 2014; Todrank et al., 2011). In particular, the olfactory sensory system of adult mice exhibits functional and neuroanatomical learning-dependent changes following olfactory fear conditioning in adulthood (Dias and Ressler, 2013; Jones et al., 2008a; Kass et al., 2014). The M71-LacZ transgenic mouse line expresses LacZ under the M71 odorant receptor (OR) promoter (encoded by the Olfr151 gene) (Vassalli et al., 2002b) in the M71 OR-expressing, acetophenone responsive population of olfactory sensory neurons (OSNs). Using this line we previously demonstrated an increased number of M71-expressing OSNs in the main olfactory epithelium (MOE) of adult mice following olfactory fear conditioning to acetophenone (Dias and Ressler, 2013; Jones et al., 2008a), an odorant that activates the M71/M72 odorant receptors (Bozza et al., 2002; Feinstein et al., 2004). This increase in receptor-specific OSNs within the MOE was directly correlated with an increase in the area of M71+ axons innervating the M71 glomeruli within the olfactory bulbs. Behaviorally, these olfactory fear conditioned mice also exhibited enhanced fear potentiated startle (FPS) and freezing specific to the conditioned odor stimulus. Notably such changes were never seen with equivalent odorant exposure alone, but only when the odorant was paired with an aversive or appetitive cue (Dias and Ressler, 2013; Jones et al., 2008a), suggesting the critical importance of behavioral learning facilitating these structural and functional alterations.

Reversing the behavioral and neuroanatomical effects of such emotional learning is important for our understanding of disorders such as post-traumatic stress disorder (PTSD), in which exposure based psychotherapy is widely used for treatment. Notably, extinction training in rodent fear conditioning models closely parallels many aspects of

exposure-based psychotherapy in humans where exposure to non-reinforced presentations of the previously acquired conditioned stimulus (CS) reduces acquired fear responses such as freezing to the CS (Myers and Davis, 2007; Pape and Pare, 2010). In the current study, we demonstrate that previously acquired structural changes within the primary olfactory system are reversed with olfactory fear extinction specific to the conditioned odorant cue.

Methods

Animals

Adult M71-IRES-tauLacZ transgenic mice (Vassalli et al., 2002b) were maintained in a mixed 129/Sv X C57BL/6 background (Jackson Laboratories) and were used in all behavioral and neuroanatomical experiments. All mice were 2-3 months old at the time of olfactory fear conditioning. For each training time course, behavioral groups were formed with mice from at least 4 litters, controlling for sex and age, such that each group was age-matched and had equivalent numbers of males and females. All mice were experiment and odor naïve at the start of the experiment. Mice were housed in a temperature-controlled vivarium on a 12 h light/dark cycle in standard group cages (≤4 mice/cage) and were given *ad libitum* access to food and water. All experiments were performed during the light cycle and were approved by Emory University Institutional Review Board following the National Institutes of Health Internal Animal Care and Use Committee standards.

Olfactory fear conditioning, extinction and testing

Fear training, testing and extinction were conducted using startle response systems (SR-LAB, San Diego Instruments) that had been modified to deliver discrete odor stimuli as previously described (Dias and Ressler, 2013; Jones et al., 2005, 2008).

For training time course 1 (Figures 2.1, Figure 2.2A-C, Figure 2.3A-C, Figure 2.5): Adult M71-IRES-tauLacZ transgenic mice were (Vassalli et al., 2002) first habituated to the training chambers 2 times (10 minutes per day) prior to training. Mice then received 3 training sessions (1 training session per day) over 3 consecutive days to ensure strong and stable odor-shock associations as previously described (Jones et al., 2005; Jones et al., 2008; Dias & Ressler, 2014). Each odor + shock training session consisted of 5 trials of 10 s odor conditioned stimulus co-terminating with a 0.25 s, 0.4 mA footshock, presented with an average 120 s inter-trial interval (ITI) (ranging from 90-150 s).

Three groups (n=~9-12 mice per group) received odor (acetophenone) + shock pairings while a fourth group (n=9 mice; n=5 male, n=4 female) remained in the home cage and received handling on all training days. Of the three groups that received odor + shock pairings one group was sacrificed three weeks after undergoing olfactory fear conditioning (n=11; n=6 male, n=5 female), a second group was sacrificed six weeks after undergoing olfactory fear conditioning (n=12; n=7 male, n=5 female) (received handling in lieu of extinction training), and the third group received extinction training three weeks after undergoing olfactory fear conditioning and was sacrificed three weeks following extinction training (n=12; n=7 male, n=5 female). Mice undergoing extinction received 1 extinction session per day for 3 consecutive days. Each extinction session

consisted of 30 non-reinforced presentations of the odorant conditioned stimulus (acetophenone) with a 60 s inter-trial interval (ITI). Prior to sacrifice, all mice were placed back in the testing chambers and were exposed to 5 presentations of the odorant conditioned stimulus (acetophenone) to assess freezing behavior. Freezing was measured throughout acquisition, extinction and during testing before sacrifice.

For training time course 1 with exposure to context and propanol (Figure 2.4A-2.4B, Figure 2.2D, Figure 2.6): A separate set of adult M71-IRES-tauLacZ transgenic mice (Vassalli et al., 2002) were habituated and received fear conditioning to acetophenone exactly as described above. Two groups (n=~12-17 mice per group) received odor (acetophenone) + shock pairings while a third group remained in the home cage and received handling on all training days (n=17; n=10 male, n=7 female). Of the two groups that received odor + shock pairings, one group was sacrificed six weeks after undergoing olfactory fear conditioning (n=12; n=9 male, n=3 female) (received handling in lieu of exposures), and the second group received exposure to the context/propanol three weeks after undergoing olfactory fear conditioning and was sacrificed three weeks following context/propanol exposure (n=12; n=9 male, n=3 female). Each propanol exposure session consisted of 30 non-reinforced presentations of the non M71-activating odorant propanol with a 60 s inter-trial interval (ITI).

Within this experimental session (same “home cage” and “train to aceto 6 weeks” group of animals as the above paragraph), an additional two groups of adult M71-IRES-tauLacZ transgenic mice underwent habituation and conditioning exactly as described above. One of the two groups underwent odor + shock conditioning to acetophenone

(n=12; n=9 male, n=3 female) and the second group underwent odor + shock conditioning to the non M71-activating odorant propanol (n=12; n=9 male, n=3 female).

For training time course 2 (Figure 2.4C-2.4D, Figure 2.7): Adult male M71-IRES-tauLacZ transgenic mice (Vassalli et al., 2002) were habituated to the training chambers 2 times (10 minutes per day) prior to training. Mice then received 3 training sessions (1 training session per day) over 3 consecutive days as described above. The day immediately following the last training session, mice underwent 3 consecutive days of extinction training (1 extinction session per day) as described above. All mice were sacrificed three weeks following the last extinction session. One group received odor (acetophenone) alone presentations, a second group received odor (acetophenone) + shock pairings, a third group received odor (acetophoneone) + shock pairings followed by extinction sessions, and finally a fourth group remained in the home cage and received handling on all behavioral session days (n=5-7 per group).

For analysis of structure three, seven, fourteen, and twenty-one days following the last olfactory fear conditioning session (Figure 2.3D and Figure 2.8): Adult male M71-IRES-tauLacZ transgenic mice (Vassalli et al., 2002) were habituated to the training chambers 2 times (10 minutes per day) prior to training. Mice then received 3 training sessions (1 training session per day) over 3 consecutive days as described above, or one group received handling and remained in the homecage (n=5-7 mice per group). One group of mice was sacrificed 3 days following the last day of fear conditioning, a second group was sacrificed 7 days following fear conditioning, a third group was sacrificed 14 days following fear conditioning, and finally a fourth group was sacrificed 21 days following fear conditioning.

Freezing behavior data analysis

Within session freezing during conditioning, extinction and testing was determined as described in Jones et al., 2005. Briefly, for each second of the 5-second activity window, voltage outputs for each animal were converted to the average voltage output. For each second of the 5-second activity window, averages that were above or below the mean voltage output of the empty cylinder (without a mouse present) were assigned an immobility score of 0 (mobile) or 1 (immobile). For each trial, a percent immobility score was determined by averaging the five immobility scores and multiplying by 100, to generate a score used as the index of freezing. Previous work has shown a high correlation between this described automated freezing index and observational ratings of freezing.

Beta-galactosidase staining of the MOE OSNs and OB glomeruli

Following sacrifice, MOE and olfactory bulbs of M71-LacZ mice were processed for Beta-galactosidase staining as previously described (Jones et al., 2008; Dias and Ressler, 2014). Lateral whole mount MOE and brains were rapidly dissected and placed into 4% paraformaldehyde (wt/vol) for 10 min at ~23 C, after which they were washed three times in 1X phosphate-buffered saline (PBS) for 5 min. MOE and brains were then stained using 45 mg of X-gal (1 mg/ml) dissolved in 600 µl of DMSO and 45 ml of a solution of 5 mM potassium ferricyanide, 5 mM potassium ferrocyanide, and 2 mM MgCl in 1 M PBS, incubated at 37 C for 3 hours.

Quantitation of M71-positive OSNs in the MOE

Following staining, the lateral whole mount MOE was imaged using a microscope-mounted digital camera, and beta-galactosidase-stained blue OSNs were

counted manually by experimenters blinded to the experimental groups. Please refer to SI Materials and Methods for a detailed description of M71+ OSN quantitation in the MOE. Following staining, the lateral whole mount MOE was imaged using a microscope-mounted digital camera, and beta-galactosidase-stained blue OSNs were counted manually by experimenters blinded to the experimental groups. Two experimenters both blinded to the experimental groups carried out this quantitation. MOE that were damaged during MOE extraction following sacrifice were not included in M71 OSN count analyses. Olfactory sensory neuron number was analyzed by 1-way ANOVA followed by Tukey post-hoc tests, and glomerular area to olfactory sensory neuron number was analyzed by linear regression. Grubbs' test was used to detect outliers; no samples were excluded from analysis of OSN number in the MOE. All data were covaried by sex, with no effect of sex observed.

Measurement of glomerular area in the olfactory bulb

M71 stained glomeruli were imaged using a microscope-mounted digital camera to capture high-resolution images of dorsal and medial glomeruli at 40X magnification. Pixel brightness distribution was exported in NIH ImageJ as gray levels from 0 = black to 255 = white. X-gal-labeled glomerular area was quantified as pixels, less than a set threshold gray level of 150 (optimized for axon versus background). Each glomerulus was traced using the lasso tool in ImageJ and the area was recorded using the histogram tool. Two experimenters both blinded to the experimental groups carried out this quantitation. Glomeruli that were damaged due to olfactory bulb extraction following sacrifice were not included in glomerular area analyses. Glomerular area was analyzed by 1-way ANOVA followed by Tukey post-hoc tests. Grubbs' test was used to detect

outliers; no samples were excluded from analysis for glomerular area in the olfactory bulb. All data were covaried by sex, with no effect of sex observed (p=0.78).

Native Chromatin Immunoprecipitation (N-ChIP) on the MOE

N-ChIP was conducted on MOE chromatin using previously described procedures (Magklara et al., 2011). The MOE were dissected, frozen on dry ice, and stored at -80C until N-ChIP was performed. Two MOE were used per sample, and each experimental group had four samples. MOE were mechanically homogenized using 2 glass homogenizers. Nuclei were extracted and digested with micrococcal nuclease (MNase) to yield a population of mono- to tri- nucleosomes that was used in chromatin immunoprecipitation assays. The antibodies used were specific to AcetylH3. Immunoprecipitated DNA was isolated by phenol-chloroform extraction and ethanol precipitation and used in quantitative PCR reactions on a Real-Time PCR machine.

Statistics

Freezing was analyzed by two-way ANOVA (Fig. 2.1B, 2.1D) or one-way ANOVA (Fig. 2.1E). Glomerular area was analyzed by one-way ANOVA (Fig. 2.3C, Fig. 2.4, Fig. 2.5, Fig. 2.6 C,D, Fig. 2.7 C,D) or Student's *t*-test (Fig. 2.3D, Fig. 2.6 B, Fig. 2.8). Olfactory sensory neuron number was analyzed by one-way ANOVA (Fig. 2.2, Fig. 2.7 A, Fig. 2.6 B, Fig. 2.7 B). Glomerular size to olfactory sensory neuron number correlation was analyzed by linear regression. All ANOVA main effects or interactions were followed by Tukey *post hoc* tests, unless otherwise noted.

Results

Behavioral responses following olfactory fear acquisition and extinction

To investigate the effects of cue-specific olfactory fear extinction, 2-3-month-old, odor naïve homozygous M71-LacZ transgenic adult mice were handled and left in their home cage (HC) or were conditioned to associate mild footshocks with acetophenone using a previously described fear conditioning protocol (Dias and Ressler, 2013; Jones et al., 2008a). Three weeks after the last olfactory fear conditioning session, mice were handled only or were exposed to an olfactory extinction training protocol consisting of a total of 90 non-reinforced odor alone presentations over 3 consecutive days, with 30 trials each day (Figure 2.1A, B). During the acquisition of olfactory fear conditioning, all groups acquired olfactory fear-like behaviors to the odor CS (as assessed by freezing behavior) at equivalent levels and rates (Figure 2.1B). Mice undergoing olfactory fear extinction training exhibited decreased freezing to the odor CS (acetophenone) across extinction trials and sessions (Figure 2.1C). One hour prior to sacrifice, all mice were exposed to 5 presentations of the odorant CS (acetophenone) to assess freezing behavior and long term olfactory fear retention. Mice that had been fear conditioned 3 weeks or 6 weeks before testing continued to exhibit enhanced freezing to the odor CS compared to home cage controls and to mice that underwent olfactory extinction 3 weeks after training (Figure 2.1D,E). These data demonstrate that olfactory fear conditioning leads to long lasting fear-related freezing for at least 6 weeks, and that olfactory extinction 3 weeks following training reduces the fear behavior to baseline when tested at the 6 week time point.

Cue-specific olfactory extinction 3 weeks following acquisition reverses M71-specific neuroanatomical enhancements

To investigate the neuroanatomical representation of neurons responsive to the conditioned odor, following sacrifice we used beta-galactosidase staining of the M71 OSNs in the MOE and the olfactory bulb (OB) glomeruli for all groups described above. Mice that were olfactory fear conditioned 3 weeks and 6 weeks prior (and that did not receive olfactory fear extinction) exhibited a significant increase in the number of M71+ OSNs in the MOE compared to home cage control mice and to mice that received olfactory fear extinction to acetophenone (Figure 2.2). Furthermore, mice that were fear conditioned to the non M71-activating odorant propanol do not exhibit an increase in the number of M71+ OSNs in the MOE compared to home cage controls (Figure 2.2D), thus replicating our previous work demonstrating that the enhanced olfactory sensory neuron counts are cue-specific. Axons of OSNs that express a particular OR gene project to and coalesce into dorsal and medial glomeruli in the olfactory bulb (Mombaerts, 2006; Mombaerts et al., 1996; Ressler et al., 1994a). Thus, as an additional measure we investigated the M71-specific glomerular area in the olfactory bulbs. At the level of the olfactory bulb, we found that mice fear conditioned 3 and 6 weeks prior (with no olfactory extinction) had significantly larger M71-specific glomeruli in the olfactory bulbs, compared with those of home cage control mice and mice that received olfactory fear extinction (Figure 2.3A-C, Figure 2.5). Glomerular area was positively correlated with increasing olfactory sensory neuron number (Figure 2.3B), as previously demonstrated (Jones et al., 2008a). Similarly, Bressel et al., 2015 recently showed strong linear correlation between OSN number in the MOE and total glomerular volume in the

OB (Bressel et al., 2016). Studies demonstrating strong OSN and glomerular size correlations point towards glomerular measurements as surrogate measurements for estimating OSN number counts in transgenic mouse lines in which OR genes are genetically tagged.

The presented neuronal and glomerular data following olfactory fear acquisition and extinction suggest that: 1) the effect of odor fear conditioning on olfactory sensory neuroanatomy is long lasting as demonstrated by the increased numbers of OSNs and increased glomerular area specific to neurons responsive to the conditioned odor that is maintained at both 3 and 6 weeks following olfactory fear conditioning; and 2) the effect of olfactory fear extinction on neuroanatomy is associated with decreased numbers of OSNs and decreased glomerular area relative to the trained groups, both of these effects are specific for the conditioned odor stimulus (acetophenone). Since the extinction group had undergone the same behavioral exposure as the 6 week trained group prior to extinction, we conclude that the findings represent a dynamic reversal of the increased odorant-specific neuronal populations generated through olfactory fear conditioning. To ensure the cue specificity of our observed extinction effect, an additional control group was run with a separate set of animals; 3 weeks following olfactory fear conditioning to acetophenone this group received 3 consecutive days of propanol odor presentations (a non M71-activating odorant), and was then sacrificed 3 weeks after the last exposure to propanol session (Figure 2.4A). Propanol was used as a control odorant for several reasons: 1) propanol has been shown to activate a region of the olfactory bulbs distinct from those activated by acetophenone as assessed by glomerular activity patterns (http://gara.bio.uci.edu), 2) previously published data have demonstrated that adult mice

are able to discriminate between acetophenone and propanol at the level of fear behavior, (Jones et al., 2005, 2008a) and 3) adult mice fear conditioned to propanol do not exhibit an enhanced M71-specific glomerular area compared to homecage controls (Jones et al., 2008a). Propanol is thus an ideal control odorant to test the cue specificity of our findings. Mice that were fear conditioned 6 weeks prior (with no olfactory extinction) and mice that were fear conditioned to acetophenone and received non-cue specific odor and context exposure (exposure to propanol), exhibited a significant increase in glomerular area at the level of the olfactory bulb compared to home cage control mice (Figure 2.4B, Figure 2.7). The observed increases in glomerular area were paralleled by increases in the number of M71 OSNs in the MOE compared to home cage controls. These data demonstrate that it is the cue-specific extinction (and not merely the exposure to the context or a non-CS olfactory cue) that results in a reversal of conditioning related glomerulus size in the OB and olfactory sensory neuron number in the MOE.

Cue-specific olfactory extinction immediately following acquisition blocks M71-specific neuroanatomical enhancements

We next wished to replicate the above observation, as well as to determine whether the reversal of structure depends on the 6-week time course from initial training. Thus, we performed an alternate time course of extinction training in which a separate group of odor and behavior-naive mice received extinction training in the three days immediately following the three days of acquisition and were sacrificed three weeks following the last extinction session (Figure 2.4C). Mice that were fear conditioned to acetophenone but did not undergo olfactory extinction exhibited enhanced dorsal and medial glomerular area as well as increased M71+ OSN numbers compared to all control

groups (Figure 2.4C-D, Figure 2.7). Notably exposure to acetophenone only without prior conditioning (odorant presentations alone) did not produce an increased M71+ glomerular size or M71+ OSN number compared to home cage controls, suggesting that it is the prior learned CS-US association that results in a corresponding enhanced neuroanatomical representation for the conditioned odor stimulus, rather than presentations of the odorant alone. Mice that received olfactory fear extinction immediately after conditioning had significantly decreased M71+ dorsal and medial glomerular area as well as decreased M71+ OSN numbers compared to mice receiving only fear conditioning. These data demonstrate that the timing of cue-specific olfactory extinction immediately after acquisition also leads to a reversal in prior olfactory fear learning effects (as measured by glomerular area in the olfactory bulbs and olfactory sensory neuron number in the MOE).

Olfactory fear acquisition and extinction are accompanied by a dynamic regulation of histone marks around the M71 locus

Epigenetic mechanisms such as histone acetylation and DNA methylation have been shown to play important roles in the mechanisms underlying fear acquisition and extinction across brain regions that include the hippocampus and the amygdala (Levenson et al., 2004; Lubin and Sweatt, 2008; Miller et al., 2008; Stefanko et al., 2009). We sought to examine whether the epigenetic status of the MOE after olfactory extinction might account for the reversal in representation for the M71 receptor. To investigate differences in histone-mediated epigenetic signatures around the M71 locus following olfactory fear acquisition and extinction, we performed native chromatin immunoprecipitation (N-ChIP) on the MOEs of mice from the groups described above.

We then immunoprecipitated MOE chromatin with antibodies recognizing the Acetyl H3 histone modifications that is known to permit transcription. Our lab has previously found that the increases in M71+ OSN number and glomerular area in mice fear conditioned with acetophenone are accompanied by more "activating" Acetyl H3 occupancy around the M71 gene in the MOE, potentially making it more permissive to transcription (Brian Dias, *unpublished data*). In the present set of experiments we found that cue-specific extinction reverses the increase in Acetyl H3 occupancy at the M71 locus. The observed decrease in Acetyl H3 occupancy at the M71 gene in animals that have undergone extinction is consistent with the above described decreases in M71 olfactory neuron numbers.

Discussion

These experiments demonstrate a reversal in neuroanatomical changes to OSN number and glomerular area specific for the conditioned odor stimulus following an extinction protocol that occurs either 3 weeks after or immediately following the fear learning event, demonstrating dynamic sensory epithelial plasticity with learning. Dynamic alterations in structural plasticity and neuroanatomical representation accompanying learning have been observed in other sensory systems; for example, studies in the primary auditory system have demonstrated that local tuning shifts produce a specific increase in the area of frequency representation within the tonotopic organization of primary auditory cortex (A1) (Bieszczad and Weinberger, 2010; Bieszczad et al., 2013). A learning dependent shift in primary representational area may be a common feature across primary sensory systems. Work in developmental rodent systems has also demonstrated behavioral and olfactory bulb neural responses following

and olfactory learning event during the pre-weanling period that is reversed with extinction training (Sullivan et al., 1991). However, the finding that at the level of the adult olfactory primary sensory system such changes are structurally reversible with a relatively small number of behavioral exposures is quite remarkable.

Learning-dependent alterations in olfactory plasticity were measured at 3 and 6 weeks following olfactory fear conditioning as alterations are not yet measureable at an earlier time point 3 days following the last day of olfactory fear conditioning session (Figure 2.3D, Figure 2.8). Our extended time course following olfactory fear conditioning, reveals that enhancements in M71 structure are not observed at three or seven days following conditioning, but are measurable at fourteen and twenty-one days following fear conditioning (Figure 2.8). Thus, the effect of olfactory fear extinction immediately after olfactory fear acquisition versus at 3 weeks following acquisition may differ mechanistically based on the finding that at 3 weeks following conditioning a neuroanatomical increase has been established, while it has not yet occurred in the 1-3 days following conditioning (Figure 2.3D, Figure 2.8). A more in-depth investigation into the time course following both the acquisition and extinction of olfactory fear could yield valuable insights into the mechanisms regulating our observed effects.

Further related to the observed time course of epithelial and glomerular structural changes after olfactory fear conditioning and extinction are their relation to changes in freezing behavior. As described above, structural changes have not yet emerged at 1-3 days after cue-specific olfactory fear conditioning or extinction, despite changes in freezing behavior. Furthermore, we demonstrate a decrease in freezing behavior between the 6 and 3 week group (though we do not observe a decrease or reversal of structural

changes in the olfactory bulb or MOE at the 6 week time point following olfactory fear conditioning to acetophenone). Thus while it does not appear that the passage of time reverses our observed olfactory structural changes, the dissociation between our behavioral and structural effects at the 6 week time point may reflect additional top down processing mechanisms that are known to regulate behavioral responses such as freezing behavior. Together, these data suggest a potential role for higher processing regions, such as the amygdala or mPFC, that may play important roles in the immediate behavioral read outs of a learning event, while changes in olfactory primary sensory representation may occur over a longer time period, thus influencing future sensitivity to the cue conditioned stimulus. Within our model, olfactory fear conditioning leading to an enhanced number of CS-responsive OSNs may serve to enhance than animals' sensitivity to an important environmental cue, whereas following olfactory fear extinction, the accompanying decrease in CS-responsive OSNs may lead to a decrease in overall sensitivity to an extinguished odor. Complementary work in adult rodent systems has shown neurophysiological evidence of an *in vivo* odor-specific enhancement in the synaptic output of OSNs following an associative learning event (Kass et al., 2013). Thus, whereas regions such as the amygdala, hippocampus, or prefrontal cortex may allow for the inhibition of fear expression or the modulation of that inhibition (Johansen et al., 2011; Pape and Pare, 2010), respectively, the primary olfactory sensory system likely plays a major role in the CS-sensitivity and responsiveness following a learning event and its extinction. A growing body of literature suggests that alterations in synaptic transmission within the BLA play an important role in the suppression of conditioned fear following extinction learning (Myers and Davis, 2007; Orsini and Maren, 2012); in

fact there is evidence of depotentiation of conditioning-related amygdala synaptic transmission which occurs following extinction training (Hong et al., 2009; Kim et al., 2010; Quirk et al., 2010). These data are in line with our observation that extinction reverses aspects of conditioning-related effects, though the contribution of regions such as the amygdala in the regulation of primary sensory system structural changes remains an important area for future investigation.

Traditionally, extinction has been thought of not as an erasure or reversal of the initial fear memory, but rather as leading to the formation of a new inhibitory memory, based on the behavioral properties of extinction such as spontaneous recovery (Quirk et al., 2010). Interestingly, we do not observe a spontaneous recovery (the return of the conditioned fear response) of freezing behavior 3 weeks following olfactory extinction (Figure 2.1D, E), suggesting a robust and long-lasting effect of cue-specific extinction both at the level of freezing behavior and primary olfactory sensory system neuroanatomy. The spontaneous recovery of fear and threat responses depends both on the depth of extinction training as well as the length of time following olfactory extinction. Additional time points beyond the one included here (3 weeks following extinction) could provide valuable insight into the long lasting effects of olfactory fear extinction. Furthermore, while the behavioral effects of auditory cue-specific fear extinction have been thoroughly investigated, the long-lasting and robust reversal of freezing behavior following olfactory cue-specific extinction in adult animals is a novel finding within the field of fear extinction.

The mechanisms underlying these striking and robust structural changes accompanying the acquisition and extinction of olfactory fear learning remain to be

elucidated. Mechanisms related to altered cell turnover of olfactory sensory neurons may play an important role. Previous work has shown that associative olfactory learning modulates the survival of newborn neurons, and increases the survival of adult-born neurons in the OB (Alonso et al., 2012; Mandairon and Linster, 2009; Mouret et al., 2008; Sultan et al., 2011). While these studies investigated the contribution of olfactory neurogenesis to learning at the level of the olfactory bulb, learning-dependent regulation of epithelial olfactory neurogenesis, in which olfactory sensory neurons are in direct contact with environmental cues, may play a similarly and perhaps even greater role in shaping sensory epithelial responses to learning. The functional significance of adult neurogenesis in the main olfactory epithelium, which occurs persistently throughout life (Arisi et al., 2011), remains to be determined within this training context, and will be explored further in Chapter 3. M71-expressing neurons may have a selectively longer survival time following olfactory fear acquisition, perhaps through the learning-dependent release of neurotrophins such as Brain-derived neurotrophic factor (BDNF) from the olfactory bulbs. BDNF belongs to the neurotrophin family and has been shown to play an important role in learning and memory (Rattiner et al., 2005; Tyler et al., 2002). BDNF signaling through its primary receptor TrkB has also been shown to play a significant role in downstream effects underlying learning (Korte et al., 1995; Minichiello, 2009; Rex et al., 2007; Tyler and Pozzo-Miller, 2003; Yoshii and Constantine-Paton, 2007). Previous data from our lab has shown increased BDNF transcription and translation in the olfactory bulb following olfactory fear conditioning (Jones et al., 2007). Furthermore, OSNs within the MOE express the BDNF receptor TrkB (Nibu et al., 2001). BDNF-TrkB signaling may thus be well situated to mediate the

learning-dependent increases in M71+ OSN numbers observed following olfactory fear conditioning. Conversely, cue-specific olfactory fear extinction may revert these neurotrophic effects, thus inducing the selective M71-specific cell death. The role of BDNF-TrkB signaling in this system will be investigated in greater depth in Chapter 4.

Epigenetic regulation of M71 receptor expression within the MOE may also play a role in the dynamic increase following training and subsequent reversal of M71-specific OSN number following extinction. In the present set of experiments, we demonstrate a reversal in the histone modification, AcetylH3, occupancy at the M71 gene locus following olfactory extinction to acetophenone. Epigenetic processes such as histone acetylation and DNA methylation have been shown to play important roles in the mechanisms underlying fear acquisition and extinction across brain regions that include the hippocampus and the amygdala (Levenson and Sweatt, 2005; Lubin and Sweatt, 2008; Miller et al., 2008; Stefanko et al., 2009). Furthermore, epigenetic mechanisms are known to regulate the choice and maintenance underlying (the singularity of) OR expression (Magklara et al., 2011; Santoro and Dulac, 2012).

Cellular mechanisms underlying learning may also include dynamic regulation of cell death and apoptotic mechanisms, based on evidence that behavioral extinction paradigms can induce the death of newborn bulbar cells previously selected to survive (Sultan et al., 2011). Processes regulating cell survival may modulate memory strength based on the biological relevance of particular odor associations in the environment. In fact, recent work has shown that a histone H2B variant, H2be, expressed exclusively by OSNs, displays activity-dependent expression, which contributes to the transcriptional activity and life span of the OSN (Santoro and Dulac, 2012). Furthermore, histone variant

exchange has been recently shown to play an important role in fear conditioning in the hippocampus and the cortex (Zovkic and Sweatt, 2013; Zovkic et al., 2014).

Dopamine signaling has been shown to play an important role in aspects of fear conditioning and extinction (Abraham et al., 2014). Dopamine neurons in the ventral tegmental area (VTA) are known to underlie aspects of prediction error, in which there is a discrepancy between expected and actual outcomes (Mackintosh, 1974; Rescorla and Wagner, 1972). When a reward is received that is greater than what is predicted, dopamine neurons, which fire tonically under baseline conditions, increase burst firing. On the other hand, when a predicted reward is omitted, dopamine neurons will inhibit tonic firing. Dopamine neuron firing thus conveys not only the hedonic value of an US, but also the corresponding expectations related to the CS. Dopaminergic signaling and circuitry in fear related behaviors involve a number of brain regions including the VTA, described above, as well as the nucleus accumbens (NAcc shell and core), the dorsal striatum, the amygdala (BLA and CeA), the substantia nigra, the hippocampus and the prefrontal cortex (IL and PL) (Abraham et al., 2014; Eshel et al., 2015; Heydari and Holroyd, 2016; Holtzman-Assif et al., 2010; Keiflin and Janak, 2015; McHugh et al., 2014). There is little known regarding the role of dopaminergic signaling in olfactory regions, however, a recent study demonstrated that specific domains of the olfactory tubercle (OT) represent distinct odor-induced motivated behaviors that are mediated via dopamine receptor subtype (D1 or D2) activation (Murata et al., 2015). Based on principles of prediction error mediated by dopamine signaling, the olfactory system may act as a "salience filter" for learned conditioned and extinguished cues, however, much additional research is required to confirm such a model.

Overall our results demonstrate that extinction training specific to a conditioned odor reverses the conditioning-associated increases in freezing behavior and structure (summary schematic in Figure 2.10). Mice undergoing olfactory fear extinction 3 weeks following acquisition exhibit decreased freezing to the odor CS across extinction sessions. The observed reduction in within session freezing during extinction is maintained 3 weeks following the extinction session, suggesting a long-term retention of extinction learning. Furthermore, the changes in freezing behavior accompanying the acquisition and extinction of olfactory fear conditioning are paralleled by neuroanatomical changes in the neuronal populations (M71+) responsive to the cue-conditioned stimulus (acetophenone). Mice fear conditioned 3 or 6 weeks prior had a larger number of M71+ OSNs in the MOE compared to controls and mice that had undergone extinction, suggesting that cue-specific olfactory extinction reverses the primary olfactory sensory neuroanatomical changes that accompany the initial learning event. Our lab has previously found that the effects of olfactory fear acquisition (increased numbers of M71 receptor expressing OSNs, increased M71-specific glomerular area, and enhanced behavioral sensitivity to acetophenone) are transmitted across generations (Dias and Ressler, 2013). While the present study investigates exclusively the effect of cue specific olfactory extinction in an adult F0 generation, the possibility that the effects of extinction may be transmitted to subsequent generations is extremely intriguing and is an important direction for future investigations. Also of note, recent observations of plasticity within the human olfactory system suggest the intriguing possibility that the phenomena observed here may occur in humans as well (Krusemark et al., 2013; Li, 2014; Li et al., 2008). Overall the data described in this chapter, support the

dynamic alterations of olfactory sensory representation with learning, and shed light on how a sensory system responds to a therapeutic intervention such as extinction learning following fear conditioning.

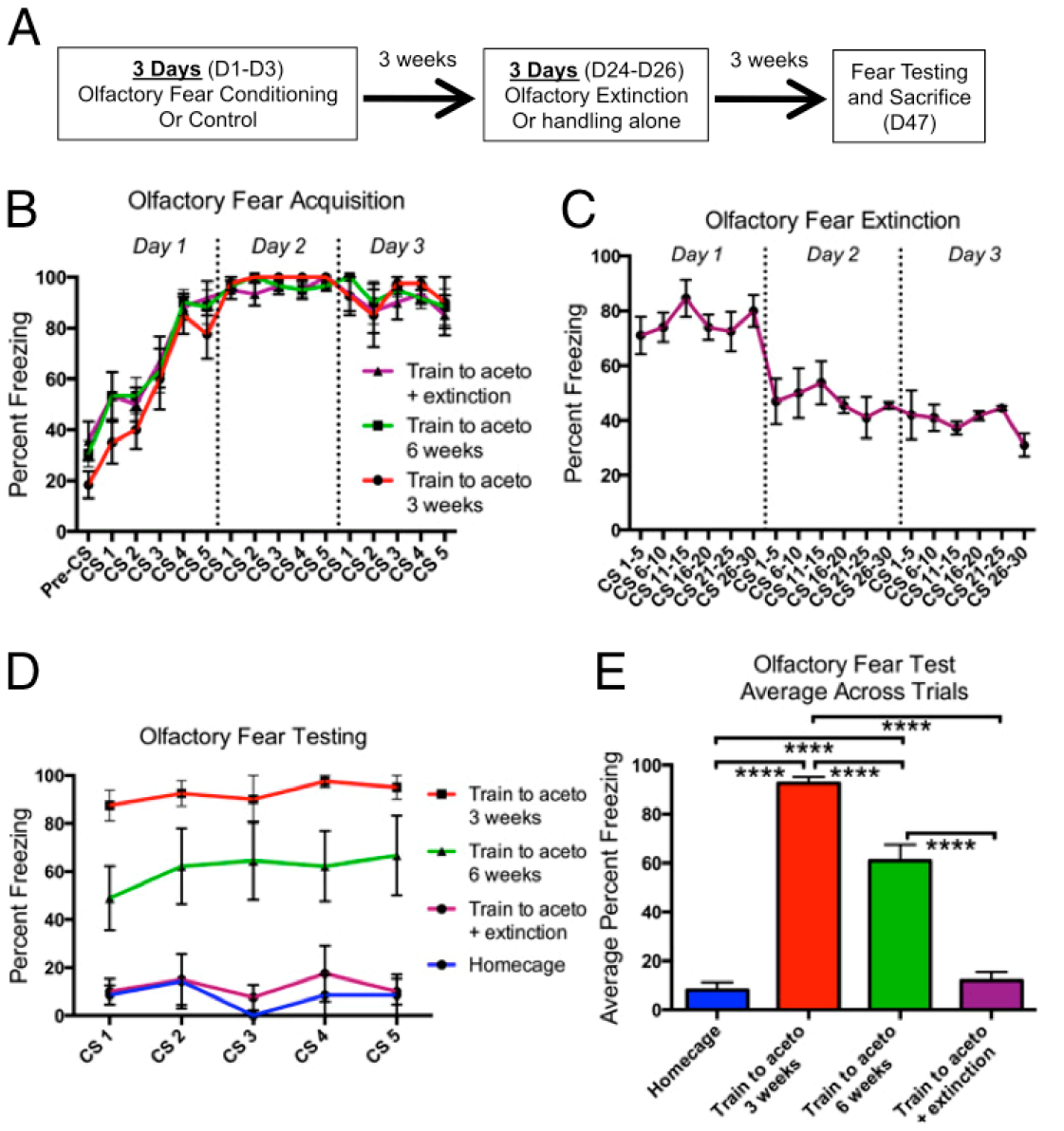

<u>Figure 2.1:</u> Olfactory fear extinction reverses conditioning associated increases in freezing behavior. (A) Experimental time line of fear conditioning, extinction and olfactory fear testing 1 hour before sacrifice. (B) Mice acquire olfactory fear at similar rates across all groups (n=9-12/group) (extinction group has not yet undergone extinction training) (two-way RM ANOVA, p=0.2314, F(2,32)=1.533). (C) Mice undergoing olfactory fear extinction exhibit decreased freezing to the odor CS across extinction sessions (n=12). (D-E) Mice fear conditioned 3 or 6 weeks prior exhibit enhanced freezing to the odor CS compared to the homecage and extinction groups (n=19-22/group) (D; two-way RM ANOVA, p<0.0001, F(3,40)=27.51) (E; ANOVA, p<0.0001, F(3,216)=23.56). Data presented as mean +/- s.e.m. *P<0.05, **P<0.01, ***P<0.001, ****P<0.0001.

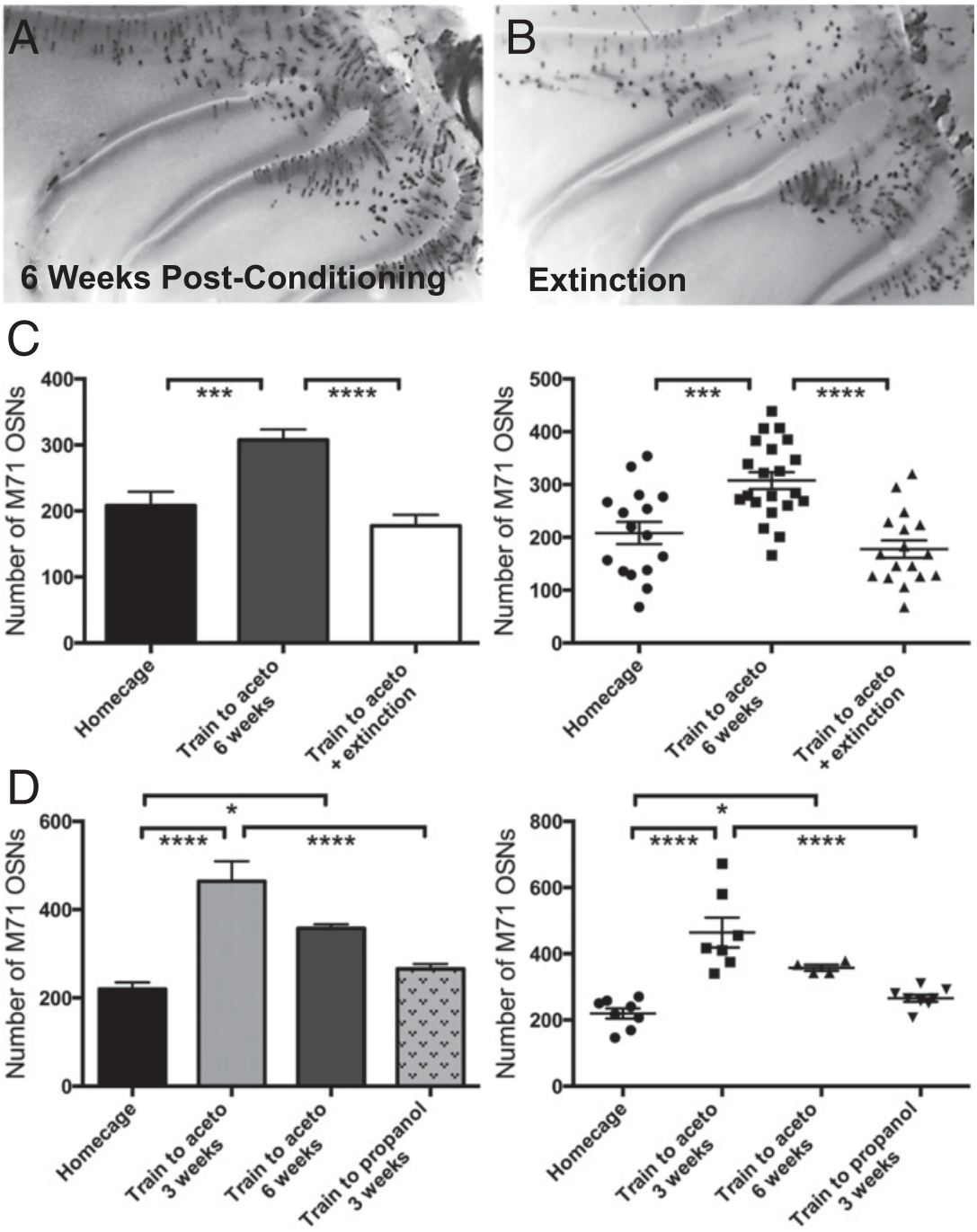

Figure 2.2: M71+ olfactory sensory neuron numbers in the MOE are reversed with cue-specific olfactory extinction training. (A-C) Mice 6 weeks post-fear conditioning (train to aceto 6 weeks) had larger number of M71 OSNs in the MOE than homecage (black bar) and extinction mice (train to aceto + extinction) (M71-LacZ: Homecage n=16; Train to aceto 6 weeks, n=21; Train to aceto + extinction, n=17; ANOVA, $P<0.0001$, $F(2,51)=15.72$; Homecage versus train to aceto 6 weeks, $P<0.001$; train to aceto 6 weeks versus train to aceto + extinction, $P<0.0001$; Homecage versus train to aceto + extinction, $P=0.2592$). (D) Mice 3 weeks post-fear conditioning (train to aceto 3

weeks) and mice 6 weeks post-fear conditioning (train to aceto 6 weeks) had an increased number of M71+ OSNs in the MOE than homecage and mice that were fear conditioned to propanol, a non M71-activating odorant (train to propanol 3 weeks) (M71-LacZ: Homecage n=8; Train to aceto 3 weeks, n=7; Train to aceto 6 weeks, n=4; Train to propanol 3 weeks, n=8; ANOVA, $P<0.0001$, $F(3, 23)=18.38$; Homecage versus Train to aceto 3 weeks, $P<0.0001$; Homecage versus train to aceto 6 weeks, $P<0.05$; Homecage versus Train to propanol 3 weeks, P=n.s.; Train to aceto 3 weeks versus Train to propanol 3 weeks, $P<0.001$; Train to aceto 3 weeks versus train to aceto 6 weeks, P=n.s.). Data presented as mean +/- s.e.m. *$P<0.05$, **$P<0.01$, ***$P<0.001$, ****$P<0.0001$.

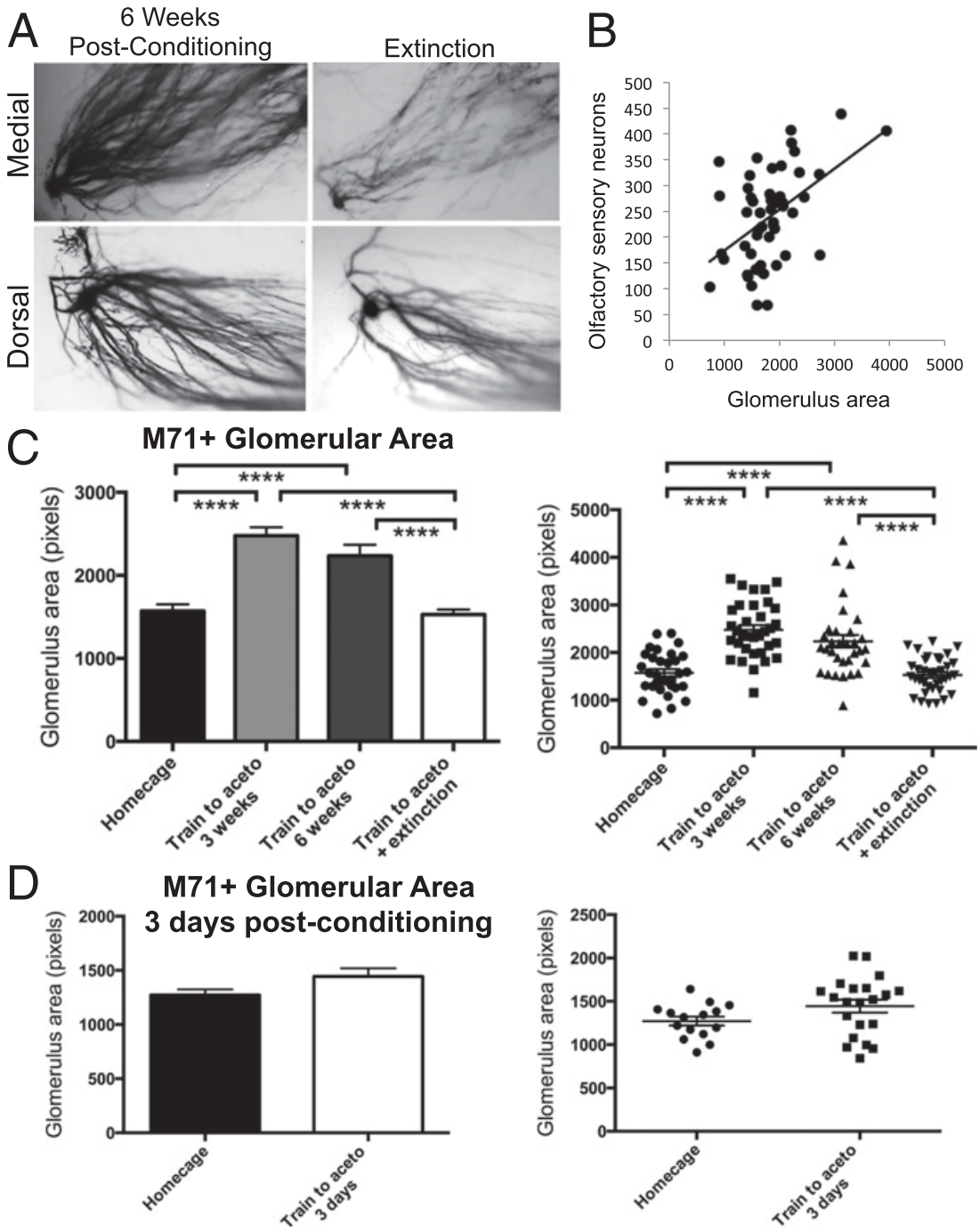

Figure 2.3: Increased M71+ glomerular size in the OB is reversed with cue-specific olfactory extinction training. (A, C) Glomerular area is greater in the acetophenone + shock groups (3 weeks and 6 weeks post-fear conditioning, gray bars) compared to home cage and extinction trained groups. (B) Glomerular size is positively correlated with increasing olfactory sensory neuron number (Pearson's correlation coefficient r=0.4844, p=0.0003, n=51 XY pairs). (C) M71 glomerular area (M71-LacZ: Homecage, n=31; 3 week, n=34; 6 week, n=32; Extinction, n=36; ANOVA, P<0.0001, F(3,129)=25.44; Homecage versus 3 week, P<0.0001; Homecage versus 6 week, P<0.0001; 3 week versus

Extinction, P<0.0001; 6 week versus Extinction, P<0.0001; Homecage versus extinction, P=0.6521). (D) There is no increase in glomerular area 3 days following olfactory fear conditioning compared to home cage (M71-LacZ: Homecage, n=15 ; Train to aceto 3 days, n=21; Homecage vs. Train to aceto 3 days, Student's t-test, P=0.08). Data presented as mean +/- s.e.m. *P<0.05, **P<0.01, ***P<0.001, ****P<0.0001.

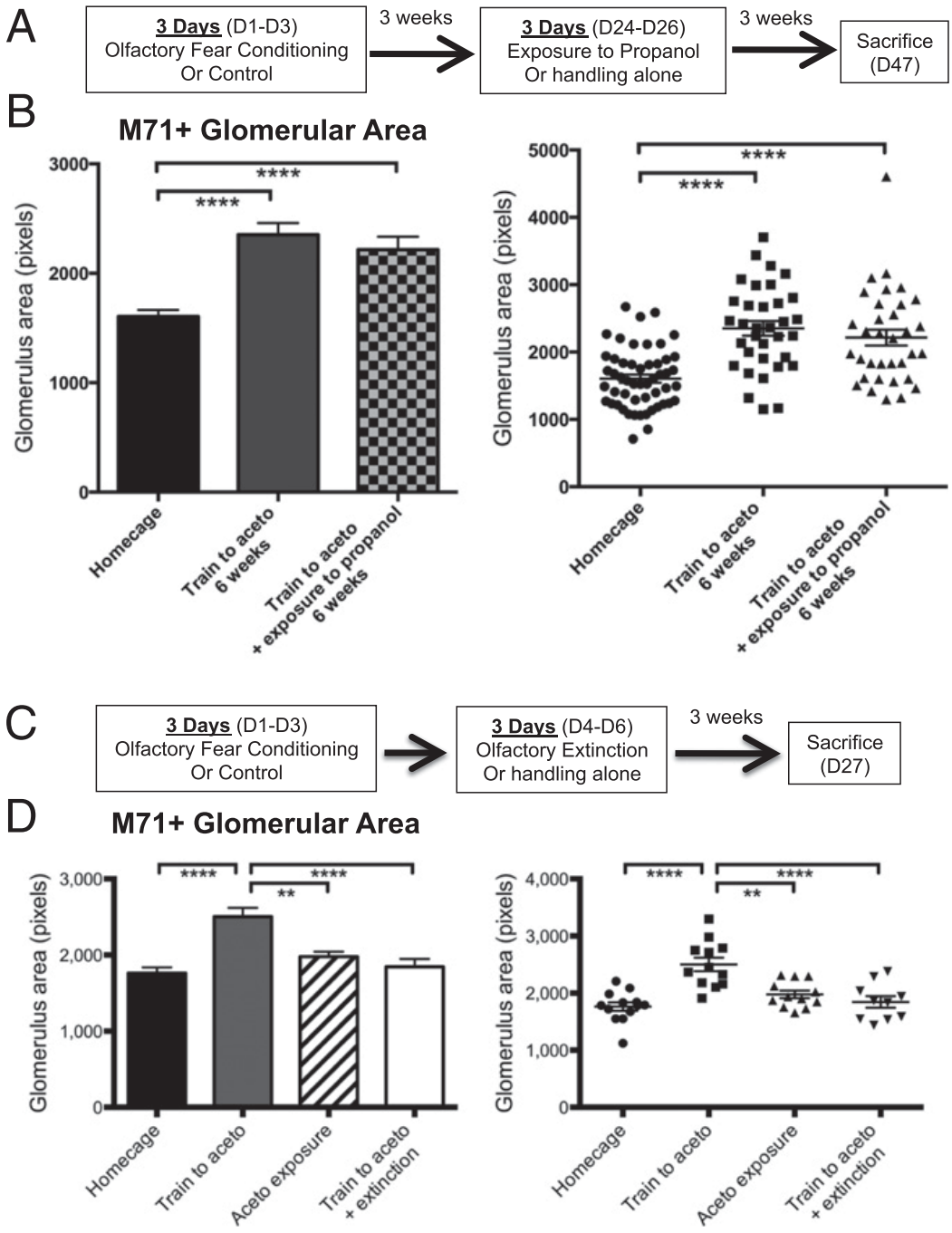

Figure 2.4: Exposure to the context and propanol (non M71-activating odorant) does not result in reversal of M71+ glomerular size in the OB. (A) Experimental time line of fear conditioning, exposure to propanol and sacrifice. The timing and extinction/exposure sessions were identical in timing and session duration as those used for the extinction to acetophenone group (except only propanol was presented). (B) Mice fear conditioned to aceto 6 weeks prior (Train to aceto 6 weeks) and mice fear conditioned to aceto that received exposure to the non M71-activating odorant propanol in lieu of extinction (Train to aceto + exposure to propanol 6 weeks) had increased M71+

glomerular area compared to home cage (M71-LacZ: Homecage, n=52; train to aceto 6 weeks, n=34; train to aceto + exposure to propanol, n=34; ANOVA, P<0.0001, F(2,117)=20.92; Homecage versus train to aceto 6 weeks, P<0.0001; Homecage versus train to aceto + exposure to propanol, P<0.0001; train to aceto 6 weeks versus train to aceto + exposure to propanol, P= n.s.). **Olfactory fear extinction immediately following acquisition supports learning related reversal of M71-specific neuroanatomical representation.** (C) Alternate experimental time line of fear conditioning, extinction and olfactory fear testing 1 hour before sacrifice. M71+ glomerular area in the OB is reversed with cue-specific olfactory extinction training that occurs immediately after conditioning. One group remained in the home cage and received handling on all behavioral session days ("Homecage"), a second group received odor (acetophenone) + shock pairings ("Train to aceto"), a third group received acetophenone odor alone presentations ("Aceto exposure"), and finally a fourth group received odor (acetophoneone) + shock pairings followed by extinction sessions ("Train to aceto + extinction") (n=5-7 per group). (d) M71 glomerular area (M71-LacZ: Homecage, n=13; Train to aceto, n=12; Aceto exposure, n=12; Train to aceto + extinction, n=10; ANOVA, P<0.0001, F(3,43)=13.42; Homecage versus Train to aceto, P<0.0001; Homecage versus Exposure to aceto, P=n.s.; Homecage versus Train to aceto + Extinction, P=n.s.; Exposure to aceto versus Train to aceto, P<0.01; Train to aceto versus Trained to aceto + Extinction, P<0.0001; Exposure to aceto versus Train to aceto + extinction, P=n.s.).

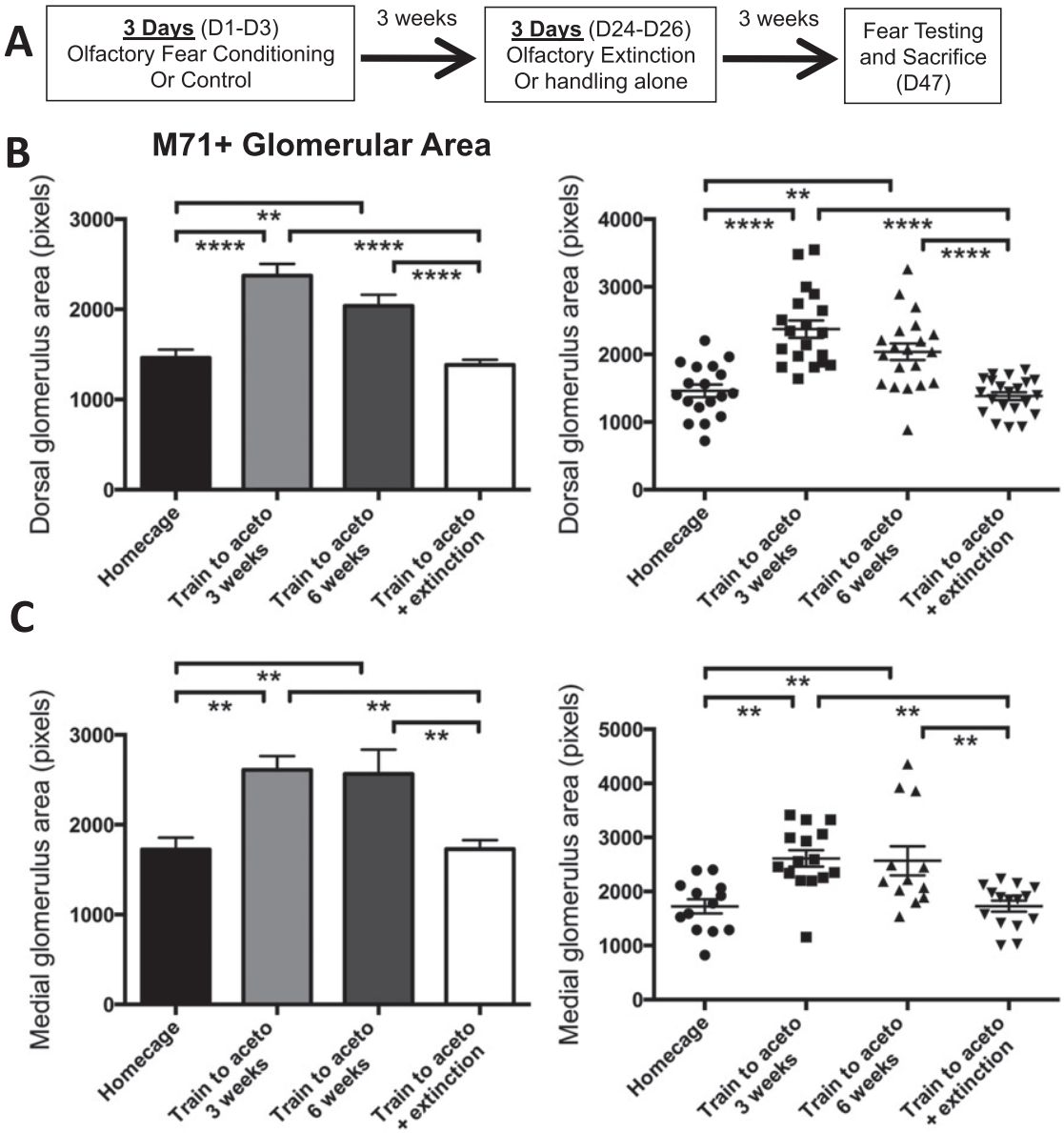

Figure 2.5: In addition to the combined total glomerulus analysis described in Figure 2.3, we have also examined the glomerular area for each medial and dorsal bulb separated. (A) Timeline of experimental design. (B) Dorsal M71 glomerular area (M71-LacZ: Homecage, n=18; Train to aceto 3 weeks, n=19; Train to aceto 6 weeks, n=20; Train to aceto + extinction, n=21; ANOVA, P<0.0001, F(3,74)=2.784; Homecage versus train to aceto 3 weeks, P<0.0001; Homecage versus train to aceto 6 weeks, P<0.01; train to aceto 3 weeks versus train to aceto + extinction, P<0.0001; train to aceto 6 weeks versus train to aceto + extinction, P<0.0001; Homecage versus train to aceto + extinction, P=4675). (C) Medial M71 glomerular area (M71-LacZ: Homecage, n=13; Train to aceto 3 weeks, n=15; Train to aceto 6 weeks, n=12; Train to aceto + extinction, n=15; ANOVA, P<0.0001, F(3,51)=1.402; Homecage versus train to aceto 3 weeks, P<0.01; Homecage versus train to aceto 6 weeks, P<0.01; train to aceto 3 weeks versus

train to aceto + extinction, P<0.01; train to aceto 6 weeks versus train to aceto + extinction, P<0.01; Homecage versus train to aceto + extinction, P=0.9827). Data presented as mean +/- s.e.m. *P<0.05, **P<0.01, ***P<0.001, ****P<0.0001.

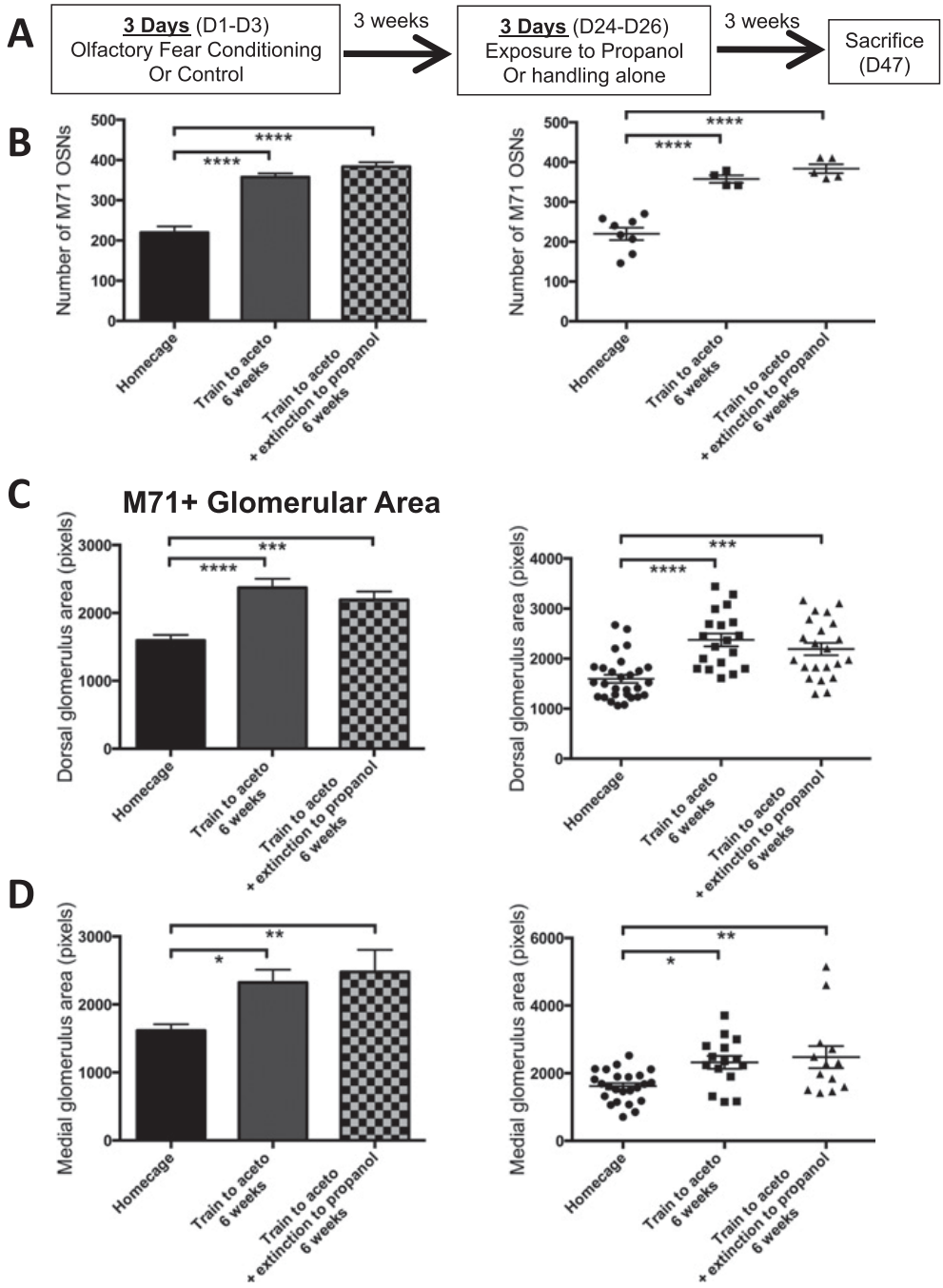

Figure 2.6: In addition to the combined total glomerulus analysis described in Figure 2.4C, we have also examined each medial and dorsal bulb separately, and the M71+ OSN counts in the MOE. (A) Alternate experimental time line of fear conditioning, extinction and olfactory fear testing 1 hour before sacrifice. M71+ glomerular area in the OB is reversed with cue-specific olfactory extinction training that occurs immediately after conditioning. One group remained in the home cage and received handling on all behavioral session days ("Homecage"), a second group received

odor (acetophenone) + shock pairings ("Train to aceto"), a third group received acetophenone odor alone presentations ("Aceto exposure"), and finally a fourth group received odor (acetophoneone) + shock pairings followed by extinction to acetophenone sessions ("Train to aceto + extinction") (n=5-7 per group). (B) M71+ olfactory sensory neuron numbers in the MOE (M71-LacZ: Homecage, n=4; Train to aceto, n=5; Exposure to aceto, n=4; Train to aceto + Extinction, n=3; ANOVA, $P<0.05$, $F(3,12)=3.915$; Homecage versus Train to aceto, *t*-test, $P=0.0541$; Homecage versus Exposure to aceto, *t*-test, $P=0.3508$; Homecage versus Train to aceto + Extinction, *t*-test, $P=0.7691$; Train to aceto versus Train to aceto + Extinction, *t*-test, $P<0.01$; Exposure to aceto versus Train to aceto + Extinction, *t*-test, $P=0.0570$; Exposure to aceto versus Train to aceto, *t*-test, $P=0.1187$). (C) Dorsal M71 glomerular area (M71-LacZ: Homecage, n=6; Train to aceto, n=6; Exposure to aceto, n=6; Train to aceto + Extinction, n=5; ANOVA, $P<0.05$, $F(3,19)=0.09007$; Homecage versus Train to aceto, $P<0.05$; Homecage versus Exposure to aceto, $P=0.06$; Homecage versus Train to aceto + Extinction, $P=0.9606$; Train to aceto versus Train to aceto + Extinction, $P<0.05$; Exposure to aceto versus Train to aceto + Extinction, $P<0.05$; Exposure to aceto versus Train to aceto, $P=0.2469$). (d) Medial M71 glomerular area (M71-LacZ: Homecage, n=7; Train to aceto, n=6; Exposure to aceto, n=6; Train to aceto + Extinction, n=5; ANOVA, $P<0.0001$, $F(3,20)=0.6732$; Homecage versus Train to aceto, $P<0.0001$; Homecage versus Exposure to aceto, $P=0.5163$; Homecage versus Train to aceto + Extinction, $P=0.9606$; Train to aceto versus Train to aceto + Extinction, $P<0.01$; Exposure to aceto versus Train to aceto + Extinction, $P<0.001$; Exposure to aceto versus Train to aceto, $P=0.6584$). Data presented as mean +/- s.e.m. *$P<0.05$, **$P<0.01$, ***$P<0.001$, ****$P<0.0001$.

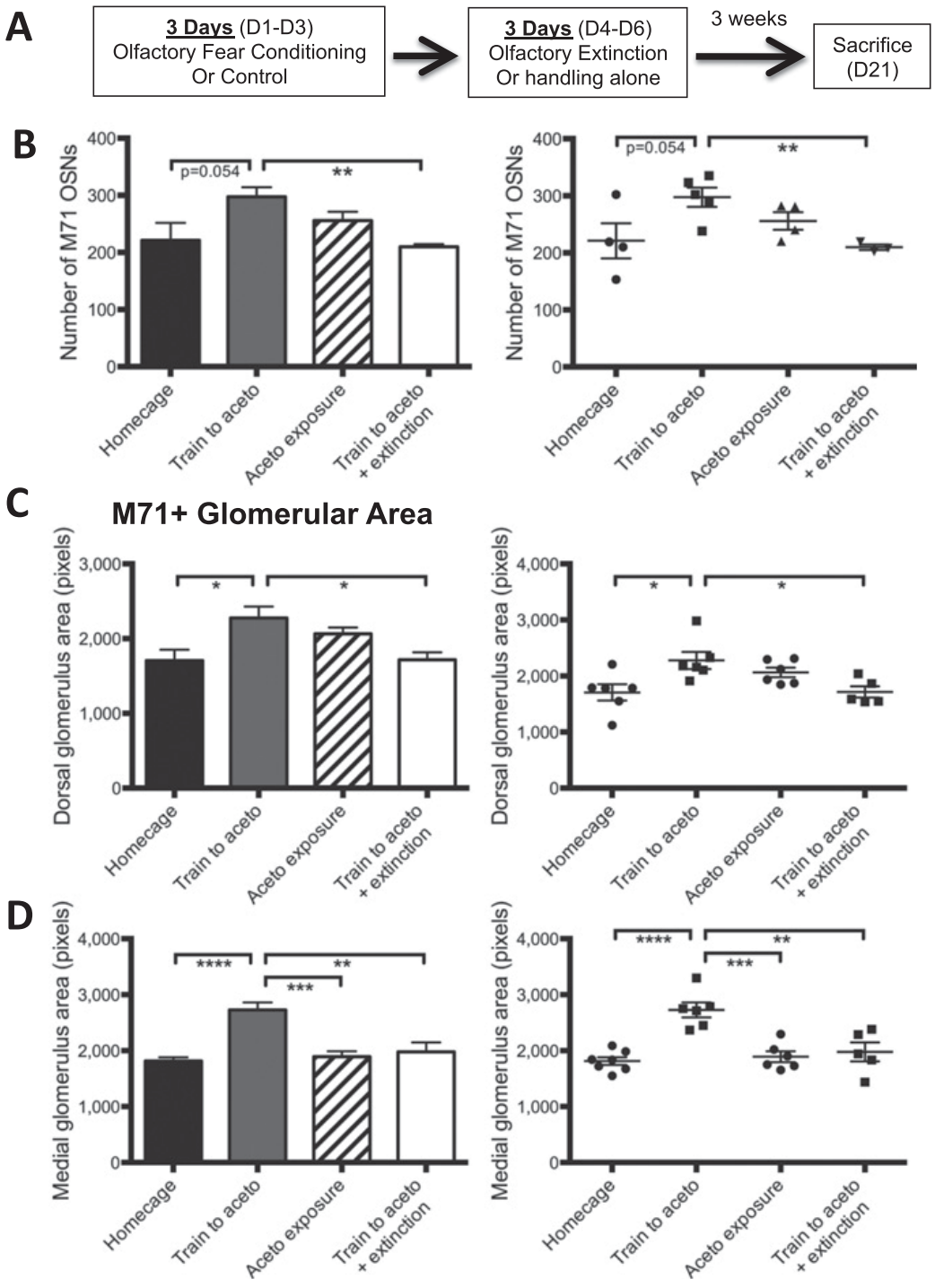

Figure 2.7: In addition to the combined total glomerulus analysis described in Figure 2.4B, we have also examined the number of M71+ OSNs in the MOE, and each M71+ medial and dorsal bulb separately. (A) Experimental time line of fear conditioning, exposure to propanol and sacrifice. The timing and extinction/exposure sessions were identical in timing and session duration as those used for the extinction to

acetophenone group (except only propanol was presented). (B) Mice fear conditioned to aceto 6 weeks prior (Train to aceto 6 weeks) and mice fear conditioned to aceto that received exposure to the non M71-activating odorant propanol in lieu of extinction (Train to aceto + exposure to propanol 6 weeks) had increased numbers of M71+ OSNs in the MOE compared to home cage (black bar) (M71-LacZ: Homecage, n=8; train to aceto 6 weeks, n=4; train to aceto + exposure to propanol, n=5; ANOVA, $P<0.0001$, $F(2,14)=40.85$; Homecage versus train to aceto 6 weeks, $P<0.0001$; Homecage versus train to aceto + exposure to propanol, $P<0.0001$; train to aceto 6 weeks versus train to aceto + exposure to propanol, P= n.s.). (C) Dorsal glomerulus area (M71-LacZ: Homecage, n=28; train to aceto 6 weeks, n=19; train to aceto + exposure to propanol, n=22; ANOVA, $P<0.0001$, $F(2,66)=15.04$; Homecage versus train to aceto 6 weeks, $P<0.0001$; Homecage versus train to aceto + exposure to propanol, $P<0.001$; train to aceto 6 weeks versus train to aceto + exposure to propanol, P= n.s.). (D) Medial glomerulus area (M71-LacZ: Homecage, n=24; train to aceto 6 weeks, n=15; train to aceto + exposure to propanol, n=12; ANOVA, $P<0.01$, $F(2,48)=6.676$; Homecage versus train to aceto 6 weeks, $P<0.01$; Homecage versus train to aceto + exposure to propanol, $P<0.05$; train to aceto 6 weeks versus train to aceto + exposure to propanol, P= n.s.). Data presented as mean +/- s.e.m. *$P<0.05$, **$P<0.01$, ***$P<0.001$, ****$P<0.0001$.

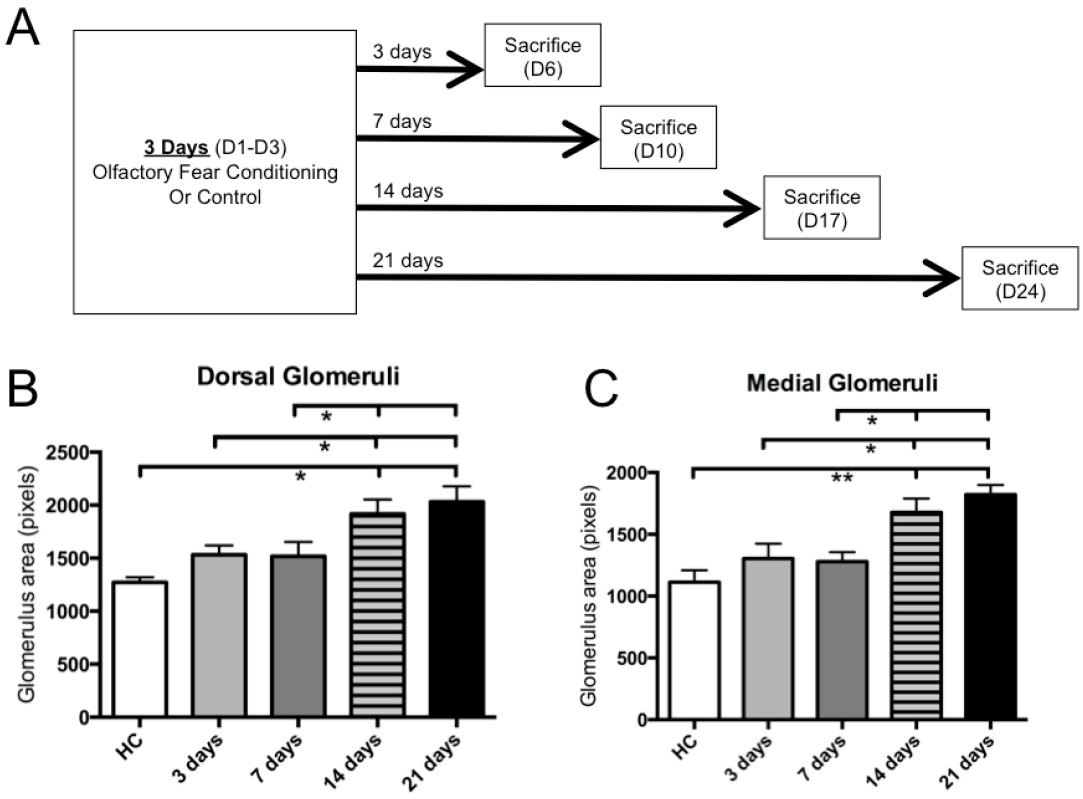

Figure 2.8: Three days following the last olfactory fear conditioning session, mice do not display significant increases in M71 expressing (A) dorsal or (B) medial glomeruli compared to home cage handled controls. (A) Experimental time line of fear conditioning and sacrifice 3 days following the last fear conditioning session. (B) Dorsal M71 glomerular area (M71-LacZ: Homecage, n=9; 3 Days, n=13; Homecage versus 3 Day, Student's *t*-test, P=0.07). (C) Medial M71 glomerular area (M71-LacZ: Homecage, n=6; 3 Days, n=8; Homecage versus 3 Day, Student's *t*-test, P=0.5897). Data presented as mean +/- s.e.m.

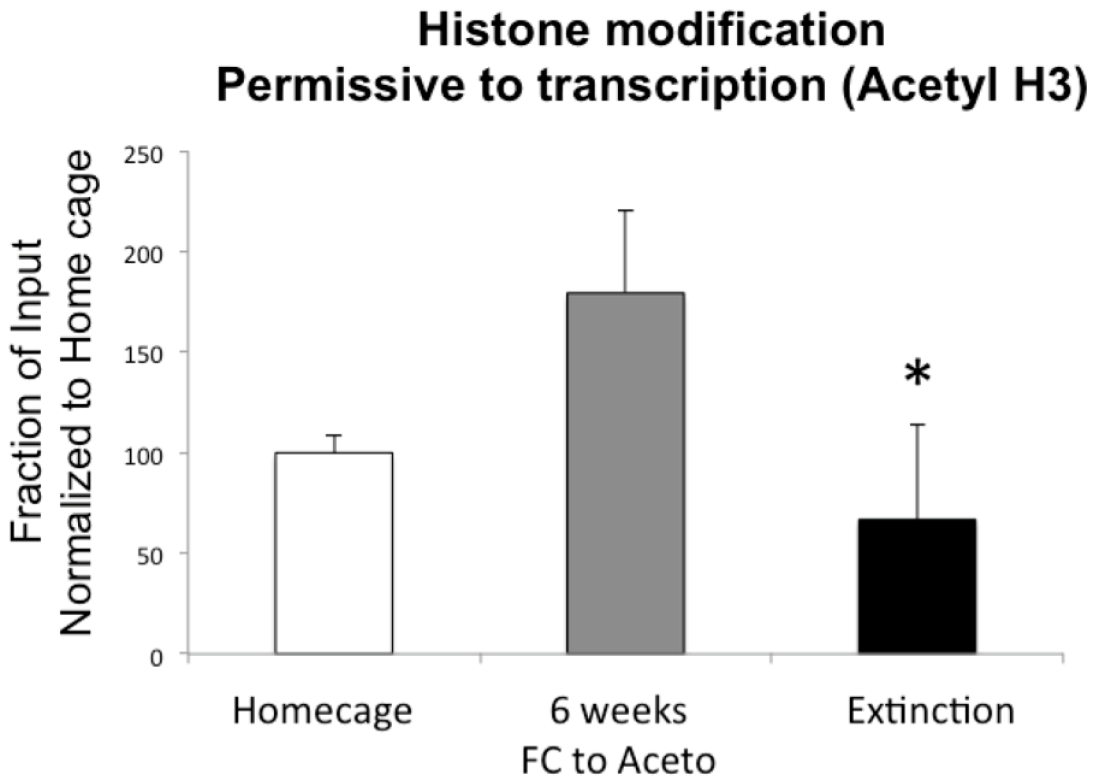

Figure 2.9: Olfactory fear acquisition and extinction are accompanied by a dynamic regulation of histone marks around the M71 locus. Extinction reverses the increase in Acetyl H3 occupancy at the M71 locus (ANOVA, quadratic trend, $F(1,10)=5.68$, $p<0.05$). Posthoc analyses (LSD test) show a significant difference between the extinction and 6 week groups for Acetyl H3 (*$p=0.05$).

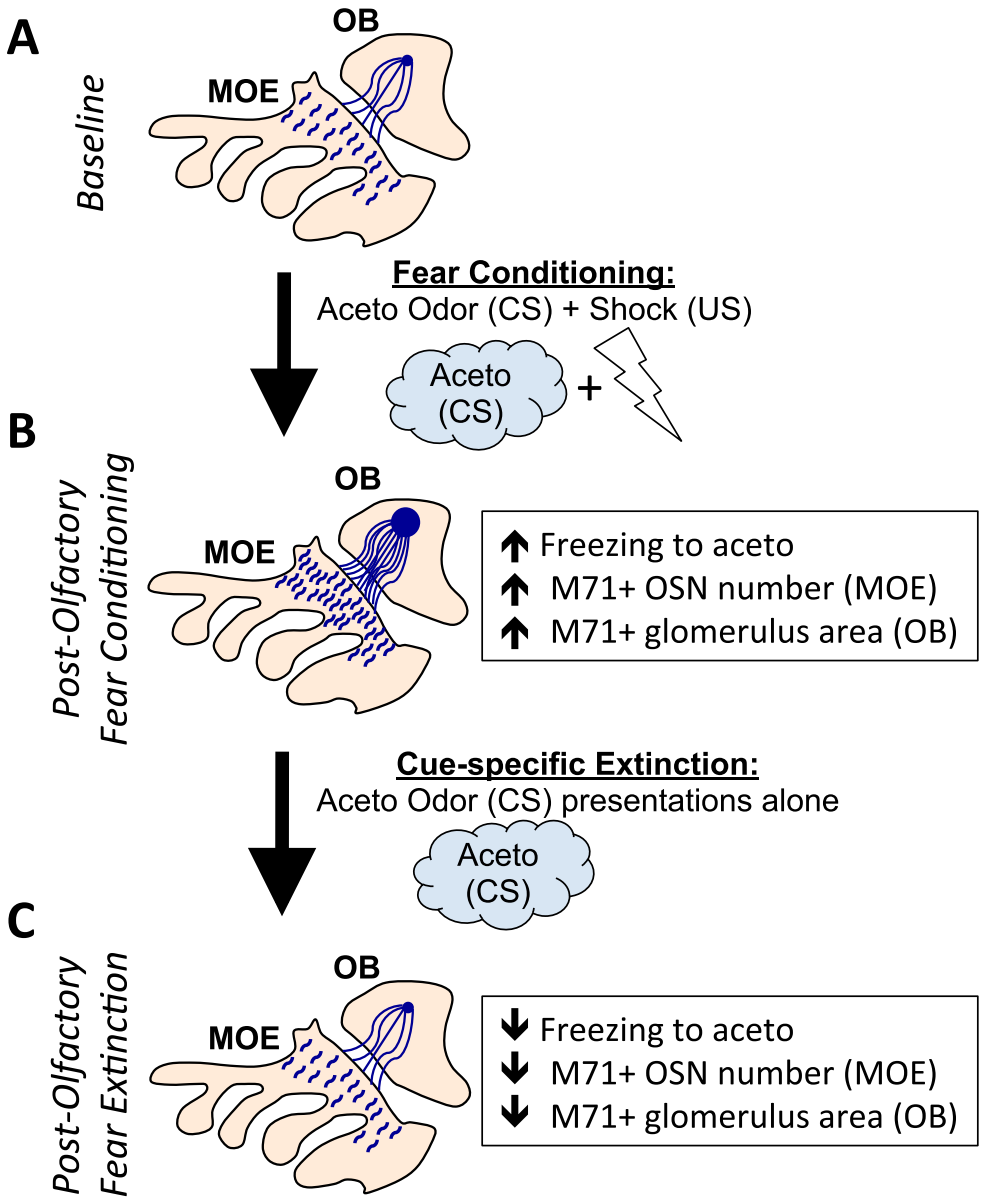

Figure 2.10: Schematic diagram of structural and behavioral changes accompanying the acquisition and extinction of cue-specific olfactory fear learning. (B) Following olfactory fear conditioning to acetophenone (M71-activating odorant), mice exhibit enhanced freezing to acetophenone, increased numbers of M71+ OSNs in the MOE, and increased M71+ glomerulus area in the OB compared to baseline controls (A) (home cage animals, animals that received acetophenone odor exposure alone, or animals that were fear conditioned to the non M71-activating odorant propanol). (C) Following cue-specific olfactory fear extinction, mice exhibit decreased freezing to acetophenone, decreased numbers of M71+ OSNs in the MOE, and decreased M71+ glomerulus area in the OB. These reductions in fear behavior and M71 specific structure are observed only

when mice are extinguished to the learned cue (acetophenone), and not if mice are extinguished to a non M71-activating odorant (propanol).

CHAPTER 3: REGULATION OF CELL SURVIVAL IN THE STRUCTURAL PLASTICITY ACCOMPANYING OLFACTORY FEAR CONDITIONING

Context, Author's Contribution, and Acknowledgement of Reproduction

The following chapter presents evidence of the regulation of cell turnover in the primary olfactory system in response to olfactory fear conditioning, using zinc sulfate induced ablation and EdU labeling methods. The context of the study was an effort to further investigate whether the learning induced increases in M71-expressing OSN cell number following olfactory fear conditioning to acetophenone are regulated by M71 specific enhancements in cell survival. The results of this study were compared to previous research from our laboratory demonstrating an enhancement in M71-specific OSN number of glomerulus area following conditioning to the M71 activating odorant, acetophenone (Jones et al., 2008). The dissertation author contributed to the paper by designing and running experiments, analyzing the data, and was a main contributor to the writing of the paper. The chapter is reproduced with minor edits from Morrison, F.G., Dias, B.G., McCullough, K.M., Ressler, K.J. Cell turnover in the primary olfactory system following associative learning. *In preparation.*

Introduction

Adult neurogenesis refers to the production, maturation and integration of new neurons throughout adult life. The hippocampus and subventricular zone (SVZ) are widely accepted as neurogenic throughout life. OB neurogenesis has been shown to play important roles in the learning and discrimination of new odors, but also in learning odor cues affecting species-specific behaviors. Enriched odor exposure has been shown to increase the number of newborn neurons in the adult OB and also lead to improvements in odor memories (Rochefort et al., 2002). Furthermore, improvements in the

discrimination of odors in mice is accompanied by elevated rates of survival of newborn OB neurons; blockade of neurogenesis prior to and during the odorant exposure period prevents the learning dependent improvements in behavioral discrimination (Moreno et al., 2009). OB neurogenesis also plays an important role in olfactory mediated reproductive and social behaviors; the pheromones of dominant males, compared to subordinate males, lead to enhanced neurogenesis in the OB and hippocampus of female mice, and these increased rates of neurogenesis correlate with female preference for dominant males over subordinate ones (Mak et al., 2007).

In addition to the olfactory bulb, the olfactory epithelium is a well-established source of local progenitor cells undergoing (Graziadei, 1973; Graziadei and Graziadei, 1979; Graziadei et al., 1978; Kittel, 1990). While many studies have investigated the role of new neurons born in the olfactory bulbs, less attention has been paid to the functional significance of adult neurogenesis in the main olfactory epithelium (MOE), which occurs persistently throughout life. The present chapter will investigate the role of neurogenesis of primary OSNs in the mouse MOE in response to an olfactory fear-learning event. In contrast to OB neurogenesis, primary OSNs are in direct contact with the outside world and as such are especially prone to external damage and environmental stimuli. The evolutionary importance of a high turnover rate of OSNs, which have such direct proximity to the external environment and are thus more prone to damage, is high, as the survival of many organisms depends on their sense of smell. The constant rate of OSN cell turnover also makes the MOE an excellent model to study how primary sensory neurons respond to changes in learned environmental cues, as such changes likely make an animal more fit in dynamic environments.

Using a transgenic mouse in which OSNs expressing the M71 odorant receptor can be visualized by LacZ histochemistry (M71-LacZ mouse line) (Vassalli et al., 2002a), our lab has demonstrated that fear conditioning with an M71-activating odorant increases the number of odorant-specific OSNs in the epithelium and the size of their glomeruli in the olfactory bulb (Jones et al., 2008a). Notably when animals receive the same odor-shock pairing to another odorant that does not activate the M71 receptor, there are no detectable changes in the M71-expressing neuron population or glomeruli. The present chapter will address mechanisms the role M71-specific turnover within this context using two approaches; 1) Zinc sulfate induced ablation of the olfactory epithelium and 2) 5-ethynyl-2'-deoxyuridine (EdU) labeling of M71-expressing OSNs.

Zinc sulfate ($ZnSO_4$) has been widely used to induce degeneration of the olfactory epithelium and ablate the olfactory sensory neurons in rodents (Dhungle et al., 2011; Ducray et al., 2002; Keller et al., 2006; Mak et al., 2007; McBride et al., 2003; Slotnick et al., 2010). We seek to utilize zinc sulfate administration to 1) observe the time course of regeneration of the olfactory epithelium following complete degeneration, and 2) investigate the contribution of the presence of OSNs to the behavioral and structural effects we have observed after our olfactory fear conditioning paradigm.

Furthermore, this chapter will clarify whether the learning dependent structural changes are due to alterations in cell survival that affect the turnover of M71 OSNs using EdU labeling of MOE OSNs. The observed cell number increase in the olfactory epithelium following olfactory fear conditioning to acetophenone could indicate a learning dependent increase in neurogenesis (selective proliferation) of the M71 neurons. However, odorant receptor specificity is thought to be determined post-mitotically by

irreversible stochastic processes, and it is thus less likely that the increase in OSNs is the result of selective proliferation. Rather, mature M71 neurons at the time of training may have a longer survival time, perhaps through the learning-dependent release of neurotrophins such as BDNF from the olfactory bulb, which will be investigated in further detail in Chapter 4. Using the olfactory fear conditioning paradigm allows us to investigate whether the formation of an olfactory fear memory is accompanied by increases in the survival of specific M71 (acetophenone-sensitive) neurons in the MOE. The present chapter utilizes EdU-labeling to specifically address cell turnover rates of M71+ OSNs following olfactory fear conditioning.

Methods

Animals

Adult M71-IRES-tauLacZ transgenic mice (Vassalli et al., 2002b) were maintained in a mixed 129/Sv X C57BL/6 background (Jackson Laboratories) and were used in all behavioral and neuroanatomical experiments related to zinc sulfate induced ablation. Adult M71-GFP transgenic mice (Feinstein et al., 2004) were maintained in a C57BL/6J background (Jackson Laboratories) and were used in all behavioral and neuroanatomical experiments using EdU labeling. These gene-targeted mice have the M71 olfactory receptor gene tagged with GFP. All mice were 2-3 months old at the time of olfactory fear conditioning. For each training time course, behavioral groups were formed with mice from at least 4 litters, controlling for sex and age, such that each group was age-matched and had equivalent numbers of males and females. All mice were experiment and odor naïve at the start of the experiment. Mice were housed in a temperature-controlled vivarium on a 12 h light/dark cycle in standard group cages (≤4

mice/cage) and were given *ad libitum* access to food and water. All experiments were performed during the light cycle and were approved by Emory University Institutional Review Board and the McLean Hospital Institutional Review Board, following the National Institutes of Health Internal Animal Care and Use Committee standards.

Olfactory fear conditioning, extinction and testing

Fear training and testing were conducted using startle response systems (SR-LAB, San Diego Instruments) that had been modified to deliver discrete odor stimuli as previously described (Jones et al., 2005; Jones et al., 2008; Dias and Ressler, 2014; Morrison et al., 2015). All fear conditioning behavior experiments followed the same behavioral protocols; adult M71-GFP transgenic mice (Feinstein et al., 2004) (2-3 months at the time of training) were first habituated to the training chambers 2 times (10 minutes per day) prior to training. Mice then received 3 training sessions (1 training session per day) over 3 consecutive days to ensure strong and stable odor-shock associations as previously described (Jones et al., 2005; Jones et al., 2008; Dias & Ressler, 2014; Morrison et al., 2015). Each odor + shock training session consisted of 5 trials of 10 s odor conditioned stimulus co-terminating with a 0.25 s, 0.4 mA footshock, presented with an average 120 s inter-trial interval (ITI) (ranging from 90-150 s). Prior to sacrifice, all mice were placed back in the testing chambers and were exposed to 5 presentations of the odorant conditioned stimulus (acetophenone) to assess freezing behavior. Freezing was measured throughout acquisition and during testing before sacrifice.

Freezing behavior data analysis

Within session freezing during conditioning and testing was determined as described in Jones et al., 2005. Briefly, for each second of the 5 second activity window,

voltage outputs for each animal were converted to the average voltage output. For each second of the 5 second activity window, averages that were above or below the mean voltage output of the empty cylinder (without a mouse present) were assigned an immobility score of 0 (mobile) or 1 (immobile). For each trial, a percent immobility score was determined by averaging the five immobility scores and multiplying by 100, to generate a score used as the index of freezing. Previous work has shown a high correlation between this described automated freezing index and observational ratings of freezing (Jones et al., 2005).

Zinc Sulfate administration and experimental timelines

Intranasal $ZnSO_4$ was performed as follows; mice were securely scruffed by the neck, and using a 1 mL syringe with a blunt end needle tip, 100 uL of 20mM $ZnSO_4$ in ddH_2O solution was administered into each naris (50 uL per naris). Following administration to the left naris, mice were allowed to rest for 10 minutes before administration to the right naris. Following $ZnSO_4$ administration, mice were closely monitored. Administration protocols yielded a 100% survival rate.

Mice were given 20mM zinc sulfate ($ZnSO_4$) (Sigma) diluted in deionized water or 0.9% saline solution. Mice were restrained by holding the back of the neck for nasal aspirations of zinc sulfate. Using a syringe with a blunted smooth needle, 50 uL was gradually dropped onto the external right nares of an awake unanesthetized mouse such that the zinc sulfate solution was aspirated into the naris through natural inhalation. Mice were allowed to rest for 5-10 minutes and the procedure was then repeated for the left naris. Control mice were treated identically except that 50 uL of saline was aspirated into

each naris. All mice were monitored closely following aspiration (every hour for 3 hours after the procedure, and at 12 hour time points thereafter).

Experiment 3.1: Time course of epithelial recovery following zinc sulfate ($ZnSO_4$) induced ablation of the MOE. 3 groups of C57BL/6J 3 month-old male mice (n=1-2 per group) received intranasal zinc sulfate administrations as described above on Day 0. A fourth group received intranasal saline (0.9% in ddH_2O) at the same time point "Saline, Day 2". 2 days later, 1 group that received intranasal $ZnSO_4$ administration (n=2, "Day 2") and the group that received intranasal saline administration (n=2) were sacrificed by decapitation. Another group that received intranasal $ZnSO_4$ administration was sacrificed 8 days following $ZnSO_4$ administration "Day 8", and finally the last group (n=1) was sacrificed 16 days following $ZnSO_4$ administration "Day 16". For all groups, following sacrifice, MOE were collected and post-fixed for 30 minutes. MOE were then transferred into a decalcification solution (100 mM EDTA, 100 mM EGTA in 1X PBS, pH 7.4) for 1 week at - 4°C, with the decalcification solution refreshed every other day. MOE were then embedded in TissueTek OCT cutting medium on dry ice and sectioned at 16 μm on a Leica cryostat at - 20°C, and mounted on 4 parallel series of slides. Cresyl violet staining was performed and epithelial thickness was measured using ImageJ in 3 regions per naris, and averaged to yield the average epithelial thickness. An overview of all groups and the experimental timeline is provided in Figure 3.2 A.

Experiment 3.2: Investigation of the OB glomeruli 2 days following zinc sulfate ($ZnSO_4$) induced ablation of the MOE. 1 group of C57BL/6J 3 month-old male mice (n=4) received intranasal zinc sulfate administrations as described above on Day 0. A second group (C57BL/6J 3 month-old male mice, n=3) received intranasal saline (0.9%

in ddH_2O) at the same time point. 2 days later ("Day 2"), both groups were sacrificed by decapitation. OB and MOE were collected, dissected, and processed for beta-galactosidase staining as described below. An overview of all groups and the experimental timeline is provided in Figure 3.3 A.

Experiment 3.3: Olfactory fear conditioning 3 days post- zinc sulfate ($ZnSO_4$) induced ablation of the MOE. 2 groups of M71-LacZ 3 month-old male mice (n=4 per group) received intranasal zinc sulfate administrations as described above on Day 0. 3 days following $ZnSO_4$ administration, one group of mice underwent 3 consecutive days of fear conditioning to acetophenone as described above. The other group remained in the home cage and received handling. 2 weeks later mice were sacrificed by decapitation. OB and MOE were collected, dissected, and processed for beta-galactosidase staining as described below. An overview of all groups and the experimental timeline is provided in Figure 3.4 A.

Experiment 3.4: Olfactory fear conditioning followed 1 week later by zinc sulfate ($ZnSO_4$) induced ablation of the MOE. 2 groups of M71-LacZ 3 month old male mice received 3 consecutive days of training to acetophenone as described above. 1 week following training, one of the trained groups (n=5) received intranasal $ZnSO_4$ administration, while the other trained group (n=5) received handling. In parallel, another group of M71-LacZ male mice (n=4) received handling alone during the fear conditioning days, and received $ZnSO_4$ administration at the same time point as the "Training + $ZnSO_4$ administration" group. A fourth group remained in the home cage throughout the experiment, did not receive $ZnSO_4$ administration, and only received handling in the home cage when other groups received experimental manipulations. 2

weeks following $ZnSO_4$ or saline administration, all mice were sacrificed by decapitation. OB and MOE were collected, dissected, and processed for beta-galactosidase staining as described below. An overview of all groups and the experimental timeline is provided in Figure 3.5 A.

EdU administration and experimental timelines

Experiment 3.5: Baseline labeling of M71+ OSNs using EdU. 1 group of M71-GFP 3 month-old male and female mice received seven I.P. injections of EdU (50 mg/kg in 0.9% Saline, 50% DMSO), with one I.P. administration per day for seven consecutive days. One week following the last EdU administration, mice were sacrificed via perfusion and OB and MOE were collected and post-fixed for 2 hours as described below. GFP+ M71 glomeruli were imaged on an inverted fluorescent microscope as described below. MOEs were prepared for sectioning, sectioned on a cryostat, and processed for EdU and GFP immunohistochemistry as described below.

Experiment 3.6: Examining the proliferation of M71+ OSNs following olfactory fear conditioning. 2 groups of M71-GFP, 3 month-old male and female mice (n=4-10 per group) received six I.P. injections of EdU (50 mg/kg in 0.9% Saline, 50% DMSO), with one I.P. administration per day for 6 consecutive days. 1 of the groups of mice (n=10) underwent cued olfactory fear conditioning on the fourth, fifth and sixth day of EdU administration (fear conditioning session began 2 hours following EdU administration). The control group (n=4) remained in the home cage and received handling alone during the equivalent training time points. Three weeks following the last EdU dose, mice received a 5 odor-CS behavioral test to assess freezing. One hour after testing, mice were sacrificed via perfusion and OB and MOE were collected and post-fixed for 2 hours as

described below. GFP+ M71 glomeruli were imaged on an inverted fluorescent microscope as described below. MOEs were prepared for sectioning, sectioned on a cryostat, and processed for EdU and GFP immunohistochemistry as described below. An overview of all groups and the experimental timeline is provided in Figure 3.8 A.

Experiment 3.7: Examining the survival of M71+ OSNs following olfactory fear conditioning. 2 groups of M71-GFP, 3 month-old male and female mice (n=8 per group) received seven I.P. injections of EdU (50 mg/kg in 0.9% Saline, 50% DMSO), with one I.P. administration per day for 7 consecutive days. 4 days following the last dose of EdU administration, one of the groups of mice (n=8) underwent 3 consecutive days of cued olfactory fear conditioning. The control group (n=8) remained in the home cage and received handling alone during the equivalent training time points. 3 weeks following the last fear conditioning session, mice received a 5 odor-CS behavioral test to assess freezing. 1 hour after testing, mice were sacrificed via perfusion and OB and MOE were collected and post-fixed for 2 hours as described below. GFP+ M71 glomeruli were imaged on an inverted fluorescent microscope as described below. MOEs were prepared for sectioning, sectioned on a cryostat, and processed for EdU and GFP immunohistochemistry as described below. An overview of all groups and the experimental timeline is provided in Figure 3.11 A.

Perfusion

Mice from experiments 3.5, 3.6 and 3.7 were anaesthetized and perfused transcardially with 4% paraformaldehyde in 0.1M phosphate buffered saline (PBS) solution (pH 7.4). Olfactory bulbs and MOE were harvested and post-fixed for 2 hours. Olfactory bulbs were then transferred to 1X PBS solution until imaging on an inverted

fluorescent microscope. MOE were transferred into a decalcification solution (100 mM EDTA, 100 mM EGTA in 1X PBS, pH 7.4) for 1 week at 4°C, with the decalcification solution refreshed every other day. MOE were then embedded in TissueTek OCT cutting medium on dry ice and sectioned at 16 µm on a Leica cryostat at - 20°C, and mounted on 10 parallel series of slides.

Beta-galactosidase staining of the MOE OSNs and OB glomeruli

Following sacrifice, MOE and olfactory bulbs of M71-LacZ mice were processed for Beta-galactosidase staining as previously described (Jones et al., 2008; Dias and Ressler, 2014; Morrison et al., 2015). Lateral whole mount MOE and brains were rapidly dissected and placed into 4% paraformaldehyde (wt/vol) for 10 min at ~23°C, after which they were washed three times in 1X phosphate-buffered saline (PBS) for 5 min. MOE and brains were then stained using 45 mg of X-gal (1 mg/ml) dissolved in 600 µl of DMSO and 45 ml of a solution of 5 mM potassium ferricyanide, 5 mM potassium ferrocyanide, and 2 mM MgCl in 1 M PBS, incubated at 37 C for 3 hours.

Quantitation of whole mount M71-positive X-gal-labeled OSNs in the MOE

Following staining, the lateral whole mount MOE was imaged using a microscope-mounted digital camera, and beta-galactosidase-stained blue OSNs were counted manually by experimenters blinded to the experimental groups. 2 experimenters both blinded to the experimental groups carried out this quantitation. MOE that were damaged during MOE extraction following sacrifice were not included in M71 OSN count analyses. Olfactory sensory neuron number was analyzed by 1-way ANOVA followed by Tukey post-hoc tests, and glomerular area to olfactory sensory neuron

number was analyzed by linear regression. Grubbs' test was used to detect outliers; no samples were excluded from analysis of OSN number in the MOE.

RNAscope investigation of the MOE

Samples for RNAscope were fresh frozen following sacrifice by decapitation. MOEs were collected and fresh frozen on dry ice. MOEs were sectioned on a cryostat with 16 um sections. Following sectioning, tissue was stored at -80C until RNAscope protocols, which were followed identically to manufacturer's instructions.

GFP, EdU, TUNEL and Caspase-3 immunohistochemical staining of the MOE

TUNEL staining: Tissue, stored at -80°C was brought to room temperature and a hydrophobic barrier was drawn around the tissue using a PAP pen. Tissue was fixed in 4% PFA for 10 minutes a room temperature. Following three washes in 1X PBS, tissue was incubated in permeabilization solution (0.1% Triton X-100, 0.1% sodium citrate) for 2 minutes on ice. Tissue was then rinsed twice with 1X PBS. TUNEL labeling solution was prepared following directions from the "Roche cell death in situ TMR red" kit and applied to samples for 60 minutes at 37°C. Tissue was then rinsed 3 times in 1X PBS before proceeding the EdU staining.

EdU protocol: Tissue, stored at -80°C was brought to room temperature and a hydrophobic barrier was drawn around the tissue using a PAP pen. Tissue was fixed in 4% PFA for 10 minutes a room temperature. Following 2 washes with 3% bovine serum albumin (BSA) in 1X PBS, tissue was them permeabilized with 0.5% Triton-X 100 in 1X PBS for 20 minutes at room temperature. Tissue was then washed twice with 3% BSA in 1X PBS, followed by incubation with Click-iT reaction cocktail containing Click-iT reaction buffer, $CuSO_4$, Alexafluor 647 Azide, and reaction buffer additive for 30

minutes at room temperature while protect from light, according to manufacturer's instructions. Tissue was then washed one with 3% BSA in 1X PBS, followed by 2 washes with 1X PBS before proceeding to GFP immunohistochemistry.

GFP immunohistochemistry protocol: Following the EdU protocol, tissue was blocked (10% normal goat serum, 3% BSA in 0.1M Tris-HCl, 0.15M NaCl) for 30 minutes at room temperature. Samples were then incubated with primary antibody diluted in blocking solution for 60 minutes at room temperature (Anti-GFP Rabbit, 1:1000). Following three washes with 0.05% Tween-20 in 0.1M Tris-HCl, 0.15M NaCl, samples were incubated in secondary antibody diluted in blocking solution for 30 minutes at room temperature (Alexa 488 Goat-anti-rabbit 1:1000, Invitrogen A11008). Slides were then washed three times with 0.05% Tween-20 in 0.1M Tris-HCl, 0.15M NaCl, counterstained with Hoescht (1:1000 in 1X PBS) for 10 minutes, washed twice with 1X PBS, and coverslipped with mowiol and stored at 4°C for short-term storage until imaging.

Quantitation of M71-positive and EdU-positive OSNs in the MOE

All MOE sections from experiments 3.5, 3.6 and 3.7 were imaged at 10X on a confocal microscope using the montage feature to create a 3x3 mm tiled image. M71+ OSN cell bodies, as well as M71+ cell bodies co-localized with EdU+ were manually counted in ImageJ by an experimenter blinded to experimental groups. 10 sections per animal were used in each quantitation and OSN counts were summed across these 10 sections.

Measurement of glomerular area in the olfactory bulb

M71-GFP or M71-LacZ glomeruli were imaged using a microscope-mounted digital camera to capture high-resolution images of dorsal and medial glomeruli at 10X

magnification. Pixel brightness distribution was exported in NIH ImageJ as gray levels from 0 = black to 255 = white. GFP of X-gal-labeled glomerular area was quantified as pixels, less than a set threshold gray level of 150 (optimized for axon versus background). Each glomerulus was traced using the lasso tool in ImageJ and the area was recorded using the histogram tool. Glomeruli that were damaged due to olfactory bulb extraction following sacrifice were not included in glomerular area analyses. Glomerular area was analyzed by Student's *t*-test. Grubbs' test was used to detect outliers; no samples were excluded from analysis for glomerular area in the olfactory bulb.

Statistics

Freezing was analyzed by two-way ANOVA (Fig. 3.8 B, 3.11 C) or Student's t-test (Fig. 3.8 D, 3.11 C). Glomerular area was analyzed by one-way ANOVA (Fig. 3.4 B-D, 3.5 B-D) or Student's *t*-test (Fig. 3.3 C-E, 3.9 A-C, 3.12 B-D). Olfactory sensory neuron number was analyzed by Student's t-test (Fig. 3.7 B, 3.10 B-D, 3.13 B-D, 3.14 A-B, 3.15 A-B). All ANOVA main effects or interactions were followed by Tukey *post hoc* tests, unless otherwise noted.

Results

RNAscope in the mouse MOE.

RNAscope provides a highly specific and sensitive method for the detection of mRNAs in fresh frozen tissues. The present work demonstrates a method for successfully labeling *M71* mRNA in fresh frozen tissue obtained for C57Bl/6J mice (Figure 3.1).

Experiment 3.1: Time course of epithelial recovery following zinc sulfate ($ZnSO_4$) induced ablation of the MOE.

We performed a time course of sacrifice following zinc sulfate-induced ablation of the nasal epithelium to investigate the regeneration of the MOE. Intranasal perfusion of zinc sulfate is one of the most commonly used methods to destroy OSNs (Alberts and Galef, 1971; Ducray et al., 2002), and previous work has demonstrated that the intranasal application of zinc sulfate produces complete ablation of OSNs in the MOE and total disruption of functional connections from the olfactory epithelium to the main olfactory bulb (McBride et al., 2003). The present set of experiments performed an even less invasive procedure by using awake un-anesthetized mice, and by using a procedure where solution is dropped onto the external nares (rather than injected into the nasal cavity).

2 days following bilateral zinc sulfate intranasal administration, there was a complete ablation of the nasal epithelium, as quantified by epithelial thickness and observable by whole mount X-Gal staining of M71-LacZ MOE (Figure 3.2 A-E). Epithelial thickness progressively re-acquired a multilayered structure and showed gradual increases in epithelial thickness as measured at eight days following ablation (Figure 3.2 B-C). Epithelial thickness continued to increase to almost complete regeneration at 16 days following ablation (Figure 3.2 B-C).

Experiment 3.2: Investigation of the OB glomeruli 2 days following zinc sulfate ($ZnSO_4$) induced ablation of the MOE.

M71 glomeruli remained intact 2 days following zinc sulfate ablation, despite the loss of OSNs in the MOE (Figure 3.3 A-E).

Experiment 3.3: Olfactory fear conditioning 3 days post- zinc sulfate ($ZnSO_4$) induced ablation of the MOE.

Zinc sulfate ablation of the olfactory epithelium followed 3 days later by cue specific olfactory fear conditioning was used to investigate the effect of olfactory fear conditioning during a highly plastic period of olfactory epithelium regeneration (Figure 3.4 A). When mice were fear conditioned during an early period of MOE regeneration following zinc sulfate ablation, we did not observe any difference in M71 glomerulus area between a "Zinc sulfate + training" group and the "Zinc sulfate + no training" control group (Figure 3.4 B-D). These data suggest that M71 OSNs are required at the time of training to observe the main effect of enhanced glomerulus area. The effect of enhanced glomerulus area following training is likely not due to training induced increases in receptor choice, as presumably during this early phase of regeneration stem cells are in the early stages of M71 differentiation. It is however, possible that our glomerular measurements reflect the "pre-ablation" glomerulus which is still intact based on the time course of OB glomeruli following ablation (Figure 3.3), although the experimental and control animals should have equivalent amounts of remaining "pre-ablation" staining, and thus any increases over baseline are due to training. Previous data combined with these studies suggest that a steady-state, but not actively regenerating epithelial layer is required for the activity-dependent increase in M71 representation. These results thus support a hypothesis in which training to acetophenone leads to an enhanced survival, rather than proliferation, of M71 specific neurons. This hypothesis will be investigated in further detail below.

Experiment 3.4: Olfactory fear conditioning followed 1 week later by zinc sulfate ($ZnSO_4$) induced ablation of the MOE.

In addition to investigating the effect of olfactory fear conditioning during a highly plastic period of MOE regeneration, we also performed a separate experiment in which mice underwent olfactory fear conditioning to acetophenone, and then received zinc sulfate or saline intranasal administration one week following the last fear conditioning session. Mice were sacrificed 2 weeks following intranasal administration, and glomerulus area was investigated (Figure 3.5). Training dependent increases in M71-specific glomerular area were maintained following zinc sulfate induced ablation of the MOE (Figure 3.5 B-D). These data, combined with results from Figure 3.4 suggest that M71-expressing OSNs are required at the time of training to observe the increased structural enhancements resulting from cue-specific training; training induced increases in glomerulus area are maintained following ablation.

EdU and TUNEL labeling of the mouse MOE

To investigate the rates of M71 specific OSN cell turnover, we utilized EdU labeling of the mouse MOE (Figure 3.6). For future experimental use, we also established the use of TUNEL co-labeling with EdU to assess more detailed rates of cell death and cell turnover. EdU is a nucleoside analog of thymidine that is incorporated in the DNA during active DNA synthesis. The EdU labeling method is based on a click reaction in which EdU administered intraperitoneally contains an alkyne group, which, in postmortem tissue, reacts and binds to an azide group co-labeled with a fluorescent Alexa Fluor dye. Based on the timing of EdU administration, this method may be used to investigate the proliferation and/or survival of neurons in response to an environmental

stimulus or experience, such as olfactory fear conditioning. TUNEL labeling protocols were also developed for future use in investigating dynamics of cell turnover (no TUNEL labeling was carried out in the present fear conditioning experiments). TUNEL is a common method for detecting DNA fragmentation resulting from apoptotic signaling cascades; the assay relies on the presence of DNA nicks that can be identified by terminal deoxynucleotidyl transferase, or TdT, which is an enzyme that catalyzes the addition of fluorescently labeled dUTs. TUNEL labeling thus allows of the labeling of cells undergoing cell death/apoptosis. Combined with anti-GFP immunohistochemistry in M71-GFP transgenic mice, EdU and TUNEL labeling may be used to identify M71 specific neurons labeled with EdU and/or TUNEL (Figure 3.6 A-C). Thus we were able to successfully implement a method and protocol for investigating rates of cell turnover in the MOE, although for the remaining experiments, we will focus exclusively on EdU labeling as a read out of cell turnover.

Experiment 3.5: Baseline labeling of M71-expressing OSNs using EdU.

In order to label and track EdU labeled M71-expressing OSNs in combination with olfactory fear behavior, we first performed an EdU pulse chase experiment in which behavior and odor naïve mice received seven I.P. doses of EdU (one administration per day for seven consecutive days). Mice were sacrificed seven days following the last EdU dose and MOEs were processed for M71-GFP and EdU labeling. Baseline labeling of M71-expressing OSNs using EdU revealed very low levels of M71/EdU co-localization (Figure 3.7 B-C). On average, only 3.3 M71-expressing OSNs per MOE were co-localized with EdU. Despite such low levels of co-localization, we hypothesized that a large labeling pulse followed by olfactory fear conditioning would lead to an increase in

EdU labeled OSNs that may then be tracked across subsequent weeks. We further explored the proliferation and survival of M71-expressing OSNs in combination with olfactory fear conditioning with differing EdU labeling strategies, as described below.

Experiment 3.6: Examining the proliferation of M71-expressing OSNs following olfactory fear conditioning.

We first sought to label neurons undergoing mitosis at the time of training, in order to investigate the effect of olfactory fear conditioning on M71 specific cell proliferation. To examine the proliferation of M71-expressing OSNs, mice received three consecutive days of EdU administration (one I.P. EdU dose per day) directly prior to training, as well as 1 hour pre-training during each of three consecutive days of odor fear conditioning (Figure 3.8 A). We hypothesized that a short pulse of EdU directly prior to training and during training would label neurons undergoing mitosis at the time of olfactory fear conditioning. If olfactory fear conditioning to acetophenone leads to an enhanced proliferation of M71 specific OSNs, we would then observe an increased number of M71 OSNs co-localized with EdU at a 3 week time point following fear conditioning. Control groups received the same quantity and timing of EdU doses, but did not undergo olfactory fear conditioning, and instead received handling in the home cage.

Mice undergoing olfactory fear conditioning to acetophenone displayed enhanced freezing to the CS across training sessions (Figure 3.8 B), and also had significantly increased freezing to the odor CS compared to home cage controls upon olfactory fear testing three weeks after conditioning (Figure 3.8 C-D). Replicating our previous findings of enhanced M71-specific glomerulus area following fear conditioning in M71-LacZ

transgenic mouse lines, we also found that M71-GFP transgenic mice had trending increases in M71-specific combined glomerulus area (Figure 3.9 A) 3 weeks following fear conditioning to acetophenone compared to home cage controls. Despite the trending increase in M71+ glomerulus area with training to acetophenone, we did not observe an increase in the overall number of M71-expressing OSNs in the MOE with training (Figure 3.10 A, C). Furthermore, we did not observe a significant difference in the number of M71-expressing OSNs co-localized with EdU in mice fear conditioned to acetophenone compared to home cage controls (Figure 3.10 A-D). Additionally, there was no significant correlation between individual measures of 1) M71 glomeruli and M71 OSNs, or 2) M71 glomeruli and M71 OSNs co-localized with EdU (data not shown). There was no difference in the overall counts of M71 OSNs, therefore the signal to noise loss makes it difficult to measure increases in OSN number, however, as in previous data (Bressel et al., 2016; Dias and Ressler, 2013; Jones et al., 2008b; Morrison et al., 2015) glomerular area was correlated with OSN number, thus our negative results are potentially a detection problem rather than a difference in the system.

Experiment 3.7: Examining the survival of M71-expressing OSNs following olfactory fear conditioning.

To examine the survival of M71+ OSNs following olfactory fear conditioning to acetophenone, we administered a 7-day pulse of EdU, as in experiment 3.5 (Figure 3.7). 4 days after the last EdU administration, 1 group of mice underwent three days of olfactory fear conditioning to acetophenone (Figure 3.11 A). Control mice received EdU at the same doses and time points, but did not undergo training to acetophenone and instead received handling in the home cage. We hypothesized that a large pulse of EdU prior to

training would maximize the number of EdU labeled mature neurons at the time of training that may then be tracked to a 3-week time point following learning.

Mice that underwent fear conditioning to acetophenone displayed increases in freezing to the CS across training sessions (Figure 3.11 B). 3 weeks following training, mice that were fear conditioned to acetophenone had significantly increased freezing to the odor CS compared to HC controls (Figure 3.11 C-D). At the level of the OB, mice that were fear conditioned to acetophenone had significantly larger dorsal and combined M71+ glomeruli compared to controls (Figure 3.12). Similarly to experiment 3.6, although we observed an increase in M71+ glomerulus area with training to acetophenone, we did not observe an overall increase in the number of M71-GFP neurons in the MOE following training (Figure 3.13 A, C). Additionally, there was no significant correlation between individual measures of 1) M71 glomeruli and M71 OSNs, or 2) M71 glomeruli and M71 OSNs co-localized with EdU (data not shown). However, as described above in previous data (Bressel et al., 2016; Dias and Ressler, 2013; Jones et al., 2008b; Morrison et al., 2015) glomerular area is correlated with OSN number, thus our negative results are potentially a detection problem rather than a difference in the system. Follow-up experiments could use confocal z-stack imaging protocols to gain a more accurate count of M71-GFP OSNs.

However, unlike experiment 3.6, there was a significant increase in the number of M71+ OSNs co-localized with EdU (Figure 3.13 A, B, D) in mice fear conditioned to acetophenone compared to home cage controls. These data suggest that cue specific olfactory fear conditioning to acetophenone resulted in an enhanced survival of M71 specific OSNs in the MOE (Figure 3.14, 3.15). These data, however, should be taken in

the context of not observing (based on our current detection methods) the main effect of increased M71+ OSNs following fear conditioning to acetophenone, despite the enhancement in M71 and EdU co-localization. Comparing the present experiment with results in which EdU methods were used to label 1) M71 OSNs at baseline control levels, and 2) M71 OSNs undergoing mitosis at the time of training, experiment 3.7 labeled mature M71 OSNs at the time of training. Our results from these studies combining EdU labeling with olfactory fear training suggest that the training induced enhancements in M71 structure are the result of M71 specific OSN survival rather than proliferation (Figure 3.14, 3.15).

Discussion

To investigate the regulation of cell turnover in the olfactory epithelium and its role in learning-induced increases in structural plasticity, we used two approaches; 1) zinc sulfate induced ablation of the olfactory epithelium and 2) EdU labeling of M71 specific OSNs. Consistent with previously published work, we observed a complete ablation of the MOE 2 days following zinc sulfate intranasal administration (Figure 3.2 A-E). MOE thickness progressively re-acquired a multilayered structure as measured at eight and sixteen days following ablation. Despite observed ablation of the MOE two days following zinc sulfate administration, we did not observe a degeneration of the M71 specific glomeruli in the OB (Figure 3.3 A-E). This discrepancy highlights the need for a more thorough characterization of the degeneration and regeneration of axons and their glomeruli following zinc sulfate ablation. Such follow-up experiments would necessitate the use of multiple tracers to be able to identify degenerating compared with new fibers entering the OB. Future experiments could investigate the time course of glomerular

degeneration and regeneration, however, tracing and labeling techniques will be necessary. Using the current transgenic model it is difficult to discern degenerating compared with newly generated axons. Notably, degenerating axons may serve as a tract for incoming regenerated axons; homotypic interactions may occur, in which leftover M71 fibers release proteins to guide developing M71 fibers into the glomeruli. Previous work has found that zinc sulfate produces total disruption of functional connections from the olfactory epithelium to the main olfactory bulb, as measured by anterograde transport of WGA following the administration of saline or zinc sulfate (Slotnick et al., 2010). These data are in parallel with our observation of remaining M71 fibers in the OB following zinc sulfate ablation of the MOE; we hypothesize that the fiber tracts may still be present following ablation (although they do not take up WGA, thus leaving a visible "space" in the OB) despite the cell body no longer being present in the MOE.

These data on the regeneration of the MOE and OSN axons also provide a specific context for understanding experiments 3.3 and 3.4 in which we performed ablation of the MOE either prior to or following fear conditioning to acetophenone and observed M71-specifc glomerulus area. In experiment 3.3 we fear conditioned mice to acetophenone 3 days after zinc sulfate ablation, during the putative window of most active MOE regeneration, and we did not observe any difference in M71-specific glomerulus area between mice that received training compared to controls. In experiment 3.4 we investigated the effect of zinc sulfate ablation 1 week after olfactory fear conditioning to acetophenone, and found that the training dependent increases in M71-specific glomerulus area were maintained if zinc sulfate ablation was performed after the conditioning event. Together, these data suggest that 1) M71-expressing OSNs are

required at the time of training to observe structural enhancements in M71-specific glomerulus area, and 2) enhancements in M71 structure following training are not due to training induced increases in receptor choice. Follow-up experiments will need to confirm these findings at the level of M71-expressing OSNs in the MOE based on the intact profile of M71 glomeruli 2 days following zinc sulfate administration.

To further explore the role of OSN turnover in the MOE, we performed EdU labeling of M71-expressing OSNs in combination with fear behavior. Data from experiments 3.5, 3.6 and 3.7 suggest that the cue specific olfactory fear conditioning to acetophenone results in an enhanced survival of M71 specific OSNs in the MOE, rather than a selective proliferation of this OSN population, as evidenced by greater number of M71-expressing OSNs co-localized with EdU in mice trained to acetophenone with EdU labeling 4 days prior to training. In the present set of experiments we performed three different labeling approaches; one to assess baseline levels of M71/EdU co-localization (Figure 3.7 B-C), one to label neurons undergoing mitosis at the time of training (Figure 3.10 A-D), and finally one to label mature neurons at the time of training, and track their survival (Figure 3.13 A-D). Given the short half-life of EdU (about 2-3 hours), it is possible that the present experimental parameters for EdU administration did not capture the full picture of M71-expressing cell turnover. An excellent follow-up experiment would be to implant osmotic mini-pumps that would continuously deliver EdU over an extended period of time, thus labeling many more M71-expressing OSNs undergoing cell turnover. Despite these limitations, we demonstrate an enhanced survival of M71 specific OSNs when we used EdU to label mature neurons and track their survival following fear conditioning to acetophenone.

The mechanisms by which fear conditioning to acetophenone leads to enhanced M71 specific cell survival remain to be determined. One potential mechanism may be the enhanced signaling of the neurotrophic factor BDNF at its receptor TrkB. The role for BDNF-TrkB signaling in the enhancement of M71 specific survival and representation will be investigated in greater detail in Chapter 4. Previous research has also shown that noradrenaline (NA) may be a potential candidate governing the integration and survival of newly born neurons (Moreno et al., 2012; Sultan et al., 2010; Vinera et al., 2015), and thus may also be an interesting candidate for further investigation.

In the present chapter, we also successfully performed RNAscope in the MOE as well as triple labeling of TUNEL, EdU, and M71 labeled OSNs in the MOE (Fig. 3.1 and 3.6). Our work shows that RNAscope may be a powerful tool for future use in primary olfactory tissues that will allow for the investigation of many different odorant receptor populations in the same tissue samples, and without the need for multiple transgenic mouse lines. Such an approach will be essential for the future comparison of multiple odorant receptor ligand pairs (within the same tissue sample) and their role in fear learning and memory. Additionally, future experiments could use the described triple labeling protocols to investigate rates of cell death (by using TUNEL) in combination with olfactory fear conditioning to gain a greater understanding of the dynamics of cell turnover in the MOE (Cowan et al., 2001; Deckner et al., 1997; Graziadei and Graziadei, 1979; Holcomb et al., 1995; Voyron et al., 1999; Magrassi and Graziadei, 1995). A time course of EdU and TUNEL labeling following olfactory fear conditioning would additionally provide interesting insight into the timing of structural increases. In addition to proliferation and survival, neuronal apoptosis is critical in both the developmental and

the adult shaping of the olfactory system (Cowan and Roskams, 2002), and previous work has suggested that apoptosis (as assessed by TUNEL labeling) is a major regulator of OSN turnover (Deckner et al., 1997). It was once believed that OSNs had a fixed and finite lifespan of about 1 month (Graziadei et al., 1978; Moulton, 1974). It is now known, as is demonstrated here, that the surrounding environment can heavily influence the longevity of OSNs (Farbman, 1990); while some OSNs have lifespans exceeding 3 months (Mackay-Sim and Kittel, 1991), most OSNs have a lifespan ranging from 30-40 days (Caggiano et al., 1994; Hunter et al., 1994), though the majority of these studies have been performed in rat models rather than in mice. Bulbectomy models have been used to show that the olfactory bulbs provide critical trophic support to maintain OSNs (Schwob, 2002), and thus, learning dependent trophic factor production by the OB may further enhance the survival by decreasing OSN cell death. Furthermore, increases in cell death are observed in newly generated immature neurons ranging from 6-7 days old, a time point that corresponds with the stage at which the axons of immature OSNs make contact with the OB (Carr and Farbman, 1992, 1993). These studies from Carr and Farbman support our current model in which training affects the survival of mature neurons rather than the selective proliferation of OSNs, as presumably newly born OSNs do not receive the same trophic support from the OB and are thus subject to enhanced rates of apoptosis.

Recent work on the role of neuron-glia communication is also intriguing in the context of shaping olfactory system plasticity. Complement proteins are present in developing CNS synapses during periods of active synapse elimination. Within this system synapses are “tagged” with complement proteins and are later eliminated by

microglial cells that express receptors for the associated complement proteins; furthermore, “tagging” and elimination by microglia appears to be regulated by neuronal activity (Bialas and Stevens, 2013; Chung et al., 2015; Hong et al., 2016; Stephan et al., 2012; Stevens et al., 2007; Wu et al., 2015). This classical complement cascade has been shown to regulate brain plasticity during development and also in adulthood in neurodegenerative diseases and injury to the central nervous system (Stephan et al., 2012). Given the activity dependent elimination of synapses by microglia, it would be interesting to investigate a role for microglia within the present set of experiments; in the context of olfactory learning dependent neuronal turnover in the MOE.

Based on our results from Chapter 2 demonstrating a reversal in M71 structure following cue specific extinction; future experiments should investigate the effects of extinction on the dynamics of OSN turnover in the MOE. Presumably, following extinction we would observe decreases in M71-specific survival and increases in M71-specific cell death, which would ultimately lead to decreases in the observed number of M71-expressing OSNs and size of the M71-specific glomeruli. Overall, the data presented in this chapter provide evidence for the odorant receptor population specific survival as a potential mechanism underlying the learning induced enhancements in OSN structural plasticity following cue specific olfactory fear conditioning.

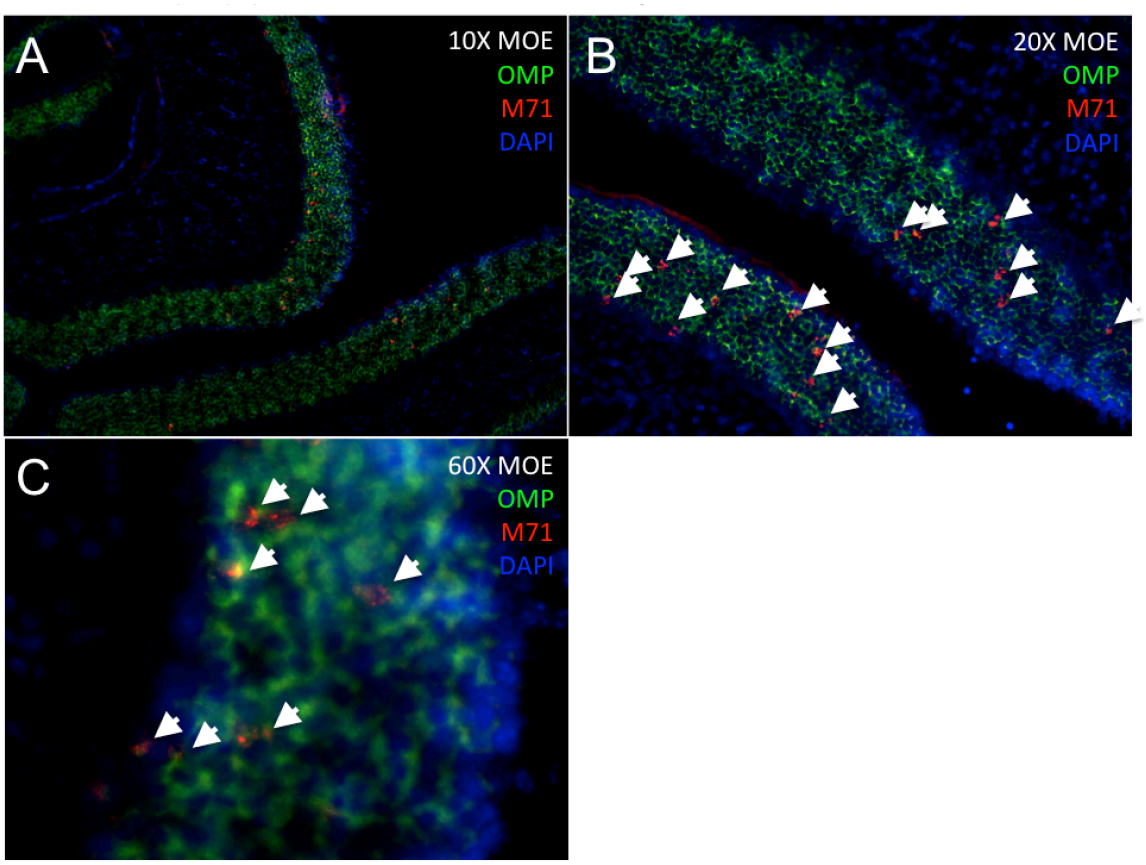

Figure 3.1: RNAscope in the mouse MOE. RNAscope using OMP (green) and M71 (red) probes in the mouse MOE. Tissue is counterstained with DAPI and shown at 10X (a), 20X (b) and 60X (c). White arrows indicate *M71* mRNA.

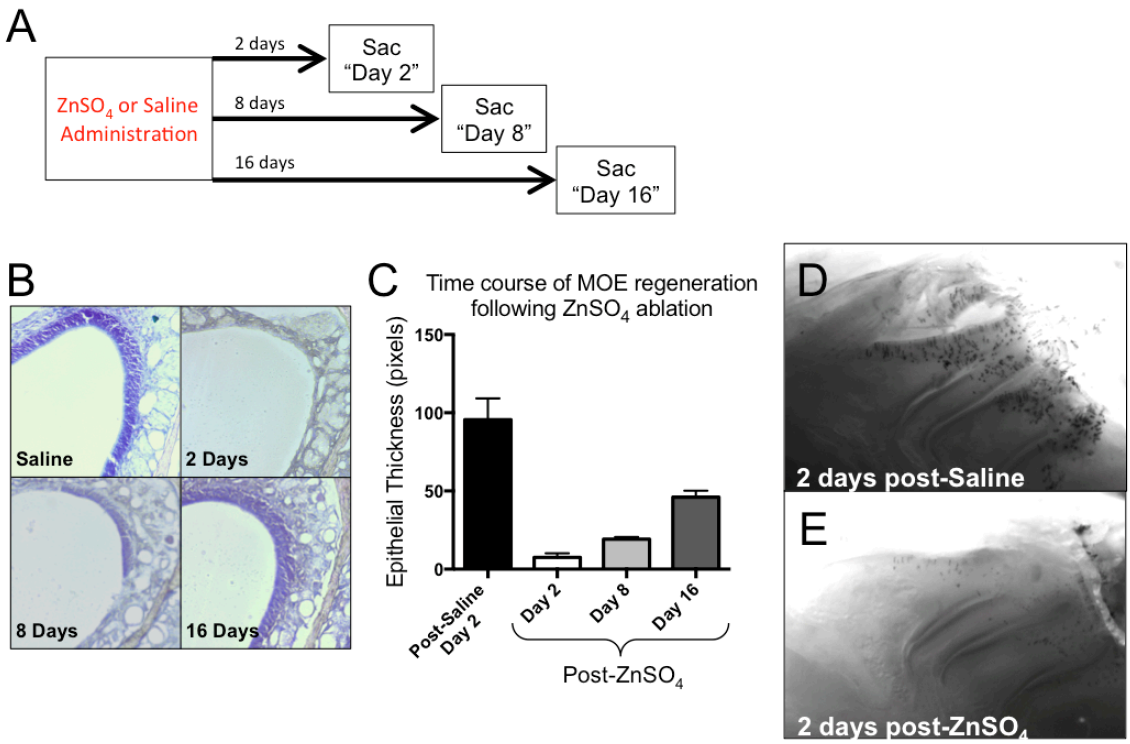

Figure 3.2: Time course of MOE recovery following zinc sulfate induced ablation. (a) Experimental timeline displaying time course of sacrifice following zinc sulfate or saline administration. (b) Regeneration of the MOE following $ZnSO_4$ administration. Epithelial thickness is intact following intranasal saline administration. Complete ablation of the MOE is observed 2 days after $ZnSO_4$ administration. MOE is partially regenerated at 8 days following $ZnSO_4$ administration. MOE regeneration is observed by 16 days following $ZnSO_4$ administration. (c) Quantitation of MOE thickness 2 days post-saline administration, 2 , 8 and 16 days post $ZnSO_4$ administration. Whole mount M71-positive X-gal labeled OSNs in the MOE 2 days post-saline (d) compared to 2 days post $ZnSO_4$ administration (e). Data presented as mean +/- s.e.m..

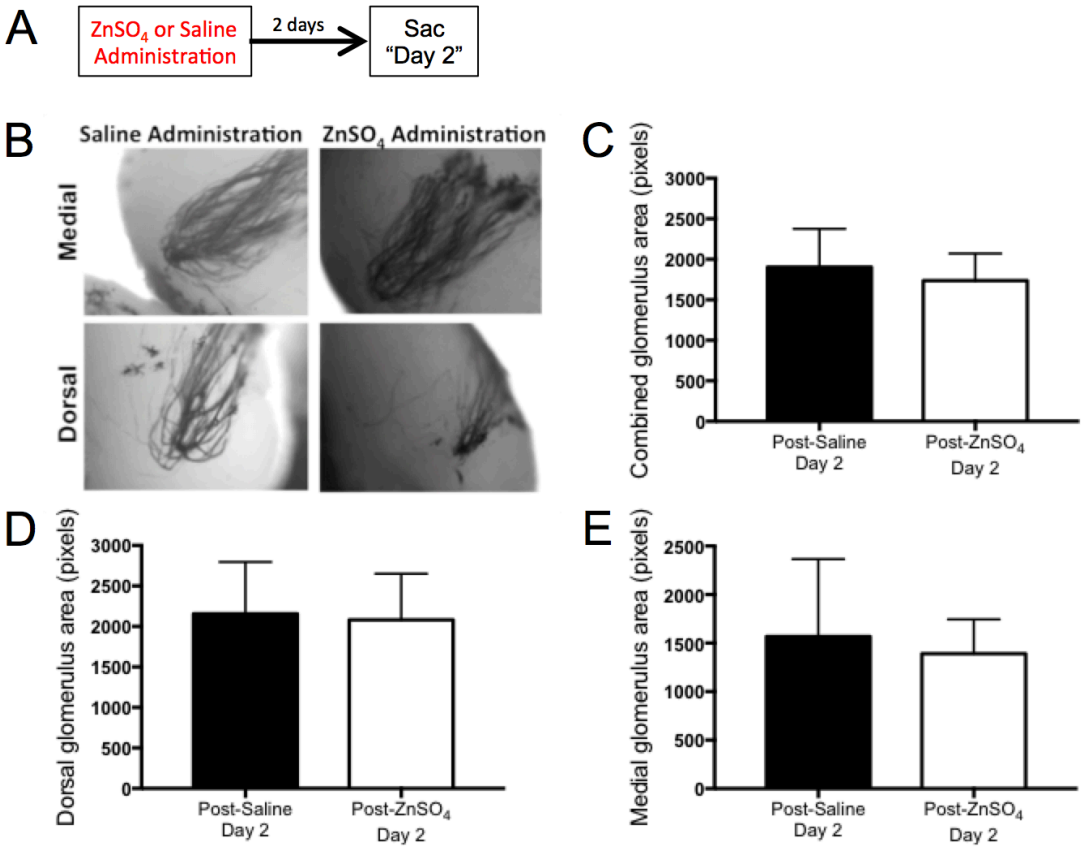

Figure 3.3: Olfactory bulb glomeruli 2 days post-zinc sulfate administration. (a) Experimental timeline of sacrifice 2 days following zinc sulfate or saline administration. (b-e) There is no significant difference in glomerular area 2 days following saline administration (black bar) compared to 2 days following $ZnSO_4$ administration (white bar). (c) M71-LacZ combined glomerulus area: Post-Saline Day 2 vs. Post- $ZnSO_4$ Day 2, Student's t-test, P= 0.78. (d) M71-LacZ dorsal glomerulus area: Post-Saline Day 2 vs. Post- $ZnSO_4$ Day 2, Student's t-test, P=0.93. (e) M71-LacZ medial glomerulus area: Post-Saline Day 2 vs. Post- $ZnSO_4$ Day 2, Student's t-test, P=0.81. Data presented as mean +/- s.e.m..

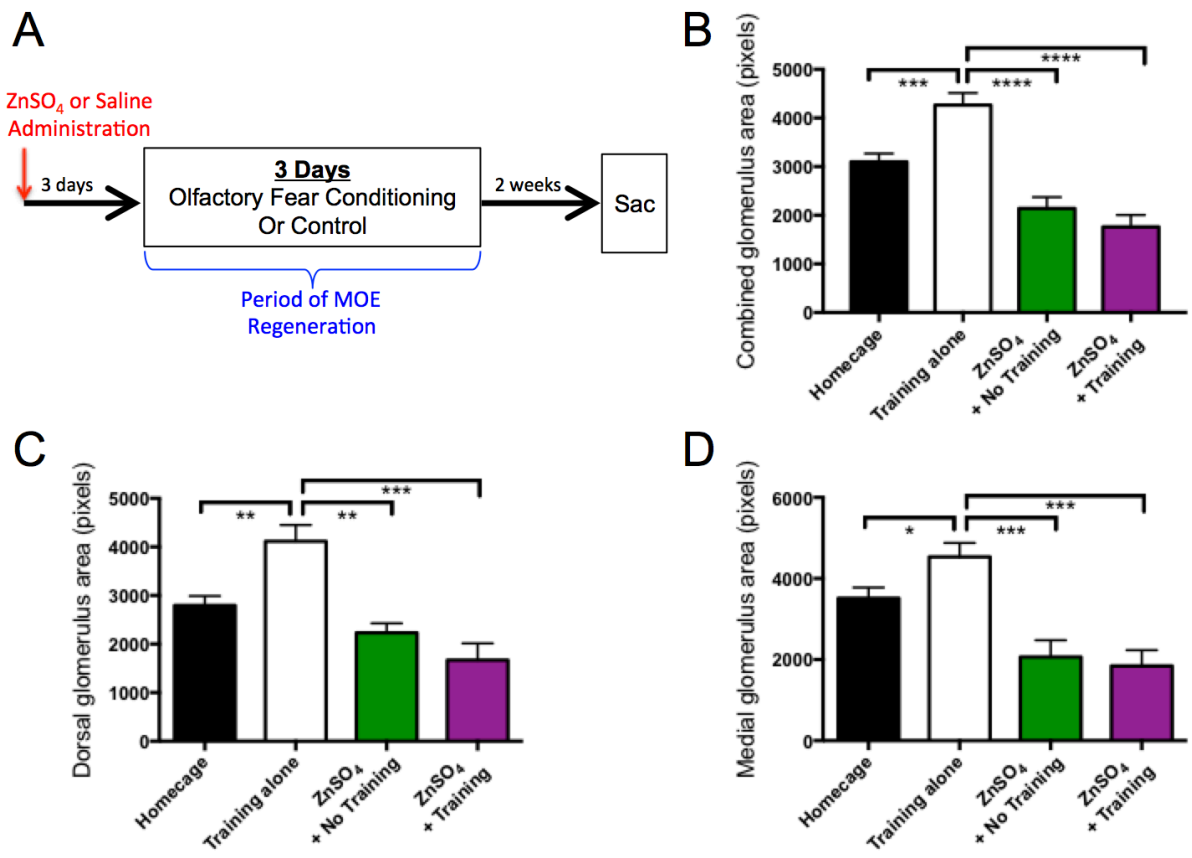

Figure 3.4: Olfactory fear conditioning during a period of active MOE regeneration has no effect on M71+ glomerulus area. (a) Experimental time line of zinc sulfate or saline administration followed by olfactory fear conditioning and sacrifice. (b-c) Glomerular area is greater in training to acetophenone alone groups (white bar) compared to home cage (black bar), $ZnSO_4$ + No Training (green bar), and $ZnSO_4$ + Training (purple bar) groups. Additionally, there is no significant difference between '$ZnSO_4$ + No Training' and '$ZnSO_4$ + Training' groups. (b) M71 combined glomerular area (M71-LacZ: Homecage, n=28; Training alone, n=25; $ZnSO_4$ + No Training, n=11; $ZnSO_4$ + Training, n=10; ANOVA, P<0.0001, F(3,70)=1.045; Homecage versus Training alone, P=0.0004; Homecage versus $ZnSO_4$ + No Training, P=0.04; Homecage versus $ZnSO_4$ + Training, P=0.003; Training alone versus $ZnSO_4$ + No Training, P<0.0001; Training alone versus $ZnSO_4$ + Training, P<0.0001; $ZnSO_4$ + No Training versus $ZnSO_4$ + Training, n.s. P=0.81). (c) M71 dorsal glomerular area (M71-LacZ: Homecage, n=16; Training alone, n=16; $ZnSO_4$ + No Training, n=5; $ZnSO_4$ + Training, n=5; ANOVA, P<0.0001, F(3,38)=0.7326; Homecage versus Training alone, P=0.004; Homecage versus $ZnSO_4$ + No Training, n.s. P=0.71; Homecage versus $ZnSO_4$ + Training, n.s. P=0.16; Training alone versus $ZnSO_4$ + No Training, P=0.0051; Training alone versus $ZnSO_4$ + Training, P=0.0002; $ZnSO_4$ + No Training versus $ZnSO_4$ + Training, n.s. P=0.82). (d) M71 medial glomerular area (M71-LacZ: Homecage, n=12; Training alone, n=9; $ZnSO_4$ + No Training, n=6; $ZnSO_4$ + Training, n=5; ANOVA, P<0.0001, F(3,28)=0.1422; Homecage versus Training alone, n.s. P=0.09; Homecage versus $ZnSO_4$ + No Training, P=0.02; Homecage versus $ZnSO_4$ + Training, P=0.01; Training alone versus $ZnSO_4$ + No

Training, P=0.0002; Training alone versus $ZnSO_4$ + Training, P=0.0002; $ZnSO_4$ + No Training versus $ZnSO_4$ + Training, n.s. P=0.98). Data presented as mean +/- s.e.m. *P<0.05, **P<0.01, ***P<0.001, ****P<0.0001.

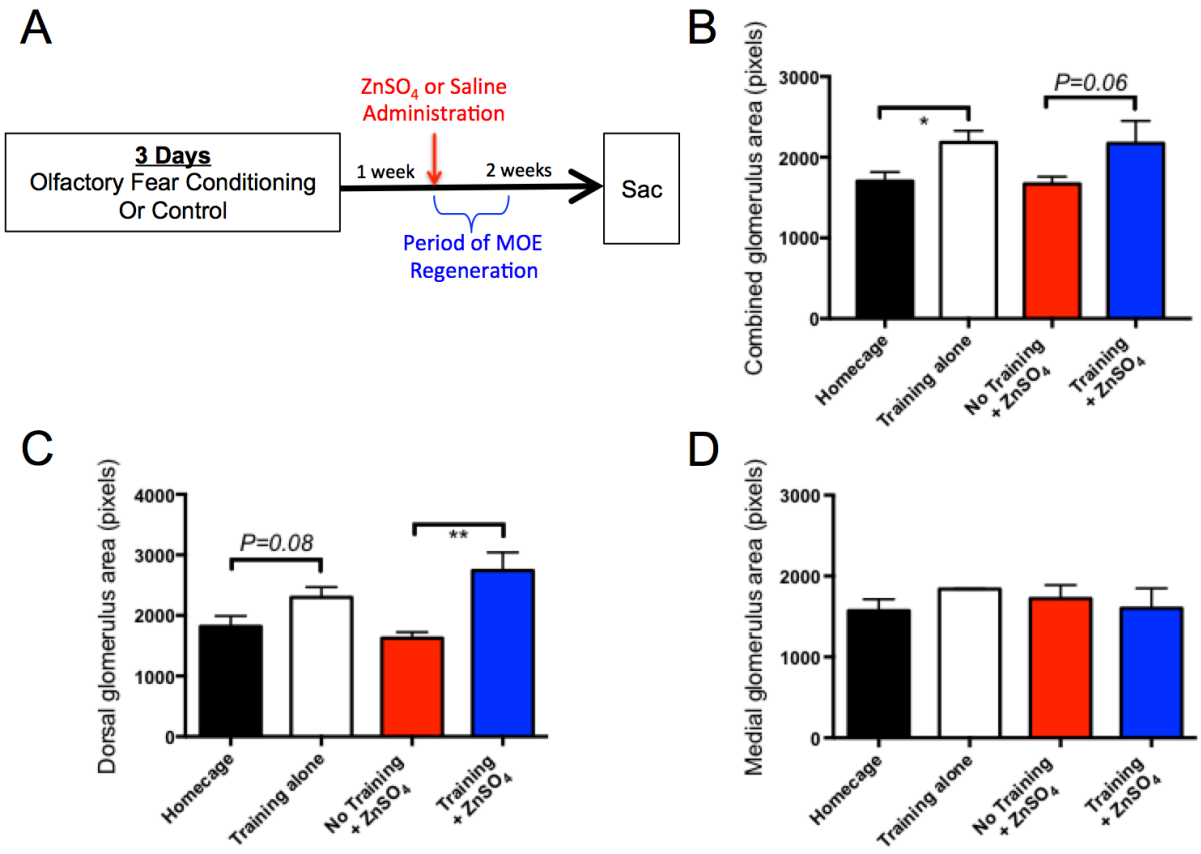

Figure 3.5: Training-dependent increases in M71+ glomerulus areas are maintained following zinc sulfate induced ablation. (a) Experimental time line of zinc sulfate or saline administration 1 week following olfactory fear conditioning. (b-c) Glomerular area is greater in training to acetophenone alone groups (white bar) compared to home cage (black bar) for combined glomerulus area groups. Additionally, there is a significant increase in combined and dorsal glomerulus area in the 'Training + $ZnSO_4$' group (blue bar) compared to 'No Training + $ZnSO_4$' group (red group). (b) M71 combined glomerular area (M71-LacZ: Homecage, n=17; Training alone, n=8; No Training + $ZnSO_4$, n=11; Training + $ZnSO_4$, n=8; ANOVA, P=0.03, F(3,40)=2.594; Homecage versus Training alone, P=0.02; Homecage versus No Training + $ZnSO_4$, n.s. P=0.99; Homecage versus Training + $ZnSO_4$, n.s. P=0.14; Training alone versus No Training + $ZnSO_4$, n.s. P=0.13; Training alone versus Training + $ZnSO_4$, n.s. P>0.99; No Training + $ZnSO_4$ versus Training + $ZnSO_4$, n.s. P=0.06). (c) M71 dorsal glomerular area (M71-LacZ: Homecage, n=9; Training alone, n=6; No Training + $ZnSO_4$, n=6; Training + $ZnSO_4$, n=4; ANOVA, P=0.003, F(3,21)=1.774; Homecage versus Training alone, P=0.08; Homecage versus No Training + $ZnSO_4$, P=n.s.; Homecage versus Training + $ZnSO_4$, P<0.05; Training alone versus No Training + $ZnSO_4$, P=n.s.; Training alone versus Training + $ZnSO_4$, P=n.s.; No Training + $ZnSO_4$ versus Training + $ZnSO_4$, P<0.01). (d) M71 medial glomerular area (M71-LacZ: Homecage, n=8; Training alone, n=2; No Training + $ZnSO_4$, n=5; Training + $ZnSO_4$, n=4; ANOVA, P=n.s., F(3,15)=0.7574; Homecage versus Training alone, P=n.s.; Homecage versus No Training + $ZnSO_4$, P=n.s.; Homecage versus Training + $ZnSO_4$, P=n.s.; Training alone versus No

Training + $ZnSO_4$, P=n.s.; Training alone versus Training + $ZnSO_4$, P=n.s.; No Training + $ZnSO_4$ versus Training + $ZnSO_4$, P=n.s.). Data presented as mean +/- s.e.m. *P<0.05, **P<0.01, ***P<0.001, ****P<0.0001.

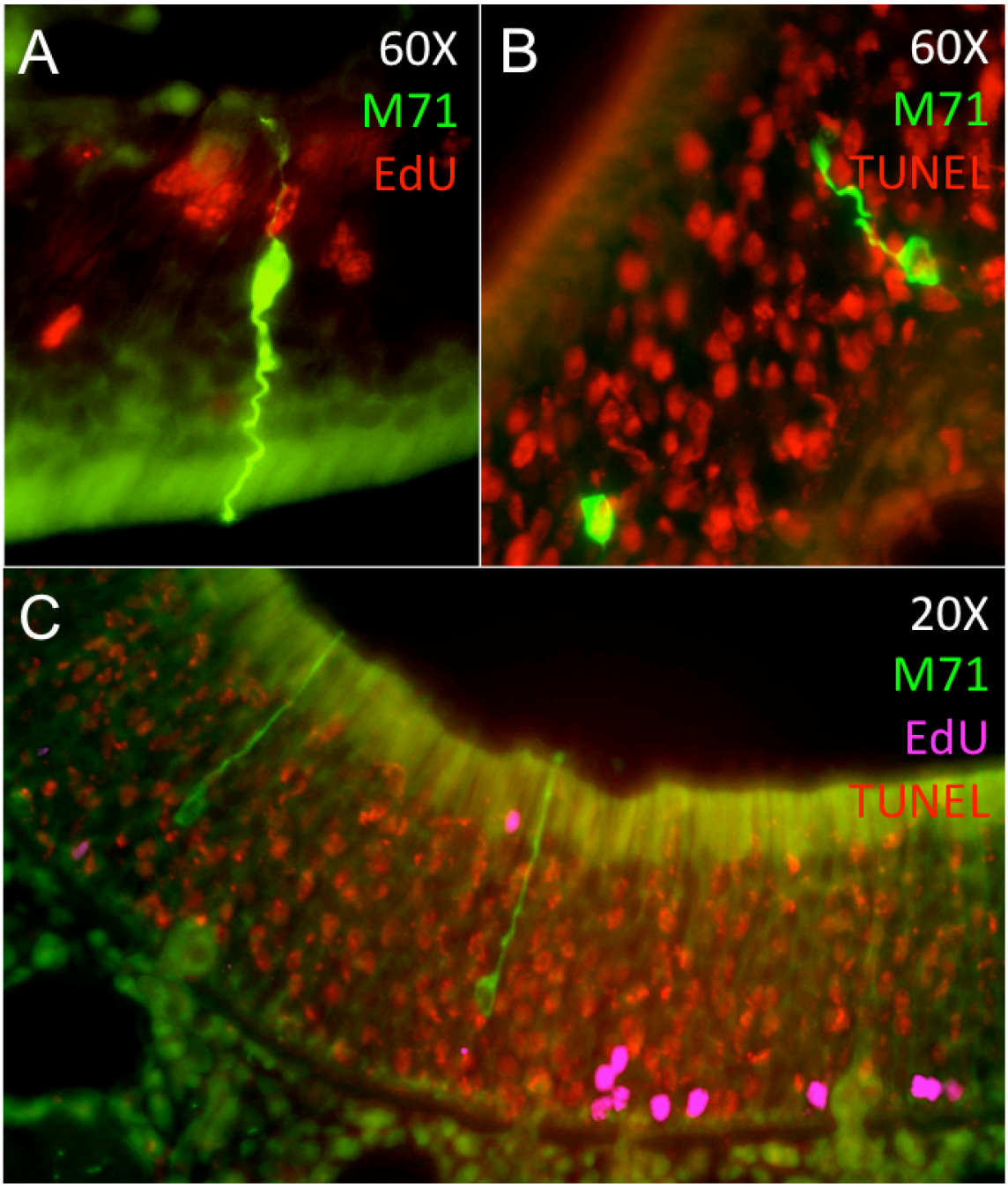

Figure 3.6: GFP, EdU and TUNEL labeling in the mouse MOE. (a) EdU (red) and M71 GFP labeled OSNs (green) in the MOE (60X). (b) TUNEL (red) and M71 GFP labeled OSNs (green) in the MOE (60X). (c) EdU (pink), TUNEL (red) and M71 GFP labeled OSNs (green) in the MOE (20X).

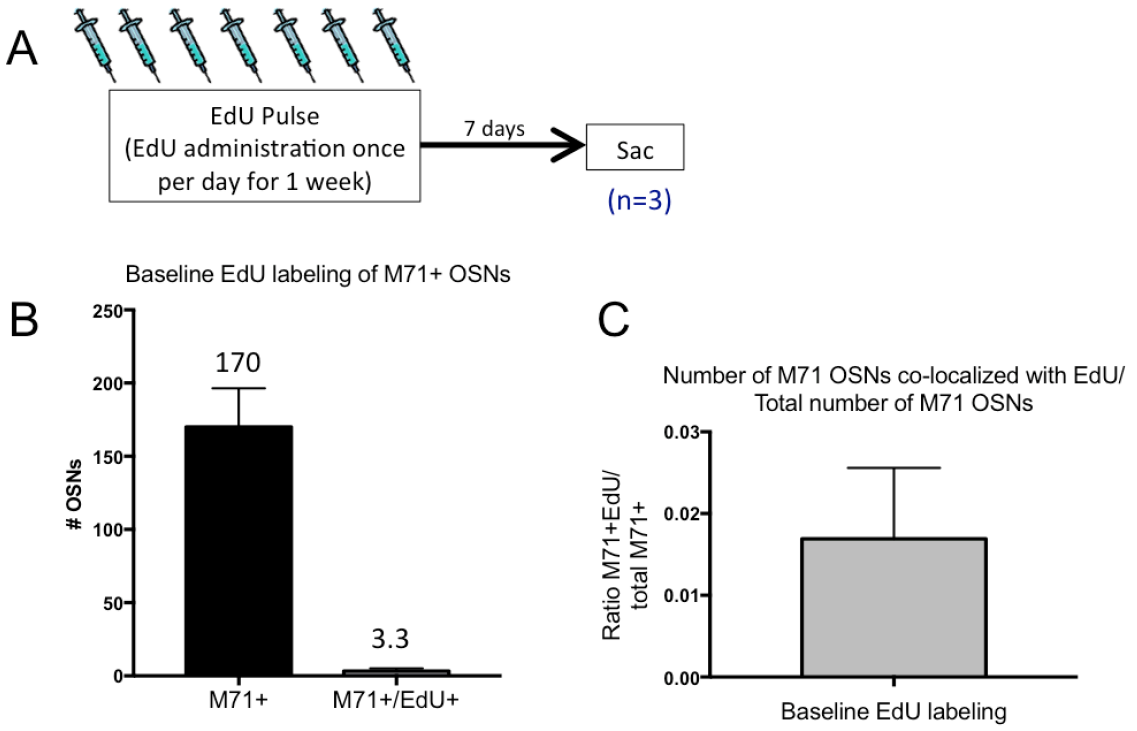

Figure 3.7: Baseline EdU labeling of M71 OSNs. (a) Experimental time line of EdU administration followed by sacrifice. (b) Number of M71 GFP labeled OSNs (black bar), and number of M71 GFP labeled OSNs co-localized with EdU (white bar). (c) Ratio of number of M71 GFP labeled OSNs co-localized with EdU to the total number of M71 OSNs. Data presented as mean +/- s.e.m..

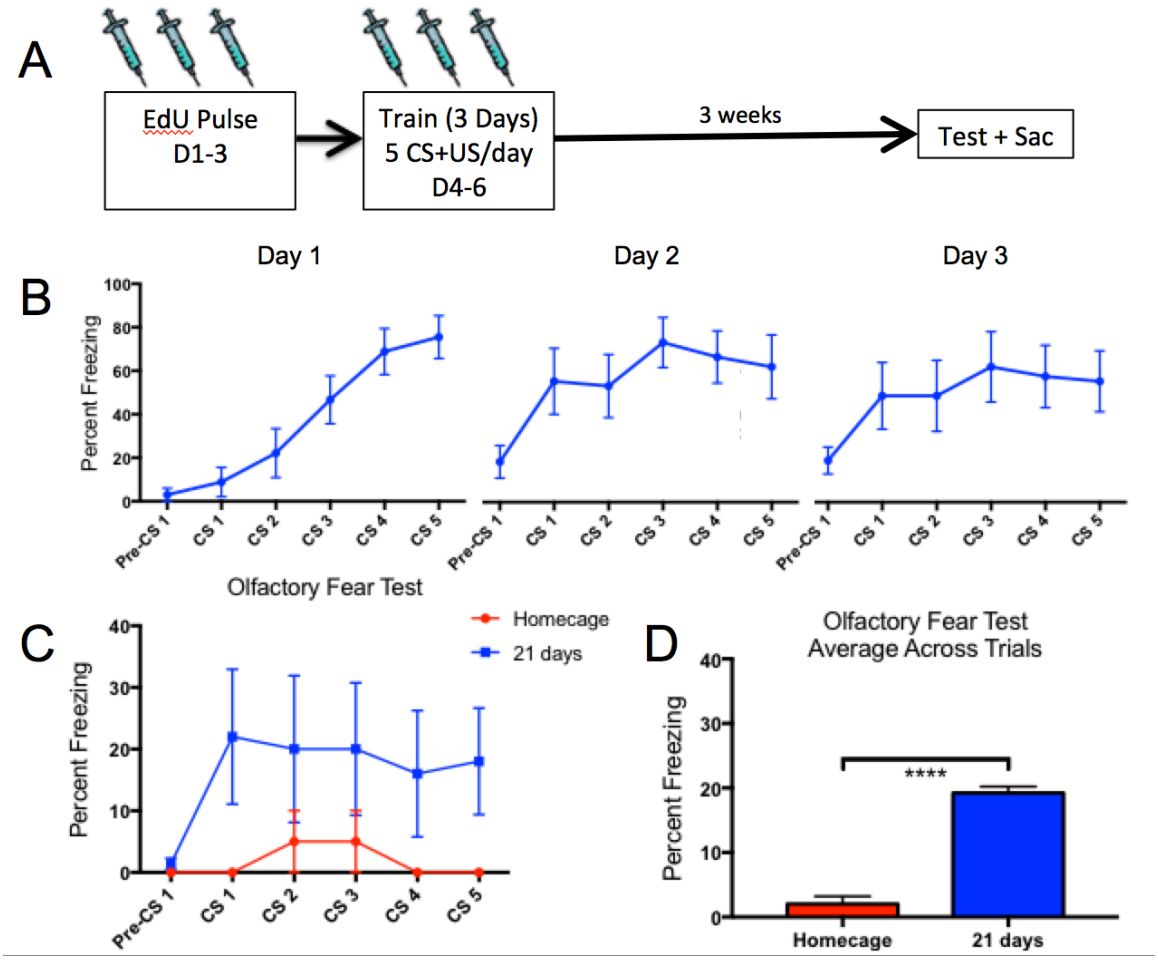

Figure 3.8: Proliferation – olfactory fear conditioning acquisition and testing. (a) Experimental time line of EdU administration, training to acetophenone and sacrifice. (b) Mice acquire olfactory fear across 3 days of olfactory fear conditioning training sessions (n=10). (c-d) Mice fear conditioned 3 weeks prior exhibit enhanced freezing to the odor CS compared to the home cage group (n=4) (C; two-way RM ANOVA, $p<0.0001$, $F(1,12)=1.172$) (D; Student's t-test, $P<0.0001$). Data presented as mean +/- s.e.m. *P<0.05, **P<0.01, ***P<0.001, ****P<0.0001.

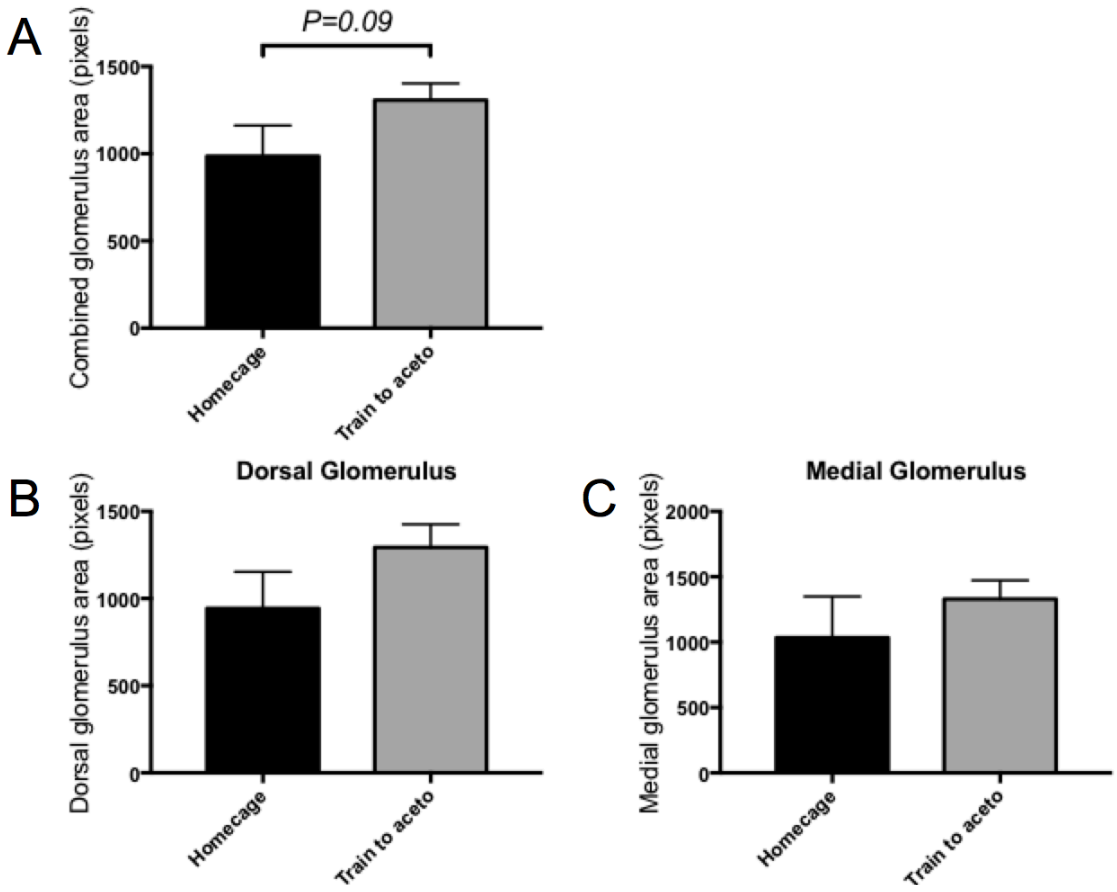

Figure 3.9: Proliferation – M71+ glomerulus area. (a-c) Glomerular area in the acetophenone + shock group (grey bar) compared to the home cage group (black bar). (A; Student's t-test, n.s., P=0.09) (B; Student's t-test, P=n.s.) (C; Student's t-test, P=n.s.). Data presented as mean +/- s.e.m..

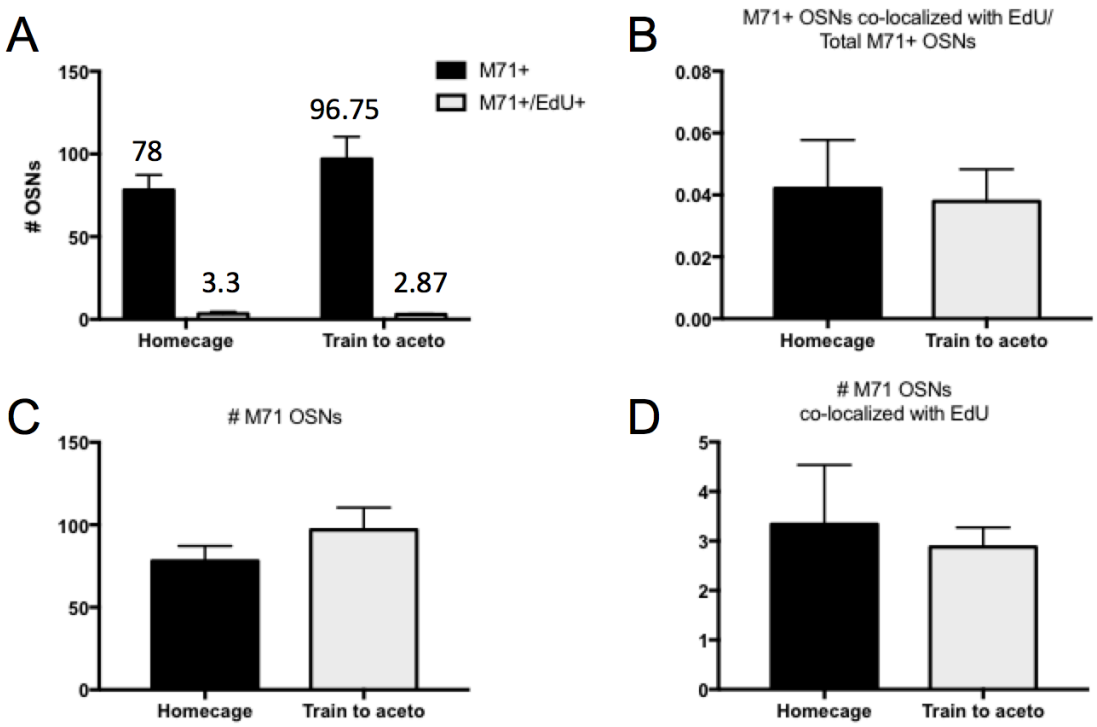

<u>Figure 3.10:</u> Proliferation – co-localization of M71+ OSNs with EdU. (a,c,d) Number of M71 GFP labeled OSNs (black bar), and number of M71 GFP labeled OSNs co-localized with EdU (grey bar) for mice in the home cage group compared to trained to acetophenone (B; Student's t-test, P=n.s.) (C; Student's t-test, P=n.s.). (b) Ratio of number of M71 GFP labeled OSNs co-localized with EdU to the total number of M71 OSNs for home cage (black bar) compared to trained to aceto (grey bar) (B; Student's t-test, P=n.s.). Data presented as mean +/- s.e.m. *P<0.05, **P<0.01, ***P<0.001, ****P<0.0001.

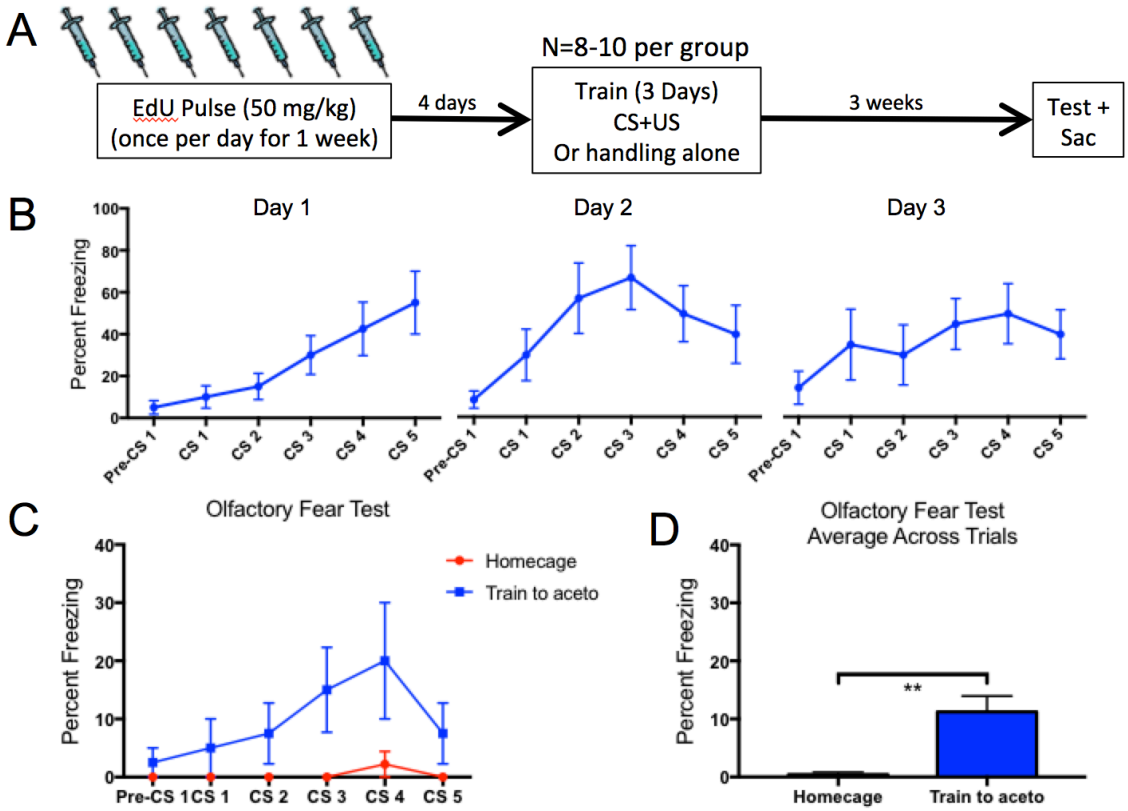

<u>Figure 3.11:</u> Survival – olfactory fear conditioning acquisition and testing. (a) Experimental time line of EdU administration, training to acetophenone and sacrifice. (b) Mice acquire olfactory fear across 3 days of olfactory fear conditioning training sessions (n=8). (c-d) Mice fear conditioned 3 weeks prior exhibit enhanced freezing to the odor CS compared to the home cage group (n=8) (C; two-way RM ANOVA, $p<0.0001$, $F(1,15)=3.921$) (D; Student's t-test, $P=0.004$). Data presented as mean +/- s.e.m. *P<0.05, **P<0.01, ***P<0.001, ****P<0.0001.

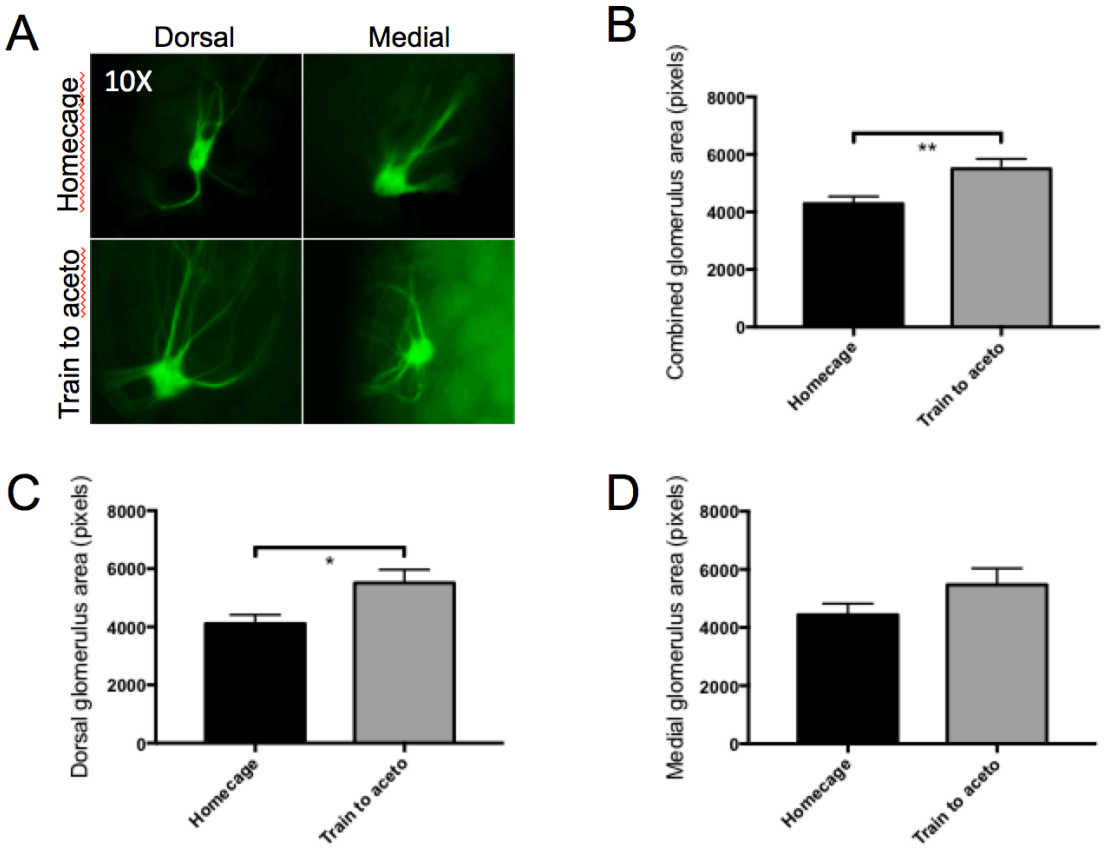

Figure 3.12: Survival – M71+ glomerulus area. (a-d) Glomerular area is greater in the acetophenone + shock group (grey bar) compared to the home cage group (black bar) (B; combined glomerulus area, Student's t-test, n.s., P=0.005) (C; dorsal glomerulus area, Student's t-test, n.s., P=0.01) (D; medial glomerulus area, Student's t-test, P=n.s.). Data presented as mean +/- s.e.m. *P<0.05, **P<0.01, ***P<0.001, ****P<0.0001.

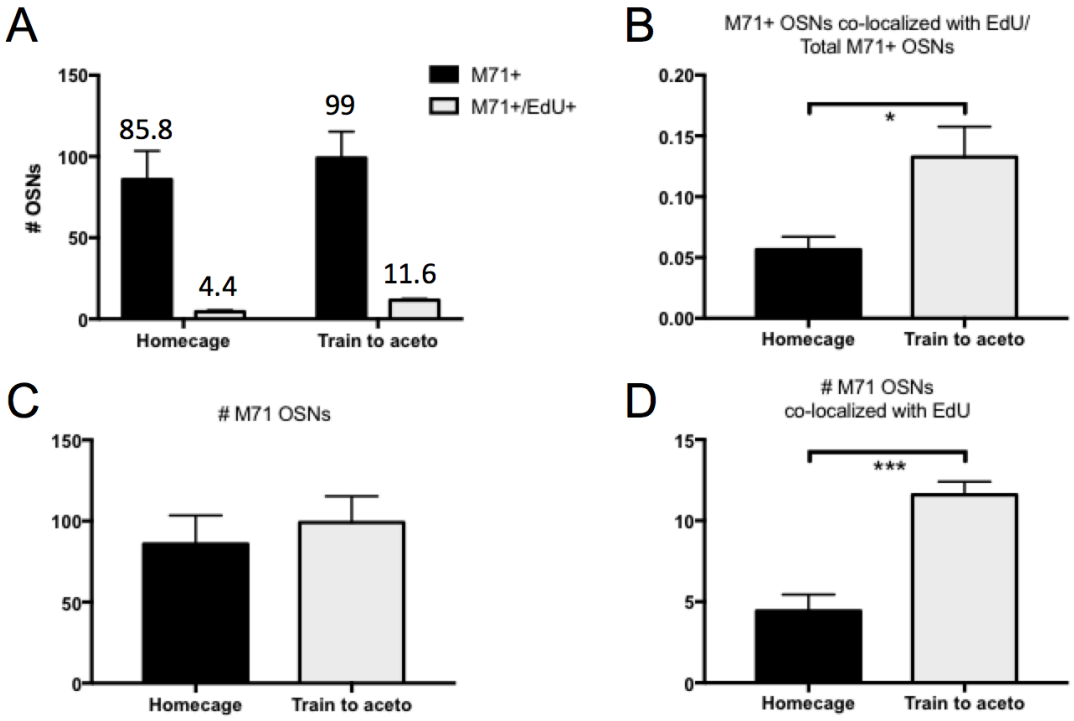

Figure 3.13: Survival – co-localization of M71+ OSNs with EdU. (a) Number of M71 GFP labeled OSNs (black bar), and number of M71 GFP labeled OSNs co-localized with EdU (grey bar) for mice in the home cage group compared to trained to acetophenone. (b) Ratio of number of M71 GFP labeled OSNs co-localized with EdU to the total number of M71 OSNs is greater for mice trained to aceto (grey bar) compared to home cage (black bar) (B; Student's t-test, P=0.01). (c) Total number of M71 OSNs (Student's t-test, P=n.s.). (d) Number of M71 OSNs co-localized with EdU is significantly greater in mice trained to aceto (grey bar) compared to home cage groups (black bar) (Student's t-test, P=0.0004). Data presented as mean +/- s.e.m. *P<0.05, **P<0.01, ***P<0.001, ****P<0.0001.

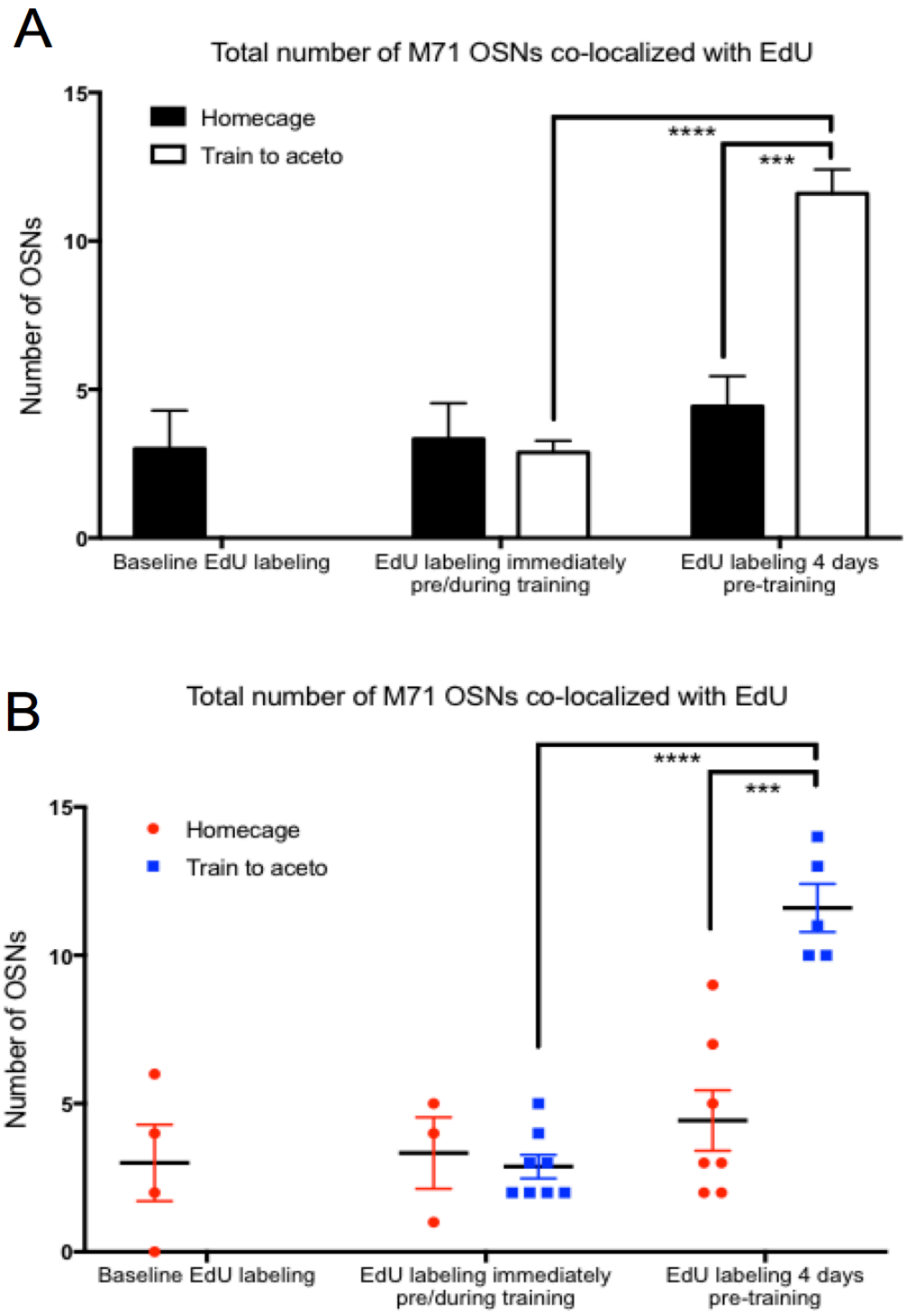

Figure 3.14: Total number M71 OSNs co-localized with EdU. (a-b) Total number of M71 OSNs co-localized with EdU in mice trained to aceto with EdU labeling 4 days prior to training is increased compared to mice fear conditioned to aceto with EdU labeling immediately prior to and during training (Student's t-test, $P<0.0001$. Number of

M71 OSNs co-localized with EdU is significantly greater in mice trained to aceto compared to home cage groups (Student's t-test, P=0.0004), as shown in Figure 3.13 D. Data presented as mean +/- s.e.m. *P<0.05, **P<0.01, ***P<0.001, ****P<0.0001.

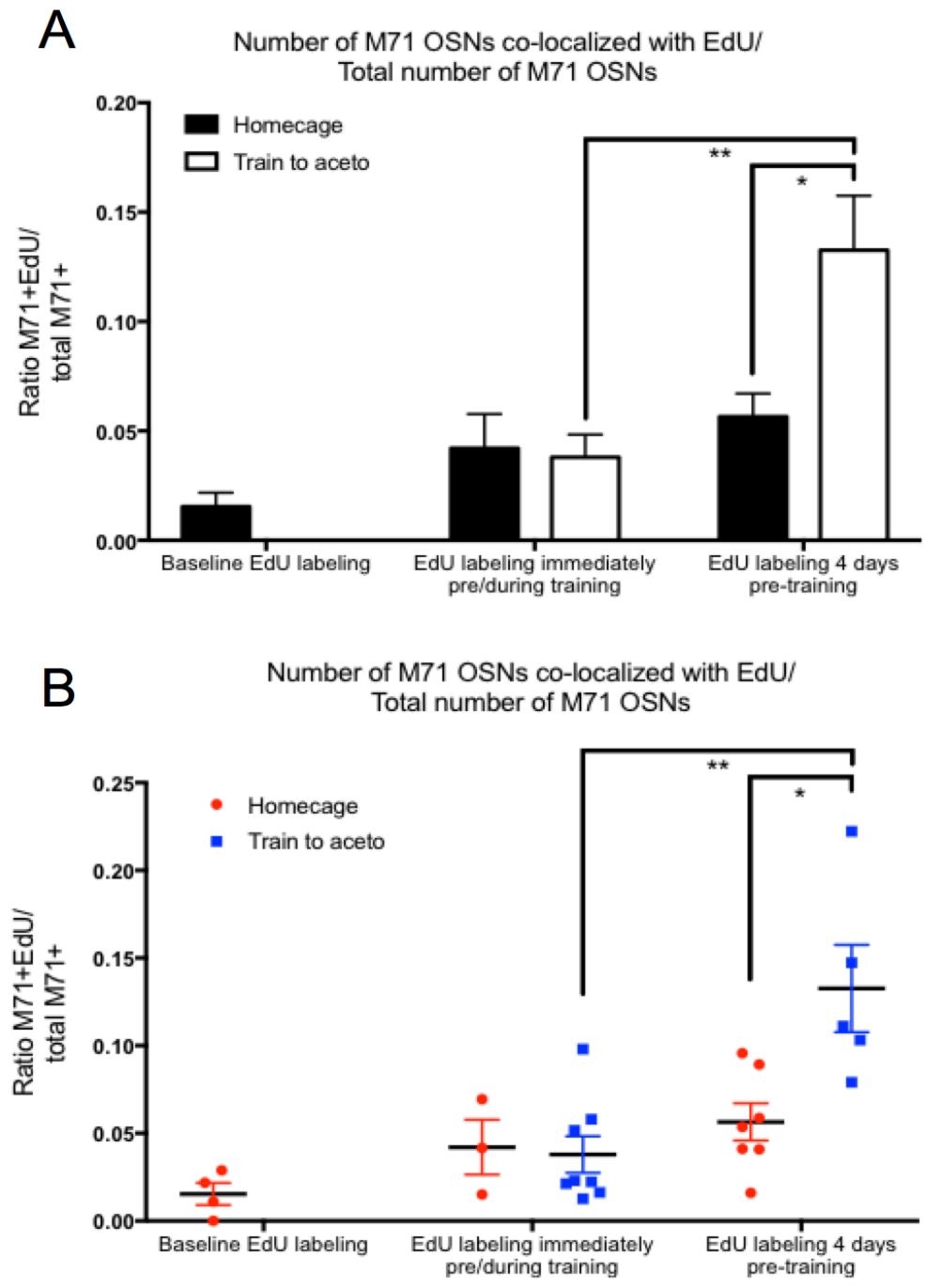

Figure 3.15: Ratio of M71 OSNs co-localized with EdU to total number of M71 OSNs. (a-b) Ratio of total number of M71 OSNs co-localized with EdU to the total number of M71 OSNs in mice trained to aceto with EdU labeling 4 days prior to training

is increased compared to mice fear conditioned to aceto with EdU labeling immediately prior to and during training (Student's t-test, P=0.0019). Ratio of total number of M71 OSNs co-localized with EdU to the total number of M71 OSNs is significantly greater in mice trained to aceto compared to home cage groups (Student's t-test, P=0.01), as shown in Figure 3.13 B. Data presented as mean +/- s.e.m. *P<0.05, **P<0.01, ***P<0.001, ****P<0.0001.

CHAPTER 4: BDNF-TRKB SIGNALING IN OLFACTORY FEAR LEARNING AND MEMORY

Context, Author's Contribution, and Acknowledgement of Reproduction

The following chapter presents evidence of a role for BDNF-TrkB signaling as a mechanism mediating the structural plasticity accompanying cue-specific olfactory fear conditioning. The context of the study was an effort to better understand the effects of TrkB agonists or antagonists in combination with olfactory fear conditioning. The dissertation author contributed to the paper by designing and running experiments, analyzing the data, and was a main contributor to the writing of the paper. This chapter is reproduced with minor edits from Morrison, F.G., McCullough, K.M., and Ressler, K.J. BDNF-TrkB signaling mechanisms underlying olfactory fear learning-dependent plasticity. *In preparation.*

Introduction

Brain-derived neurotrophic factor (BDNF) and its action at the Tropomysin receptor kinase B (TrkB) receptor play a significant role in both the acquisition and extinction of fear learning in both human PTSD and in animal models of fear conditioning and extinction (Andero and Ressler, 2012). BDNF signaling through its primary receptor TrkB is also known to play a significant role in downstream effects underlying learning such as long-term synaptic plasticity (Korte et al., 1995), morphological changes in dendritic spines (Rex et al., 2007; Tyler and Pozzo-Miller, 2003), gene transcription via cAMP response element-binding protein (CREB) (Minichiello, 2009), and the recruitment of postsynaptic density protein 95 (PSD-95) to the synapse (Yoshii and Constantine-Paton, 2007). Furthermore, BDNF-TrkB signaling may play a significant role in olfactory learning processes (Jones et al., 2007; Nibu et al.,

2001). In the present set of experiments, we investigate a role for BDNF-TrkB signaling in olfactory fear learning and memory, through the administration of TrkB agonists and antagonists in combination with olfactory fear conditioning of mouse transgenic models.

Brain-derived neurotrophic factor (BDNF) signaling mechanisms in PTSD and fear learning

The Val66Met polymorphism is a single nucleotide polymorphism (SNP) in the pro-region of *BDNF* that consists of a Met substitution for Val at position 66 and has been implicated in several psychiatric disorders including depression, schizophrenia and PTSD (Frielingsdorf et al., 2010). Individuals with the Val66Met SNP release less BDNF peptide, have decreased hippocampal volume and exhibit deficits in declarative memory and deficits in fear extinction (Bueller et al., 2006; Egan et al., 2003; Soliman et al., 2010). These data suggest that this polymorphism in the *BDNF* gene may disrupt BDNF signaling and, in so doing, affect emotional learning and memory.

To investigate the importance of the Val66Met SNP experimentally in a rodent model, investigators generated mice with the knock-in allele of the human Val66Met allele. Knock-in mice display reduced hippocampal dendritic arborization, decreased hippocampal volume and impaired LTP as well as deficits in declarative memory and decreased fear extinction (Bath et al., 2012; Frielingsdorf et al., 2010; Ninan et al., 2010; Pattwell et al., 2012; Spencer et al., 2010; Yu et al., 2009; Cao et al., 2007), indicating similar phenotypes between transgenic mice and human carriers of the Val66Met SNP. Furthermore, knock-in mice display impaired NMDA receptor-dependent synaptic plasticity in the hippocampus, and DCS appears to rescue the *BDNF* Val66Met extinction deficit of conditioned aversive memories (Yu et al., 2009).

In support of these findings, studies in rodent models have demonstrated that BDNF-TrkB signaling is necessary for the acquisition of fear conditioning and the consolidation of fear extinction in the amygdala, the hippocampus and the PFC (Chhatwal et al., 2006; Rattiner et al., 2004). In the amygdala, BDNF transcription is upregulated in extinction-trained rats compared to non-extinction trained controls. Furthermore, intra-BLA infusions of a lentiviral vector expressing the dominant-negative TrkB isoform (TrkB.t1) prior to extinction training resulted in deficits in extinction retention, suggesting an important role for TrkB in the consolidation of extinction memory (Chhatwal et al., 2006). *Bdnf* deletion by injecting Cre recombinase expressing lentivirus into the brain of floxed *Bdnf* transgenic mice provides a useful technique to investigate the regional dependent effects of BDNF (Heldt and Ressler, 2009; Heldt et al., 2007). *Bdnf* deletion in the hippocampus results in deficits in fear extinction but has no effects on fear consolidation (Heldt and Ressler, 2009). BDNF also plays a role in distinct regions of the PFC in fear extinction. Direct BDNF infusion in the infralimbic (IL) region enhances fear extinction (Peters et al., 2010). In contrast, *Bdnf* deletion in the prelimbic (PL) region of the PFC results in deficits in fear acquisition but does not affect fear extinction. *Bdnf* deletion-induced fear acquisition deficits in the PL may be rescued by administration of 7,8-DHF, a small molecule compound that activates the TrkB receptor, thus mimicking the actions of endogenous BDNF (Choi et al., 2010).

A number of agonists and antagonists of the TrkB receptor have been identified and used to query to role of BDNF-TrkB signaling *in vivo*. 7,8-DHF has been identified as a relatively specific TrkB receptor agonist which, when systemically administered in mice, crosses the blood brain barrier (BBB) to initiate TrkB receptor dimerization, auto-

phosphorylation and activation of downstream signaling (Jang et al., 2010). Systemic administration of a single dose of 7,8-DHF has been found to activate TrkB receptors in the amygdala and also enhance the acquisition and extinction of fear in mice (Andero et al., 2011). 7,8-DHF also rescues the extinction deficit present in a mouse model of stress using the immobilization on boards stressor paradigm (IMO) as well as in mouse models of chronic stress (Andero and Ressler, 2012). K252a is a potent inhibitor of the tyrosine kinase activity of neurotrophin receptors and has been used extensively as a pharmacological Trk receptor antagonist (Tapley et al., 1992). Bilateral infusion of K252a into the BLA prior to and after auditory fear conditioning results in impairments in fear-conditioned learning upon testing 48 hours later (Rattiner et al., 2004). More recently, a low-molecular weight TrkB-specific ligand, ANA-12, has been identified (Cazorla et al., 2011). ANA-12 directly and selectively binds the TrkB receptor to inhibit processes downstream of TrkB, and does not act at TrkA or TrkC receptors. Systemic administration of ANA-12 has been shown to reduce anxiety and depression-like behaviors in mice (Cazorla et al., 2011; Ren et al., 2015; Vassoler et al., 2013).

BDNF-TrkB signaling in the olfactory system

Together, these data suggest an important role for BDNF in fear learning and memory. Previous data from our lab has shown increased BDNF transcription and translation in the olfactory bulb following olfactory fear conditioning (Jones et al., 2007). Furthermore, OSNs within the MOE express the BDNF receptor, TrkB (Deckner et al., 1993; Nibu et al., 2001). BDNF-TrkB signaling is thus well-situated to mediate the learning-dependent increases in M71-expressing OSN number we have observed following olfactory fear conditioning; because mature OSN axons express TrkB, BDNF

expressed in the OB as a result of olfactory fear conditioning may promote the activity-dependent survival of olfactory sensory neurons in the MOE (Carter and Roskams, 2002).

This chapter will further investigate the role of BDNF-TrkB signaling in olfactory fear learning and memory by examining the effects of administration of TrkB agonists or antagonists during training at the behavioral and neuroanatomical level. We hypothesize that administration of TrkB agonists or antagonists will result in increases and decreases, respectively, in M71 specific OSN number and glomerular size.

Methods

Animals

Adult M71-IRES-tauLacZ transgenic mice (Vassalli et al., 2002) were maintained in a mixed 129/Sv X C57BL/6 background (Jackson Laboratories) and were used in all behavioral and neuroanatomical experiments. All mice were 2-3 months old at the time of olfactory fear conditioning. For each training time course, behavioral groups were formed with mice from at least 4 litters, controlling for sex and age, such that each group was age-matched and had equivalent numbers of males and females. All mice were experiment and odor naïve at the start of the experiment. Mice were housed in a temperature-controlled vivarium on a 12 h light/dark cycle in standard group cages (≤4 mice/cage) and were given *ad libitum* access to food and water. All experiments were performed during the light cycle and were approved by Emory University Institutional Review Board and the McLean Hospital Institutional Review Board, following the National Institutes of Health Internal Animal Care and Use Committee standards.

Drug administration

7,8-DHF (obtained from Tokyo Chemical Industry, catalog no. D1916) was administered either intraperitoneally at a dose of 5 mg/kg in a vehicle of 17% dimethylsulfoxide (DMSO) in phosphate-buffered saline (PBS), or intranasally at a dose of 20 mM in a vehicle of 17% DMSO in PBS with 50 ul per naris. The same vehicle was also used in vehicle administered control groups. K252a (obtained from Calbiochem, La Jolla, CA) was administered intranasally at a dose of 20 mM in a vehicle of 17% DMSO in PBS with 50 ul per naris. The same vehicle was used in vehicle administered control groups. ANA-12 was administered either intraperitoneally at a dose of 0.5 mg/kg in a vehicle of 17% DMSO PBS, or intranasally at a dose of 2 mM in a vehicle of 17% DMSO in PBS with 50 ul per naris. The same vehicle was also used in vehicle administered control groups.

Olfactory fear conditioning and testing

Fear training and testing were conducted using startle response systems (SR-LAB, San Diego Instruments) that had been modified to deliver discrete odor stimuli as previously described (Jones et al., 2005; Jones et al., 2008; Dias and Ressler, 2014; Morrison et al., 2015). All fear conditioning behavior experiments followed the same behavioral protocols; adult M71-IRES-tauLacZ transgenic mice (Vassalli et al., 2002) were first habituated to the training chambers 2 times (10 minutes per day) prior to training. Mice then received either 1 training session, or 3 training sessions (1 training session per day) over 3 consecutive days to ensure strong and stable odor-shock associations as previously described (Jones et al., 2005; Jones et al., 2008; Dias & Ressler, 2014; Morrison et al., 2015). Each odor + shock training session consisted of 5

trials of 10 s odor conditioned stimulus co-terminating with a 0.25 s, 0.4 mA footshock, presented with an average 120 s inter-trial interval (ITI) (ranging from 90-150 s). Prior to sacrifice, all mice were placed back in the testing chambers and were exposed to 5 presentations of the odorant conditioned stimulus (acetophenone) to assess freezing behavior. Freezing was measured throughout acquisition and during testing before sacrifice.

Experiment 4.1: Effect of parallel administration of either I.P. or intranasal TrkB agonist 7,8-DHF prior to olfactory fear conditioning. Three groups of M71-LacZ (2-3 month-old male and female mice, n=9-12 per group) underwent one day of cued olfactory fear conditioning. One of these groups received training alone, with no vehicle, a second group received I.P. 7,8-DHF administration 1 hour prior to training ("Train to aceto + I.P. 7,8-DHF"), and the third group received intranasal 7,8-DHF administration 1 hour prior to training ("Train to aceto + intranasal 7,8-DHF"). A fourth group remained in the home cage and received handling during training time points. 3 weeks following olfactory fear acquisition, all mice received a 5 odor-CS behavioral test to assess freezing. One hour after testing, mice were sacrificed by decapitation. OB and MOE were collected, dissected, and processed for beta-galactosidase staining as described below. An overview of all groups and the experimental timeline is provided in Figure 4.1 A.

Experiment 4.2: Intranasal administration of the TrkB agonist 7,8-DHF or vehicle prior to olfactory fear conditioning. Two groups of M71-LacZ (2-3 month-old male and female mice, n=10 per group) underwent one day of cued olfactory fear conditioning. One group received intranasal vehicle administration 1 hour prior to training ("Train (1 day) + intranasal vehicle", n=5 male mice, n=5 female mice), and the other group

received intranasal 7,8-DHF 1 hour prior to training ("Train (1 day) + intranasal 7,8-DHF", n=5 male mice, n=5 female mice). A third group remained in the home cage and received handling during training time points (n=5 male mice, n=5 female mice). 3 weeks following olfactory fear acquisition, all mice received a 5 odor-CS behavioral test to assess freezing. One hour after testing, mice were sacrificed by decapitation. OB and MOE were collected, dissected, and processed for beta-galactosidase staining as described below. An overview of all groups and the experimental timeline is provided in Figure 4.4 A.

Experiment 4.3: Intranasal administration of the broad spectrum TrkB antagonist K252a or vehicle prior to olfactory fear conditioning. Two groups of M71-LacZ (2-3 month-old male mice, n=8-10 per group) underwent one day of cued olfactory fear conditioning. One group received intranasal vehicle administration 30 minutes prior to training ("Train (1 day) + intranasal vehicle", n=5 male mice, n=5 female mice), and the other group received intranasal K252a 30 minutes prior to training ("Train (1 day) + intranasal K252a"). A third group remained in the home cage and received handling during training time points. 3 weeks following olfactory fear acquisition, all mice received a 5 odor-CS behavioral test to assess freezing. One hour after testing, mice were sacrificed by decapitation. OB and MOE were collected, dissected, and processed for beta-galactosidase staining as described below. An overview of all groups and the experimental timeline is provided in Figure 4.6 A.

Experiment 4.4: I.P. administration of the TrkB antagonist ANA-12 prior to olfactory fear conditioning.

Two groups of M71-LacZ (2-3 month-old male and female mice, n=9 per group) underwent 3 days of cued olfactory fear conditioning. One group received I.P. vehicle administration 30 minutes prior to training ("Train (3 day) + I.P. vehicle", n=6 male mice, n=3 female mice), and the other group received I.P. ANA-12 30 minutes prior to training ("Train (3 days) + I.P. ANA-12", n=6 male mice, n=3 female mice). A third group remained in the home cage and received handling during training time points (n=3 male mice, n=3 female mice). 3 weeks following olfactory fear acquisition, mice were sacrificed by decapitation. OB and MOE were collected, dissected, and processed for beta-galactosidase staining as described below. An overview of all groups and the experimental timeline is provided in Figure 4.8 A.

Experiment 4.5: Intranasal administration of the TrkB antagonist ANA-12 prior to olfactory fear conditioning. Two groups of M71-LacZ (2-3 month-old male and female mice, n=8-10 per group) underwent three days of cued olfactory fear conditioning. One group received intranasal vehicle administration 1 hour prior to training ("Train (3 days) + intranasal vehicle", n=5 male mice, n=5 female mice), and the other group received intranasal 7,8-DHF 1 hour prior to training ("Train (3 days) + intranasal ANA-12", n=5 male mice, n=5 female mice). All behavioral conditioning and drug administration was performed in parallel to experiment 4.2. 3 weeks following olfactory fear acquisition, all mice received a 5 odor-CS behavioral test to assess freezing. One hour after testing, mice were sacrificed by decapitation. OB and MOE were collected, dissected, and processed for beta-galactosidase staining as described below. An overview of all groups and the experimental timeline is provided in Figure 4.10 A.

Freezing behavior data analysis

Within session freezing during conditioning and testing was determined as described in Jones et al., 2005. Briefly, for each second of the 5 second activity window, voltage outputs for each animal were converted to the average voltage output. For each second of the 5-second activity window, averages that were above or below the mean voltage output of the empty cylinder (without a mouse present) were assigned an immobility score of 0 (mobile) or 1 (immobile). For each trial, a percent immobility score was determined by averaging the five immobility scores and multiplying by 100, to generate a score used as the index of freezing. Previous work has shown a high correlation between this described automated freezing index and observational ratings of freezing (Jones et al., 2005).

Beta-galactosidase staining of the MOE OSNs and OB glomeruli

Following sacrifice, MOE and olfactory bulbs of M71-LacZ mice were processed for Beta-galactosidase staining as previously described (Jones et al., 2008; Dias and Ressler, 2014; Morrison et al., 2015). Lateral whole mount MOE and brains were rapidly dissected and placed into 4% paraformaldehyde (wt/vol) for 10 min at ~23 C, after which they were washed three times in 1X phosphate-buffered saline (PBS) for 5 min. MOE and brains were then stained using 45 mg of X-gal (1 mg/ml) dissolved in 600 µl of DMSO and 45 ml of a solution of 5 mM potassium ferricyanide, 5 mM potassium ferrocyanide, and 2 mM MgCl in 1 M PBS, incubated at 37 C for 3 hours.

Quantitation of M71-positive OSNs in the MOE

Following staining, the lateral whole mount MOE was imaged using a microscope-mounted digital camera, and beta-galactosidase-stained blue OSNs were

counted manually by experimenters blinded to the experimental groups. Two experimenters both blinded to the experimental groups carried out this quantitation. MOE that were damaged during MOE extraction following sacrifice were not included in M71 OSN count analyses. Olfactory sensory neuron number was analyzed by 1-way ANOVA followed by Tukey post-hoc tests, and glomerular area to olfactory sensory neuron number was analyzed by linear regression. Grubbs' test was used to detect outliers; no samples were excluded from analysis of OSN number in the MOE.

Measurement of glomerular area in the olfactory bulb

M71 stained glomeruli were imaged using a microscope-mounted digital camera to capture high-resolution images of dorsal and medial glomeruli at 40X magnification. Pixel brightness distribution was exported in NIH ImageJ as gray levels from 0 = black to 255 = white. X-gal-labeled glomerular area was quantified as pixels, less than a set threshold gray level of 150 (optimized for axon versus background). Each glomerulus was traced using the lasso tool in ImageJ and the area was recorded using the histogram tool. Two experimenters both blinded to the experimental groups carried out this quantitation. Glomeruli that were damaged due to olfactory bulb extraction following sacrifice were not included in glomerular area analyses. Glomerular area was analyzed by 1-way ANOVA followed by Tukey post-hoc tests. Grubbs' test was used to detect outliers; no samples were excluded from analysis for glomerular area in the olfactory bulb due to Grubbs' test outlier analysis.

Statistics

Freezing was analyzed by two-way ANOVA (Fig. 4.1 B-C, 4.4 B-C, 4.6 B-C, 4.8 B, 4.10 B-C) or one-way ANOVA (Fig. 4.1 D, 4.4 D, 4.6 D, 4.10 D). Glomerular area

was analyzed by one-way ANOVA (Fig. 4.3 A-C, Fig. 4.5 B-D, Fig. 4.7 A-C, Fig. 4.9 A-C, Fig. 4.11 B-D). Olfactory sensory neuron number was analyzed by one-way ANOVA (Fig. 4.2 D) or Student's t-test (Fig. 4.5 A, 4.11 A). All ANOVA main effects or interactions were followed by Tukey *post hoc* tests, unless otherwise noted.

Results

Experiment 4.1: Both I.P. and intranasal administration of the TrkB agonist 7,8-DHF prior to olfactory fear conditioning lead to increases in M71 structure.

To begin investigating the potential role of BDNF-TrkB signaling in the olfactory system during a learning event, we tested whether the I.P. or intranasal administration of the TrkB specific agonist 7,8-DHF, which binds with high affinity to the TrkB receptor, prior to training results in increases in M71 structure. Mice received either training alone, or I.P. 7,8-DHF or intranasal 7,8-DHF 1 hour prior to training (Figure 4.1, A). The use of I.P. compared to intranasal administration allows for the ability to investigate the effect of 7,8-DHF throughout both the periphery and the entire brain (I.P.) or locally at the level of the MOE (intranasally). Mice underwent 1 day of olfactory fear conditioning to acetophenone to minimize potential ceiling effects. Three weeks after conditioning, all groups received a brief 5 CS odor fear test to assess freezing levels, and were sacrificed 1 hour following test to investigate M71 neuroanatomy. We found no significant difference between groups at the level of behavior; training alone and 7,8-DHF drug administered groups acquired fear at equivalent rates (Figure 4.1, B) and all three trained groups displayed enhanced freezing to the odor CS upon testing three weeks alter compared to home cage controls (Figure 4.1, C-D). At the level of the MOE, M71+ OSN numbers were increased with I.P. or intranasal administration of 7,8-DHF prior to training,

compared to animals that had training alone (Figure 4.2, A-D). Additionally, I.P. or intranasal administration of 7,8-DHF prior to training resulted in increased M71+ dorsal and combined glomerulus area in the OB (Figure 4.3, A-C). Although this experiment demonstrates increases in M71+ structure with 7,8-DHF administration at the level of the MOE and OB, importantly, the training control did not receive an I.P. or intranasal vehicle manipulation, and thus it is unclear from experiment 4.1 whether the observed effect 7,8-DHF is specific to TrkB signaling or the stress of I.P. or intranasal administration.

Experiment 4.2: Intranasal administration of the TrkB agonist 7,8-DHF prior to olfactory fear conditioning leads to increases in M71 structure, but no differences in freezing behavior, compared to vehicle-administered controls.

To further clarify the effects of the TrkB agonist 7,8-DHF prior to olfactory fear conditioning, a follow-up experiment was performed in which mice received either intranasal vehicle or intranasal 7,8-DHF 1 hour prior to training (Figure 4.4). Groups that received either vehicle or 7,8-DHF administration acquired fear as assessed by freezing behavior at equivalent rates (Figure 4.4, B) and also displayed enhanced freezing to the odor CS upon testing three weeks later (Figure 4.4, C-D) compared to home cage controls. Mice fear conditioned to acetophenone (1 day) that received vehicle had a trending increase in the number of M71-expressing OSNs (Figure 4.5 A). There was no observable increase in M71-expressing OSNs in mice that received intranasal administration 7,8-DHF prior to training compared to home cage controls; this may be due to low number of samples of satisfactory quality for performing cell counts (many samples were damaged during dissection) (Figure 4.5 A). Intranasal administration of

either vehicle or 7,8-DHF prior to training led to a significant increase in the size of the M71 specific glomerulus in the OB (Fig. 4.5 B-D). There was no observable significant difference between the vehicle + training and the 7,8-DHF + training groups; this may be due to 1) a ceiling effect in which the structural adaptation to learning cannot be pushed any further, or 2) the stress of intranasal administration which may play a role in structural enhancements in M71.

Experiment 4.3: Intranasal administration of the broad spectrum TrkB antagonist K252a prior to olfactory fear conditioning leads to decreases in M71 structure, but no differences in freezing behavior, compared to vehicle-administered controls.

We next examined the effect of administering the broad-spectrum Trk antagonist K252a 30 minutes prior to training (Figure 4.6, A). Mice received either intranasal vehicle or intranasal K252a 30 minutes prior to training. Experiment 4.3 was run in parallel with experiment 4.2, thus trained animals received only 1 day of olfactory fear conditioning to acetophenone. There was no difference between trained groups during acquisition; mice that received intranasal vehicle or K252a acquired fear at equivalent rates (Figure 4.6, B). Upon testing 3 weeks after conditioning, both trained groups displayed enhanced freezing to the odor CS compared to home cage handled controls (Figure 4.6, C-D). Following sacrifice we examined the M71 specific glomerulus area at the level of the OB. MOE were fresh frozen and saved for a separate experiment in which N-ChIP protocols were used to investigate histone modifications at the M71 gene (data not shown here), thus we do not have data demonstrating MOE M71 specific OSN changes. At the level of the OB, mice that received intranasal K252a administration prior to training showed no significant increase in the size of the M71 glomerulus compared to

control home cage mice (Figure 4.7 A-C). These data suggest that the broad antagonism of Trk receptors leads to a block in the structural effects of olfactory fear conditioning. However, K252a is a broad-spectrum antagonist of all Trk receptors, and thus does not specifically target the TrkB receptor. To more specifically target the TrkB receptor, we next investigated the effects of the TrkB specific antagonist ANA-12 in experiment 4.4.

Experiment 4.4: I.P. administration of the TrkB antagonist ANA-12 prior to olfactory fear conditioning leads to decreases in M71 structure compared to vehicle-administered controls.

We first investigated the I.P. administration of the selective TrkB antagonist ANA-12 prior to olfactory fear conditioning. Mice underwent three consecutive days of olfactory fear conditioning to acetophenone. Prior to each training session, one group received I.P. vehicle administration, and a second group received I.P. ANA-12 administration. Both trained groups received vehicle or drug administration 1 hour prior to each fear conditioning session (Figure 4.8 A). A separate control group remained in the home cage and received handling alone at equivalent experimental session times. There was no difference between trained groups receiving vehicle or ANA-12 during acquisition; all mice acquired fear at equivalent rates as exhibited by freezing (Figure 4.8 B). All mice were sacrificed three weeks after the last training session. MOE were fresh frozen and saved for a separate experiment in which N-ChIP protocols were used to investigate histone modifications at the M71 gene (data not shown here), thus we do not have data demonstrating MOE OSN changes. At the level of the OB, mice that received I.P. ANA-12 had a significant decrease in the size of the combined M71 specific glomeruli (Figure 4.9, A-C). These data suggest that the specific antagonism of ANA-12,

administered I.P., and thus acting both peripherally and centrally, blocks the structural glomerular effects of olfactory fear learning.

Experiment 4.5: Intranasal administration of the TrkB antagonist ANA-12 prior to olfactory fear conditioning leads to decreases in M71 structure, but no differences in freezing behavior, compared to vehicle administered controls.

Despite our observation of a block in M71 glomerulus enhancement with I.P. ANA-12 in experiment 4.4, we cannot specifically state that the observed structural effect is specific to ANA-12's action at the level of the MOE, based on the fact that when drug is administered I.P. its actions occur throughout the peripheral and central nervous system. To more specifically investigate the effect of ANA-12 at the level of the primary olfactory system, we performed an experiment in which we administered either intranasal vehicle or intranasal ANA-12 prior to olfactory fear conditioning to acetophenone. One group received intranasal vehicle administration, and a second group received intranasal ANA-12 administration. Both trained groups received vehicle or drug administration 1 hour prior to each fear conditioning session (Figure 4.10, A). A separate control group remained in the home cage and received handling alone at equivalent times as the experimental sessions. As in experiment 4.4, there was no difference between trained groups receiving vehicle or ANA-12 throughout behavioral training; mice undergoing training acquired fear at equivalent rates as exhibited by freezing levels (Figure 4.10, B), and also exhibited equivalent levels of freezing upon testing to the odor CS three weeks following the last training session (Figure 4.10, C-D). At the level of the MOE, mice that received intranasal administration of ANA-12 prior to training showed no difference in the number of M71+ OSNs compared to home cage controls, while mice that received

vehicle showed a trending increase in the number of M71-expressing OSNs compared to home cage controls. At the level of the OB, mice that received intranasal ANA-12 prior to training show significantly decreased combined and medial M71 specific glomerulus area compared to mice that received vehicle prior to training. These data demonstrate that the specific antagonism of TrkB receptors of OSNs in the primary olfactory system leads to a block in the structural effects of fear conditioning.

Discussion

To investigate the role of BDNF-TrkB signaling in olfactory fear learning and memory, we administered TrkB agonists or antagonists prior to olfactory fear conditioning and examined the effects at the level of 1) behavior by investigating freezing during acquisition and testing, and 2) neuroanatomy by investigating M71 specific OSN number and glomerulus size.

Following I.P. or intranasal administration of the TrkB agonist 7,8-DHF or vehicle alone prior to training, 1) M71-expressing OSN numbers in the MOE are increased and 2) M71 specific glomerular size in the OB is increased. However, there was no significant difference between vehicle and 7,8-DHF groups. The present set of experiments cannot definitively tell us whether 7,8-DHF administration enhances the structural effects of olfactory fear conditioning. It is possible that we have reached a ceiling effect, in which we cannot push the training related enhancement in M71 representation any further. Additionally, it's possible that learning leads to receptor saturation, and thus we will only observe an effect with blockade of the receptor. Follow-up experiments could use a less stringent fear conditioning protocol (by decreasing the

number of CS-US pairings, or decreasing the intensity of the US) to further investigate these changes.

To investigate whether the blockade of the TrkB receptors in the MOE prior to training blocks our observed effects on primary sensory neuroanatomy, we intranasally administered the broad-spectrum Trk antagonist K252a prior to training and observed decreased M71 specific glomerular size in the OB. To more specifically query the blockade of the TrkB receptor we performed a follow-up experiment in which we intraperitoneally administered the specific TrkB antagonist ANA-12 prior to training and observed a decrease in M71 specific glomerular size in the OB compared to vehicle administered controls. To more specifically assess the role of TrkB antagonism at the level of the primary olfactory system, and not throughout the entire brain and periphery, we administered ANA-12 intranasally and observed a decrease in the size of the M71 specific glomerulus compared to vehicle-administered controls. Together, these data provide strong evidence to support a role for BDNF-TrkB signaling as a contributing mechanism underlying the acquisition of olfactory fear learning and memory. In this scenario, during olfactory fear conditioning to acetophenone, increases in BDNF may act at TrkB receptors in the MOE; the dual activation of TrkB receptors and M71 receptors, along with other signaling mechanisms or top down pathways, may promote the enhanced survival of M71 specific neurons.

Interestingly, although we observe a significant block of learning induced structural plasticity with intranasal or I.P. administration of the Trk antagonist K252a or the specific TrkB antagonist ANA-12, we do not observe any differences in freezing levels between vehicle and drug administered groups during acquisition. Furthermore, we

do not observe any difference between vehicle and ANA-12 administered groups upon fear testing 3 weeks after fear conditioning. These data demonstrate an interesting dissociation between observed fear behaviors and M71 specific neuroanatomy, potentially suggesting that acetophenone-sensitive M71 OSNs themselves do not "hold" the olfactory fear memory but rather reflect a strategy to alter the organism's sensitivity to the conditioned cue. The observed dissociation between freezing behavior and M71 neuroanatomy being unique to the primary sensory system is supported by previous research demonstrating that at the level of the amygdala, the inhibition of BDNF signaling in the amygdala impairs both the acquisition and consolidation of auditory fear conditioning (Chhatwal et al., 2006).

Future experiments will need to confirm the activation or inhibition of TrkB receptors following intranasal administration of the drugs used in these experiments within the MOE using immunoblot investigation of TrkB, phospho-TrkB, and phospho-mitogen-activated protein kinase (p-MAPK). Additionally, to more specifically investigate the mechanisms underlying the effects described in the present chapter, future experiments are needed to assess the necessity and sufficiency of BDNF-TrkB signaling in olfactory cued fear learning and memory. The use of transgenic mouse models would provide one approach for investigating the effects of genetic deletion of TrkB specifically in M71+ OSNs. We hypothesize that the deletion of TrkB receptors would prevent the conditioning associated increases in M71+ OSN number and glomerular area following fear conditioning to acetophenone. Additional experiments using transgenic mouse models could investigate the inducible deletion of *Bdnf* at the level of the olfactory bulb, with the hypothesis that the inducible deletion of *Bdnf* in the OB would prevent the

activity-dependent increases in M71+ OSN number and glomerular size in animals following olfactory fear conditioning. It would be interesting to observe the effect of such transgenic manipulations at the level of behavior, based on the finding that we do not observe any differences in freezing levels during acquisition or testing with the administration of TrkB agonists or antagonists.

Future investigations would also allow us to determine the source of BDNF during fear conditioning. Neurotrophins are soluble and may be retrogradely transported across large distances away from their site of synthesis and secretion (Roskams et al., 1996). Previous research has demonstrated low levels of *Bdnf* mRNA within the mitral cells of the olfactory bulb, in addition to cells in the granule cell layer (Deckner et al., 1993). At the level of the MOE, BDNF immunoreactivity appears to be restricted to the basal cell layer (Buckland and Cunningham); *Bdnf* mRNA has not been localized within the MOE, thus it is unclear whether BDNF is made by or transported to MOE basal cells.

The results of the present chapter, which support a model in which olfactory bulb BDNF promotes the survival of MOE OSNs, are consistent with previous work using bulbectomy models demonstrating that the olfactory bulb provides critical trophic support in maintaining mature OSNs and preventing their undergoing apoptosis (Schwob, 2002). Future research should combine the methods used in the present chapter, and Chapter 3 (investigation of OSN turnover in the MOE) to investigate the effect of TrkB agonist and antagonist administration prior to training on the dynamics of OSN turnover in the MOE. If, as we would hypothesize, BDNF signaling at its receptor TrkB during training promotes the survival of M71-expressing OSNs, we would observe increases in M71 co-localization with EdU following training, when a survival labeling protocol is used.

Interestingly, however, our lab has previously demonstrated increases in BDNF mRNA in response to odor + shock sessions, as well as with odor exposure alone; our results thus suggest that while TrkB signaling may be necessary for the learning induced enhancements in M71 structure, BDNF-TrkB signaling may play a permissive role in promoting OSN survival and may required an additional factor that is released in response to the shock (Jones et al., 2007). Future investigations will be necessary to identify additional pathways mediating observed olfactory structural plasticity, and may test the role of noradrenaline or serotonin signaling or HPA axis modulation based on their known roles in other olfactory learning paradigms (Moreno et al., 2012; Rincón-cortés et al., 2015; Siopi et al., 2016; Sullivan and Holman, 2010; Vinera et al., 2015).

Based on our findings in Chapter 2 in which cue-specific extinction leads to a reversal in M71 representation, future experiments could additionally investigate the role of BDNF-TrkB signaling in the context of olfactory extinction. Future studies could investigate whether the administration of TrkB agonists prior to extinction enhance the reversal in M71 structure, and also whether the administration of TrkB antagonists block the effects of extinction induced decreases in M71 structural representation. Overall the results presented in this chapter support a role for the signaling of BDNF at its receptor TrkB in the learning dependent enhancements in olfactory cue specific neuronal number and glomerulus area.

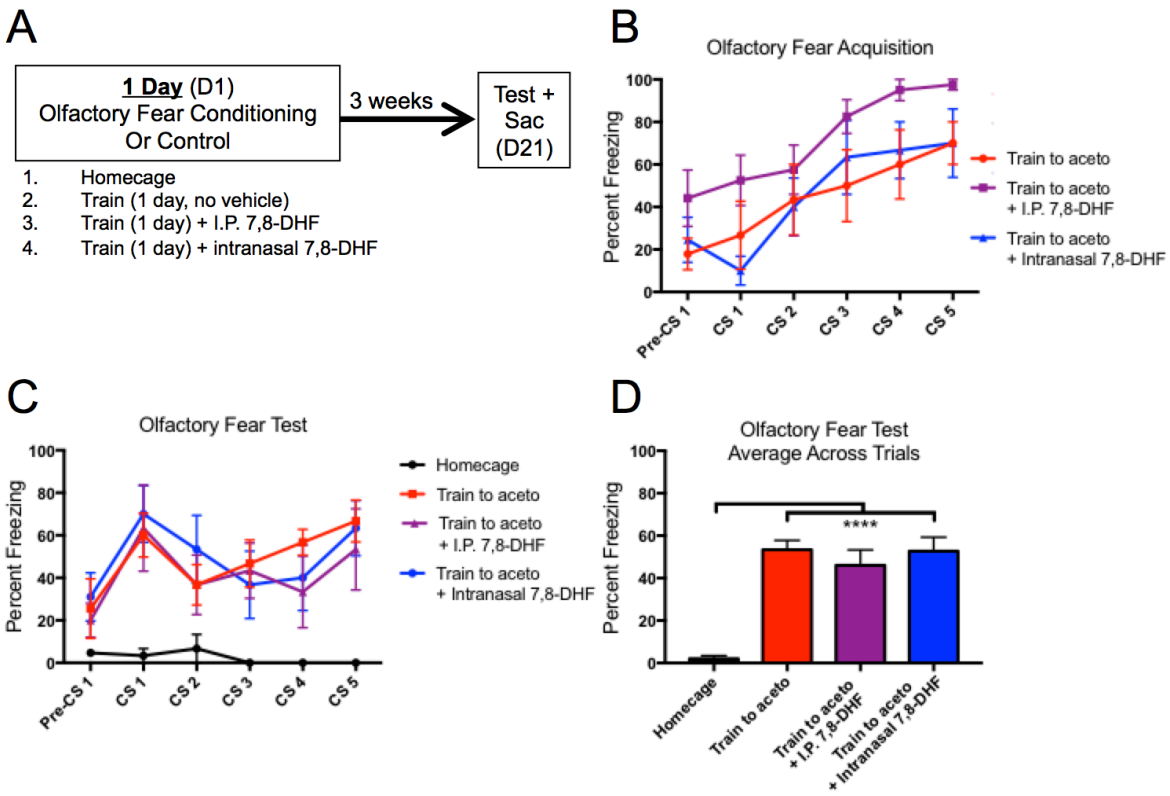

Figure 4.1: Effect of the TrkB agonist 7,8-DHF prior to training on the acquisition and maintenance of olfactory fear learning. (a) Experimental time line of drug administration, fear conditioning and olfactory fear testing 1 hour before sacrifice. (b) Mice acquire olfactory fear at similar rates across all groups (n=9-12/group) (two-way RM ANOVA, $p=0.0891$, $F(2,17)=2.796$). (c-d) Mice fear conditioned without drug (red, n=9), with I.P. 7,8-DHF (purple, n=12), and with intranasal 7,8-DHF (blue, n=10) exhibit enhanced freezing to the odor CS compared to the home cage groups (black, n=9) (C; two-way RM ANOVA, $p=0.0051$, $F(3,20)=5.799$) (D; ANOVA, $p<0.0001$, $F(3,116)=26.03$). Data presented as mean +/- s.e.m. *P<0.05, **P<0.01, ***P<0.001, ****P<0.0001.

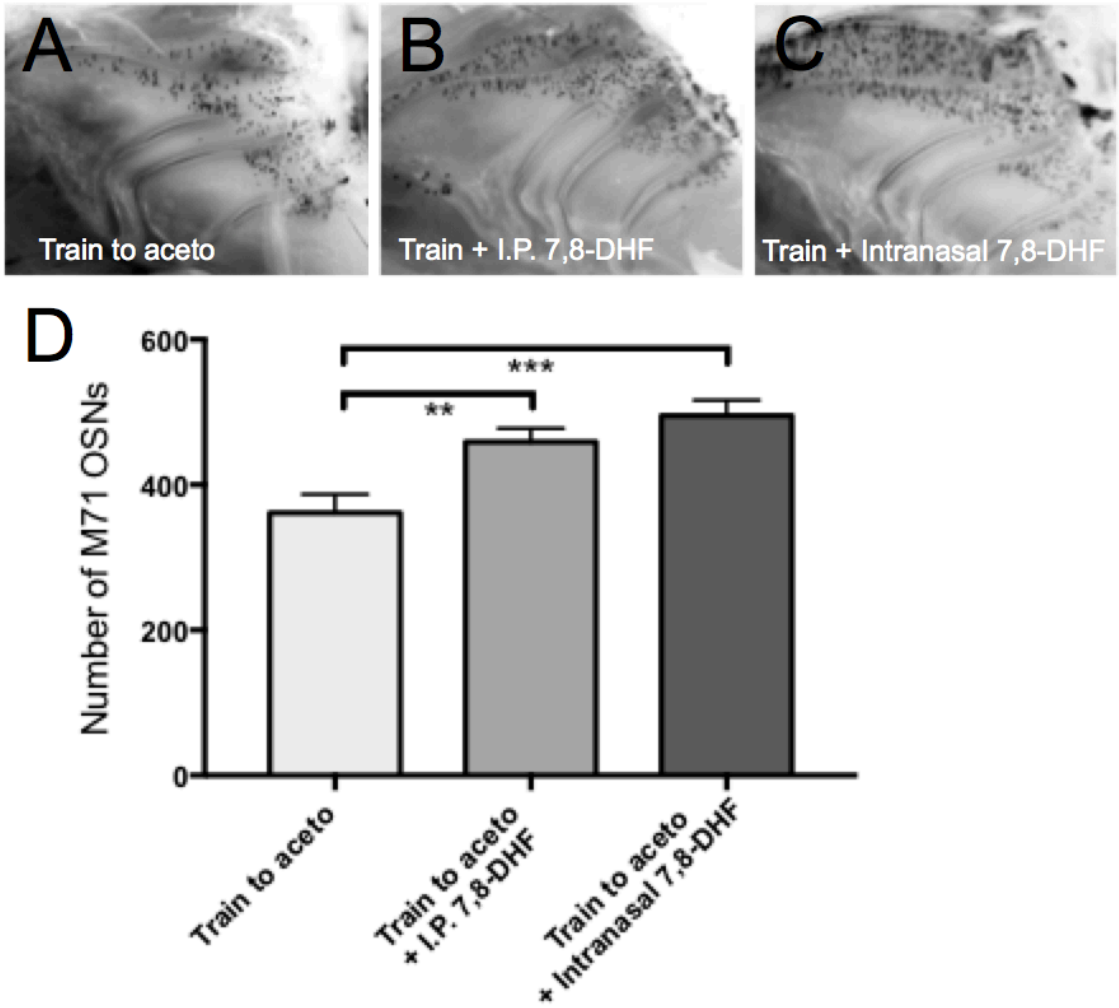

<u>Figure 4.2:</u> Effect of the TrkB agonist 7,8-DHF prior to training on M71 neuron number in the MOE. (a-d) Mice that received I.P. (medium grey bar) or intranasal 7,8-DHF (dark grey bar) prior to training have a larger number of M71 OSNs in the MOE than mice that received training without drug (light grey bar) (D; M71-LacZ: train to aceto, n=12; Train to aceto + I.P. 7,8-DHF, n=18; Train to aceto + intranasal 7,8-DHF, n=10; ANOVA, P=0.0007, F(2,37)=0.202; Train to aceto versus train to aceto + I.P. 7,8-DHF, P=0.006; Train to aceto versus train to aceto + intranasal 7,8-DHF, P=0.001; Train to aceto + I.P. 7,8-DHF versus train to aceto + intranasal 7,8-DHF, P=n.s.). Data presented as mean +/- s.e.m. *P<0.05, **P<0.01, ***P<0.001, ****P<0.0001.

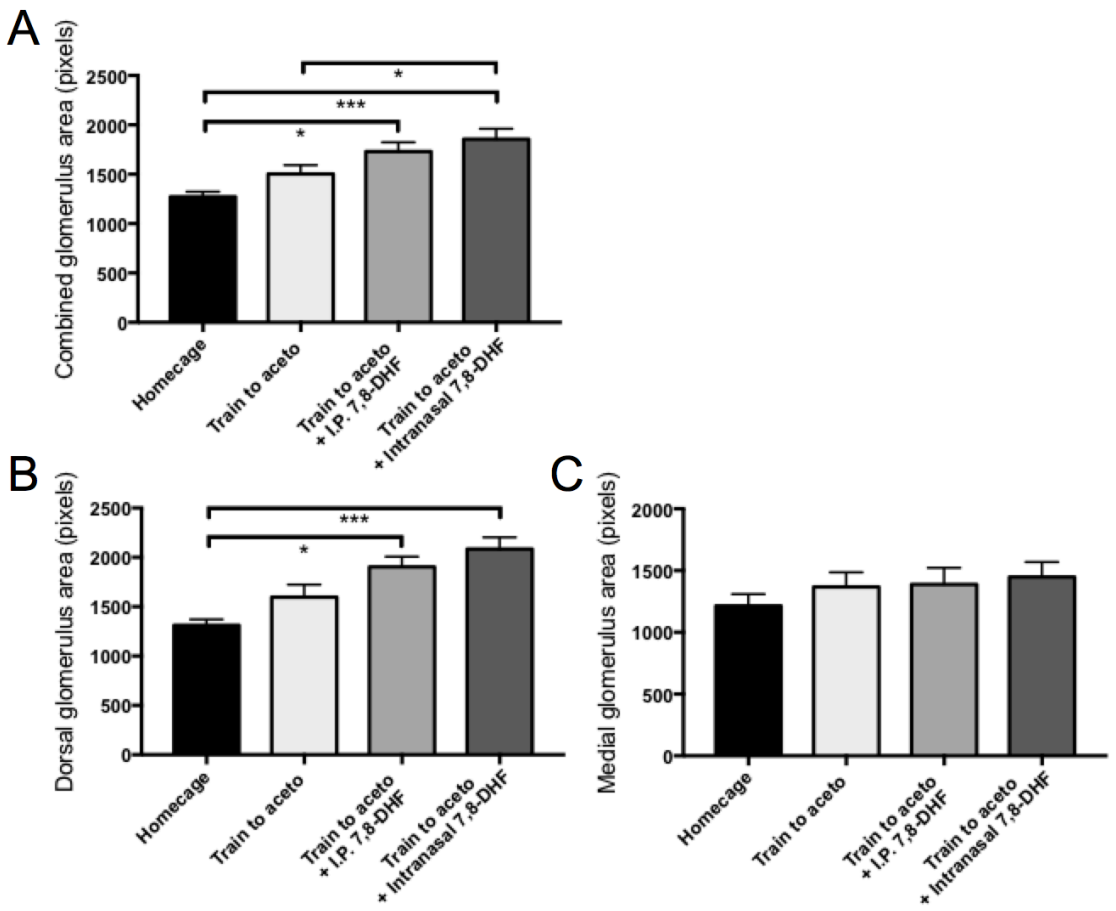

Figure 4.3: Effect of the TrkB agonist 7,8-DHF prior to training on M71 glomerulus area in the OB. (a-c) Mice that received I.P. (medium grey bar) or intranasal 7,8-DHF (dark grey bar) prior to training have a larger M71 glomerulus area in the OB than home cage control mice (black bar) (A; Combined M71 glomerulus area: Home cage, n=15; Train to aceto, n=29; Train to aceto + I.P. 7,8-DHF, n=30; Train to aceto + intranasal 7,8-DHF, n=28; ANOVA, P=0.001, F(3,98)=0.022; Home cage versus Train to aceto, P=n.s.; Home cage versus Train to aceto + I.P. 7,8-DHF, P=0.01; Home cage versus Train to aceto + intranasal 7,8-DHF, P=0.001; Train to aceto versus Train to aceto + I.P. 7,8-DHF, P=n.s.; Train to aceto versus Train to aceto + intranasal 7,8-DHF, P=0.03; Train to aceto + I.P. 7,8-DHF versus train to aceto + intranasal 7,8-DHF, P=n.s.). (B; Dorsal M71 glomerulus area: Home cage, n=9; Train to aceto, n=17; Train to aceto + I.P. 7,8-DHF, n=20; Train to aceto + intranasal 7,8-DHF, n=18; ANOVA, P=0.0005, F(3,60)=1.898; Home cage versus Train to aceto, P=n.s.; Home cage versus Train to aceto + I.P. 7,8-DHF, P=0.01; Home cage versus Train to aceto + intranasal 7,8-DHF, P=0.0009; Train to aceto versus Train to aceto + I.P. 7,8-DHF, P=n.s.; Train to aceto versus Train to aceto + intranasal 7,8-DHF, P=0.01; Train to aceto + I.P. 7,8-DHF versus train to aceto + intranasal 7,8-DHF, P=n.s.). (C; Medial M71 glomerulus area: Home cage, n=6; Train to aceto, n=12; Train to aceto + I.P. 7,8-DHF, n=10; Train to aceto + intranasal 7,8-DHF, n=10; ANOVA, P=n.s., F(3,34)=0.3268; Home cage versus Train to aceto, P=n.s.; Home cage versus Train to aceto + I.P. 7,8-DHF, P=n.s.; Home cage versus Train to aceto + intranasal 7,8-DHF, P=n.s.; Train to aceto versus Train to aceto + I.P. 7,8-DHF, P=n.s.;

Train to aceto versus Train to aceto + intranasal 7,8-DHF, P=n.s.; Train to aceto + I.P. 7,8-DHF versus train to aceto + intranasal 7,8-DHF, P=n.s.). Data presented as mean +/- s.e.m. *P<0.05, **P<0.01, ***P<0.001, ****P<0.0001.

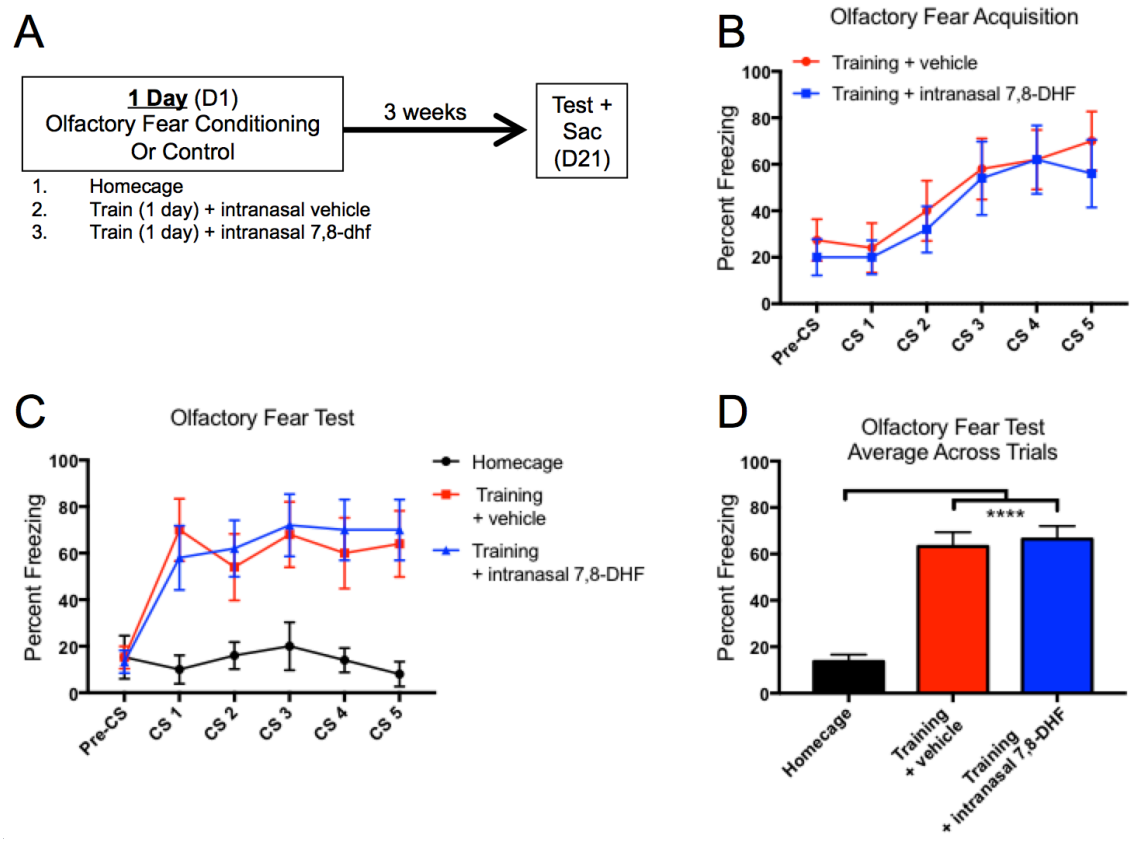

Figure 4.4: Effect of intranasal administration of the TrkB agonist 7,8-DHF prior to training on the acquisition and maintenance of olfactory fear learning. (a) Experimental time line of drug administration, fear conditioning and olfactory fear testing 1 hour before sacrifice. (b) Mice acquire olfactory fear at similar rates across all groups (n=10/group) (two-way RM ANOVA, p=0.6574, F(1,18)=0.2034). (c-d) Mice fear conditioned vehicle (red, n=10), and with intranasal 7,8-DHF (blue, n=10) exhibit enhanced freezing to the odor CS compared to the home cage groups (black, n=10) (C; two-way RM ANOVA, p=0.0034, F(2,27)=7.081) (D; ANOVA, p<0.0001, F(2,147)=8.789). Data presented as mean +/- s.e.m. *P<0.05, **P<0.01, ***P<0.001, ****P<0.0001.

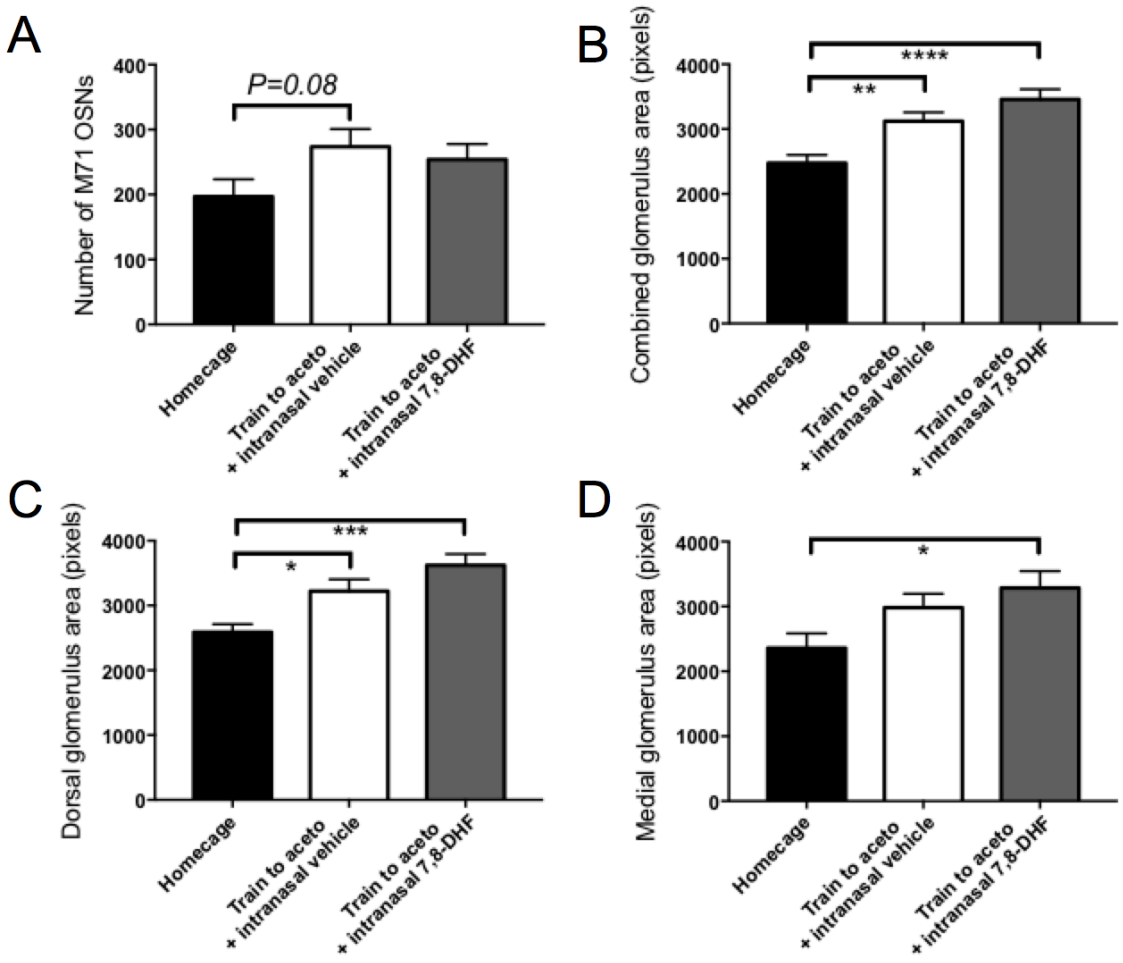

<u>Figure 4.5:</u> Effect of intranasal administration of the TrkB agonist 7,8-DHF prior to training on M71 neuron number in the MOE and M71 glomerulus area in the OB. (a) Mice that received intranasal vehicle (white bar) or intranasal 7,8-DHF (dark grey bar) prior to training have a trending increase in the number of M71 OSNs in the MOE compared to homecage control mice (black bar) (A; M71-LacZ: Home cage, n=6; Train to aceto + intranasal vehicle, n=4; Train to aceto + intranasal 7,8-DHF, n=6; ANOVA, P=0.1424, F(2,13)=0.201; Homecage versus Train to aceto + intranasal vehicle, P=n.s.; Homecage versus train to aceto + intranasal 7,8-DHF, P=n.s.; Train to aceto + intranasal vehicle versus Train to aceto + intranasal 7,8-DHF, P=n.s.) (Student's t-test; Homecage versus Train to aceto + intranasal vehicle, P=0.0086). (b-d) Mice that received intranasal vehicle (white bar) or intranasal 7,8-DHF (dark grey bar) prior to training have a larger M71 glomerulus area in the OB than home cage control mice (black bar) (B; Combined M71 glomerulus area: Home cage, n=34; Train to aceto + intranasal vehicle, n=33; Train to aceto + intranasal 7,8-DHF, n=37; ANOVA, P<0.0001, F(2,101)=1.651; Home cage versus Train to aceto + intranasal vehicle, P=0.0061.; Home cage versus Train to aceto + intranasal 7,8-DHF, P<0.0001; Train to aceto + intranasal vehicle versus train to aceto + intranasal 7,8-DHF, P=n.s.) (C; Combined M71 glomerulus area: Home cage, n=17; Train to aceto + intranasal vehicle, n=19; Train to aceto + intranasal 7,8-DHF, n=19; ANOVA, P=0.0003, F(2,52)=0.2831; Home cage versus Train to aceto + intranasal

vehicle, P=0.0259; Home cage versus Train to aceto + intranasal 7,8-DHF, P=0.0002; Train to aceto + intranasal vehicle versus train to aceto + intranasal 7,8-DHF, P=n.s.) (D; Medial M71 glomerulus area: Home cage, n=17; Train to aceto + intranasal vehicle, n=14; Train to aceto + intranasal 7,8-DHF, n=18; ANOVA, P=0.0237, F(2,46)=1.681; Home cage versus Train to aceto + intranasal vehicle, P=n.s.; Home cage versus Train to aceto + intranasal 7,8-DHF, P=0.0195; Train to aceto + intranasal vehicle versus train to aceto + intranasal 7,8-DHF, P=n.s.). Data presented as mean +/- s.e.m. *P<0.05, **P<0.01, ***P<0.001, ****P<0.0001.

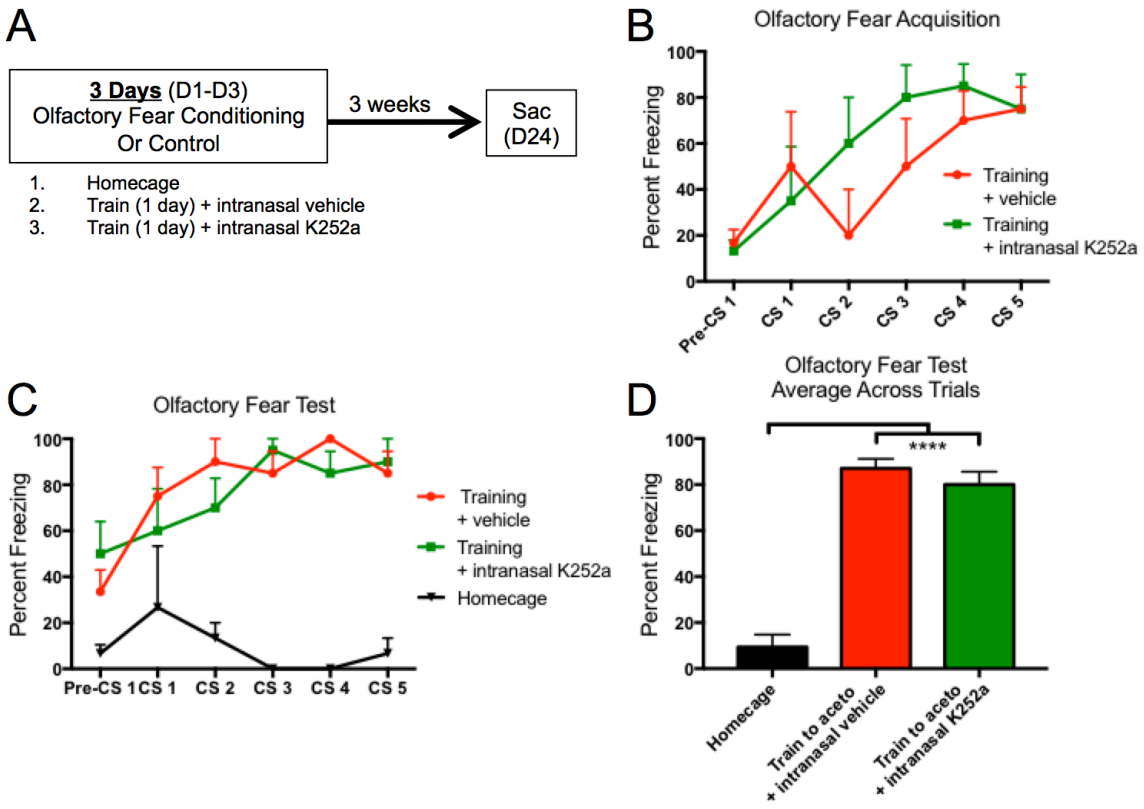

Figure 4.6: Effect of intranasal administration of the Trk antagonist K252a prior to training on the acquisition and maintenance of olfactory fear learning. (a) Experimental time line of drug administration, fear conditioning and olfactory fear testing 1 hour before sacrifice. (b) Mice acquire olfactory fear at similar rates across all groups (n=10/group) (two-way RM ANOVA, p=0.5265, F(1,6)=0.4518. (c-d) Mice fear conditioned and receiving vehicle prior to training (red, n=6), or receiving intranasal K252a prior to training (green, n=6) exhibit enhanced freezing to the odor CS compared to the home cage groups (black, n=6) (C; two-way RM ANOVA, p=0.0003, F(2,8)=27.1) (D; ANOVA, p<0.0001, F(2,52)=1.444). Data presented as mean +/- s.e.m. *P<0.05, **P<0.01, ***P<0.001, ****P<0.0001.

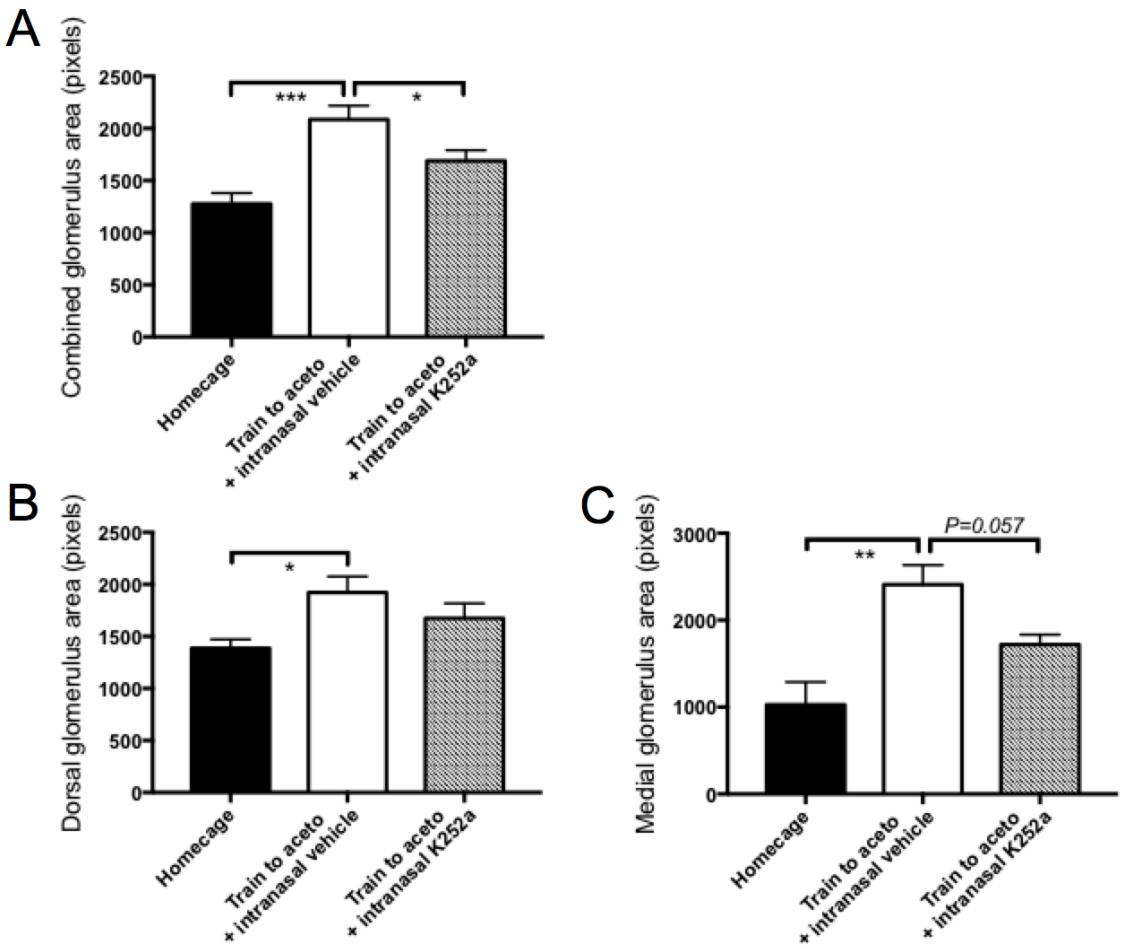

<u>Figure 4.7:</u> Effect of intranasal administration of the Trk antagonist K252a prior to training on M71 glomerulus area in the OB. (a-c) Mice that received intranasal vehicle (white bar) prior to training have a larger M71 glomerulus area in the OB than home cage control mice (black bar) and mice that received intranasal K252a (striped bar) prior to training. (A; Combined M71 glomerulus area: Home cage, n=13; Train to aceto + intranasal vehicle, n=21; Train to aceto + intranasal K252a, n=19; ANOVA, P=0.0002, F(2,50)=1.372; Home cage versus Train to aceto + intranasal vehicle, P=0.0001; Home cage versus Train to aceto + intranasal K252a, P=0.0709; Train to aceto + intranasal vehicle versus train to aceto + intranasal K252a, P=0.0443) (B; Dorsal M71 glomerulus area: Home cage, n=9; Train to aceto + intranasal vehicle, n=14; Train to aceto + intranasal K252a, n=13; ANOVA, P=0.0514, F(2,33)=1.87; Home cage versus Train to aceto + intranasal vehicle, P=0.0412; Home cage versus Train to aceto + intranasal K252a, P=n.s.; Train to aceto + intranasal vehicle versus train to aceto + intranasal K252a, P=n.s.) (C; Dorsal M71 glomerulus area: Home cage, n=4; Train to aceto + intranasal vehicle, n=7; Train to aceto + intranasal K252a, n=6; ANOVA, P=0.0017, F(2,14)=0.5636; Home cage versus Train to aceto + intranasal vehicle, P=0.0013; Home cage versus Train to aceto + intranasal K252a, P=n.s.; Train to aceto + intranasal vehicle versus train to aceto + intranasal K252a, P=0.0579). Data presented as mean +/- s.e.m. *P<0.05, **P<0.01, ***P<0.001, ****P<0.0001.

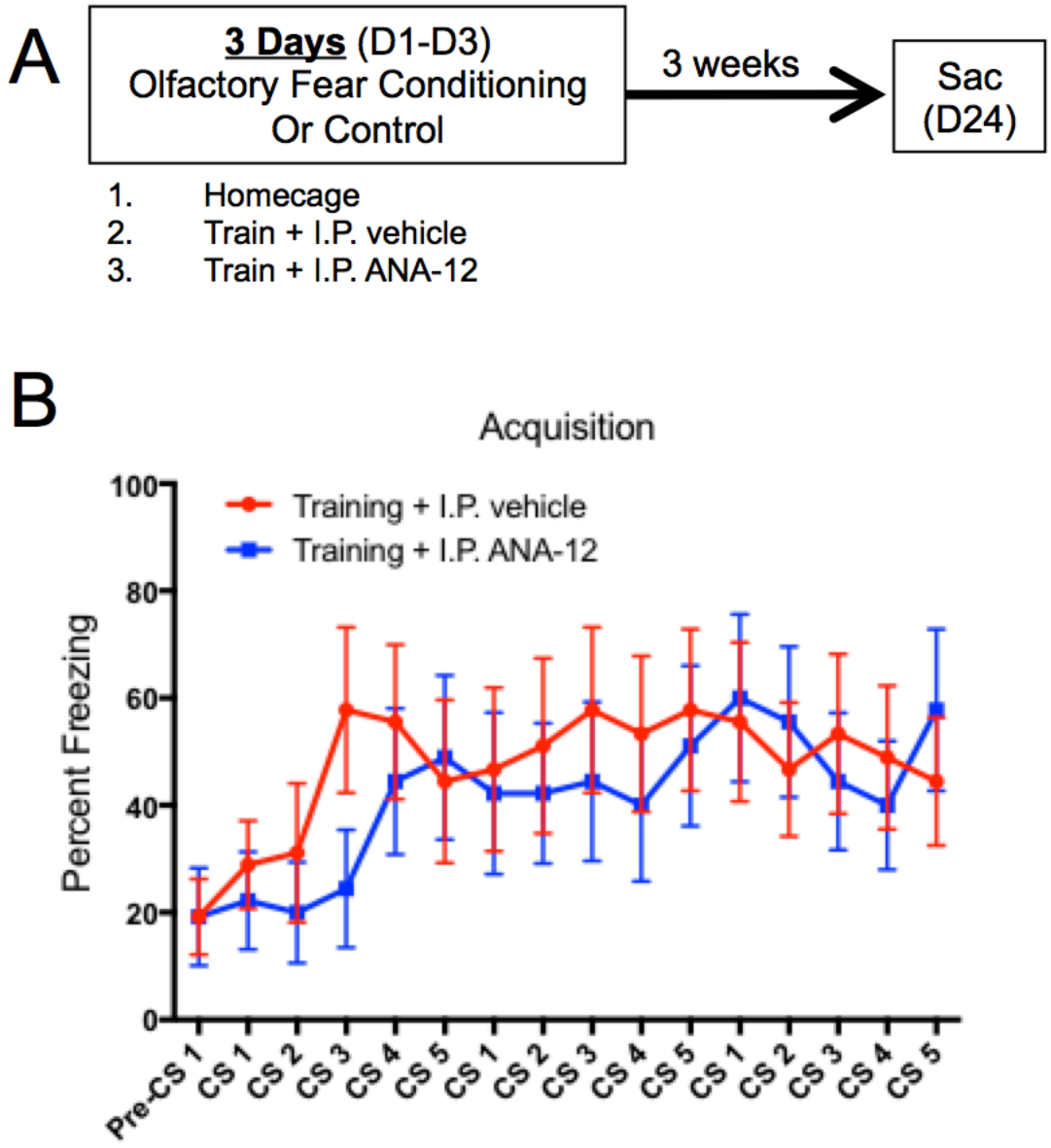

Figure 4.8: Effect of I.P. administration of the TrkB antagonist ANA-12 prior to training on the acquisition of olfactory fear learning. (a) Experimental time line of drug administration and fear conditioning. (b) Mice acquire olfactory fear at similar rates across all groups (n=9/group) (two-way RM ANOVA, P=0.7255, F(1,16)=0.1277). Data presented as mean +/- s.e.m..

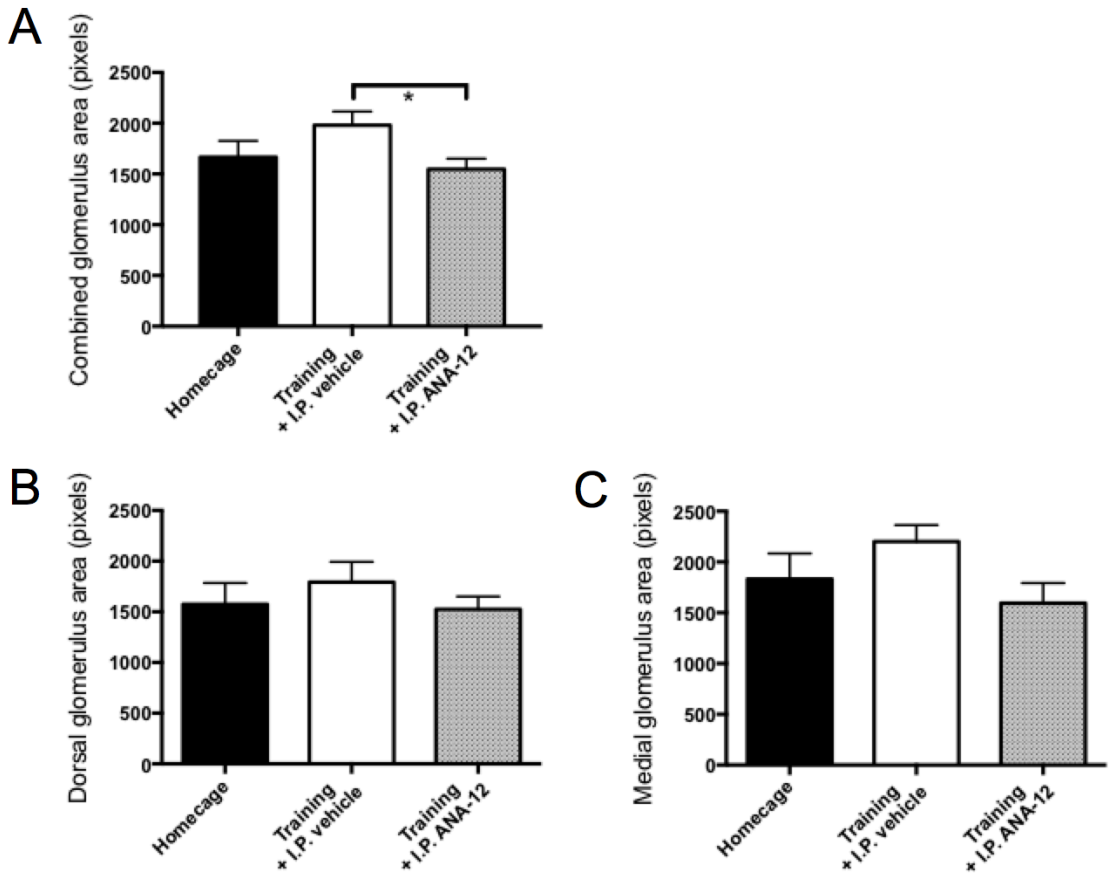

Figure 4.9: Effect of I.P. administration of the TrkB antagonist ANA-12 prior to training on M71 glomerulus area in the OB. (a-c) Mice that received I.P. vehicle (white bar) prior to training have a larger combined M71 glomerulus area in the OB compared to mice that received I.P. ANA-12 (grey dotted bar) prior to training. (A; Combined M71 glomerulus area: Home cage, n=14; Train to aceto + I.P. vehicle, n=24; Train to aceto + I.P. ANA-12, n=22; ANOVA, P=0.0455, F(2,57)=1.26; Home cage versus Train to aceto + I.P. vehicle, P=0.2619; Home cage versus Train to aceto + I.P. ANA-12, P=n.s.; Train to aceto + intranasal vehicle versus train to aceto + I.P. ANA-12, P=0.0415) (B; Dorsal M71 glomerulus area: Home cage, n=9; Train to aceto + I.P. vehicle, n=13; Train to aceto + I.P. ANA-12, n=15; ANOVA, P=0.4957, F(2,34)=0.1373; Home cage versus Train to aceto + I.P. vehicle, P=n.s.; Home cage versus Train to aceto + I.P. ANA-12, P=n.s.; Train to aceto + intranasal vehicle versus train to aceto + I.P. ANA-12, P=n.s.) (C; Medial M71 glomerulus area: Home cage, n=5; Train to aceto + I.P. vehicle, n=11; Train to aceto + I.P. ANA-12, n=7, ANOVA, P=0.0831, F(2,20)=0.0282; Home cage versus Train to aceto + I.P. vehicle, P=n.s.; Home cage versus Train to aceto + I.P. ANA-12, P=n.s.; Train to aceto + intranasal vehicle versus train to aceto + I.P. ANA-12, P=n.s.). Data presented as mean +/- s.e.m. *P<0.05, **P<0.01, ***P<0.001, ****P<0.0001.

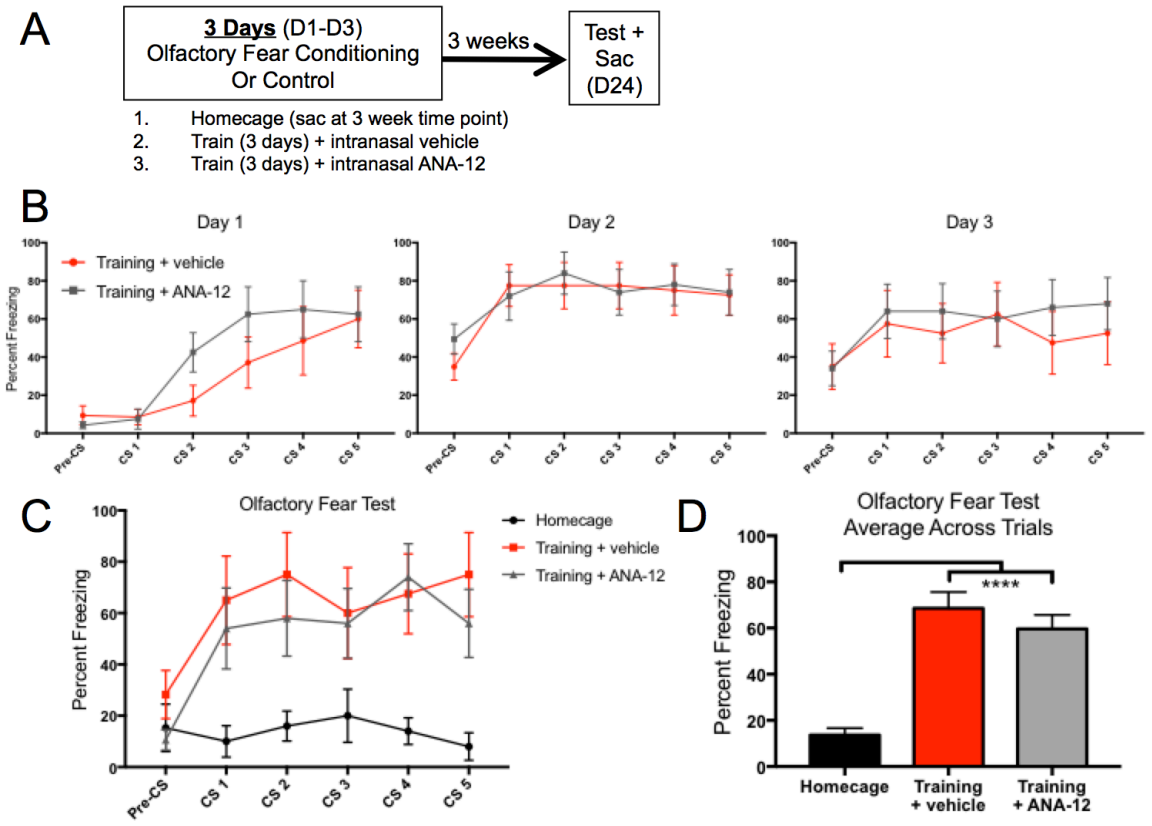

Figure 4.10: Effect of intranasal administration of the TrkB antagonist ANA-12 prior to training on the acquisition and maintenance of olfactory fear learning. (a) Experimental time line of drug administration, fear conditioning and olfactory fear testing 1 hour before sacrifice. (b) Mice acquire olfactory fear at similar rates across all groups (n=8-10/group) (Day 1; two-way RM ANOVA, p=n.s., F(1,13)=0.691) (Day 2; two-way RM ANOVA, p=n.s., F(1,16)=0.84) (Day 3; two-way RM ANOVA, p=n.s., F(1,16)=0.1699). (c-d) Mice fear conditioned vehicle (red, n=8), and with intranasal 7,8-DHF (grey, n=10) exhibit enhanced freezing to the odor CS compared to the home cage groups (black, n=10) (C; two-way RM ANOVA, p=0.0047, F(2,25)=6.704) (D; ANOVA, p<0.0001, F(2,137)=8.22). Data presented as mean +/- s.e.m. *P<0.05, **P<0.01, ***P<0.001, ****P<0.0001.

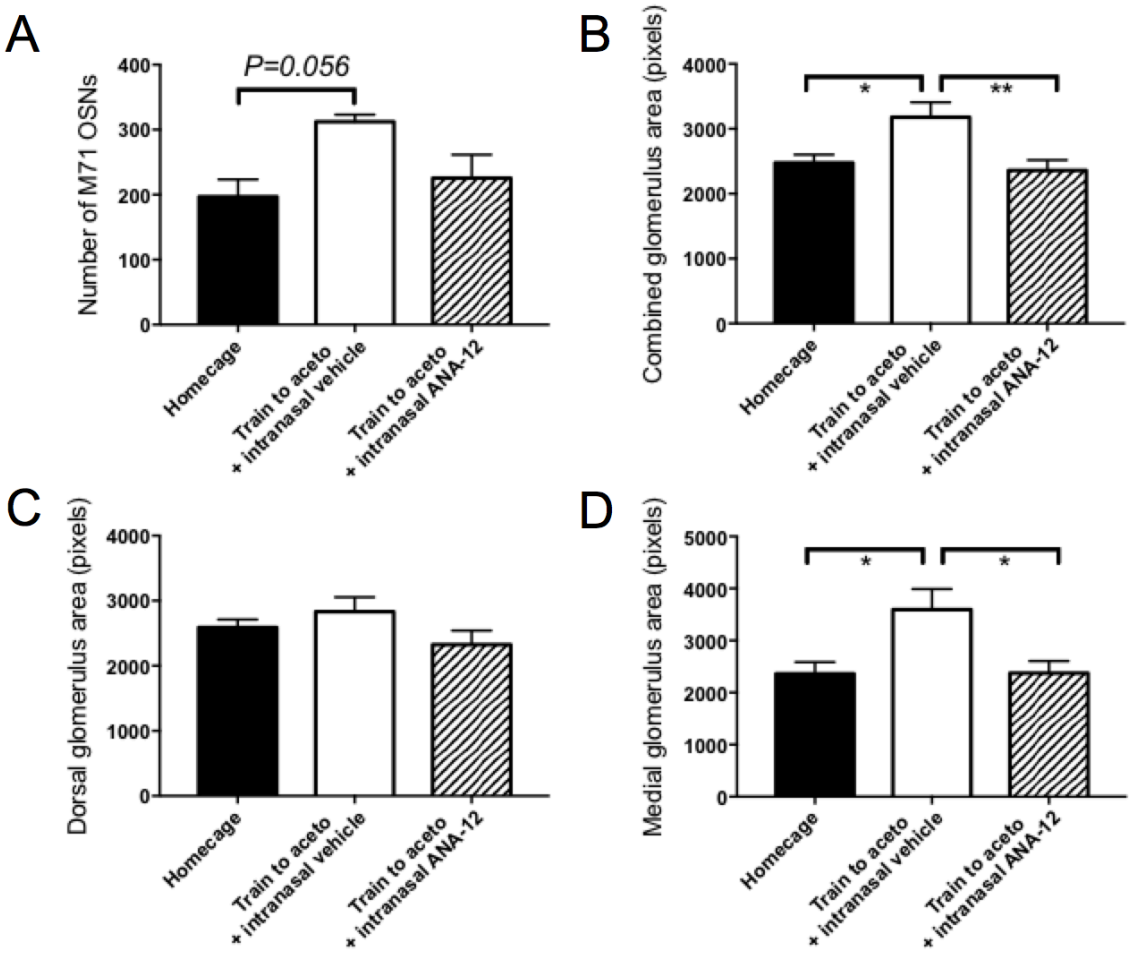

<u>Figure 4.11:</u> Effect of intranasal administration of the TrkB antagonist ANA-12 prior to training on M71 neuron number in the MOE and M71 glomerulus area in the OB.

(a) Mice that received intranasal vehicle (white bar) prior to training have a larger number of M71 OSNs in the MOE than homecage control mice (black bar) and mice that received intranasal ANA-12 prior to training (striped bar) (A; M71-LacZ: Home cage, n=6; Train to aceto + intranasal vehicle, n=2; Train to aceto + intranasal ANA-12, n=5; ANOVA, P=0.1724, F(2,10)=1.407; Homecage versus Train to aceto + intranasal vehicle, P=n.s.; Homecage versus train to aceto + intranasal ANA-12, P=n.s.; Train to aceto + intranasal vehicle versus Train to aceto + intranasal ANA-12, P=n.s.) (Student's t-test; Homecage versus Train to aceto + intranasal vehicle, P=0.0560). (b-d) Mice that received intranasal vehicle (white bar) prior to training have a larger M71 glomerulus area in the OB than home cage control mice (black bar) and mice that received intranasal ANA-12 prior to training (B; Combined M71 glomerulus area: Home cage, n=34; Train to aceto + intranasal vehicle, n=24; Train to aceto + intranasal ANA-12, n=31; ANOVA, P=0.0027, F(2,86)=1.967; Home cage versus Train to aceto + intranasal vehicle, P=0.0125; Home cage versus Train to aceto + intranasal ANA-12, P=n.s.; Train to aceto + intranasal vehicle versus train to aceto + intranasal ANA-12, P=0.0035) (C; Dorsal M71 glomerulus area: Home cage, n=17; Train to aceto + intranasal vehicle, n=13; Train

to aceto + intranasal ANA-12, n=13; ANOVA, P=n.s., F(2,40)=1.458; Home cage versus Train to aceto + intranasal vehicle, P=n.s.; Home cage versus Train to aceto + intranasal ANA-12, P=n.s.; Train to aceto + intranasal vehicle versus train to aceto + intranasal ANA-12, P=n.s.) (D; Medial M71 glomerulus area: Home cage, n=17; Train to aceto + intranasal vehicle, n=11; Train to aceto + intranasal ANA-12, n=18; ANOVA, P=0.0067, F(2,43)=1.15; Home cage versus Train to aceto + intranasal vehicle, P=0.0116; Home cage versus Train to aceto + intranasal ANA-12, P=n.s.; Train to aceto + intranasal vehicle versus train to aceto + intranasal ANA-12, P=0.0117). Data presented as mean +/- s.e.m. *P<0.05, **P<0.01, ***P<0.001, ****P<0.0001.

CHAPTER 5: DISCUSSION

Summary of results

Based on prior evidence in the literature, this dissertation sought to determine the effects of olfactory extinction at the level of the primary sensory system, and also to investigate the mechanisms underlying learning dependent olfactory structural plasticity.

In Chapter 2, we demonstrate that following olfactory fear conditioning to acetophenone, mice show gradual decreases in freezing across extinction sessions, and the decreases in freezing following extinction are pronounced and long-lasting up to at least 3 weeks following extinction training. At the level of the primary olfactory sensory system, we found that mice that received cue-specific extinction show a reversal in the number of M71-expressing neurons as well as a decrease in the size of the M71 specific glomerulus area. In another experiment, we found that the effects of olfactory fear extinction were specific to the conditioned stimulus; mice that were fear conditioned to acetophenone, but extinguished in the exact same manner to propanol (a non-M71 activating control odorant), did not show decreases in the number of M71-expressing OSNs or the size of the M71 specific glomerulus. We also investigated an alternate time course of extinction and found that mice receiving extinction immediately after fear conditioning also show the same reversal in M71 structure. The effect of immediate extinction following conditioning compared to extinction performed 3 weeks following conditioning may differ mechanistically based on the finding that at 3 weeks after conditioning the learning related increases in structure have been established, whereas these enhancements have not yet occurred in the one to three days following conditioning. Finally, using N-ChIP protocols, we demonstrate that consistent with the decreases in M71-expressing OSN numbers with extinction, we also observe a reversal in

occupancy of the "activating" histone modification Acetyl H3 at the *M71* gene in animals that have undergone extinction.

In Chapter 3 we tested the hypothesis that the observed enhancement in M71-expressing OSN number and glomerulus area following fear conditioning to acetophenone is mediated by increases in M71 specific cell survival. We first characterized a time course of regeneration following zinc sulfate induced ablation of the MOE and found that the MOE, but not the glomeruli in the OB, is fully degenerated 2 days following intranasal administration of zinc sulfate. By combining ablation methods with olfactory fear conditioning, we demonstrate that 1) OSNs are required at the time of training to observe the learning induced enhancements in M71 structure, and 2) learning induced enhancements in M71 structure are likely not due to cue specific increases in receptor choice. To further investigate the effect of olfactory fear conditioning on the dynamics of OSN turnover in the MOE, we used EdU methods to label 1) M71-expressing OSNs at baseline control levels, 2) M71-expressing OSNs undergoing mitosis at the time of training, and 3) mature M71-expressing OSNs at the time of training. Our results from these studies combining EdU labeling with olfactory fear training suggest that the training induced enhancements in M71 structure are the result of M71 specific OSN survival rather than proliferation, however, replication experiments are needed to truly confirm these results, as we did not replicate the main effect of enhanced M71-expressing neurons following fear conditioning compared to controls.

In Chapter 4 we tested the effects of TrkB agonist and antagonist administration prior to olfactory fear conditioning on olfactory fear acquisition and memory retention and primary olfactory sensory system representation. Previous research has shown that

BDNF-TrkB signaling plays a critical role in learning and memory, and prior data from our laboratory found that *Bdnf* mRNA is increases in animals receiving paired odor-foot shocks in the OB, anterior and posterior piriform cortex, and the BLA. Based on research showing the expression of TrkB receptors in the MOE, we hypothesized that during olfactory fear conditioning, increases in BDNF may act at TrkB receptors in the MOE, and the dual activation of TrkB receptors with M71 receptors (potentially with additional factors or top down pathways) may lead to the enhanced survival of M71 specific OSNs. To begin testing this hypothesis, we first administered either intranasal or I.P. 7,8-DHF (TrkB agonist) prior to training and found no significant increase compared to vehicle administered groups. However, upon administration of the Trk antagonist K252a, or the TrkB specific antagonist ANA-12 prior to training, we observed a block in M71 specific increases in OSN number and glomerulus area, suggesting that BDNF signaling at TrkB may in part mediate the structural plasticity accompanying learning. We did not observe any difference in freezing behavior during acquisition or testing, suggesting a striking dissociation between neuroanatomical and behavioral responses.

Altogether, the results of this dissertation support the following findings; 1) cue specific olfactory fear extinction reverses the learning induced changes in behavior, primary sensory system neuronatomy and histone modification occupancy at the *M71* gene, 2) the learning induced increases in M71 structure may be the result of M71 specific OSN survival following olfactory fear conditioning to the M71 activating odorant acetophenone, and finally 3) BDNF-TrkB signaling is a mediator of the learning induced enhancement in M71 structure following fear conditioning to acetophenone.

Integration of findings

Prior data from our laboratory have demonstrated that olfactory fear conditioning to acetophenone leads to enhanced behavioral responses (as measured by freezing and fear potentiated startle) to the conditioned odorant, along with increases in acetophenone responsive M71-expressing OSN number and glomerulus area (Jones et al., 2005, 2008a). Furthermore, recent work from our laboratory has shown that the effects of fear conditioning to acetophenone in a parental F0 generation result in behavioral sensitivity of the F1 and F2 generations to acetophenone as well as an enhanced neuroanatomical representation of the M71 pathway. An extremely intriguing question that follows the research presented in this dissertation is whether the extinction of olfactory learning in an F0 parental generation may be transmitted to subsequent F1 and F2 generations. Furthermore, it would be interesting to investigate the effect of extinction training in the F1 generation, and whether such extinction could reverse the transmitted olfactory response.

Previous work and the studies in this dissertation show alterations in freezing behavior following olfactory fear acquisition and extinction. An important question is whether these changes in behavior are the result of enhanced sensitivity to the conditioned odorant. Electroolfactogram (EOG) recordings provide a technique to measure MOE response patterns upon odorant presentation (Coppola et al., 2013; Cygnar et al., 2010; Scott and Sherrill, 2008; Scott et al., 2006). Preliminary studies done by the dissertation author (data not shown) using EOG recordings of zone 1 of the MOE following fear conditioning to acetophenone suggest that at very low concentrations, mice fear conditioned to acetophenone have a higher acetophenone to propanol response

pattern both at 3 and 6 weeks following fear conditioning, suggesting an enhanced sensitivity to the odor CS. Follow-up studies are needed to confirm enhancements in sensitivity as measured by EOG recordings of the MOE, and should also be performed following olfactory fear extinction to determine whether extinction results in corresponding decreases in sensitivity to the odor CS.

Based on the findings from Chapters 3 and 4 investigating the regulation of cell survival and BDNF-TrkB signaling, future experiments are needed to definitively demonstrate the role of BDNF in promoting activity dependent survival of M71-specific OSNs. Interestingly, previous research from our lab showed increases in BDNF mRNA with odor regardless of it being paired to a shock; our results thus suggest that while TrkB signaling may be necessary for the learning induced enhancements in M71 structure, BDNF-TrkB signaling may play a permissive role in promoting OSN survival and may require an additional factor that is released in response to the shock US (Jones et al., 2007).

Such an additional required factor may be the result of top-down control of olfactory perception that may be regulated by olfactory cortical regions, including the amygdala. The results of this dissertation lay an important foundation for future research to examine the regulation of the primary olfactory sensory system via the amygdala and traditional fear circuitry. Future experiments could use muscimol inactivation of the amygdala or other olfactory cortical regions such as the piriform cortex prior to olfactory fear conditioning to investigate the effect of these brain regions on M71 sensory system representation (via M71-expressing OSN number and glomerulus area) and fear behavior. Tying these areas together is promising in its potential to further our understanding of

neural systems biology and has the possibility of leading to profound discoveries related to emotion regulation of sensory function.

A growing body of literature supports a model of plasticity in sensory systems during learning. At the level of the somatosensory system, work has recently investigated a fear conditioning paradigm in which whisker stimulation in freely exploring mice is used as a conditioned stimulus paired with a foot shock (Gdalyahu et al., 2012). Following conditioning, mice exhibited enhanced freezing to stimulation of the whisker CS, with freezing being specific to the trained whisker and not generalized to a distinct, distant, untrained whisker. Behavioral learning was reflected in the rodent primary somatosensory cortex, or barrel cortex, which receives tactile information from distinct whiskers on the facial pad. The authors found that in the region of barrel cortex mapping the trained whisker, fewer neurons responded to stimulation of the whisker CS, however, despite this decrease, the responses of these neurons were significantly stronger than those in control mice that received unpaired conditioning. The authors hypothesize that the observed emergence of combined sparse neuronal responding with increased response strength likely represents an organisms strategy to improve signal to noise following an emotional learning event, while regulating metabolic efficiency. This model is referred to as spare network coding, and represents one strategy by which the somatosensory cortex encodes a learned stimulus associated with an emotional learning event. Further work investigating neural plasticity in the rodent somatosensory cortex has investigated the laminar plasticity following learning; layer 4 of the cortex is thought to be highly plastic only in very young mice, while layer 2/3 remains plastic in adults (Feldman and Brecht, 2005). Additionally, learning-induced plasticity in receptive fields has been studied

extensively in the auditory system, by studying the cortical map expansion following learning to a specific auditory cue. Following learning to a specific cue, the cortical representation of the stimulus expands (Bieszczad and Weinberger, 2010), and the magnitude of cortical map plasticity is also proportional to the level of behavioral motivation associated with the cue stimulus (Weinberger, 2007). Recent findings further indicate that map plasticity enhancements in learning are transient (Molina-Luna et al., 2008; Reed et al., 2011; Yotsumoto et al., 2008). A model has recently been proposed in which auditory cortical map expansion undergoes two phases; 1) the first involves a transient expansion of the neurons responding to the trained stimulus, and 2) the second involves an active selection of efficient circuitry from the expanded pool. Such a model supports the idea of a transient expansion in map plasticity when neurons are recruited by learning, followed by decreases to a more baseline efficient level.

Implications and future directions

The results of this dissertation integrate olfactory sensory biology and fear learning processes, and further a model for understanding the regulation of sensory function as well as altered function associated with symptoms of trauma-related disorders. As we continue to gain a greater understanding of the mechanisms of fear learning and sensory regulation in animal models, we will be able to translate these findings to enhancing therapeutic and diagnostic approaches in humans. Below we will briefly review recent research investigating associative plasticity in human olfactory pathways in health individuals and individuals with PTSD. Additionally, we will place the results from the present dissertation into the larger context of potential translational approaches.

Associative plasticity in the human olfactory sensory system

While the work from the present dissertation only provides evidence for learning induced plasticity of the olfactory sensory system in mice, there is a growing body of literature suggesting that associative learning also induces olfactory neuroplasticity in humans. In a sophisticated series of experiments combining functional magnetic resonance imaging (fMRI) with multivariate analytical techniques, Li et al. investigated the effects of aversive olfactory conditioning on the neural responses to and perceptual changes of odor cues (Li et al., 2008). The authors used perceptually identical odor enantiomers to determine whether aversive odor-footshock conditioning to one enantiomer and not the other would allow individuals the ability to discriminate between the two odors that were previously indistinguishable. Participants underwent conditioning in which one enantiomer was paired with a foot shock, and the other was not. In a forced choice discrimination task, participants that had undergone the aversive associative conditioning were able to pick the odor that had served as the conditioned stimulus, at a rate greater than chance, and also exceeding their preconditioning performance. Accompanying the observed behavioral accuracy in discrimination between the two initially indistinguishable odor enantiomers, the authors also observed spatial divergence of ensemble activity patterns in the posterior piriform cortex, suggesting a major effect of discriminative learning on neural plasticity. This important work highlighted the idea that while prior work investigating threat conditioning has highlighted the role of the conditioned stimulus in the production of behavioral responses, an important consideration should also be how threat conditioning alters the sensory processing and

representation of the conditioned stimulus itself; thus resulting in perceptual learning, enhanced sensitivity and discrimination.

A major question in the field has been whether the alterations in how a learned cue is perceived following a learning event is the result of attentional or perceptual processes; that is, whether attention is acting as a filter for the large amount of environmental sensory stimuli, and these attentional processes are altered with learning, or on the other hand, whether the perceptual processing of sensory cues is heightened with learning. A number of studies have sought to dissociate attentional vs. perceptual processes underlying both olfactory learning as well as PTSD symptomology. In the below section we will review several studies that have shed some light on this problem. The above described Li et al., 2008 work addressed the potential for aversive conditioning leading to heightened attention to the conditioned stimulus; however, the authors found no changes in the anterior piriform cortex, a region purported to play a significant role in human olfactory attention, suggesting that aversive learning may alter odor quality representations rather than modulating attention or arousal.

Follow-up work has not only replicated the behavioral results from Li et al., 2008, but has also demonstrated that aversive learning can also increase the participants' sensitivity to the conditioned odor stimulus (Ahs et al., 2013). Ahs et al., 2013 performed aversive conditioning followed by a force discrimination task as used by Li et al., 2008, and assessed the absolute detection threshold for the conditioned odor stimulus both before and after conditioning, and also investigated the long-term behavioral effects of aversive conditioning on odor sensitivity by testing the odor detection threshold 8 weeks following the conditioning session. Following the conditioning protocol, in addition to

having enhanced discrimination between the two previously indistinguishable enantiomers, participants also showed decreased detection threshold of the odor CS, indicating that threat conditioning enhanced odor sensitivity in an odorant-specific manner. However, the effects on both discrimination and sensitivity were short lasting, with the odor detection threshold levels returning to baseline when tested eight weeks following the initial conditioning. The short lasting effects on discrimination and sensitivity may be due to a relatively short and non-intensive training protocol, as other studies have found long lasting effects of odor learning with more robust training paradigms. Furthermore, the participants did not rate the conditioned odor as more intense, again suggesting that altered discriminative ability is independent of conscious cognitive processes such as attention or expectancy; processes which would be exerted through the top-down modulation of sensory inputs. The present studies provide evidence that olfactory learning affects underlying perceptual, rather than attentional, processes.

Olfactory cues potent and salient trauma reminders and triggers in individuals with posttraumatic stress disorder (PTSD)

The human work described above was performed exclusively in healthy participants with no history of trauma or anxiety like disorders. Olfactory cues may be paired with traumatic experiences in humans (for example the smell of a physical abuser, etc.) and the subsequent exposure to the odor cue may serve as a potent reminder of the traumatic event and may trigger anxiety, phobia, and other PTSD symptoms. Estimates from epidemiological studies indicate that PTSD occurs in up to 10% of the general population (Kessler et al., 2005), and populations that are exposed to chronic physical and emotional trauma experience even higher lifetime rates of PTSD of up to 20-30%

(Breslau et al., 1990; Breslau et al., 2001). While fear learning is at times an adaptive and evolutionarily advantageous response to traumatic events, dysregulated fear processes, resulting in the sensitization and over-generalization to sensory stimuli associated with a traumatic experience, can be extremely harmful to the individual. Recent work supports the hypothesis that PTSD trauma-related odors may serve as extremely salient and potent emotional reminders and triggers. In fact, many individuals suffering from PTSD, report that odors related to trauma experiences serve as potent reminders of past traumatic events. Odors have been shown to enhance the retrieval of trauma memories, trigger physiological arousal (Chu and Downes, 2002; Herz, 2004; Cupchik, 1995; Willander and Larsson, 2006; Saive et al., 2014; Masaoka et al., 2012) and flashbacks (Kline and Rausch, 1985; Vermetten and Bremner, 2003), and olfactory hallucinations have been reported following trauma.

Using PET imaging of cerebral blood flow combined with assessment of psychophysiological and behavioral symptoms, Vermetten et al., 2007 investigated behavioral and neural responses to a range of combat-related odors as well as negative and pleasant odors in male combat veterans with and without PTSD. PTSD combat veterans consistently rated diesel odor as unpleasant and distressing, and also showed increased PTSD symptoms in response to diesel odor exposure compared to combat controls. At the level of PET imaging, exposure to diesel odor evoked increases in regional blood flow in the amygdala, insula, medial prefrontal cortex (mPFC), anterior cingulate cortex (ACC), and decreased blood flow in the lateral prefrontal cortex (lPFC) in veterans with PTSD compared with combat controls.

Another characteristic symptom of PTSD is the presence of posttraumatic nightmares; individuals with PTSD often suffer major sleep disturbances that may include recurrent nightmares (Fontana and Rosenheck, 2008; Leskin et al., 2002), which may persist form many years following the initial trauma (Blagrove et al., 2004) and significantly disturb daytime waking functioning and day-to-day activities and wellbeing. Recent work has suggested that the presence of olfactory sensations as part of nightmares, although rare, may be a possible index of nightmare intensity, and is also related to decreased treatment response outcomes (Harb et al., 2012).

In a recent study, Cortese et al., 2015 investigated behavioral responses to a wide range of odors with different qualities using a self-report strategy in which odor-elicited distress could be examined in combat veterans with and without PTSD. Combat veterans with PTSD reported increased distress to a limited number of odors that included fuel, blood, gunpowder and burning hair, compared to both healthy controls and combat veterans without PTSD. However, in parallel to this observed increase in sensitivity, combat veterans with or without PTSD also displayed lower rates of distress to negative hedonic odors and also lower rates of relaxation in response to positive hedonic odors compared to non-combat healthy controls. One possible mechanisms by which individuals with combat related PTSD experience both an enhancement in sensitivity to select odors with a co-occurring blunting of responses to other odors, may be a parallel strategy that includes both sensitivity and also attentional bias towards threat odors, and a selective ignoring of non-important distractor cues.

The data presented in this thesis demonstrating structural changes following olfactory fear conditioning may underlie the olfactory sensitivity symptoms observed in

PTSD patients described above, and may also underlie multiple chemical sensitivity syndrome, in which an individual becomes hypersensitive to certain odorants (Bell et al., 1992). Multiple chemical sensitivity syndrome is an idiopathic disorder that is thought to manifest following an aversive olfactory experience and the subsequent odor sensitization. Patients suffering from this disorder, as a result of aversive olfactory experiences, may exhibit enhanced structural representations of specific olfactory receptor pathways at the level of primary sensory neurons, causing them to exhibit enhanced sensitivity to these odors.

Clinical relevance of the olfactory system and its potential for inclusion in therapeutic treatment

The results from this dissertation along with evidence from work across rodent models and human clinical research support a model for primary sensory systems, and particularly the olfactory sensory system, as potential tractable and plastic targets that may be manipulated in the treatment of anxiety-like disorders such as PTSD. Hypersensitivity to environmental cues is a characteristic symptom in disorders such as PTSD. A number of factors make the olfactory system particularly well suited for clinical investigations. The non-thalamic connectivity of the olfactory system heightens access to emotional and memory related brain regions, thus making this system a clinically relevant trigger as well as a potentially powerful vector for therapy. Such clinical relevance could be achieved at the level of behavior, based on our results from chapter 2 demonstrating a long lasting and significant reversal in both behavioral and neuroanatomical representations of a learned olfactory trauma cue in mice. Furthermore, the two time courses of extinction training presented in chapter 2 (extinction either

immediately after fear conditioning or three weeks later) have important implications in the timing of exposure-based therapy following a trauma experience.

While fear inhibition can be tested using fear extinction, as described above, it may also be tested using conditioned inhibition, in which a separate stimulus is not paired with the unconditioned stimulus and is instead a safety signal. Conditional discrimination is a more recently developed way to test fear inhibition and is based on learning an AX+ danger signal (which predicts the US), a BX- safety signal (no CS), and an AB transfer test in which the presentation of both A and B results in overall decreased startle responses compared to responses to A, due to the fact that B has become inhibitory (Jovanovic and Ressler, 2010; Jovanovic et al., 2005, 2010; Myers and Davis, 2004). The conditional discrimination paradigm has been used to demonstrate conditioned inhibition in healthy individuals, and an inability to transfer fear inhibition in individuals with PTSD (Jovanovic et al., 2009). Preliminary evidence from the dissertation authors' work (not presented in this thesis) suggests that mice are able to learn an olfactory safety signal following a safety learning behavioral protocol. Thus, one potential for clinical translation would be to co-opt the olfactory system to enhance safety learning and fear inhibition in the treatment of PTSD.

In addition to a behavioral advantage in clinical translation, the olfactory system also possesses a number of advantages for drug delivery and biopsy measures. In chapter 4 we presented evidence of intranasal administration of TrkB agonists and antagonists during fear conditioning and their effects at the level of behavior and olfactory neuroanatomy. Neuroepithelium-to-brain drug delivery may provide one approach for further investigation in clinical research. Additionally, olfactory biopsies may be easily

obtained from human subjects in a non-invasive procedure and may then be used as a source of neural tissue (for cell culture, immunohistochemistry, or epigenetic approaches, etc.) and as a potential way to probe biomarkers related to psychiatric disorders. Overall, we propose a re-conceptualization of the approach to understanding fear related disorders such as PTSD to include acquired changes at the level of primary sensory systems.

Conclusion

The experiments contained in this thesis have investigated the mechanisms underlying the behavioral and structural plasticity of the olfactory system in mice following the acquisition and extinction of cued olfactory fear. This work has continued to develop olfactory fear conditioning as a behavioral paradigm used to model and understand dysregulated fear responses underlying fear-related disorders such as PTSD. An understanding of how primary sensory neurons perceive and regulate the perception of environmental stimuli greatly enhances our understanding of emotional fear regulation and our hope is that this line of research will lead to improved treatment strategies for anxiety disorders such as PTSD, in which the environmental cue associated with the trauma incident can often be recalled. The strength of our fear conditioning paradigm lies in the specificity of the olfactory system, which is both intricately laid out and also plastic and responsive to environmental cues throughout life due to the ongoing adult neurogenesis in olfactory regions. The studies contained in this dissertation contribute to the growing body literature suggesting a critical role for primary sensory systems, particularly the olfactory system, in emotional learning and memory. Looking forward, we hope that these studies will inform new and ongoing translational research in humans to better understand and treat PTSD and other fear and anxiety related disorders.

REFERENCES

Abraham, A.D., Neve, K.A., and Lattal, K.M. (2014). Dopamine and extinction: A convergence of theory with fear and reward circuitry. Neurobiol. Learn. Mem. *108*, 65–77.

Agren, T., Engman, J., Frick, A., Björkstrand, J., Larsson, E.-M., Furmark, T., and Fredrikson, M. (2012). Disruption of reconsolidation erases a fear memory trace in the human amygdala. Science *337*, 1550–1552.

Alberini, C.M., Milekic, M.H., and Tronel, S. (2006). Mechanisms of memory stabilization and de-stabilization. *63*, 999–1008.

Alberts, J.R., and Galef, B.G. (1971). Acute anosmia in the rat: A behavioral test of a peripherally-induced olfactory deficit. Physiol. Behav. *6*, 619–621.

Alonso, M., Lepousez, G., Sebastien, W., Bardy, C., Gabellec, M.-M., Torquet, N., and Lledo, P.-M. (2012). Activation of adult-born neurons facilitates learning and memory. Nat. Neurosci. *15*, 897–904.

Andero, R., and Ressler, K.J. (2012). Fear extinction and BDNF: translating animal models of PTSD to the clinic. Genes. Brain. Behav. *11*, 503–512.

Andero, R., Ph, D., Heldt, S.A., Ye, K., Liu, X., Armario, A., and Ressler, K.J. (2011). TrkB Agonist , on Emotional Learning. 163–172.

Arisi, G.M., Foresti, M.L., Mukherjee, S., and Shapiro, L. a (2011). The role of olfactory stimulus in adult mammalian neurogenesis. Behav. Brain Res.

Banerjee, S.B., Morrison, F.G., Ressler, K.J., (2017). Genetic approaches for the study of PTSD: Advances and challenges. Neurosci. Lett.

Bath, K.G., Chuang, J., Spencer-Segal, J.L., Amso, D., Altemus, M., McEwen, B.S., and Lee, F.S. (2012). Variant brain-derived neurotrophic factor (Valine66Methionine) polymorphism contributes to developmental and estrous stage-specific expression of anxiety-like behavior in female mice. Biol. Psychiatry *72*, 499–504.

Belnoue, L., Grosjean, N., Abrous, D.N., and Koehl, M. (2011). A critical time window for the recruitment of bulbar newborn neurons by olfactory discrimination learning. J. Neurosci. *31*, 1010–1016.

Belzung, C., and Philippot, P. (2007). Anxiety from a phylogenetic perspective: is there a qualitative difference between human and animal anxiety? Neural Plast. *2007*, 59676.

Bialas, A.R., and Stevens, B. (2013). supplemental_TGF-β signaling regulates neuronal C1q expression and developmental synaptic refinement. Nat. Neurosci. *16*, 1773–1782.

Bieszczad, K.M., and Weinberger, N.M. (2010). Representational gain in cortical area underlies increase of memory strength. Proc. Natl. Acad. Sci. U. S. A. *107*, 3793–3798.

Bieszczad, K.M., Miasnikov, a a, and Weinberger, N.M. (2013). Remodeling sensory cortical maps implants specific behavioral memory. Neuroscience *246*, 40–51.

Binder, E.B. (2009). The role of FKBP5, a co-chaperone of the glucocorticoid receptor in the pathogenesis and therapy of affective and anxiety disorders. Psychoneuroendocrinology *34 Suppl 1*, S186-95.

Binder, E.B., Salyakina, D., Lichtner, P., Wochnik, G.M., Ising, M., Pütz, B., Papiol, S., Seaman, S., Lucae, S., Kohli, M. a, et al. (2004). Polymorphisms in FKBP5 are

associated with increased recurrence of depressive episodes and rapid response to antidepressant treatment. Nat. Genet. *36*, 1319–1325.

Binder, E.B., Bradley, R.G., Epstein, M.P., Deveau, T.C., Mercer, K.B., Heim, C.M., Nemeroff, C.B., Schwartz, A.C., and Cubells, J.F. (2008). Association of FKBP5 Polymorphisms and Childhood Abuse With Risk of Posttraumatic Stress Disorder Symptoms in Adults. *299*.

Blair, H.T., Schafe, G.E., Bauer, E.P., Rodrigues, S.M., and LeDoux, J.E. (2001). Synaptic plasticity in the lateral amygdala: a cellular hypothesis of fear conditioning. Learn. Mem. *8*, 229–242.

Bonmpo, A., Panza, K.E., and Bloch, M.H. (2013). Meta-Analysis: D-cycloserine Augmentation of Behavioral Therapy for the Treatment of Anxiety Disorders. J. Clin. Psychiatry *73*, 533–537.

Bozza, T., Feinstein, P., Zheng, C., and Mombaerts, P. (2002). Odorant receptor expression defines functional units in the mouse olfactory system. J. Neurosci. *22*, 3033–3043.

Bozza, T., Mcgann, J.P., Mombaerts, P., and Wachowiak, M. (2004). *In Vivo* Imaging of Neuronal Activity Neurotechnique by Targeted Expression of a Genetically Encoded Probe in the Mouse. *42*, 9–21.

Brain, B., Cohen, N.J., Memory, H., and Memory, L.R. (1998). Selected references What is the amygdala□? *21*, 323–331.

Breslau, N., and Ph, D. (2001). The Epidemiology of Posttraumatic Stress Disorder□: What Is the Extent of the Problem□? rig ht a du rig Pr. *62*.

Bressel, O.C., Khan, M., and Mombaerts, P. (2016). Linear correlation between the number of olfactory sensory neurons expressing a given mouse odorant receptor gene and the total volume of the corresponding glomeruli in the olfactory bulb. J. Comp. Neurol. *524*, 199–209.

Breton-Provencher, V., Lemasson, M., Peralta, M.R., and Saghatelyan, A. (2009). Interneurons produced in adulthood are required for the normal functioning of the olfactory bulb network and for the execution of selected olfactory behaviors. J. Neurosci. *29*, 15245–15257.

Buck, L., and Axel, R. (1991). A novel multigene family may encode odorant receptors: a molecular basis for odor recognition. Cell *65*, 175–187.

Bueller, J. a, Aftab, M., Sen, S., Gomez-Hassan, D., Burmeister, M., and Zubieta, J.-K. (2006). BDNF Val66Met allele is associated with reduced hippocampal volume in healthy subjects. Biol. Psychiatry *59*, 812–815.

Caggiano, M., Kauer, J.S., and Hunter, D.D. (1994). G lobose Basal Cells Are Neuronal Progenitors in the O lfactory Epithelium□: A lineage Analysis Using a Replication-Incompetent Retrovirus. *13*, 339–352.

Cain, C.K., Maynard, G.D., and Kehne, J.H. (2012). Targeting memory processes with drugs to prevent or cure PTSD. Expert Opin. Investig. Drugs *21*, 1323–1350.

Callaghan, B.L., Sullivan, R.M., Howell, B., and Tottenham, N. (2014). The international society for developmental psychobiology sackler symposium: Early adversity and the maturation of emotion circuits-A cross-species analysis. Dev. Psychobiol.

Camp, L.L., and Rudy, J.W. (1988). Chanqes in the Cateqorization of Appetitive and Aversive Events During Postnatal Development of the Rat. *21*, 25–42.

Campeau, S., and Davis, M. (1995). Involvement of subcortical and cortical afferents to

the lateral nucleus of the amygdala in fear conditioning measured with fear-potentiated startle in rats trained concurrently with auditory and visual conditioned stimuli. J. Neurosci. *15*, 2312–2327.

Carr, V.M., and Farbman, A.I. (1992). Ablation of the olfactory bulb up-regulates the rate of neurogenesis and induces precocious cell death in olfactory epithelium. Exp. Neurol. *115*, 55–59.

Carr, V.M., and Farbman, A.I. (1993). The dynamics of cell death in the olfactory epithelium. Exp. Neurol. *124*, 308–314.

Cazorla, M., Pr??mont, J., Mann, A., Girard, N., Kellendonk, C., and Rognan, D. (2011). Identification of a low-molecular weight TrkB antagonist with anxiolytic and antidepressant activity in mice. J. Clin. Invest. *121*, 1846–1857.

Chhatwal, J.P., Stanek-Rattiner, L., Davis, M., and Ressler, K.J. (2006). Amygdala BDNF signaling is required for consolidation but not encoding of extinction. Nat. Neurosci. *9*, 870–872.

Choi, D.C., Maguschak, K. a, Ye, K., Jang, S.-W., Myers, K.M., and Ressler, K.J. (2010). Prelimbic cortical BDNF is required for memory of learned fear but not extinction or innate fear. Proc. Natl. Acad. Sci. U. S. A. *107*, 2675–2680.

Chung, W.-S., Welsh, C.A., Barres, B.A., and Stevens, B. (2015). Do glia drive synaptic and cognitive impairment in disease? Nat. Publ. Gr. *18*, 1539–1545.

Ciocchi, S., Herry, C., Grenier, F., Wolff, S.B.E., Letzkus, J.J., Vlachos, I., Ehrlich, I., Sprengel, R., Deisseroth, K., Stadler, M.B., et al. (2010). Encoding of conditioned fear in central amygdala inhibitory circuits. Nature *468*, 277–282.

Coppola, D.M., Waggener, C.T., Radwani, S.M., and Brooks, D. a (2013). An electroolfactogram study of odor response patterns from the mouse olfactory epithelium with reference to receptor zones and odor sorptiveness. J. Neurophysiol. *109*, 2179–2191.

Corotto, F.S., Henegar, J.R., and Maruniak, J.A. (1994). Odor deprivation leads to reduced neurogenesis and reduced neuronal survival in the olfactory bulb of the adult mouse. Neuroscience *61*, 739–744.

Cowan, C.M., and Roskams, a J. (2002). Apoptosis in the mature and developing olfactory neuroepithelium. Microsc. Res. Tech. *58*, 204–215.

Cowan, C.M., Thai, J., Krajewski, S., Reed, J.C., Nicholson, D.W., Kaufmann, S.H., and Roskams, a J. (2001). Caspases 3 and 9 send a pro-apoptotic signal from synapse to cell body in olfactory receptor neurons. J. Neurosci. *21*, 7099–7109.

Cukor, J., Spitalnick, J., Difede, J., Rizzo, A., and Rothbaum, B.O. (2009). Emerging treatments for PTSD. Clin. Psychol. Rev. *29*, 715–726.

Cygnar, K.D., Stephan, A.B., and Zhao, H. (2010). Analyzing responses of mouse olfactory sensory neurons using the air-phase electroolfactogram recording. J. Vis. Exp. 1–5.

Davis, M. (1992). The role of the amygdala in fear and anxiety. Annu. Rev. Neurosci. *15*, 353–375.

Deckner, M.L., Frisén, J., Verge, V.M., Hökfelt, T., and Risling, M. (1993). Localization of neurotrophin receptors in olfactory epithelium and bulb. Neuroreport *5*, 301–304.

Deckner, M.L., Risling, M., and Frisén, J. (1997). Apoptotic death of olfactory sensory neurons in the adult rat. Exp. Neurol. *143*, 132–140.

Dias, B.G., and Ressler, K.J. (2013). Parental olfactory experience influences behavior and neural structure in subsequent generations. Nat. Neurosci.

Ducray, A., Bondier, J.-R., Michel, G., Bon, K., Propper, A., and Kastner, A. (2002). Recovery following peripheral destruction of olfactory neurons in young and adult mice. Eur. J. Neurosci. *15*, 1907–1917.

Dudchenko, P.A., Wood, E.R., and Eichenbaum, H. (2000). Neurotoxic hippocampal lesions have no effect on odor span and little effect on odor recognition memory but produce significant impairments on spatial span, recognition, and alternation. J. Neurosci. *20*, 2964–2977.

Egan, M.F., Kojima, M., Callicott, J.H., Goldberg, T.E., Kolachana, B.S., Bertolino, A., Zaitsev, E., Gold, B., Goldman, D., Dean, M., et al. (2003). The BDNF val66met polymorphism affects activity-dependent secretion of BDNF and human memory and hippocampal function. Cell *112*, 257–269.

Eshel, N., Bukwich, M., Rao, V., Hemmelder, V., Tian, J., and Uchida, N. (2015). Arithmetic and local circuitry underlying dopamine prediction errors. Nature *525*, 243–246.

Etkin, A., and Wager, T.D. (2012). Functional Neuroimaging of Anxiety: A Meta-Analysis of Emotional Processing in PTSD, Social Anxiety Disorder, and Specific Phobia. Am. J Psychiatry *164*, 1476–1488.

Falls, W. a, Miserendino, M.J., and Davis, M. (1992). Extinction of fear-potentiated startle: blockade by infusion of an NMDA antagonist into the amygdala. J. Neurosci. *12*, 854–863.

Fani, N., King, T.Z., Brewster, R., Srivastava, A., Stevens, J.S., Glover, E.M., Norrholm, S.D., Bradley, B., Ressler, K.J., and Jovanovic, T. (2014). Fear-potentiated startle during extinction is associated with white matter microstructure and functional connectivity. Cortex. *64C*, 249–259.

Fanselow, M.S., and Ledoux, J.E. (1999). Pavlovian Fear Conditioning Occurs in the Basolateral Amygdala. *23*, 229–232.

Farbman, A.I. (1990). Olfactory neurogenesis: genetic or environmental controls? Trends Neurosci. *13*, 362–365.

Feinstein, P., Bozza, T., Rodriguez, I., Vassalli, A., and Mombaerts, P. (2004). Axon guidance of mouse olfactory sensory neurons by odorant receptors and the beta2 adrenergic receptor. Cell *117*, 833–846.

Feldman, D.E., and Brecht, M. (2005). Map plasticity in somatosensory cortex. Science (80-.). *310*, 810–815.

Frielingsdorf, H., Bath, K.G., Soliman, F., and Difede, J. (2010). Variant brain-derived neurotrophic factor Val66Met endophenotypes: implications or posttraumatic stress disorder. *1208*, 150–157.

Gdalyahu, A., Tring, E., Polack, P., Gruver, R., Golshani, P., Fanselow, M.S., Silva, A.J., and Trachtenberg, J.T. (2012). Associative Fear Learning Enhances Sparse Network Coding in Primary Sensory Cortex. 121–132.

Goldman, A.L., Van Der Goes Van Naters, W., Lessing, D., Warr, C.G., and Carlson, J.R. (2005). Coexpression of two functional odor receptors in one neuron. Neuron *45*, 661–666.

Graziadei, P.P.C. (1973). Cell dynamics in the olfactory mucosa. Tissue Cell *5*, 113–131.

Graziadei, P.P., and Graziadei, G. a (1979). Neurogenesis and neuron regeneration in the

olfactory system of mammals. I. Morphological aspects of differentiation and structural organization of the olfactory sensory neurons. J Neurocytol *8*, 1–18.

Graziadei, P.P., Levine, R.R., and Graziadei, G.A. (1978). Regeneration of olfactory axons and synapse formation in the forebrain after bulbectomy in neonatal mice. Proc. Natl. Acad. Sci. U. S. A. *75*, 5230–5234.

Haubensak, W., Kunwar, P.S., Cai, H., Ciocchi, S., Wall, N.R., Ponnusamy, R., Biag, J., Dong, H.-W., Deisseroth, K., Callaway, E.M., et al. (2010). Genetic dissection of an amygdala microcircuit that gates conditioned fear. Nature *468*, 270–276.

Heldt, S. a, and Ressler, K.J. (2009). The Use of Lentiviral Vectors and Cre/loxP to Investigate the Function of Genes in Complex Behaviors. Front. Mol. Neurosci. *2*, 22.

Heldt, S. a, Stanek, L., Chhatwal, J.P., and Ressler, K.J. (2007). Hippocampus-specific deletion of BDNF in adult mice impairs spatial memory and extinction of aversive memories. Mol. Psychiatry *12*, 656–670.

Heydari, S., and Holroyd, C.B. (2016). Reward positivity: Reward prediction error or salience prediction error? Psychophysiology *53*, 1185–1192.

Holcomb, J.D., Mumm, J.S., and Calof, A.L. (1995). Apoptosis in the neuronal lineage of the mouse olfactory epithelium: regulation *in vivo* and in vitro. Dev. Biol. *172*, 307–323.

Holtzman-Assif, O., Laurent, V., and Westbrook, R.F. (2010). Blockade of dopamine activity in the nucleus accumbens impairs learning extinction of conditioned fear. Learn. Mem. *17*, 71–75.

Hong, I., Song, B., Lee, S., Kim, J., Kim, J., and Choi, S. (2009). Extinction of cued fear memory involves a distinct form of depotentiation at cortical input synapses onto the lateral amygdala. Eur. J. Neurosci. *30*, 2089–2099.

Hong, S., Dissing-Olesen, L., and Stevens, B. (2016). New insights on the role of microglia in synaptic pruning in health and disease. Curr. Opin. Neurobiol. *36*, 128–134.

Hunter, D.D., Caggiano, M., and Kauer, J.S. (1994). Lineage analysis of the olfactory epithelium using a replication-incompetent retrovirus. Chem Senses *19*, 683–693.

Jang, S.-W., Liu, X., Yepes, M., Shepherd, K.R., Miller, G.W., Liu, Y., Wilson, W.D., Xiao, G., Blanchi, B., Sun, Y.E., et al. (2010). A selective TrkB agonist with potent neurotrophic activities by 7,8-dihydroxyflavone. Proc. Natl. Acad. Sci. U. S. A. *107*, 2687–2692.

Johansen, J.P., Cain, C.K., Ostroff, L.E., and LeDoux, J.E. (2011). Molecular mechanisms of fear learning and memory. Cell *147*, 509–524.

Jones, S. V, Heldt, S. a, Davis, M., and Ressler, K.J. (2005). Olfactory-mediated fear conditioning in mice: simultaneous measurements of fear-potentiated startle and freezing. Behav. Neurosci. *119*, 329–335.

Jones, S. V, Stanek-Rattiner, L., Davis, M., and Ressler, K.J. (2007). Differential regional expression of brain-derived neurotrophic factor following olfactory fear learning. Learn. Mem. *14*, 816–820.

Jones, S. V, Choi, D.C., Davis, M., and Ressler, K.J. (2008a). Learning-Dependent Structural Plasticity in the Adult Olfactory Pathway. *28*, 13106–13111.

Jones, S. V, Choi, D.C., Davis, M., and Ressler, K.J. (2008b). Learning-dependent structural plasticity in the adult olfactory pathway. J. Neurosci. *28*, 13106–13111.

Jovanovic, T., and Ressler, K.J. (2010). How the neurocircuitry and genetics of fear inhibition may inform our understanding of PTSD. Am. J. Psychiatry *167*, 648–662.

Jovanovic, T., Keyes, M., Fiallos, A., Myers, K.M., Davis, M., and Duncan, E.J. (2005). Fear potentiation and fear inhibition in a human fear-potentiated startle paradigm. Biol. Psychiatry *57*, 1559–1564.

Jovanovic, T., Blanding, N.Q., Norrholm, S.D., Duncan, E., Bradley, B., and Ressler, K.J. (2009). Childhood abuse is associated with increased startle reactivity in adulthood. Depress. Anxiety *26*, 1018–1026.

Jovanovic, T., Norrholm, S.D., Blanding, N.Q., Davis, M., Duncan, E., Bradley, B., and Ressler, K.J. (2010). Impaired fear inhibition is a biomarker of PTSD but not depression. Depress. Anxiety *27*, 244–251.

Kass, M.D., Rosenthal, M.C., Pottackal, J., and McGann, J.P. (2013). Fear Learning Enhances Neural Responses to Threat-Predictive Sensory Stimuli. Science (80-.). *342*, 1389–1392.

Kass, M.D., Rosenthal, M.C., Pottackal, J., and Mcgann, J.P. (2014). NIH Public Access. *342*, 1389–1392.

Keiflin, R., and Janak, P.H. (2015). Dopamine Prediction Errors in Reward Learning and Addiction: From Theory to Neural Circuitry. Neuron *88*, 247–263.

Kermen, F., Midroit, M., Kuczewski, N., Forest, J., Thévenet, M., Sacquet, J., Benetollo, C., Richard, M., Didier, A., and Mandairon, N. (2016). Topographical representation of odor hedonics in the olfactory bulb.

Kerr, M. a, and Belluscio, L. (2006). Olfactory experience accelerates glomerular refinement in the mammalian olfactory bulb. Nat. Neurosci. *9*, 484–486.

Kessler, R.C., Berglund, P., Demler, O., Jin, R., Merikangas, K.R., and Walters, E.E. (2005). Lifetime prevalence and age-of-onset distributions of DSM-IV disorders in the National Comorbidity Survey Replication. Arch. Gen. Psychiatry *62*, 593–602.

Kim, J., Song, B., Hong, I., Kim, J., Lee, J., Park, S., Yong Eom, J., Lee, C.J., Lee, S., and Choi, S. (2010). Reactivation of Fear Memory Renders Consolidated Amygdala Synapses Labile. J. Neurosci. *30*, 9631–9640.

King, E.C., Pattwell, S.S., Glatt, C.E., and Lee, F.S. (2013). Sensitive periods in fear learning and memory. Stress *3890*, 1–9.

Kitte, P.W. (1990). On the Life Span of Olfactory Receptor Neurons. *3*.

de Kleine, R. a, Hendriks, G.-J., Kusters, W.J.C., Broekman, T.G., and van Minnen, A. (2012). A randomized placebo-controlled trial of D-cycloserine to enhance exposure therapy for posttraumatic stress disorder. Biol. Psychiatry *71*, 962–968.

Klengel, T., Mehta, D., Anacker, C., Rex-haffner, M., Pruessner, J.C., Pariante, C.M., Pace, T.W.W., Mercer, K.B., Mayberg, H.S., Bradley, B., et al. (2012). Allele-specific FKBP5 DNA demethylation mediates gene – childhood trauma interactions. Nat. Neurosci. 1–12.

Knight, D.C., Smith, C.N., Cheng, D.T., Stein, E. a, and Helmstetter, F.J. (2004). Amygdala and hippocampal activity during acquisition and extinction of human fear conditioning. Cogn. Affect. Behav. Neurosci. *4*, 317–325.

Kobayakawa, K., Kobayakawa, R., Matsumoto, H., Oka, Y., Imai, T., Ikawa, M., Okabe, M., Ikeda, T., Itohara, S., Kikusui, T., et al. (2007). Innate versus learned odour

processing in the mouse olfactory bulb. Nature *450*, 503–508.
Korte, M., Carrolltt, P., Wolf, E., Brem, G., Thoenent, H., and Bonhoeffer, T. (1995). brain-derived neurotrophic. *92*, 8856–8860.
Krusemark, E. a, Novak, L.R., Gitelman, D.R., and Li, W. (2013). When the sense of smell meets emotion: anxiety-state-dependent olfactory processing and neural circuitry adaptation. J. Neurosci. *33*, 15324–15332.
Kushner, M.G., Kim, S.W., Donahue, C., Thuras, P., Adson, D., Kotlyar, M., McCabe, J., Peterson, J., and Foa, E.B. (2007). D-cycloserine augmented exposure therapy for obsessive-compulsive disorder. Biol. Psychiatry *62*, 835–838.
Landers, M.S., and Sullivan, R.M. (2012). The Development and Neurobiology of Infant Attachment and Fear. Dev. Neurosci. *10016*, 1–14.
Lang, P.J., Davis, M., and Ohman, a (2000). Fear and anxiety: animal models and human cognitive psychophysiology. J. Affect. Disord. *61*, 137–159.
Lanuza, E., Nader, K., and Ledoux, J.E. (2004). Unconditioned stimulus pathways to the amygdala: effects of posterior thalamic and cortical lesions on fear conditioning. Neuroscience *125*, 305–315.
Lapid, H., Shushan, S., Plotkin, A., Voet, H., Roth, Y., Hummel, T., Schneidman, E., and Sobel, N. (2011). Neural activity at the human olfactory epithelium reflects olfactory perception. Nat. Neurosci. *14*, 1455–1461.
Lazarini, F., and Lledo, P.-M. (2011). Is adult neurogenesis essential for olfaction? Trends Neurosci. *34*, 20–30.
Ledoux, J.E., Romanski, M., and Xagoraris, A. (1990). The Lateral Amygdaloid in Fear Conditioning Nucleus□: Sensory Interface Amygdala.
LeDoux, J.E., Iwata, J., Cicchetti, P., and Reis, D.J. (1988). Different projections of the central amygdaloid nucleus mediate autonomic and behavioral correlates of conditioned fear. J. Neurosci. *8*, 2517–2529.
Levenson, J.M., and Sweatt, J.D. (2005). Epigenetic mechanisms in memory formation. Nat. Rev. Neurosci. *6*, 108–118.
Levenson, J.M., O'Riordan, K.J., Brown, K.D., Trinh, M. a, Molfese, D.L., and Sweatt, J.D. (2004). Regulation of histone acetylation during memory formation in the hippocampus. J. Biol. Chem. *279*, 40545–40559.
Li, W. (2014). Learning to smell danger: acquired associative representation of threat in the olfactory cortex. Front. Behav. Neurosci. *8*, 98.
Li, J., Ishii, T., Feinstein, P., and Mombaerts, P. (2004). Odorant receptor gene choice is reset by nuclear transfer from mouse olfactory sensory neurons. Nature *428*, 393–399.
Li, W., Howard, J.D., Parrish, T.B., and Gottfried, J.A. (2008). Aversive Learning Enhances Perceptual and Cortical Discrimination of Indiscriminable Odor Cues. *964*, 1842–1846.
Lledo, P., Alonso, M., and Grubb, M.S. (2006). Adult neurogenesis and functional. *7*, 179–193.
Lodovichi, C., and Belluscio, L. (2012). Odorant receptors in the formation of the olfactory bulb circuitry. Physiology (Bethesda). *27*, 200–212.
Lovelace, C.T., and Slotnick, B.M. (1995). Memory for brief, widely spaced odor presentations in the rat. Chem. Senses *20*, 183–190.
Lubin, F.D., and Sweatt, J.D. (2008). NIH Public Access. *55*, 942–957.

Luskin, M.B., and Price, J.L. (1983). The topographic organization of associational fibers of the olfactory system in the rat, including centrifugal fibers to the olfactory bulb. J. Comp. Neurol. *216*, 264–291.

Magklara, A., and Lomvardas, S. (2013). Stochastic gene expression in mammals: lessons from olfaction. Trends Cell Biol. 1–8.

Magklara, A., Yen, A., Colquitt, B.M., Clowney, E.J., Allen, W., Markenscoff-Papadimitriou, E., Evans, Z. a, Kheradpour, P., Mountoufaris, G., Carey, C., et al. (2011). An epigenetic signature for monoallelic olfactory receptor expression. Cell *145*, 555–570.

Mahan, A.L., and Ressler, K.J. (2012). Fear conditioning, synaptic plasticity and the amygdala: implications for posttraumatic stress disorder. Trends Neurosci. *35*, 24–35.

Mak, G.K., Enwere, E.K., Gregg, C., Pakarainen, T., Poutanen, M., Huhtaniemi, I., and Weiss, S. (2007). Male pheromone-stimulated neurogenesis in the adult female brain: possible role in mating behavior. Nat. Neurosci. *10*, 1003–1011.

Mandairon, N., and Linster, C. (2009). Odor perception and olfactory bulb plasticity in adult mammals. J. Neurophysiol. *101*, 2204–2209.

Maren, S. (2005). Synaptic mechanisms of associative memory in the amygdala. Neuron *47*, 783–786.

McBride, K., Slotnick, B., and Margolis, F.L. (2003). Does intranasal application of zinc sulfate produce anosmia in the mouse? An olfactometric and anatomical study. Chem. Senses *28*, 659–670.

McHugh, S.B., Barkus, C., Huber, A., Capitão, L., Lima, J., Lowry, J.P., and Bannerman, D.M. (2014). Aversive prediction error signals in the amygdala. J. Neurosci. *34*, 9024–9033.

McKernan, M.G., and Shinnick-Gallagher, P. (1997). Fear conditioning induces a lasting potentiation of synaptic currents in vitro. Nature *390*, 607–611.

Mehta, D., and Binder, E.B. (2012). Gene × environment vulnerability factors for PTSD: the HPA-axis. Neuropharmacology *62*, 654–662.

Milad, M.R., Wright, C.I., Orr, S.P., Pitman, R.K., Quirk, G.J., and Rauch, S.L. (2007). Recall of fear extinction in humans activates the ventromedial prefrontal cortex and hippocampus in concert. Biol. Psychiatry *62*, 446–454.

Milad, M.R., Orr, S.P., Lasko, N.B., Chang, Y., Rauch, S.L., and Pitman, R.K. (2008). Presence and acquired origin of reduced recall for fear extinction in PTSD: results of a twin study. J. Psychiatr. Res. *42*, 515–520.

Miller, C. a, Campbell, S.L., and Sweatt, J.D. (2008). DNA methylation and histone acetylation work in concert to regulate memory formation and synaptic plasticity. Neurobiol. Learn. Mem. *89*, 599–603.

Minichiello, L. (2009). TrkB signalling pathways in LTP and learning. Nat. Rev. Neurosci. *10*, 850–860.

Molina-Luna, K., Hertler, B., Buitrago, M.M., and Luft, A.R. (2008). Motor learning transiently changes cortical somatotopy. Neuroimage *40*, 1748–1754.

Mombaerts, P. (2004). Genes and ligands for odorant, vomeronasal and taste receptors. Nat. Rev. Neurosci. *5*, 263–278.

Mombaerts, P. (2006). Axonal wiring in the mouse olfactory system. Annu. Rev. Cell Dev. Biol. *22*, 713–737.

Mombaerts, P., Wang, F., Dulac, C., Chao, S.K., Nemes, a, Mendelsohn, M., Edmondson, J., and Axel, R. (1996). Visualizing an olfactory sensory map. Cell *87*, 675–686.

Monahan, K., and Lomvardas, S. (2015). Monoallelic Expression of Olfactory Receptors. Annu. Rev. Cell Dev. Biol. *31*, 721–740.

Moreno, M.M., Linster, C., Escanilla, O., Sacquet, J., Didier, A., and Mandairon, N. (2009). Olfactory perceptual learning requires adult neurogenesis. Proc. Natl. Acad. Sci. U. S. A. *106*, 17980–17985.

Moreno, M.M., Bath, K., Kuczewski, N., Sacquet, J., Didier, a., and Mandairon, N. (2012). Action of the Noradrenergic System on Adult-Born Cells Is Required for Olfactory Learning in Mice. J. Neurosci. *32*, 3748–3758.

Mori, K., and Sakano, H. (2011). How is the olfactory map formed and interpreted in the mammalian brain? Annu. Rev. Neurosci. *34*, 467–499.

Moriceau, S., and Sullivan, R.M. (2006). Maternal presence serves as a switch between learning fear and attraction in infancy. *9*, 1004–1006.

Moriceau, S., Wilson, D. a, Levine, S., and Sullivan, R.M. (2006). Dual circuitry for odor-shock conditioning during infancy: corticosterone switches between fear and attraction via amygdala. J. Neurosci. *26*, 6737–6748.

Moriceau, S., Raineki, C., Holman, J.G.J.D., and Sullivan, R.M. (2009). Enduring neurobehavioral effects of early life trauma mediated through learning and corticosterone suppression. Front. Behav. Neurosci. *3*, 22.

Morrison, F.G., Dias, B.G., and Ressler, K.J. (2015). Extinction reverses olfactory fear-conditioned increases in neuron number and glomerular size. Proc. Natl. Acad. Sci. *112*, 12846–12851.

Moulton, D.G. (1974). Dynamics of Cell Populations in the Olfactory Epithelium. Ann. N. Y. Acad. Sci. *237*, 52–61.

Mouret, A., Gheusi, G., Gabellec, M.-M., de Chaumont, F., Olivo-Marin, J.-C., and Lledo, P.-M. (2008). Learning and survival of newly generated neurons: when time matters. J. Neurosci. *28*, 11511–11516.

Mouret, A., Lepousez, G., Gras, J., Gabellec, M.-M., and Lledo, P.-M. (2009). Turnover of newborn olfactory bulb neurons optimizes olfaction. J. Neurosci. *29*, 12302–12314.

Myers, K.M., and Davis, M. (2004). AX+, BX- Discrimination Learning in the Fear-Potentiated Startle Paradigm: Possible Relevance to Inhibitory Fear Learning in Extinction. Learn. Mem. *11*, 464–475.

Myers, K.M., and Davis, M. (2007). Mechanisms of fear extinction. 120–150.

Nakatani, H., Serizawa, S., Nakajima, M., Imai, T., and Sakano, H. (2003). Developmental elimination of ectopic projection sites for the transgenic OR gene that has lost zone specificity in the olfactory epithelium. Eur. J. Neurosci. *18*, 2425–2432.

Nibu, K., Kondo, C.A.K., Ohta, Y., Ishibashi, T., Rothstein, J.L., and Kaga, K. (2001). Expression of NeuroD and TrkB in developing and aged mouse olfactory epithelium. *12*, 1615–1619.

Ninan, I., Bath, K.G., Dagar, K., Perez-Castro, R., Plummer, M.R., Lee, F.S., and Chao, M. V (2010). The BDNF Val66Met polymorphism impairs NMDA receptor-dependent synaptic plasticity in the hippocampus. J. Neurosci. *30*, 8866–8870.

Norberg, M.M., Krystal, J.H., and Tolin, D.F. (2008). A meta-analysis of D-cycloserine and the facilitation of fear extinction and exposure therapy. Biol. Psychiatry *63*, 1118–1126.

Orsini, C. a, and Maren, S. (2012). Neural and cellular mechanisms of fear and extinction memory formation. Neurosci. Biobehav. Rev. *36*, 1773–1802.

Pape, H., and Pare, D. (2010). Plastic Synaptic Networks of the Amygdala for the Acquisition , Expression , and Extinction of Conditioned Fear. 419–463.

Parsons, R.G., and Ressler, K.J. (2013). Implications of memory modulation for post-traumatic stress and fear disorders. Nat. Neurosci. *16*, 146–153.

Paschall, G.Y., and Davis, M. (2002a). Olfactory-mediated fear-potentiated startle. Behav. Neurosci. *116*, 4–12.

Paschall, G.Y., and Davis, M. (2002b). Second-order olfactory-mediated fear-potentiated startle. Learn. Mem. *9*, 395–401.

Pattwell, S.S., Bath, K.G., Perez-Castro, R., Lee, F.S., Chao, M. V, and Ninan, I. (2012). The BDNF Val66Met polymorphism impairs synaptic transmission and plasticity in the infralimbic medial prefrontal cortex. J. Neurosci. *32*, 2410–2421.

Pedersen, P.E., and Blass, E.M. (1982). Determinants of the 1st Suckliny Episode in Albino Rats. *15*, 349–355.

Peters, J., Dieppa-Perea, L.M., Melendez, L.M., and Quirk, G.J. (2010). Induction of fear extinction with hippocampal-infralimbic BDNF. Science *328*, 1288–1290.

Petreanu, L., and Alvarez-Buylla, A. (2002). Maturation and death of adult-born olfactory bulb granule neurons: role of olfaction. J. Neurosci. *22*, 6106–6113.

Phelps, E. a, Delgado, M.R., Nearing, K.I., and LeDoux, J.E. (2004). Extinction learning in humans: role of the amygdala and vmPFC. Neuron *43*, 897–905.

Potter, S.M., Zheng, C., Koos, D.S., Feinstein, P., Fraser, S.E., and Mombaerts, P. (2001). Structure and emergence of specific olfactory glomeruli in the mouse. J. Neurosci. *21*, 9713–9723.

Quirk, G.J., Paré, D., Richardson, R., Herry, C., Monfils, M.H., Schiller, D., and Vicentic, A. (2010). Erasing fear memories with extinction training. J. Neurosci. *30*, 14993–14997.

Raineki, C., Moriceau, S., and Sullivan, R.M. (2010). Developing a neurobehavioral animal model of infant attachment to an abusive caregiver. Biol. Psychiatry *67*, 1137–1145.

Raineki, C., Rinco, M., Belnoue, L., and Sullivan, R.M. (2012). Effects of Early-Life Abuse Differ across Development : Infant Social Behavior Deficits Are Followed by Adolescent Depressive-Like Behaviors Mediated by the Amygdala. *32*, 7758–7765.

Rattiner, L.M., Davis, M., French, C.T., and Ressler, K.J. (2004). Brain-derived neurotrophic factor and tyrosine kinase receptor B involvement in amygdala-dependent fear conditioning. J. Neurosci. *24*, 4796–4806.

Rattiner, L.M., Davis, M., and Ressler, K.J. (2005). Brain-derived neurotrophic factor in amygdala-dependent learning. Neuroscientist *11*, 323–333.

Reed, A., Riley, J., Carraway, R., Carrasco, A., Perez, C., Jakkamsetti, V., and Kilgard, M.P. (2011). Cortical Map Plasticity Improves Learning but Is Not Necessary for Improved Performance. Neuron *70*, 121–131.

Ren, Q., Ma, M., Yang, C., Zhang, J.-C., Yao, W., and Hashimoto, K. (2015). BDNF-

TrkB signaling in the nucleus accumbens shell of mice has key role in methamphetamine withdrawal symptoms. Transl Psychiatry *5*, e666.

Ressler, K.J., Sullivan, S.L., and Buck, L.B. (1993). A zonal organization of odorant receptor gene expression in the olfactory epithelium. Cell *73*, 597–609.

Ressler, K.J., Sullivan, S.L., and Buck, L.B. (1994a). Information coding in the olfactory system: evidence for a stereotyped and highly organized epitope map in the olfactory bulb. Cell *79*, 1245–1255.

Ressler, K.J., Sullivan, S.L., and Buck, L.B. (1994b). A molecular dissection of spatial patterning in the olfactory system. Curr. Opin. Neurobiol. *4*, 588–596.

Ressler, K.J., Rothbaum, B.O., Tannenbaum, L., and Anderson, P. (2013). Cognitive Enhancers as Adjuncts to Psychotherapy. *61*.

Rex, C.S., Lin, C.-Y., Kramár, E. a, Chen, L.Y., Gall, C.M., and Lynch, G. (2007). Brain-derived neurotrophic factor promotes long-term potentiation-related cytoskeletal changes in adult hippocampus. J. Neurosci. *27*, 3017–3029.

Rincón-cortés, M., Barr, G.A., Marie, A., Shionoya, K., and Nuñez, B.S. (2015). Enduring good memories of infant trauma : Rescue of adult neurobehavioral deficits via amygdala serotonin and corticosterone interaction. *112*.

Rincón-Cortés, M., and Sullivan, R.M. (2014). Early life trauma and attachment: immediate and enduring effects on neurobehavioral and stress axis development. Front. Endocrinol. (Lausanne). *5*, 33.

Rochefort, C., Gheusi, G., Vincent, J.-D., and Lledo, P.-M. (2002). Enriched odor exposure increases the number of newborn neurons in the adult olfactory bulb and improves odor memory. J. Neurosci. *22*, 2679–2689.

Roskams, a J., Bethel, M. a, Hurt, K.J., and Ronnett, G. V (1996). Sequential expression of Trks A, B, and C in the regenerating olfactory neuroepithelium. J. Neurosci. *16*, 1294–1307.

Rothbaum, B.O., Kearns, M.C., Price, M., Malcoun, E., Davis, M., Ressler, K.J., Lang, D., and Houry, D. (2012). Early Intervention May Prevent the Development of Posttraumatic Stress Disorder: A Randomized Pilot Civilian Study with Modified Prolonged Exposure. Biol. Psychiatry.

Rudy, J.W., and Cheatle, M.D. (1977). Odor-Aversion Learning in Neonatal Rats. Science (80-.). *198*, 845–846.

Saghatelyan, A., Roux, P., Migliore, M., Rochefort, C., Desmaisons, D., Charneau, P., Shepherd, G.M., and Lledo, P.M. (2005). Activity-dependent adjustments of the inhibitory network in the olfactory bulb following early postnatal deprivation. Neuron *46*, 103–116.

Sah, P., Westbrook, R.F., and Lüthi, a (2008). Fear conditioning and long-term potentiation in the amygdala: what really is the connection? Ann. N. Y. Acad. Sci. *1129*, 88–95.

Sakamoto, M., Kageyama, R., and Imayoshi, I. (2014). The functional significance of newly born neurons integrated into olfactory bulb circuits. Front. Neurosci. *8*, 1–9.

Santoro, S.W., and Dulac, C. (2012). The activity-dependent histone variant H2BE modulates the life span of olfactory neurons. Elife *1*, e00070.

Schwob, J.E. (2002). Neural regeneration and the peripheral olfactory system. Anat. Rec. *269*, 33–49.

Scott, J.W., and Sherrill, L. (2008). Effects of Odor Stimulation on Antidromic Spikes in Olfactory Sensory Neurons. 3074–3085.

Scott, J.W., Acevedo, H.P., and Sherrill, L. (2006). Effects of concentration and sniff flow rate on the rat electroolfactogram. Chem. Senses *31*, 581–593.

Shi, C., and Davis, M. (1999). Pain pathways involved in fear conditioning measured with fear-potentiated startle: lesion studies. J. Neurosci. *19*, 420–430.

Shykind, B.M., Rohani, S.C., O'Donnell, S., Nemes, A., Mendelsohn, M., Sun, Y., Axel, R., and Barnea, G. (2004). Gene switching and the stability of odorant receptor gene choice. Cell *117*, 801–815.

Sierra-Mercado, D., Padilla-Coreano, N., and Quirk, G.J. (2011). Dissociable roles of prelimbic and infralimbic cortices, ventral hippocampus, and basolateral amygdala in the expression and extinction of conditioned fear. Neuropsychopharmacology *36*, 529–538.

Sigurdsson, T., Doyère, V., Cain, C.K., and LeDoux, J.E. (2007). Long-term potentiation in the amygdala: a cellular mechanism of fear learning and memory. Neuropharmacology *52*, 215–227.

Siopi, E., Denizet, M., Gabellec, M.-M., de Chaumont, F., Olivo-Marin, J.-C., Guilloux, J.-P., Lledo, P.-M., and Lazarini, F. (2016). Anxiety- and Depression-Like States Lead to Pronounced Olfactory Deficits and Impaired Adult Neurogenesis in Mice. J. Neurosci. *36*, 518–531.

Soliman, F., Glatt, C.E., Bath, K.G., Levita, L., Jones, R.M., Pattwell, S.S., Jing, D., Tottenham, N., Amso, D., Somerville, L.H., et al. (2010). A genetic variant BDNF polymorphism alters extinction learning in both mouse and human. Science *327*, 863–866.

Spencer, J.L., Waters, E.M., Milner, T. a, Lee, F.S., and McEwen, B.S. (2010). BDNF variant Val66Met interacts with estrous cycle in the control of hippocampal function. Proc. Natl. Acad. Sci. U. S. A. *107*, 4395–4400.

Steckler, T., and Risbrough, V. (2012). Pharmacological treatment of PTSD - established and new approaches. Neuropharmacology *62*, 617–627.

Stefanko, D.P., Barrett, R.M., Ly, A.R., Reolon, G.K., and Wood, M. a (2009). Modulation of long-term memory for object recognition via HDAC inhibition. Proc. Natl. Acad. Sci. U. S. A. *106*, 9447–9452.

Stephan, A.H., Barres, B. a., and Stevens, B. (2012). The Complement System: An Unexpected Role in Synaptic Pruning During Development and Disease. Annu. Rev. Neurosci. *35*, 369–389.

Stevens, B., Allen, N.J., Vazquez, L.E., Howell, G.R., Christopherson, K.S., Nouri, N., Micheva, K.D., Mehalow, A.K., Huberman, A.D., Stafford, B., et al. (2007). The Classical Complement Cascade Mediates CNS Synapse Elimination. Cell *131*, 1164–1178.

Sullivan, R.M., and Holman, P.J. (2010). Transitions in sensitive period attachment learning in infancy: the role of corticosterone. Neurosci. Biobehav. Rev. *34*, 835–844.

Sullivan, R.M., and Wilson, D. a (2003). Molecular biology of early olfactory memory. Learn. Mem. *10*, 1–4.

Sullivan, R.M., Hofer, M.A., and Brake, S.C. (1986). Olfactory-guided orientation in neonatal rats is enhanced by a conditioned change in behavioral state. Dev.

Psychobiol. *19*, 615–623.
Sultan, S., Mandairon, N., Kermen, F., Garcia, S., Sacquet, J., and Didier, a (2010). Learning-dependent neurogenesis in the olfactory bulb determines long-term olfactory memory. FASEB J. *24*, 2355–2363.
Sultan, S., Rey, N., Sacquet, J., Mandairon, N., and Didier, a. (2011). Newborn Neurons in the Olfactory Bulb Selected for Long-Term Survival through Olfactory Learning Are Prematurely Suppressed When the Olfactory Memory Is Erased. J. Neurosci. *31*, 14893–14898.
Teicher, M.H., and Blass, E.M. (1977). First suckling response of the newborn albino rat: the roles of olfaction and amniotic fluid. Science *198*, 635–636.
Todrank, J., Heth, G., and Restrepo, D. (2011). Effects of *in utero* odorant exposure on neuroanatomical development of the olfactory bulb and odour preferences. Proc. Biol. Sci. *278*, 1949–1955.
Tsvetkov, E., Carlezon, W. a, Benes, F.M., Kandel, E.R., and Bolshakov, V.Y. (2002). Fear conditioning occludes LTP-induced presynaptic enhancement of synaptic transmission in the cortical pathway to the lateral amygdala. Neuron *34*, 289–300.
Tyler, W.J., and Pozzo-Miller, L. (2003). Miniature synaptic transmission and BDNF modulate dendritic spine growth and form in rat CA1 neurones. J. Physiol. *553*, 497–509.
Tyler, W.J., Alonso, M., Bramham, C.R., and Pozzo-Miller, L.D. (2002). From acquisition to consolidation: on the role of brain-derived neurotrophic factor signaling in hippocampal-dependent learning. Learn. Mem. *9*, 224–237.
Valley, M.T., Mullen, T.R., Schultz, L.C., Sagdullaev, B.T., and Firestein, S. (2009). Ablation of mouse adult neurogenesis alters olfactory bulb structure and olfactory fear conditioning. Front. Neurosci. *3*, 51.
Vassalli, A., Rothman, A., Feinstein, P., Zapotocky, M., and Mombaerts, P. (2002a). Minigenes impart odorant receptor-specific axon guidance in the olfactory bulb. Neuron *35*, 681–696.
Vassalli, A., Rothman, A., Feinstein, P., Zapotocky, M., and Mombaerts, P. (2002b). Minigenes impart odorant receptor-specific axon guidance in the olfactory bulb. Neuron *35*, 681–696.
Vassar, R., Chao, S.K., Sitcheran, R., Nuiiez, M., Vosshall, L.B., and Axel, R. (1994). Topographic O rganization of Sensory Projection to the O lfactory Bulb. *79*.
Vassoler, F.M., White, S.L., Schmidt, H.D., Sadri-Vakili, G., and Pierce, R.C. (2013). Epigenetic inheritance of a cocaine-resistance phenotype. Nat. Neurosci. *16*, 42–47.
Vinera, J., Kermen, F., Didier, A., Mandairon, N., and Richard, M. (2015). Olfactory perceptual learning requires action of noradrenaline in the olfactory bulb : comparison with olfactory associative learning. 192–197.
Voyron, S., Giacobini, P., Tarozzo, G., Cappello, P., Perroteau, I., and Fasolo, A. (1999). Apoptosis in the development of the mouse olfactory epithelium. Brain Res. Dev. Brain Res. *115*, 49–55.
Walker, D.L., Ressler, K.J., Lu, K.-T., and Davis, M. (2002). Facilitation of conditioned fear extinction by systemic administration or intra-amygdala infusions of D-cycloserine as assessed with fear-potentiated startle in rats. J. Neurosci. *22*, 2343–2351.

Weinberger, N.M. (2007). Associative representational plasticity in the auditory cortex: a synthesis of two disciplines. Learn. Mem. *14*, 1–16.

Wilensky, A.E., Schafe, G.E., Kristensen, M.P., and LeDoux, J.E. (2006). Rethinking the fear circuit: the central nucleus of the amygdala is required for the acquisition, consolidation, and expression of Pavlovian fear conditioning. J. Neurosci. *26*, 12387–12396.

Wilson, D. a, Best, a R., and Sullivan, R.M. (2004). Plasticity in the olfactory system: lessons for the neurobiology of memory. Neuroscientist *10*, 513–524.

Wu, Y., Dissing-Olesen, L., MacVicar, B.A., and Stevens, B. (2015). Microglia: Dynamic Mediators of Synapse Development and Plasticity. Trends Immunol. *36*, 605–613.

Yamaguchi, M., and Mori, K. (2005). Critical period for sensory experience-dependent survival of newly generated granule cells in the adult mouse olfactory bulb. Proc. Natl. Acad. Sci. U. S. A. *102*, 9697–9702.

Yehuda, R., and LeDoux, J. (2007). Response variation following trauma: a translational neuroscience approach to understanding PTSD. Neuron *56*, 19–32.

Yoshii, A., and Constantine-Paton, M. (2007). BDNF induces transport of PSD-95 to dendrites through PI3K-AKT signaling after NMDA receptor activation. Nat. Neurosci. *10*, 702–711.

Yu, H., Wang, Y., Pattwell, S., Jing, D., Liu, T., Zhang, Y., Bath, K.G., Lee, F.S., and Chen, Z.-Y. (2009). Variant BDNF Val66Met polymorphism affects extinction of conditioned aversive memory. J. Neurosci. *29*, 4056–4064.

Zovkic, I.B., and Sweatt, J.D. (2013). Epigenetic mechanisms in learned fear: implications for PTSD. Neuropsychopharmacology *38*, 77–93.

Zovkic, I.B., Paulukaitis, B.S., Day, J.J., Etikala, D.M., and Sweatt, J.D. (2014). Histone H2A.Z subunit exchange controls consolidation of recent and remote memory. Nature.

TABLE 1 – REFERENCES

Andero R, Brothers SP, Jovanovic T et al. . Amygdala-dependent fear is regulated by Oprl1 in mice and humans with PTSD. Science translational medicine 2013;5:188ra73.

Andre JM, Leach PT, Gould TJ. Nicotine ameliorates NMDA receptor antagonist-induced deficits in contextual fear conditioning through high-affinity nicotinic acetylcholine receptors in the hippocampus. Neuropharmacology 2011;60(4):617-25.

Berlau DJ, McGaugh JL. Enhancement of extinction memory consolidation: the role of the noradrenergic and GABAergic systems within the basolateral amygdala. Neurobiology of learning and memory 2006;86:123-32.

Biojone C, Casarotto PC, Resstel LB et al. . Anti-aversive effects of the atypical antipsychotic, aripiprazole, in animal models of anxiety. J Psychopharmacol 2011;25(6):801-7.

Borowski TB, Kokkinidis L. Contribution of ventral tegmental area dopamine neurons to expression of conditional fear: effects of electrical stimulation, excitotoxin lesions, and quinpirole infusion on potentiated startle in rats. Behav Neurosci 1996;110(6):1349-64.

Cain CK, Blouin AM, Barad M. Adrenergic transmission facilitates extinction of conditional fear in mice. Learning & memory (Cold Spring Harbor, N.Y.) 2004;11:179-87.

Chess AC, Landers AM, Bucci DJ. L-kynurenine treatment alters contextual fear conditioning and context discrimination but not cue-specific fear conditioning. Behav Brain Res 2009;201(2):325-31.

Chhatwal JP, Gutman AR, Maguschak Ka et al. . Functional interactions between endocannabinoid and CCK neurotransmitter systems may be critical for extinction learning. Neuropsychopharmacology : official publication of the American College of Neuropsychopharmacology 2009;34:509-21.

Corbit LH, Janak PH. Posterior dorsomedial striatum is critical for both selective instrumental and Pavlovian reward learning. Eur J Neurosci 2010;31(7):1312-21.

Davis JA, Gould TJ. beta2 subunit-containing nicotinic receptors mediate the enhancing effect of nicotine on trace cued fear conditioning in C57BL/6 mice. Psychopharmacology (Berl) 2007;190(3):343-52.

de Oliveira MR, da Rocha RF, Stertz L et al. . Total and mitochondrial nitrosative stress, decreased brain-derived neurotrophic factor (BDNF) levels and glutamate uptake, and evidence of endoplasmic reticulum stress in the hippocampus of vitamin A-treated rats. Neurochem Res 2011;36(3):506-17.

Delamater AR, Campese V, Westbrook RF. Renewal and spontaneous recovery, but not latent inhibition, are mediated by gamma-aminobutyric acid in appetitive conditioning. J Exp Psychol Anim Behav Process 2009;35(2):224-37.

Fanselow MS, Bolles RC. Naloxone and shock-elicited freezing in the rat. J Comp Physiol Psychol 1979;93(4):736-44.

Fanselow MS. Opiate modulation of the active and inactive components of the postshock reaction: parallels between naloxone pretreatment and shock intensity. Behav Neurosci 1984;98(2):269-77.

Fu AL, Yan XB, Sui L. Down-regulation of beta1-adrenoceptors gene expression by short interfering RNA impairs the memory retrieval in the basolateral amygdala of rats. Neurosci Lett 2007;428(2-3):77-81.

Good AJ, Westbrook RF. Effects of a microinjection of morphine into the amygdala on the acquisition and expression of conditioned fear and hypoalgesia in rats. Behav Neurosci 1995;109(4):631-41.

Greba Q, Kokkinidis L. Peripheral and intraamygdalar administration of the dopamine D1 receptor antagonist SCH 23390 blocks fear-potentiated startle but not shock reactivity or the shock sensitization of acoustic startle. Behav Neurosci 2000;114(2):262-72.

Greba Q, Gifkins a, Kokkinidis L. Inhibition of amygdaloid dopamine D2 receptors impairs emotional learning measured with fear-potentiated startle. Brain research 2001;899:218-26.

Guarraci Fa, Frohardt RJ, Kapp BS. Amygdaloid D1 dopamine receptor involvement in Pavlovian fear conditioning. Brain research 1999;827:28-40.

Holbrook TL, Galarneau MR, Dye JL et al. . Morphine use after combat injury in Iraq and post-traumatic stress disorder. The New England journal of medicine 2010;362:110-7.

Kenney JW, Wilkinson DS, Gould TJ. The enhancement of contextual fear conditioning by ABT-418. Behav Pharmacol 2010;21(3):246-9.

Lazzaro SC, Hou M, Cunha C et al. . Antagonism of lateral amygdala alpha1-adrenergic receptors facilitates fear conditioning and long-term potentiation. Learn Mem 2010;17(10):489-93.

Lisboa SF, Reis DG, da Silva AL et al. . Cannabinoid CB1 receptors in the medial prefrontal cortex modulate the expression of contextual fear conditioning. Int J Neuropsychopharmacol 2010;13(9):1163-73.

McGaugh JL, Castellano C, Brioni J. Picrotoxin enhances latent extinction of conditioned fear. Behav Neurosci 1990;104(2):264-7.Wiltgen BJ, Godsil BP, Peng Z et al. The alpha1 subunit of the GABA(A) receptor modulates fear learning and plasticity in the lateral amygdala. Front Behav Neurosci 2009;3:37.

McNally GP, Westbrook RF. Opioid receptors regulate the extinction of Pavlovian fear conditioning. Behav Neurosci 2003;117(6):1292-301.

McNally GP, Pigg M, Weidemann G. Opioid receptors in the midbrain periaqueductal gray regulate extinction of pavlovian fear conditioning. The Journal of neuroscience : the official journal of the Society for Neuroscience 2004;24:6912-9.

Mueller D, Bravo-Rivera C, Quirk GJ. Infralimbic D2 receptors are necessary for fear extinction and extinction-related tone responses. Biological psychiatry 2010;68:1055-60.

Nader K, LeDoux J. The dopaminergic modulation of fear: quinpirole impairs the recall of emotional memories in rats. Behav Neurosci 1999;113(1):152-65.

Ortiz O, Delgado-Garcia JM, Espadas I et al. . Associative learning and CA3-CA1 synaptic plasticity are impaired in D1R null, Drd1a-/- mice and in hippocampal siRNA silenced Drd1a mice. J Neurosci 2010;30(37):12288-300.

Ponnusamy R, Nissim Ha, Barad M. Systemic blockade of D2-like dopamine receptors facilitates extinction of conditioned fear in mice. Learning & memory (Cold Spring Harbor, N.Y.) 2005;12:399-406.

Prado-Alcalá Ra, Haiek M, Rivas S et al. . Reversal of extinction by scopolamine. Physiology & behavior 1994;56:27-30.

Raybuck JD, Lattal KM. Double dissociation of amygdala and hippocampal contributions to trace and delay fear conditioning. PloS one 2011;6:e15982.

Saxe G, Stoddard F, Courtney D et al. . Relationship between acute morphine and the course of PTSD in children with burns. J Am Acad Child Adolesc Psychiatry 2001;40(8):915-21.

Van't Veer A, Yano JM, Carroll FI et al. . Corticotropin-releasing factor (CRF)-induced disruption of attention in rats is blocked by the κ-opioid receptor antagonist JDTic. Neuropsychopharmacology : official publication of the American College of Neuropsychopharmacology 2012;37:2809-16.